

Bay Area Air Quality Management District
Community Air Protection Program
Annual Report #1 – Grant #17-CAPP-3
April 18, 2019

The Bay Area Air Quality Management District is submitting this Annual Report in compliance with requirements of the agreement governing the use of the funds provided through the Community Air Protection Grant #17-CAPP-3. **This Annual Report covers activities and expenditures for the period of March 1, 2018 through February 28, 2019.**

As of February 28, 2019, the Air District expended \$2,640,637 supporting the implementation of AB 617 in the Bay Area and earned \$44,189 in interest. The fund balance, including earned interest, is \$2,203,552. A breakdown of expenditures by spending plan element is provided in the Table A below.

The main activities that occurred during the reporting period included identifying priority communities with the Bay Area; selecting one community, West Oakland, for the development of community air protection plan; selecting one community, the Richmond-San Pablo area, for the development of a monitoring plan; identification of potential Best Available Retrofit Control Technologies for stationary sources subject to the requirements of Cap and Trade Regulation; updated modeling of regional, background particulate matter and toxic emissions impacting West Oakland; an updated local inventory of emissions occurring within West Oakland; modeling of local concentrations of diesel particulate matter and PM_{2.5} in West Oakland, as well as modeling of cancer risks from toxics emissions; and design of a mobile monitoring van.

The Air District has posted online agendas, presentations and documents developed with support from Community Air Protection Grant at <http://www.baaqmd.gov/community-health/community-health-protection-program>. There were two draft technical studies completed during the reporting period that have not yet been posted to the Air District's website. These draft studies are included in the electronic submittal of this Annual Report.

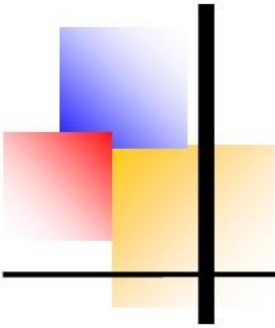
An updated Spending Plan for the Community Air Protection Grant #17-CAPP-3 is included with this Annual Report. The changes to the Spending Plan are prompted by a shift to more mobile monitoring and special studies in the near-term, and delaying potential development of additional permanent, regulatory monitoring stations. Delays in the adoption of final state-wide emissions reporting requirements and lower than expected initial costs for the BARCT review have also lowered our expected first year program costs.

Table A

**Bay Area Air Quality Management District
 Assembly Bill 617 Implementation
 Expenditures – March 1, 2018 to February 28, 2019
 Grant #G17-CAPP-3**

Program Component	Major Activities	Staff Costs	Capital Costs and Professional Services
Community Engagement	<ul style="list-style-type: none"> • Adoption of Year 1 and Years 2-5 priority AB 617 communities. • Held ten (10) community workshops as part of the selection of AB 617 communities. • Conducted two online Open Air Forum surveys to gather input on the criteria for selecting AB 617 communities. • In cooperation with the West Oakland Environmental Indicators Project, convened a Steering Committee for the development of the West Oakland Community Action Plan. • Hosted 7 meetings of the Steering Committee for the West Oakland Community Action Plan. • Hosted 6 community meetings in Richmond, CA as part of the development of the Richmond-San Pablo Area Monitoring Plan. • Professional Facilitation for the West Oakland Community Action Plan. • Professional Facilitation for the Richmond-San Pablo Area Monitoring Plan. • Ongoing capacity building with local communities. 	\$370,812	\$71,627
Implementation of Best Available Retrofit Technology	<ul style="list-style-type: none"> • Review of existing controls at over 3,000 sources that contribute to emissions at facilities subject to Cap-and-Trade. • Identification of feasible Best Available Retrofit Control Technologies • CEQA review on schedule to implement new BARCT requirements. • Adoption by the Board of Directors of a schedule for adoption of rules to implement new BARCT requirements. 	\$180,024	\$33,586

Community Emission Reduction Plans	<ul style="list-style-type: none"> • Development of the West Oakland Community Action Plan, in cooperation with the West Oakland Environmental Indicators Project. • Development of a detailed emissions inventory for West Oakland. • Fine Particulate Matter Analysis and Regional Modeling in the San Francisco Bay Area in Support of AB 617. • Local scale modeling of emissions concentrations and cancer risks from emissions sources within West Oakland. 	\$1,266,066	\$50,308
Community Monitoring	<ul style="list-style-type: none"> • Participation in and support for the development of the Richmond-San Pablo Area Monitoring Plan. • New equipment and van for short-term mobile monitoring studies. 	\$416,844	\$190
Overhead	<ul style="list-style-type: none"> • Executive Management to coordinate/oversee AB 617 program development. • Legal Services for CEQA analysis and regulatory development. • Administrative Services. 	\$142,417	\$30,162



BAY AREA
AIR QUALITY
MANAGEMENT
DISTRICT

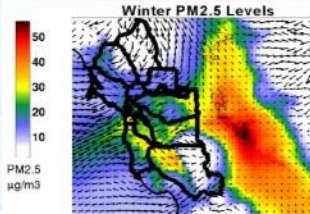
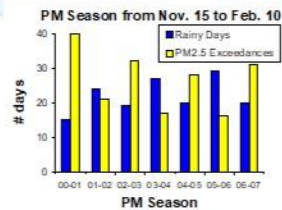
375 Beale Street, San Francisco, CA 94105

Air Quality Modeling and Analysis Section Publication No. 201903-019-Toxics

Air Toxics Data Analysis and Regional Modeling In the San Francisco Bay Area to Support AB617

Draft Report—Version 1

April, 2019



Prepared by the Air Quality Modeling and Analysis Section:

Saffet Tanrikulu, Manager
Bonyoung Koo, Senior Atmospheric Modeler
Stephen Reid, Senior Atmospheric Modeler
Yuanyuan Fang, Statistician
Yiqin Jia, Atmospheric Modeler
James Cordova, Air Quality Meteorologist
Jeff Matsuoka, Research Analyst

Contributors from Ramboll US Corporation

Michele Jimenez
Tejas Shah
Chris Emery

Disclaimer

This draft report presents results from analyses of ambient measurement data and air quality modeling performed by the District. The models were tested and evaluated for many cases in the Bay Area, and their performance has been iteratively improved. In addition, ambient and emissions data used in the analyses were carefully evaluated. The simulations in this report utilize the best-performing configurations of the models. However, the results presented should be viewed as interim because further refinements may still be made to emissions estimates, meteorological fields, and other modeling-related data. The District plans to improve upon these interim results and minimize uncertainties via its on-going modeling and analysis efforts. As significant improvements are made, this draft report may be updated.

Air Toxics Data Analysis and Regional Modeling in the San Francisco Bay Area to Support AB617

1. Introduction

1.1 Background

The adoption of Assembly Bill 617 (AB617) established collaborative programs to reduce community exposure to air pollutants in neighborhoods most impacted by air pollution. Air District staff have been working closely with the California Air Resources Board (ARB), other local air districts, community groups, community members, environmental organizations, regulated industries, and other key stakeholders to reduce harmful air pollutants in Bay Area communities.

One purpose of this data analysis and regional modeling effort is to support the District's AB617 activities by assessing pollutant formation, quantifying the relative contribution of emission sources to ambient pollution levels, and assessing population exposures and the benefits of emission controls in impacted communities around the Bay Area. Another purpose is to support the AB617 activities by identifying geographic areas that are significantly overburdened relative to the Bay Area as a whole, prioritizing among the overburdened areas for AB617 community selection and characterizing relative ambient concentrations in rural, suburban and urban areas. Results of this effort are expected to help identify strategies for reducing regional concentrations of key species of air toxics. Analyses in this report focus on air toxics concentrations in the whole Bay Area with an emphasis on West Oakland. Follow-up analyses will include other Bay Area communities.

For the air toxics analyses, we evaluated ambient meteorological and air quality data, and applied the U.S. EPA's Community Multi-Scale Air Quality (CMAQ) model to simulate pollutant concentrations at a 1-km horizontal resolution over the entire Bay Area for 2016 (Figure 1.1). Then we repeated the simulation with West Oakland's anthropogenic emissions removed from the modeling inventory, leaving all other model input parameters unchanged. We calculated annual average air toxics concentrations using the output of each simulation. The first simulation provided the annual average air toxics concentrations for 2016 over the entire Bay Area, which will be used for air toxics cancer risk evaluation. The second simulation provided an estimate of background air toxics levels in West Oakland (i.e., the air toxics concentrations that would exist in the absence of local West Oakland sources).

Background air toxics concentrations will be combined with local-scale modeling of West Oakland sources using the AERMOD dispersion model to provide a complete picture of air toxics levels in the community and the relative contribution of different emission sources to those levels. Figure 1.2 shows the AERMOD modeling domain for West Oakland. The area outlined in blue represents the "source domain," and all significant emissions sources in that

area will be modeled in the AERMOD simulations. The red hatched area represents the “receptor domain,” or the area for which pollutant concentrations will be calculated by AERMOD.

The application of the CMAQ model involves the preparation of meteorological and emissions inputs, model runs, analysis of simulated pollutant concentrations, and the evaluation of model performance via comparison between simulated and observed pollutant concentrations. A simulation year of 2016 was selected because (1) this is a recent year that is likely to be representative of current conditions in West Oakland and other communities; and (2) special measurement studies that took place in 2016 provide additional ambient data to support evaluations of model performance.

A total of 11 air toxics were simulated: diesel particulate matter (DPM), 5 toxic gases (acetaldehyde, acrolein, benzene, 1,3-butadiene, and formaldehyde), and 5 trace metals (cadmium, chromium VI, lead, mercury, and nickel). Previous analyses have indicated that DPM and the 5 toxic gases cumulatively account for more than 90% of toxic air contaminant emissions in the Bay Area (Tanrikulu et al., 2011).

District staff have been applying and evaluating the CMAQ model in the Bay Area over the last several years, along with the Weather Research and Forecasting (WRF) model, which provides meteorological inputs for CMAQ. Findings from previous modeling work are documented in District reports on air toxics data analysis and modeling (Tanrikulu et al., 2009 and 2011) and PM_{2.5} data analysis and modeling (Tanrikulu et al., 2019), as well as in the District’s 2017 Clean Air Plan (BAAQMD, 2017). Both the CMAQ and WRF models were tested and evaluated for many cases in the Bay Area, and their performance has been iteratively improved. The 2016 simulations used the best-performing configuration of the model. The 2016 emissions inputs have been updated to reflect ARB’s most recent estimates and have been evaluated to the extent possible.

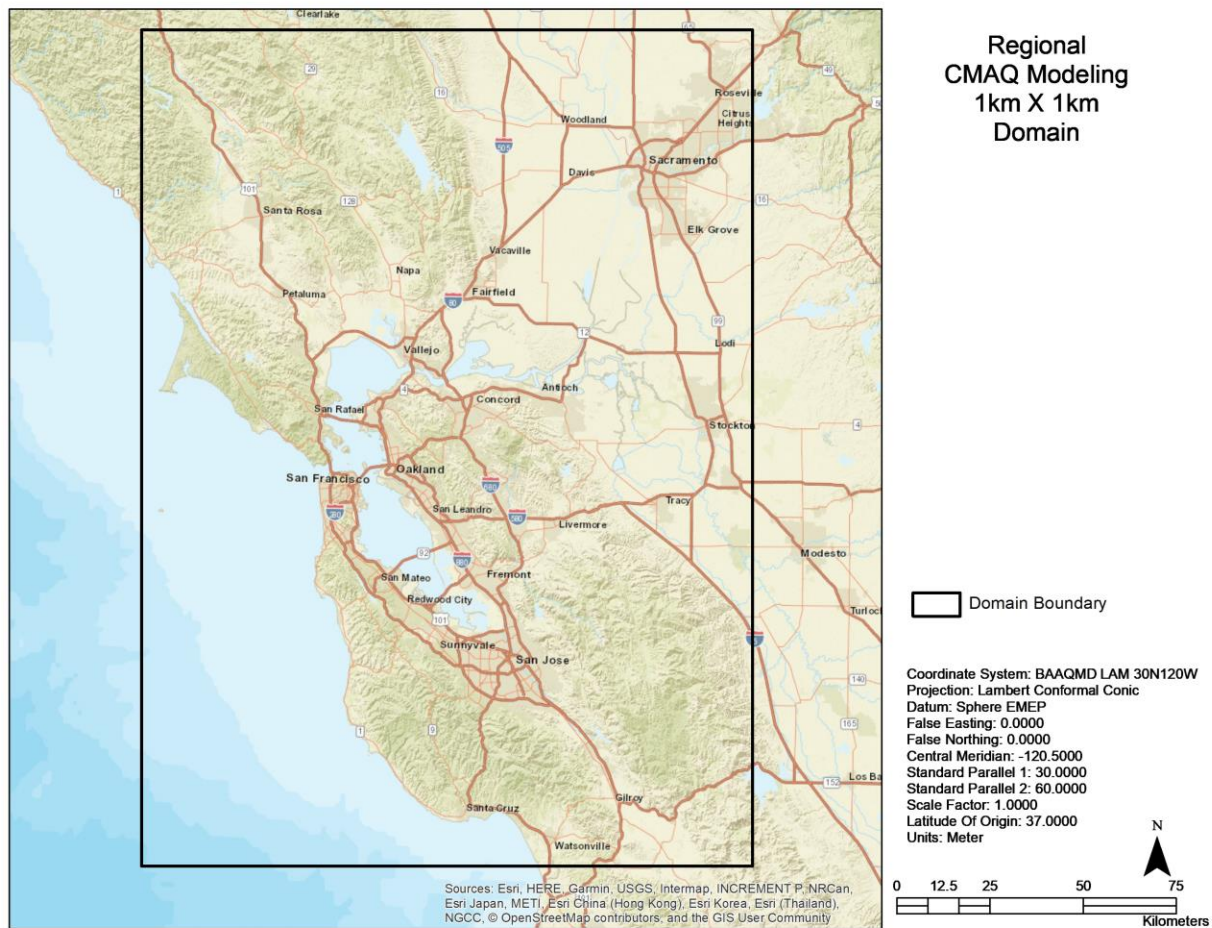


Figure 1.1: The regional 1-km modeling domain used for CMAQ simulations.

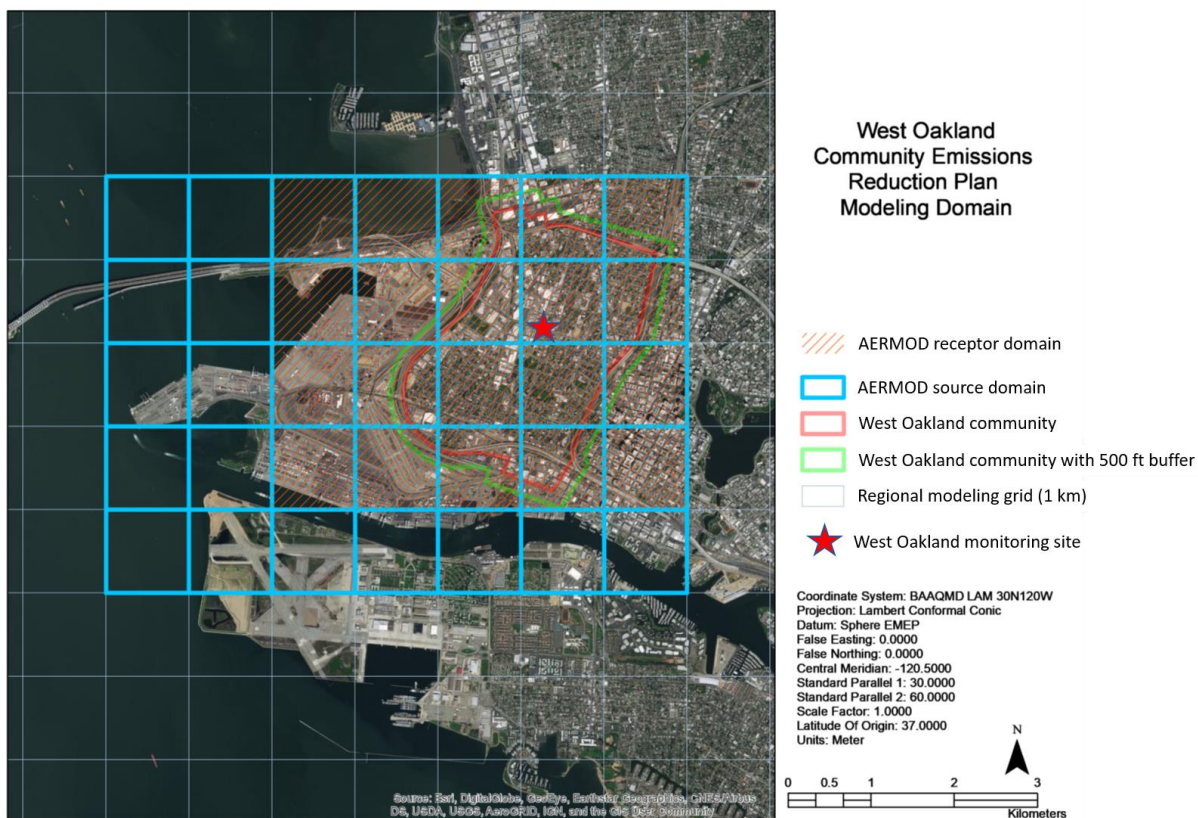


Figure 1.2: The West Oakland AERMOD modeling domain. The area outlined in blue represents the AERMOD source domain, and the red hatched area represents the AERMOD receptor domain.

1.2 Air Toxics and Their Health Impacts

Air toxics are a complex mixture of gases, suspended particles and liquid droplets in the atmosphere. Most air toxics originate from human-made sources, including mobile sources (e.g., cars, trucks, buses) and stationary sources (e.g., factories, refineries, power plants), as well as indoor sources (e.g., some building materials and cleaning solvents). Some air toxics are also released from natural sources such as forest fires.

One of the major human health outcomes resulting from air toxics exposure is cancer risk. The unit risk factor describes the excess cancer risk associated with an inhalation exposure to a concentration of $1 \mu\text{g}/\text{m}^3$ of a given toxic air contaminant (assuming a 70-year lifetime exposure). Table 1.1 lists unit risk factors for the modeled air toxics that were recently updated based on CAPCOA recommendations. Unit risk factors for toxic metals tend to be higher than those of other air toxics; for example, the unit risk factor for hexavalent chromium is orders-of-magnitude higher than unit risk factors for other air toxics. However, typical atmospheric concentrations of toxic metals are much smaller than those of other toxics; thus, overall cancer risks due to the metals are relatively small.

Table 1.1: Inhalation unit cancer risk factors for the air toxic species included in this study.

Air Toxics¹	Unit Risk Factor (($\mu\text{g}/\text{m}^3$)⁻¹)
Formaldehyde	0.000014
Acetaldehyde	0.000068
Benzene	0.000068
1,3-Butadiene	0.00041
Diesel PM	0.00074
Hexavalent Chromium	0.38
Nickel	0.00062
Cadmium	0.010
Lead	0.00066

¹Acrolein and mercury were also simulated in this study; however, they have no known cancer risk. Therefore, they are not included in this table.

Section 2 of this report presents a summary of air toxics observations in the Bay Area and results of analysis of observed data; Section 3 presents modeling methods, including emissions inventory preparation, preparation of meteorological inputs and application of the CMAQ model. Section 4 presents model evaluation. Section 5 presents the excess cancer risk associated with air toxics. Section 6 presents a summary and discussion of overall results.

There are several appendices that provide additional details on air toxics emissions estimates (Appendix A), primary vs. secondary air toxics formation (Appendix B), simulation of toxics metals (Appendix C), and West Oakland-specific cancer risk evaluation (Appendix D).

Simulation of toxics metals is discussed in Appendix C rather than the main body of this report because the emissions estimates for these species are preliminary and uncertain. In the absence of local data, emission estimates for metals were taken from the EPA’s 2014 National Air Toxics Assessment (NATA) inventory and may be unrepresentative of 2016 emission levels in Bay Area communities. Simulated metal concentrations presented in Appendix C are preliminary and will be updated when improved emissions estimates are available. Note that, while these preliminary contributions of metals to Bay Area total cancer risk are included in the overall results, at their currently estimated levels, metals contribute only about 2% to the total Bay Area cancer risk.

2. Observations and Data Analysis

2.1 Ambient Measurements

Ambient air toxics data have been continuously collected in the Bay Area for many years. In 2016, there were 20 air toxics monitoring stations operating in the Bay Area. These stations, which are listed in Table 2.1 along with their sampling schedules, can be categorized into two types: (1) National Air Toxics Trend Stations (NATTS); and (2) Hazardous Air Pollutants Stations (HAPS). There is one NATTS station (San Jose – Jackson Street) and nineteen HAPS stations (all others) in the Bay Area.

Four air toxics species (formaldehyde, acetaldehyde, 1,3-butadiene and benzene) were measured at the San Jose NATTS every 6 days in 2016. Two air toxics species (1,3-butadiene and benzene) were measured at HAPS every 12 days. Chromium, cadmium, nickel, lead, and mercury were sampled as part of PM_{2.5} speciation at Livermore, Oakland West and Vallejo every 6 days and at San Jose – Jackson Street every 3 days.

Acrolein was not measured in the Bay Area in 2016. The air quality monitoring network plan published by BAAQMD (Knoderer et al., 2017) provides additional details on the District’s monitoring network.

All ambient data used in this study were subjected to quality assurance checks and validated prior to being used. These data were used for the establishment of relationships among emissions, meteorology and air quality, and the evaluation of models. Daily average data are used for most analyses and model evaluation, but annual averages are presented here for brevity.

Table 2.1: A list of air toxics monitoring stations in the Bay Area with their sampling schedule for 2016. Highlighted columns and rows show measurement schedule.

Station	Formaldehyde	Acetaldehyde	Benzene	1,3-butadiene	EC	Chromium	Cadmium	Lead	Nickel	Mercury
NATTS										
San Jose -Jackson St.	1 in 6 days					1 in 3 days				
HAPS and speciated PM_{2.5}										
Livermore			1 in 12 days			1 in 6 days				
Oakland West										
Vallejo										

HAPS											
Berkeley			1 in 12 days								
Bethel Island											
Concord											
Crockett											
Fort Cronkhite											
Laney College											
Martinez											
Napa											
Oakland East											
Redwood City											
Richmond – 7 th St.											
San Francisco											
San Jose – Knox Ave.											
San Pablo											
San Rafael											
Sebastopol											

2.2 Data Analysis

Table 2.2 shows the annual average observed air toxics concentrations for 2016. Concentrations below the minimum detection limit are not included in the annual averages. Stations with no annual average concentration value for a given pollutant either did not have measurements for that pollutant in 2016 or did not capture any samples above the minimum detection limit. Highlighted values in Table 2.2 represent averages calculated from less than 12 samples above the detection limit.

Formaldehyde and acetaldehyde were measured only at San Jose – Jackson Street. The annual average concentrations of these species were 2.18 $\mu\text{g}/\text{m}^3$ and 1.39 $\mu\text{g}/\text{m}^3$, respectively. Over 70% of atmospheric formaldehyde forms as an intermediate product of the oxidation (combustion) of methane and other carbon compounds (Zemba et al, 2019). The remaining atmospheric formaldehyde is directly emitted to the atmosphere, mainly from its use in industrial processes such as oil refining and the production of resins for particle board and coatings. Acetaldehyde forms as an intermediate product of the oxidation of ethylene and ethanol.

Benzene and 1,3-butadiene were monitored at all Bay Area toxics monitoring stations. The highest annual average benzene concentration in the Bay Area (0.39 ppb) was at San Jose – Knox Avenue. At seven other air monitoring stations (Berkeley, Napa, Vallejo, Oakland West, Oakland East, Redwood City and San Jose – Jackson Street), the annual average benzene concentrations exceeded 0.2 ppb. Benzene is used as a constituent in motor fuels; as a solvent for

fats, waxes, resins, oils, inks, paints, plastics, and rubber; in the extraction of oils from seeds and nuts; and in photogravure printing.

The highest Bay Area annual average 1,3-butadiene concentration (0.1 ppb) was measured at the San Jose – Knox Avenue air monitoring station. Concentrations at Sebastopol, Vallejo, San Jose – Jackson Street, Redwood City and Oakland West were above 0.07 ppb, higher than the remaining Bay Area stations. Emission sources of 1,3-butadiene include: motor vehicle exhaust, manufacturing and processing facilities, forest fires or other combustion, and cigarette smoke. Higher levels of 1,3-butadiene may be found in highly industrialized cities or near oil refineries, chemical manufacturing plants, and plastic and rubber factories.

As mentioned, PM samples were speciated at four Bay Area air monitoring stations (San Jose – Jackson Street, Vallejo, Livermore and Oakland West), and concentrations of EC and five metals were extracted, among other species. As shown in Table 2.2, the annual average EC concentration at San Jose – Jackson Street is the lowest among the four stations. However, while samples were speciated at San Jose – Jackson Street throughout 2016 and averaged over the entire year, they were speciated only during winter, spring and fall months at the other three stations and averaged over those three seasons. Since PM concentrations are higher during winter months than summer months in the Bay Area, this mismatched averaging period led to lower annual average concentration at San Jose – Jackson Street compared to other three stations.

The annual average lead concentrations are significantly higher at Oakland West than at the other 3 stations (Livermore, San Jose – Jackson Street and Vallejo). At Oakland West, there were six samples during 2016 with concentrations around 100 ng/m³ and above; as a result, the annual average concentration at this station stands out.

Table 2.2: Annual average observed air toxics concentrations for 2016. Highlighted values represent averages calculated from less than 12 valid samples.

Site	Formaldehyde	Acetaldehyde	Benzene	1,3-Butadiene	EC	Chromium	Cadmium	Lead	Nickel	Mercury
	[$\mu\text{g}/\text{m}^3$]	[$\mu\text{g}/\text{m}^3$]	[ppb]	[ppb]	[$\mu\text{g}/\text{m}^3$]	[ng/m^3]	[ng/m^3]	[ng/m^3]	[ng/m^3]	[ng/m^3]
Berkeley			0.2108							
Bethel Island			0.1263							
Concord			0.1356							
Crockett			0.1399	0.0540						
Fort Cronkhite			0.0796							
Laney College			0.1991	0.0635						
Livermore			0.1785	0.0638	0.5981		11.6242	3.8260	2.2144	2.6552
Martinez			0.1494	0.0670						
Napa			0.2192	0.0666						
Oakland East			0.2360	0.0606						
Oakland West			0.2239	0.0779	0.5580		9.0201	56.9884	4.4872	2.2439
Redwood City			0.2210	0.0703						
Richmond - 7th St			0.1424	0.0370						
San Francisco			0.1731	0.0485						
San Jose - Jackson St.	2.1871	1.3921	0.2609	0.0741	0.3608	8.4436		17.4300	4.1820	
San Jose - Knox Av			0.3971	0.1067						
San Pablo			0.1841							
San Rafael			0.1602	0.0625						
Sebastopol			0.1583	0.0850						
Vallejo			0.2027	0.0838	0.4915		8.8598	3.1431	1.3480	2.7547

Data for EC and metals are components of speciated $\text{PM}_{2.5}$.

Data for chromium include all oxidation states.

3. Modeling

3.1 Emissions Inventory Preparation

Emissions inputs for the CMAQ model were prepared using the Sparse Matrix Operator Kernel Emissions (SMOKE) processing system, version 4.5, which converts emissions inventory data to the spatial, temporal, and chemical resolution required by the air quality model. CMAQ-ready emissions inputs for 2016 included 11 air toxics: diesel particulate matter (DPM), 5 toxic gases (acetaldehyde, acrolein, benzene, 1,3-butadiene, and formaldehyde), and 5 trace metals (cadmium, chromium VI, lead, mercury, and nickel).

The starting point for the emissions processing was the 2016 criteria pollutant inventories previously assembled for 1-km PM_{2.5} modeling (Tanrikulu et al., 2019). These 2016 data, which include estimates for area sources,¹ point sources, onroad mobile sources, nonroad mobile sources, and biogenic sources, were assembled from a variety of data sources, including the District's in-house emissions estimates, emissions data from ARB, and outputs from ARB's EMFAC2017 model. Additional details on data sources and processing steps for air toxics emissions estimates are provided below.

3.1.1 Toxic Gases

SMOKE disaggregates total organic (TOG) and PM_{2.5} emissions into a series of model species that CMAQ uses to represent atmospheric chemistry. For the 2016 PM_{2.5} modeling, speciation profiles developed for the SAPRC07 chemical mechanism were applied to TOG emissions from all sources, and profiles developed for the AERO6 aerosol module (AE6) were applied to PM_{2.5} emissions from all sources (Tanrikulu et al., 2019).

The SAPRC07 mechanism treats some toxic species explicitly, including acetaldehyde, benzene, and formaldehyde. However, other air toxics are lumped into model species that act as surrogates for multiple compounds with similar mass and reactivity. For the 2016 toxics modeling, existing SAPRC07 speciation profiles for TOG were modified to treat additional air toxics (acrolein and 1,3-butadiene) explicitly.² Once the revised speciation profiles were generated, the District used SMOKE to speciate existing 2016 TOG emissions estimates into the 5 toxic gases of interest, as well as other model species used by the SAPRC07 chemical mechanism.

3.1.2 Diesel Particulate Matter

To track DPM emissions separately from other PM emissions, speciation profiles related to diesel exhaust were edited to include DPM tracer species. For example, speciation profile

¹ Area sources are stationary sources such as dry cleaners that are too small or numerous to treat as individual point sources.

² The District contracted with Ramboll to perform this work.

91106 (for heavy duty diesel vehicle exhaust) was modified to include the DPM components shown in Table 1 below.

Table 3.1: DPM components for speciation profile 91106.

Component	Description	Weight fraction
DIESEL_PMEC	Elemental carbon	0.7712
DIESEL_PMOC	Organic carbon	0.1756
DIESEL_PMFINE	Unspeciated PM _{2.5}	0.049109
DIESEL_PMSO4	Sulfate	0.00295
DIESEL_PMNO3	Nitrate	0.001141

Running SMOKE with these revised diesel exhaust profiles produced separate DPM species that could be used to estimate DPM concentrations in CMAQ.

3.1.3 Trace Metals

The toxic metals of interest are not included in the AE6 mechanism; therefore, emission estimates for these species were taken from the EPA’s 2014 NATA inventory. The 2014 NATA data includes air toxics emissions estimates for the entire U.S. at the county (for area, nonroad, and onroad sources) or facility (for point sources) level. Emissions records for cadmium, chromium VI, lead, mercury, and nickel were extracted from the NATA data for all counties in the 1-km modeling domain, processed through SMOKE, and merged with emissions data for the remaining toxic species being modeled.

Additional details on SMOKE processing steps, including ancillary data sets (e.g., spatial surrogates) used in SMOKE, are provided in a companion report on the 2016 PM_{2.5} modeling for the Bay Area (Tanrikulu et al., 2019).

3.1.4 Emissions Summaries

This subsection provides emissions density plots and summary tables for DPM, the main driver of cancer risk in the Bay Area. Similar information for additional air toxics can be found in Appendix A. Figure 3.1 shows annual average DPM emissions for the 1-km modeling domain. Table 3.2 summarizes the annual average DPM emissions by county and source sector, as reported by the SMOKE emissions model. Within the District’s jurisdiction, annual average DPM emissions total 4.2 tons per day (tpd). Nonroad and onroad mobile sources account for 57% and 41%, respectively, of total DPM emissions in the Bay Area.

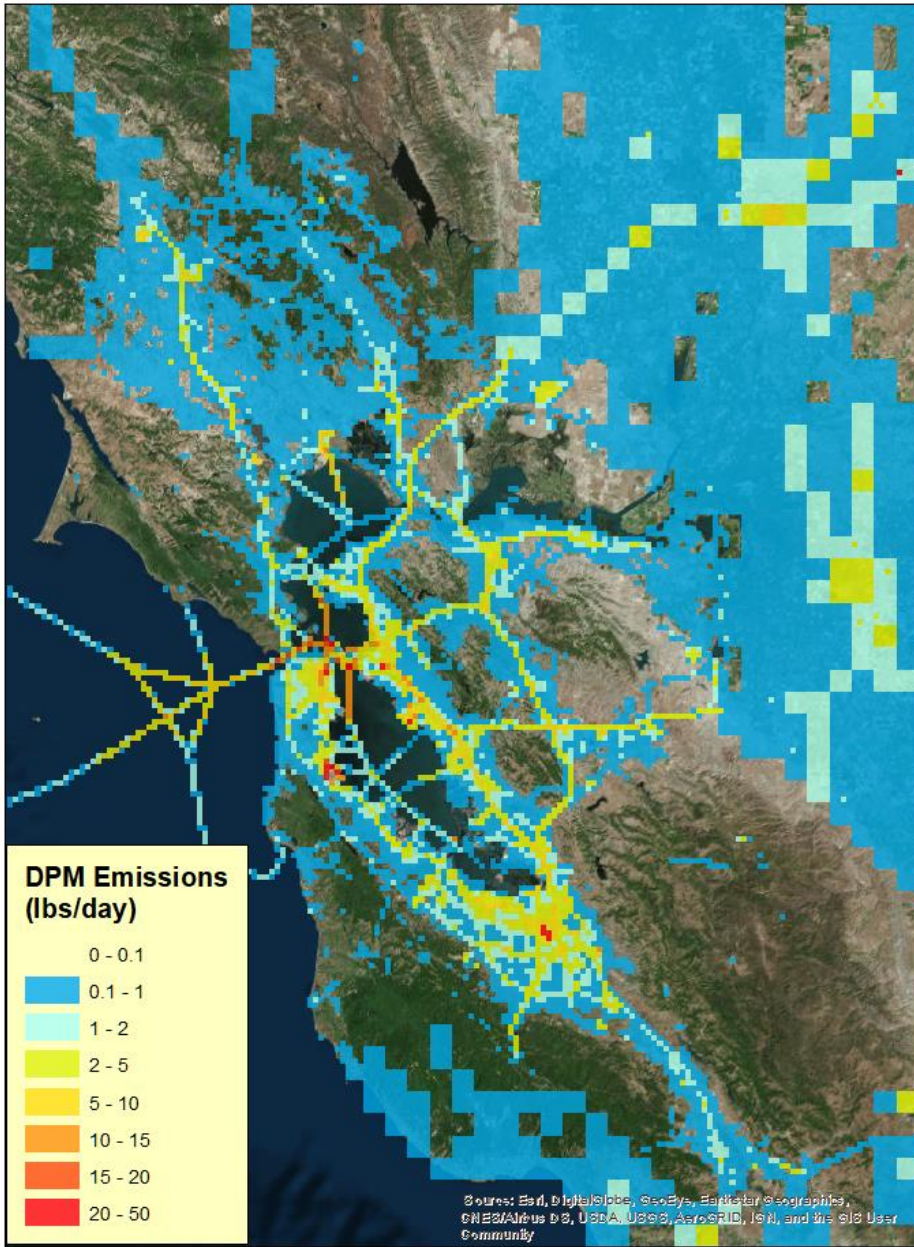


Figure 3.1: Spatial distribution of annual average DPM emissions for the 1-km modeling domain for 2016.

Table 3.2: Summary of 2016 DPM10 emissions (tpd) by geographic area and source sector.

Geographic Area	Area	Nonroad	Onroad	Point	Total
Alameda	0.00	0.30	0.56	0.03	0.88
Contra Costa	0.00	0.23	0.23	0.00	0.47
Marin	0.00	0.09	0.05	0.00	0.14
Napa	0.00	0.10	0.06	0.00	0.16
San Francisco	0.00	0.65	0.11	0.01	0.76
San Mateo	0.00	0.38	0.10	0.01	0.49
Santa Clara	0.00	0.36	0.39	0.02	0.77

Solano ^a	0.00	0.06	0.10	0.00	0.17
Sonoma ^a	0.00	0.22	0.13	0.00	0.35
<i>BAAQMD Subtotal</i>	<i>0.00</i>	<i>2.38</i>	<i>1.74</i>	<i>0.08</i>	<i>4.19</i>
Non-BAAQMD Counties	0.02	1.44	1.11	0.03	2.60
Domain Total	0.02	3.81	2.85	0.11	6.79

^aEmissions totals for Solano and Sonoma counties only include the portion of those counties in BAAQMD's jurisdiction.

For the West Oakland AERMOD modeling domain, annual average DPM_{2.5} emissions total 0.1 tpd, or 2.4% of the BAAQMD total. Figure 3.2 shows that the distribution of emissions by source sector in West Oakland differs from the District as a whole. In West Oakland, onroad and nonroad mobile sources account for 85% of total DPM_{2.5} emissions, while the same sources account for 98% of total PM_{2.5} emissions districtwide. Figure 3.3 shows the spatial distribution of DPM emissions across the 1-km grid cells that coincide with the local-scale AERMOD modeling domain. Grid cells with high DPM emissions along the western edge of the domain are impacted by motor vehicle emissions from the Bay Bridge and marine vessel activity. Grid cells with high DPM emissions in the eastern portion of the modeling domain are impacted by motor vehicle emissions, especially from the I-880/I-980 and I-580/I-980 interchanges.

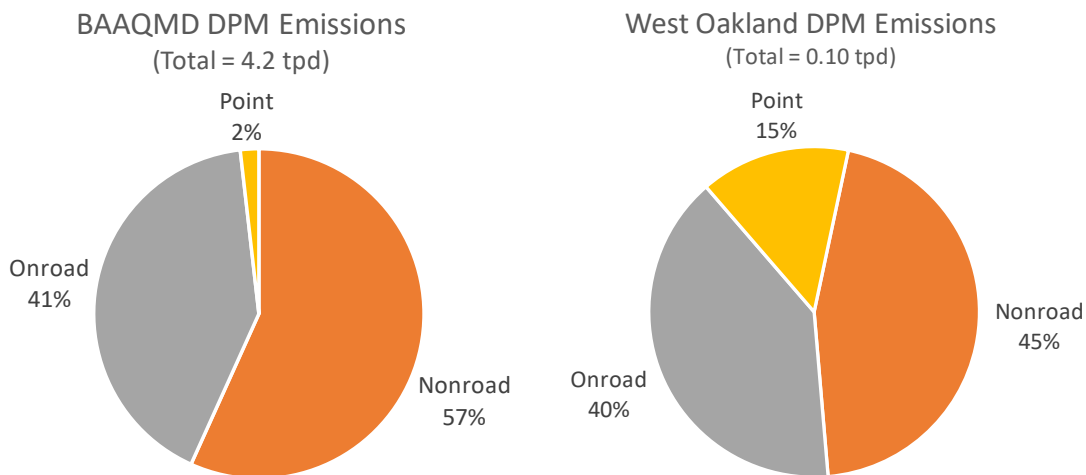


Figure 3.2: DPM emissions by source sector for the District (left) and West Oakland (right) for 2016.

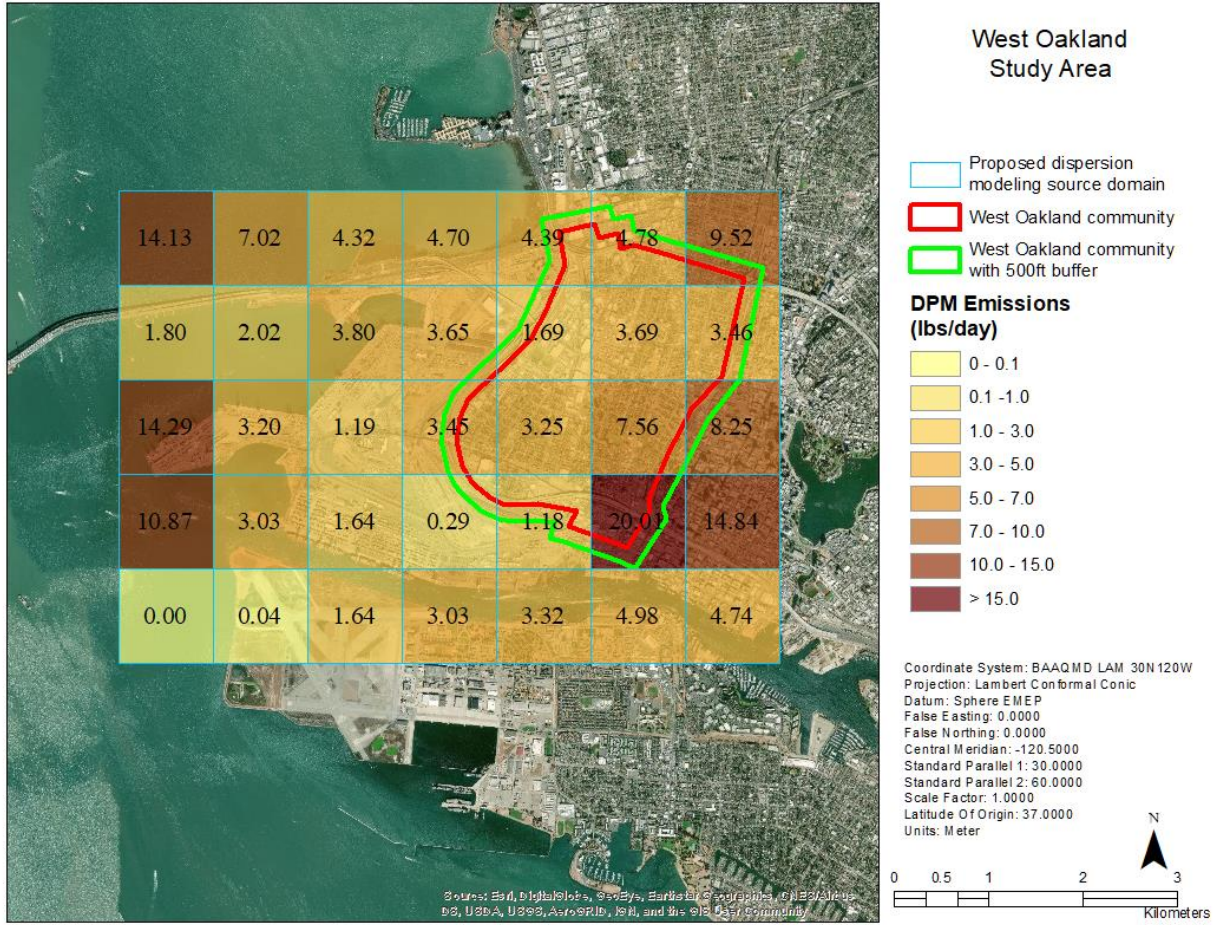


Figure 3.3: Spatial distribution of annual average DPM emissions in West Oakland for 2016.

3.2 Meteorological Modeling

The Weather Research and Forecasting (WRF) Model version 3.8 was used to prepare meteorological inputs to CMAQ. Four nested modeling domains were used (Figure 3.4). The outer domain covered the entire western United States at 36-km horizontal grid resolution to capture synoptic (large-scale) flow features and the impact of these features on local meteorology. The second domain covered California and portions of Nevada at 12-km horizontal resolution to capture mesoscale (sub-regional) flow features and their impacts on local meteorology. The third domain covered Central California at 4-km resolution to capture localized air flow features. The 4-km domain included the Bay Area, San Joaquin Valley, and Sacramento Valley, as well as portions of the Pacific Ocean and the Sierra Nevada mountains. The fourth domain covered the Bay Area and surrounding regions at 1-km resolution. All four domains employed 50 vertical layers with thickness increasing with height from the surface to the top of the modeling domain (about 18 km).

Meteorological variables are estimated at the layer midpoints in WRF. The thickness of the lowest layer to the surface was about 25 m. Thus, meteorological variables near the surface were estimated at about 12.5 m above ground level. The model configuration was tested using available physics options, including: (1) planetary boundary layer processes and time-based evaluation of mixing heights; (2) cumulus parameterization; (3) four-dimensional data assimilation (FDDA) strategy; (4) horizontal and vertical diffusion; (5) advection scheme; and (6) microphysics and radiation scheme. The final choice of options was the one that best characterized meteorology in the domain.

WRF was applied for 2016 to estimate parameters required by the air quality model, including hourly wind speed and direction, temperature, humidity, cloud cover, rain and solar radiation levels. Observations were assimilated into the model during the simulations to minimize the difference between simulations and real-world measurements. Two types of nudging methods were employed (analysis and observation). The National Centers for Environmental Prediction (NCEP) North America Mesoscale (NAM) 12-km analyzed meteorological fields were used for analysis nudging as well as for initializing the model. The NCEP ADP Global Surface and Upper Air Observational Weather Data were used for observational nudging. The analysis nudging was applied to the 36-km and 12-km domains. Frequency of surface analysis nudging was every three hours, while the frequency of 3D analysis nudging was every six hours. The 3D analysis nudging of winds was performed over all model layers, but the 3D analysis nudging of temperature and humidity was limited to layers above the planetary boundary layer. The observation nudging of wind was applied to all four domains every three hours.

The WRF model was rigorously evaluated for accuracy. Observations used to evaluate WRF were taken from the EPA's Air Quality System, the BAAQMD meteorological network, and the National Climate Data Center. Hourly and daily time series plots of observed and simulated wind, temperature and humidity were generated at each observation station and compared to each other hour by hour and day by day. Simulated hourly areal plots of wind, temperature,

humidity, planetary boundary layer height, pressure and other fields were generated and quantitatively compared against observations where observations were available.

WPS Domain Configuration

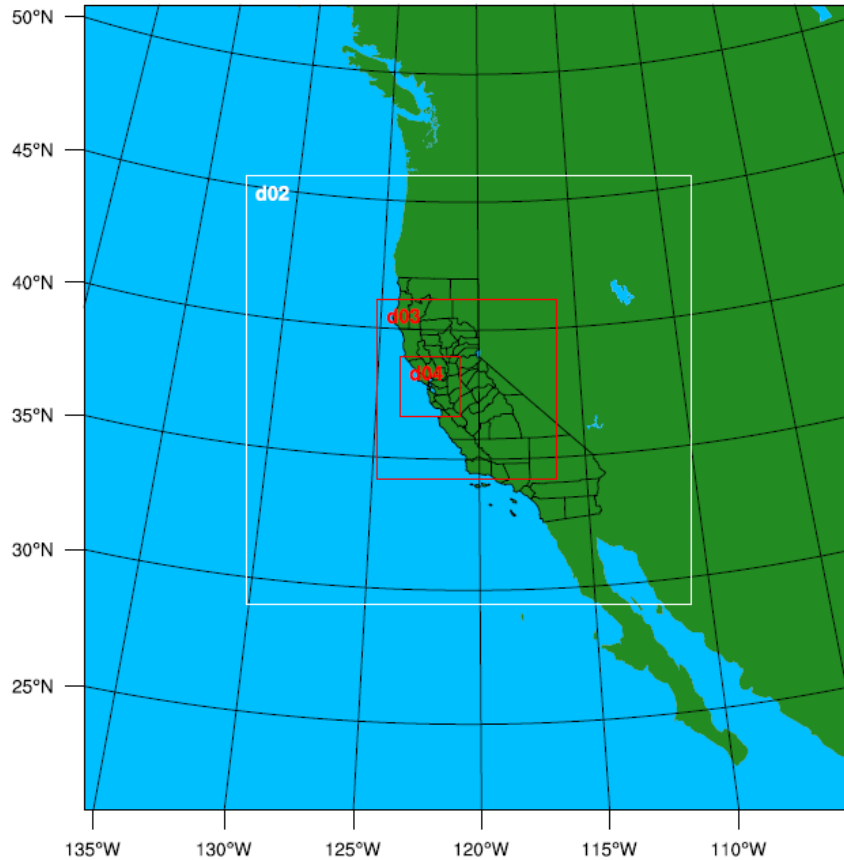


Figure 3.4: Nested WRF modeling domains.

These plots were also qualitatively evaluated for known meteorological features of the modeling domain, especially at 4-km and 1-km resolutions. These features include slope flows, channeled flows, sea breeze and low-level jet. The vertical profile of observed and simulated meteorological fields was compared at several upper air meteorological stations, including Oakland, Medford, Reno and Las Vegas, and at a temporary station established at Bodega Bay. Ramboll's METSTAT program (Emery et al., 2001) was used to statistically evaluate the performance of WRF.

The WRF model performed reasonably well in every evaluation category. The estimated bias, gross error, root mean square error (RMSE), and index of agreement (IOA) are within established criteria for acceptable model performance for every day of 2016. In other words, performance obtained from the Bay Area applications of WRF is similar or slightly better than performance obtained from applications elsewhere, available from literature. Additional information on model application and evaluation can be found in Tanrikulu et al., 2019.

3.3 Air Quality Modeling

U.S. EPA's Community Multiscale Air Quality (CMAQ) modeling system version 5.2 was used to simulate gaseous and particulate air toxics. The modeling domain is similar to that used for the District's previous air toxics modeling (Tanrikulu et al., 2009; 2011), focusing on the Bay Area at 1-km horizontal grid resolution, but extending further inland to include more surrounding regions (Figure 1.1). The vertical grid has 28 layers that extend to the lower stratosphere (~18 km) with a surface layer thickness of about 25 m. Below 1,500 m, the CMAQ layers match the WRF layers, while above 1,500 m, CMAQ layers span several meteorological model layers, which is a common practice in air quality modeling to improve computational efficiency.

The initial and boundary conditions for the 1-km modeling domain were primarily derived from the District's recent regional air quality modeling that simulated ozone and PM over the Bay Area, San Joaquin Valley and Sacramento Valley at 4-km grid resolution (Tanrikulu et al., 2019).

The standard Statewide Air Pollution Research Council Toxics Species version 2007 (SAPRC07TC) chemistry mechanism implemented in CMAQ v5.2 includes gaseous air toxics such as formaldehyde, acetaldehyde, acrolein, benzene and 1,3-butadiene (Hutzell et al., 2012). It also separately tracks direct emissions of formaldehyde, acetaldehyde and acrolein, since these compounds include a significant proportion of chemical production in the atmosphere (i.e., "secondary" production) from the oxidation of other organic compounds.

For the Bay Area application, the standard chemistry mechanism was modified to include atmospheric mercury and chemical reactions that oxidize elemental mercury to divalent mercury in both gaseous and particle-bound forms. Gaseous elemental mercury, the predominant form in the atmosphere, is relatively inert and can be transported over long distances with an atmospheric lifetime ranging from several months to a year, while both forms of oxidized mercury (often referred to as gaseous oxidized mercury and particulate bound mercury) are quickly removed from the atmosphere via wet and dry deposition, limiting their impact to a local/regional scale (AMAP/UNEP, 2013).

Formation of methylmercury by microorganisms and its bioaccumulation in the aquatic food chain are not addressed in this study. Other toxic metals added to the mechanism for the Bay Area applications include hexavalent chromium, nickel, cadmium and lead. Explicit particle emission components from diesel exhaust were also added to separately track diesel PM. The initial and boundary concentrations for the newly added species were set to a lower bound value (a negligible, but non-zero value) to avoid potential numerical problems in the model.

The CMAQ modeling was conducted for the whole year of 2016 using the complete air toxics emissions inventories described in Section 3.1 (base case) and with all anthropogenic emissions from West Oakland removed (control case). The base case represents ambient concentrations of the air toxics for 2016 over the entire Bay Area, which will be used for model evaluation and health impact assessment. The control case estimates background levels of the air toxics in

West Oakland, which will complement local-scale air dispersion model simulations to determine detailed source-receptor relationships for the area.

The simulated annual average concentrations of gaseous air toxics are discussed in section 3.3.1, diesel PM in section 3.3.2, and toxics metals in section 3.3.3.

3.3.1 Gaseous Air Toxics

Figures 3.5 through 3.9 show annual average concentrations of five gaseous air toxics (formaldehyde, acetaldehyde, acrolein, 1,3-butadiene, and benzene) from the base case CMAQ simulation over the 1-km modeling domain. The annual average concentrations are a total of primary and secondary components for species with secondary production pathways.

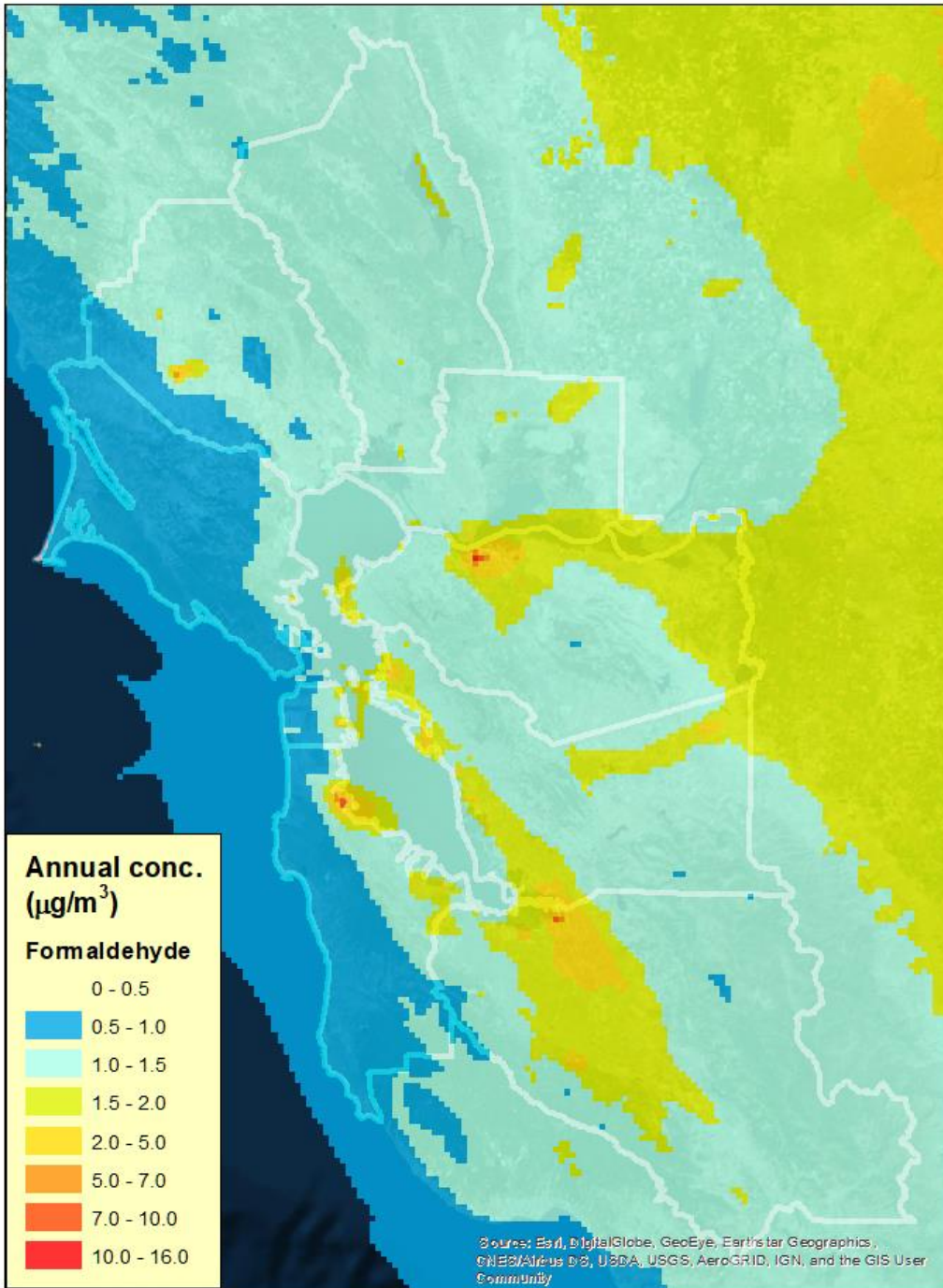
The highest annual average formaldehyde concentration is simulated at Martinez in the vicinity of the Shell Refinery, reaching $15.7 \mu\text{g}/\text{m}^3$. Other hot spots are simulated near a wastewater treatment facility in northern San Jose ($8.7 \mu\text{g}/\text{m}^3$), at San Francisco International Airport ($8.2 \mu\text{g}/\text{m}^3$), in northwestern Petaluma near a regional landfill ($6.6 \mu\text{g}/\text{m}^3$), and near Emeryville ($5.1 \mu\text{g}/\text{m}^3$). Simulated concentrations range from 2 to $5 \mu\text{g}/\text{m}^3$ in the areas surrounding these hot spots as well as at a landfill east of Livermore, and near Richmond, Oakland International Airport, Redwood City and southern San Jose. Similar concentrations are simulated along the Delta, the I-580 corridor in Livermore, and the I-880 corridor between San Leandro and San Jose.

The annual average acetaldehyde concentrations are highest at San Francisco International Airport ($2.7 \mu\text{g}/\text{m}^3$). Concentrations are also high (above $0.8 \mu\text{g}/\text{m}^3$) on the east side of the Bay Bridge, at Oakland International Airport, and in San Jose. Portions of I-80, I-880, I-680, I-101, and I-580 have elevated concentrations.

While formaldehyde and acetaldehyde in most of the modeling domain are largely due to secondary production, hot spot areas tend to exhibit relatively higher primary fractions, indicating significant contributions of local sources (see Appendix B for a discussion of primary vs. secondary toxics formation).

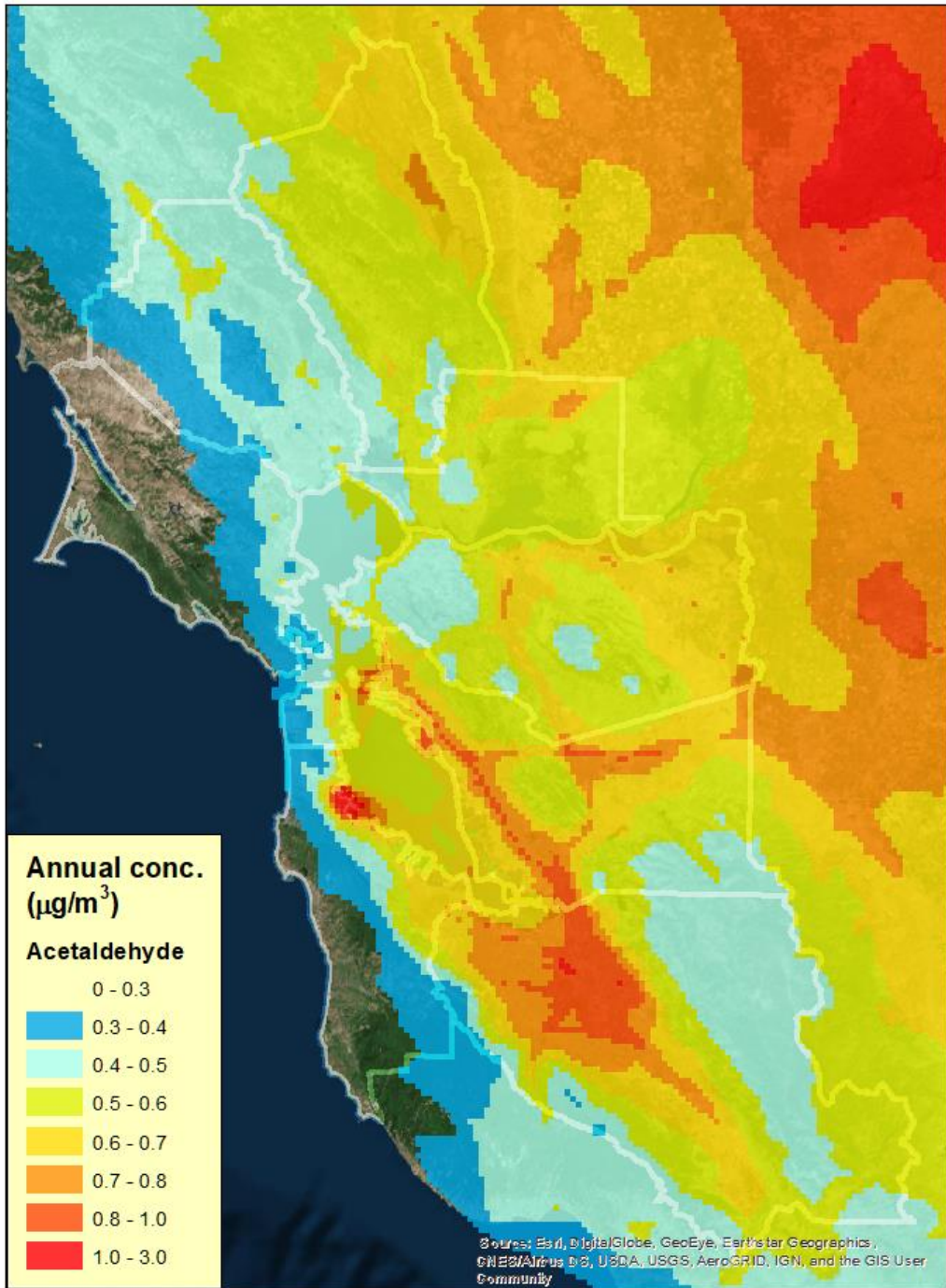
Concentration patterns of acrolein and 1,3-butadiene are similar, with both showing the highest annual average concentration at San Francisco International Airport ($1.1 \mu\text{g}/\text{m}^3$ for acrolein and $0.9 \mu\text{g}/\text{m}^3$ for 1,3-butadiene). Secondary production pathways of acrolein include atmospheric oxidation of 1,3-butadiene.

For benzene, annual average concentrations above $1 \mu\text{g}/\text{m}^3$ occur in Richmond, Martinez, northern San Jose, Mountain View, and at the San Francisco International Airport.



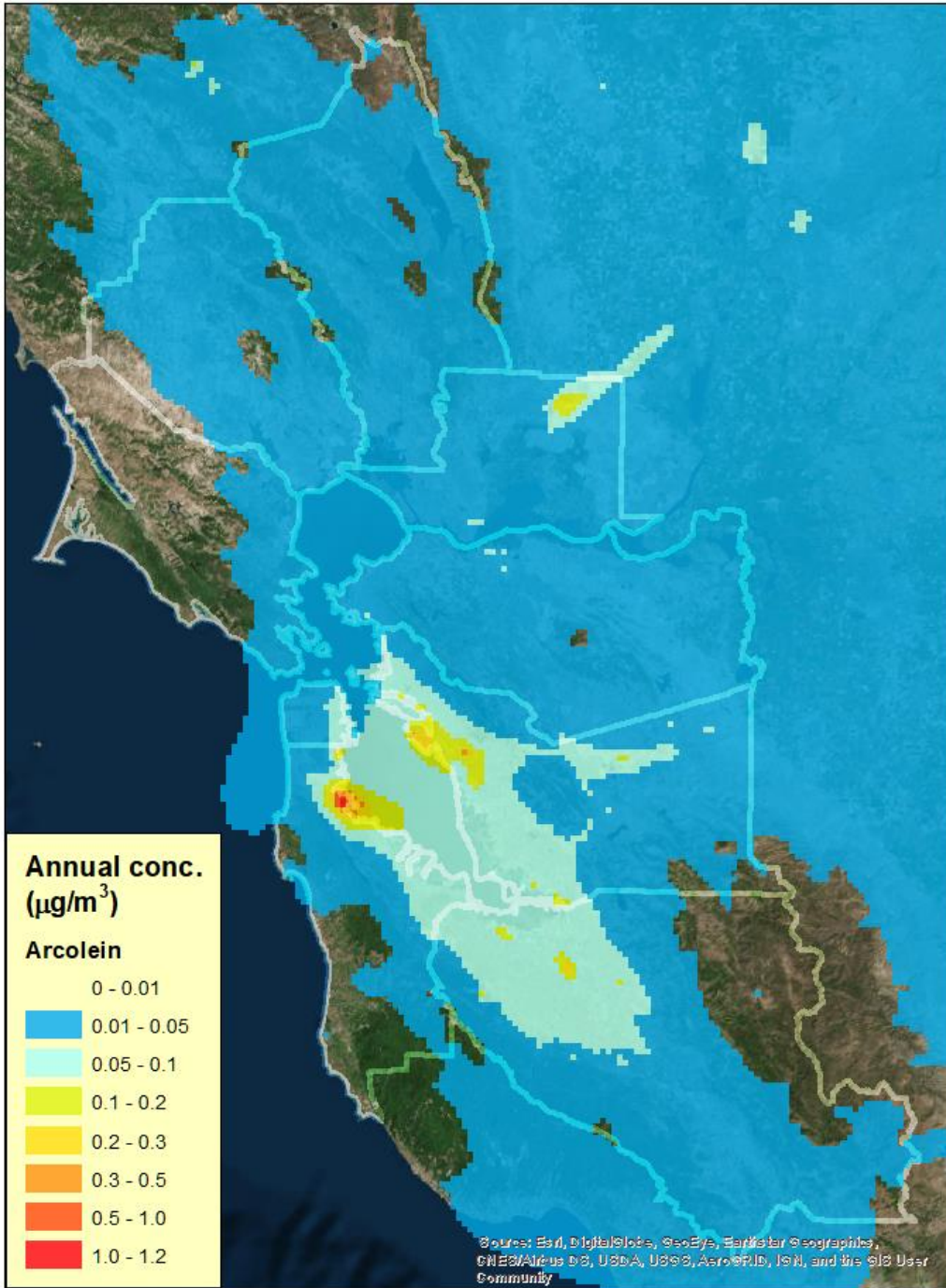
Maximum: 15.7

Figure 3.5: Annual average simulated formaldehyde concentrations for 2016.



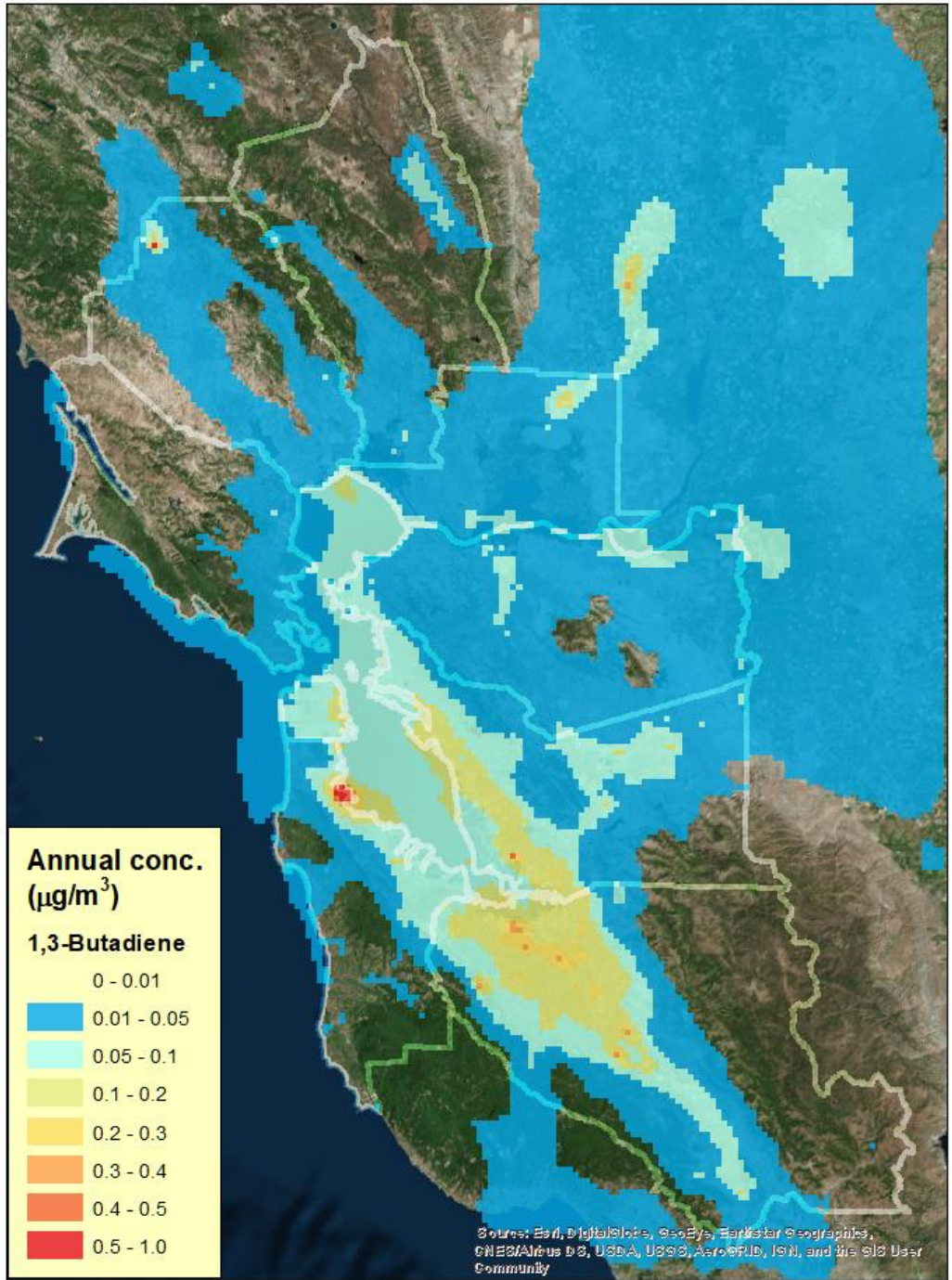
Maximum: 2.7

Figure 3.6: Annual average simulated acetaldehyde concentrations for 2016.



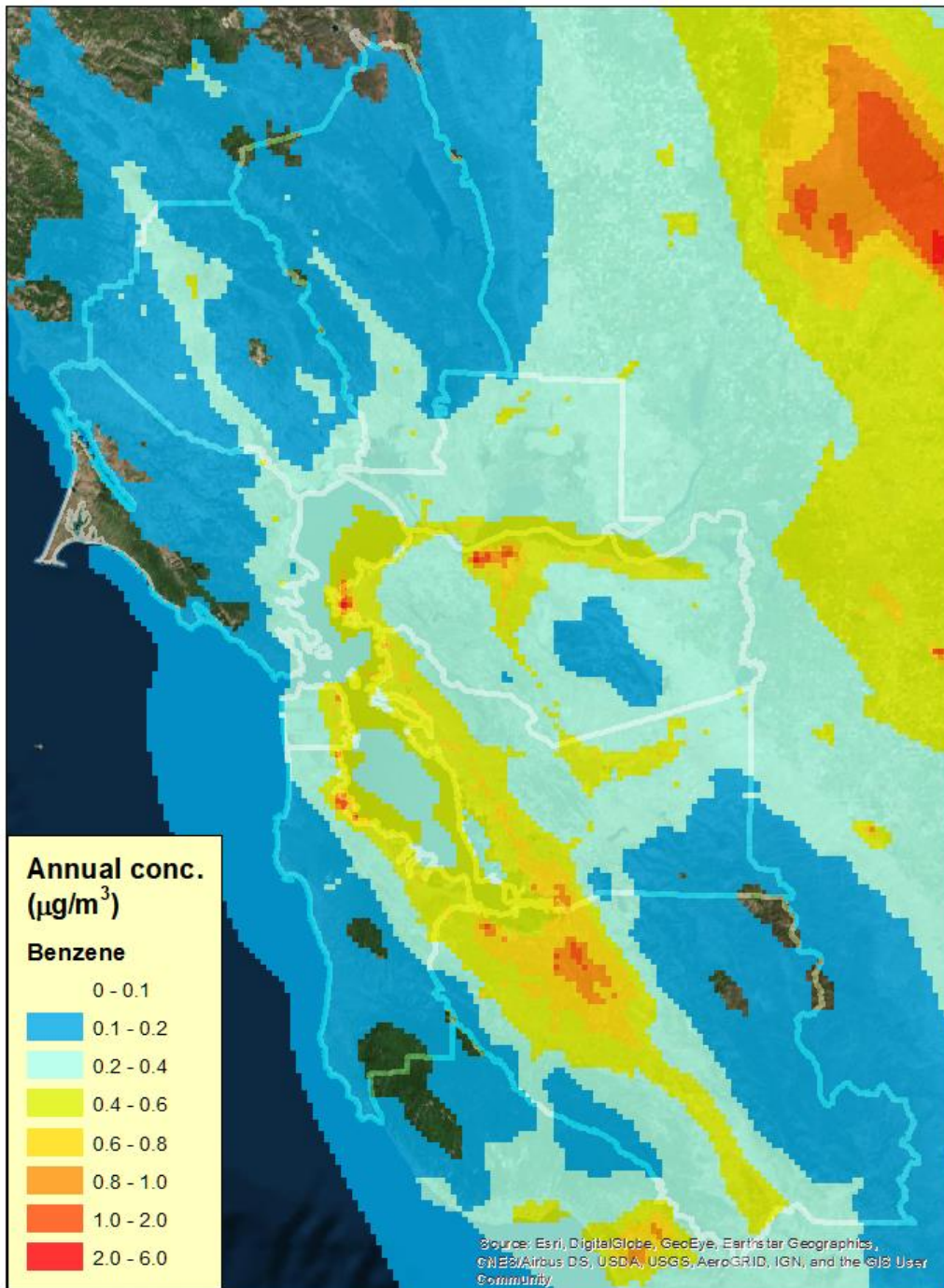
Maximum: 1.1

Figure 3.7: Annual average simulated acrolein concentrations for 2016.



Maximum: 0.9

Figure 3.8: Annual average simulated 1,3 butadiene concentrations for 2016.

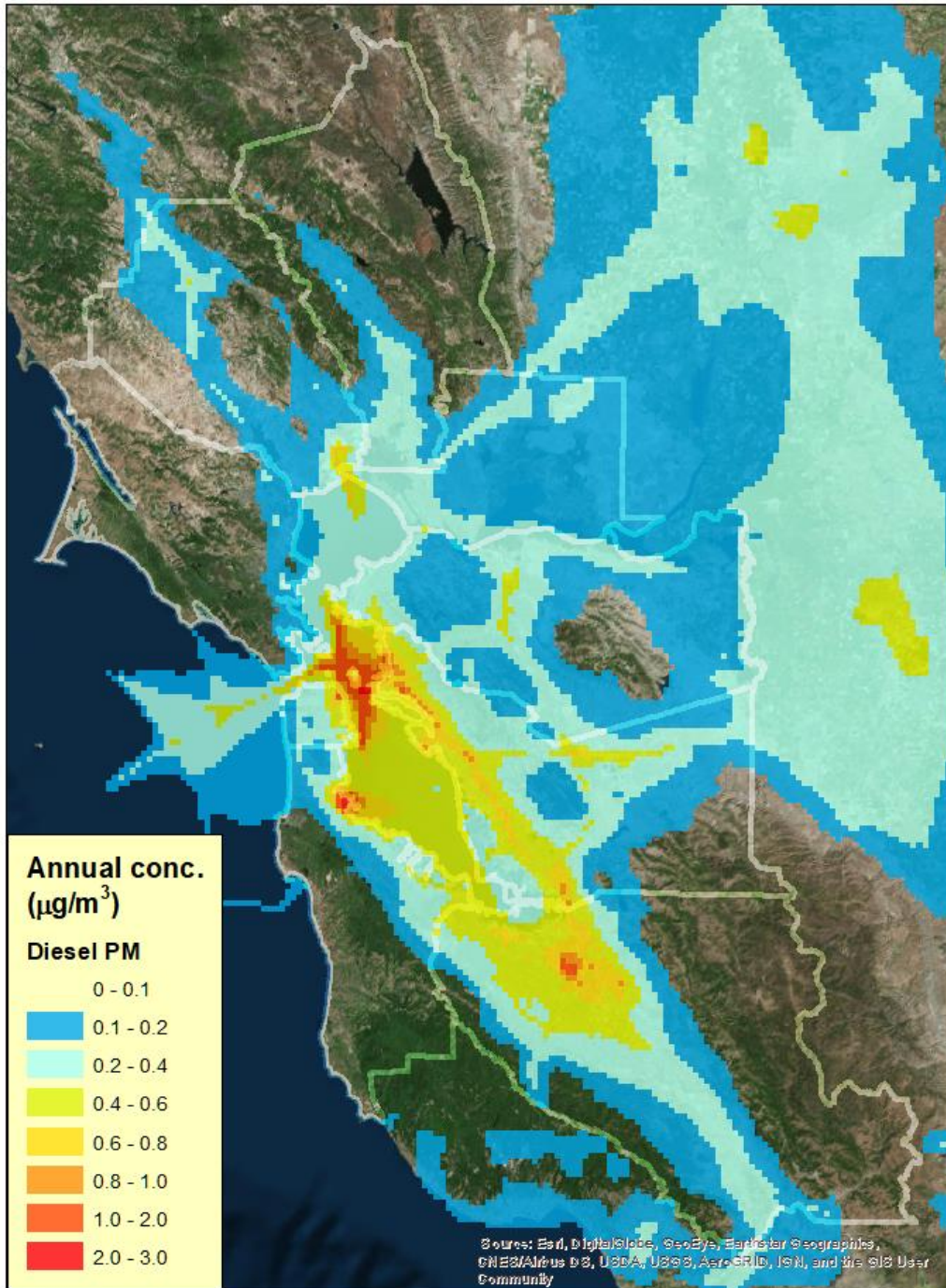


Maximum: 5.5

Figure 3.9: Annual average simulated benzene concentrations for 2016.

3.3.2 Diesel PM

Figure 3.10 shows the annual average concentrations of diesel PM. The highest concentration is $2.7 \mu\text{g}/\text{m}^3$ at San Francisco International Airport. Concentrations are also high (above $1 \mu\text{g}/\text{m}^3$) along the Bay Area ship routes, peaking at $2.6 \mu\text{g}/\text{m}^3$ near Yerba Buena Island, as well as in downtown Oakland and San Jose International Airport. Concentrations at Oakland International Airport reach $0.9 \mu\text{g}/\text{m}^3$. Concentrations along I-880 between Oakland and San Jose range mostly from 0.6 to $0.8 \mu\text{g}/\text{m}^3$ with some grid cells having concentrations above $0.8 \mu\text{g}/\text{m}^3$. The northern edge of San Pablo Bay, a portion of I-580 around Dublin, the Dumbarton Bridge, and a portion of US 101 north of Sunnyvale also show concentrations of 0.6 to $0.8 \mu\text{g}/\text{m}^3$.



Maximum: 2.7

Figure 3.10: Simulated annual average diesel PM concentrations for 2016.

3.3.3 Toxic Metals

Five toxic metals (hexavalent chromium, cadmium, lead, nickel, and mercury) were simulated, and their annual average concentrations were estimated. Emission estimates for these metals were taken from the EPA’s 2014 National Air Toxics Assessment (NATA) inventory and may not

be representative of Bay Area emission levels for 2016. Therefore, the estimated annual average concentrations are considered to be preliminary. A summary of simulated metal concentrations is presented in Appendix C.

4. Model Performance Evaluation

The simulated air toxics concentrations were compared against available observations for the purpose of evaluating the CMAQ model. The District collects ambient air toxics data at 20 air monitoring stations, as discussed in Section 2.1. Locations of these stations are shown Figure 4.1. Samples of elemental carbon (EC) were used as a surrogate for evaluating diesel PM since diesel PM cannot be directly distinguished in the measurements.

Figure 4.2 shows scatter plots of observed vs. modeled formaldehyde and acetaldehyde concentrations at the San Jose-Jackson Street air monitoring station. The model tends to underestimate concentrations of these species but shows reasonable agreement with observations, aside from a few outliers.

Figure 4.3 shows scatter plots of observed vs. modeled benzene and 1,3-butadiene at the 20 toxics monitoring sites. Again, the model performance is reasonable but with slight underestimation. The underestimation biases at Oakland West are somewhat higher than the overall biases across all 20 sites, but agreement between the model and observations is still reasonable.

Figure 4.4 presents scatter plots of observed EC vs. modeled diesel PM. At Oakland West and San Jose-Jackson Street, modeled diesel PM concentrations are generally higher than observed EC. Assuming the predominant source of observed EC is diesel exhaust, this is expected because simulated diesel PM consists of PM components other than EC (e.g., organic carbon).

The modeled diesel PM tends to be lower than observed EC at Vallejo and Livermore, especially in winter and fall, suggesting EC sources other than diesel exhaust are influencing these sites (e.g., wood smoke). These discrepancies are also an indication of pollutant transport from outside the region defined in the modeling domain. While observations included the impact of such transport, the modeled concentrations did not because no diesel PM concentrations are specified along the model boundary. Overall, modeled diesel PM and observed EC are close enough to demonstrate their correlation.

Figure 4.5 compares observed and modeled concentrations of nickel, cadmium, lead and particulate-bound mercury. The model greatly underestimates the observed metal concentrations, indicating substantial uncertainty in emissions estimates for metals. This finding indicates that modeled cancer risks associated with toxic metals are also underestimated.

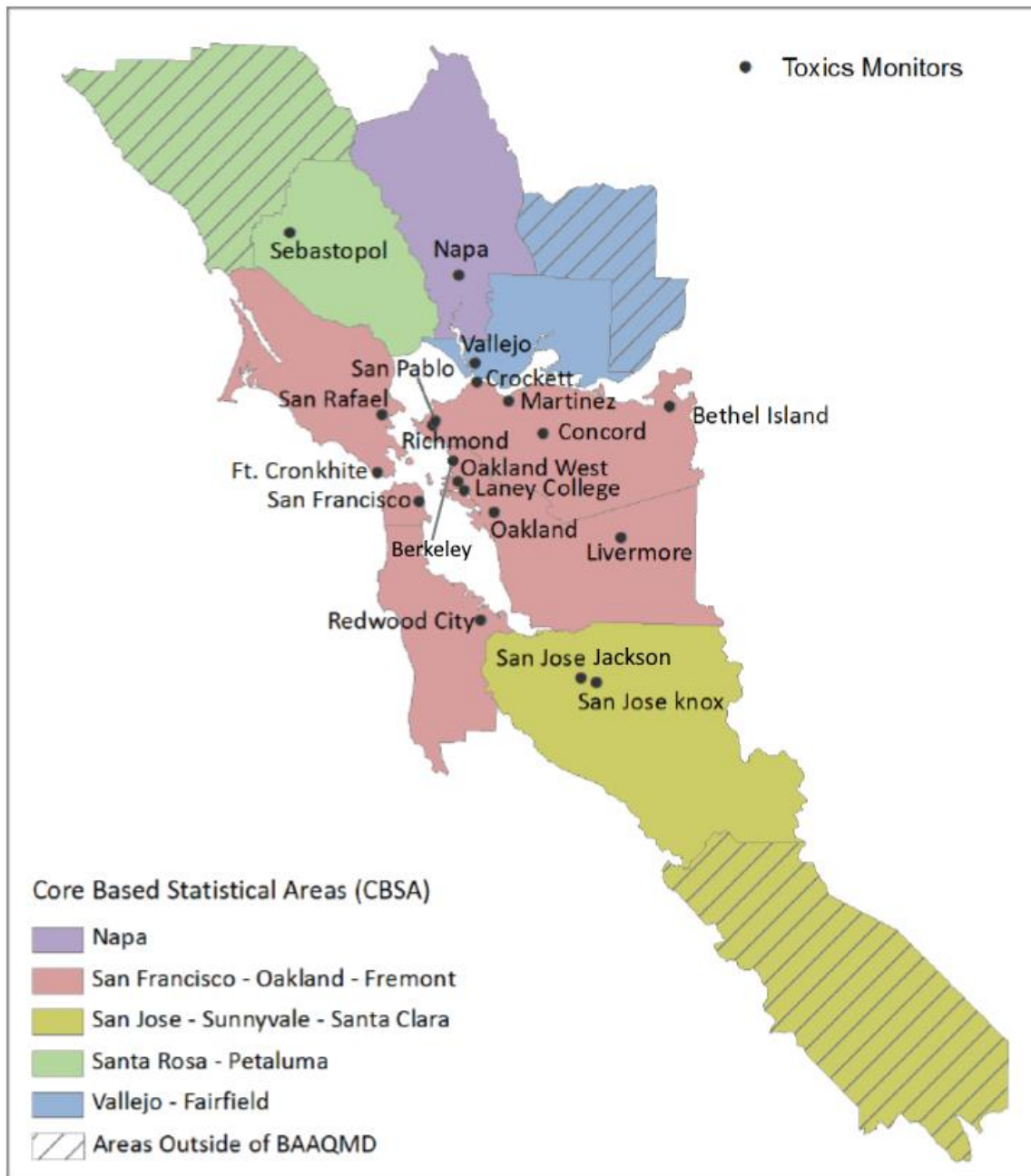
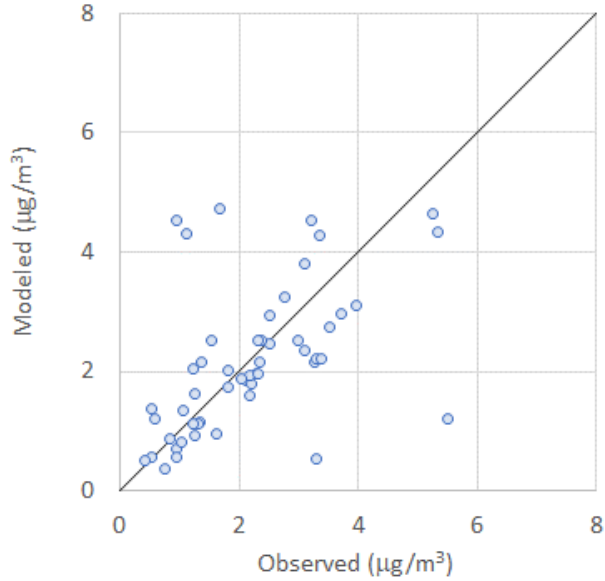


Figure 4.1: Map of BAAQMD toxics monitoring sites in 2016; reprinted from Knoderer et al. (2017). The location of the Berkeley site, which began operation on July 1, 2016, was added.

(a) Formaldehyde

NMB	-1.8%
NME	35%



(b) Acetaldehyde

NMB	-31%
NME	46%

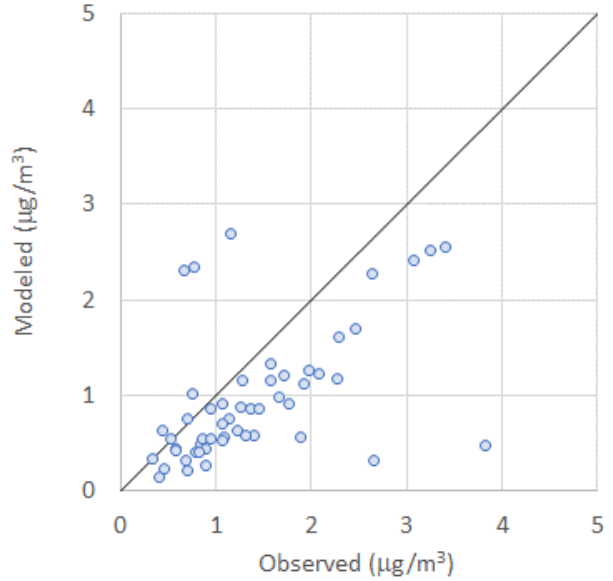


Figure 4.2: Observed vs. modeled 24-hr average concentrations of formaldehyde and acetaldehyde at the San Jose-Jackson St. site. Performance statistics shown are normalized mean bias (NMB) and normalized mean error (NME).

(a) Benzene

	All Sites	Oakland West
NMB	-16%	-29%
NME	40%	34%

(b) 1,3-butadiene

	All Sites	Oakland West
NMB	-5.7%	-28%
NME	44%	36%

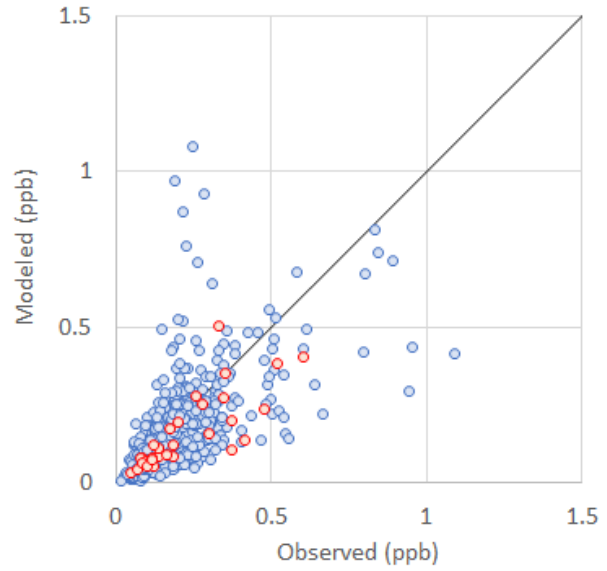
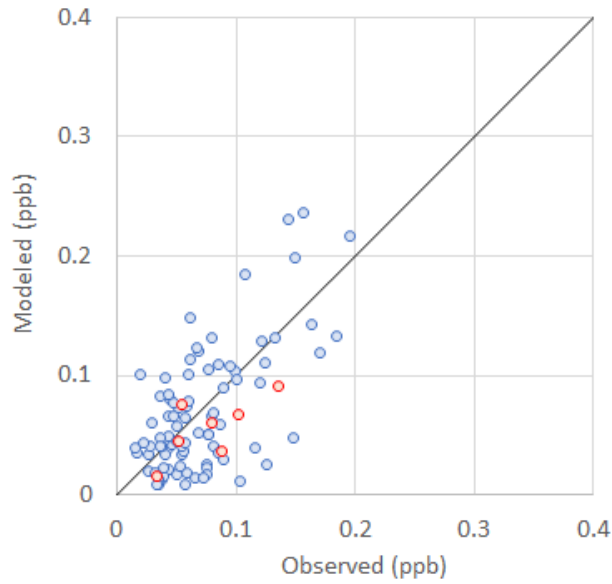


Figure 4.3: Observed vs. modeled 24-hr average concentrations of benzene and 1,3-butadiene at 20 toxics monitoring sites (values at the Oakland West site are shown in red). Normalized mean bias (NMB) and normalized mean error (NME) were calculated over all 20 sites, as well as at the Oakland West site alone.

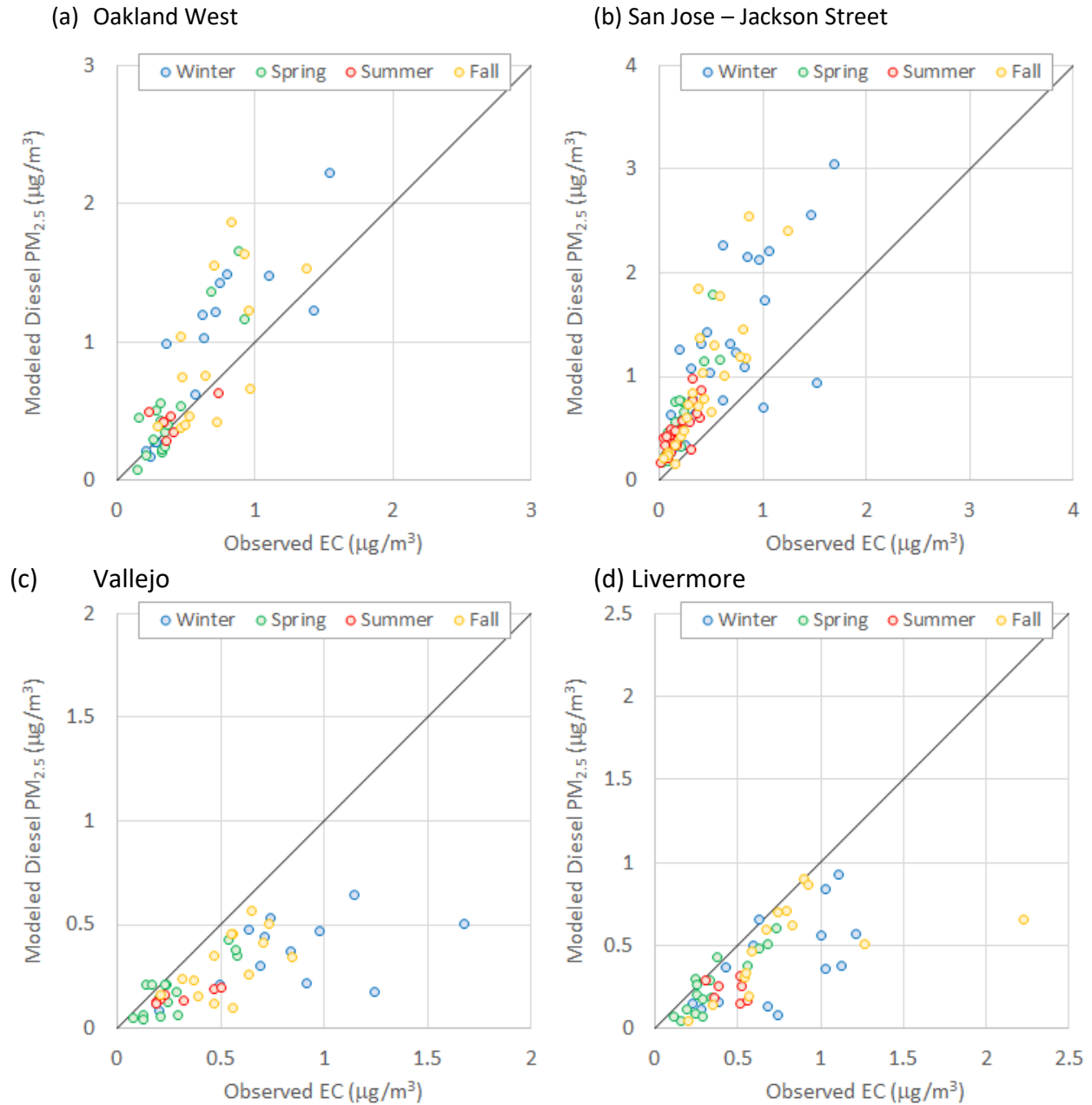
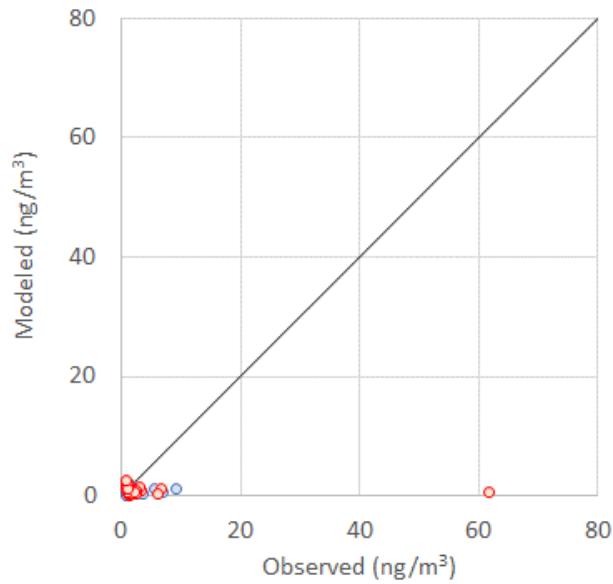
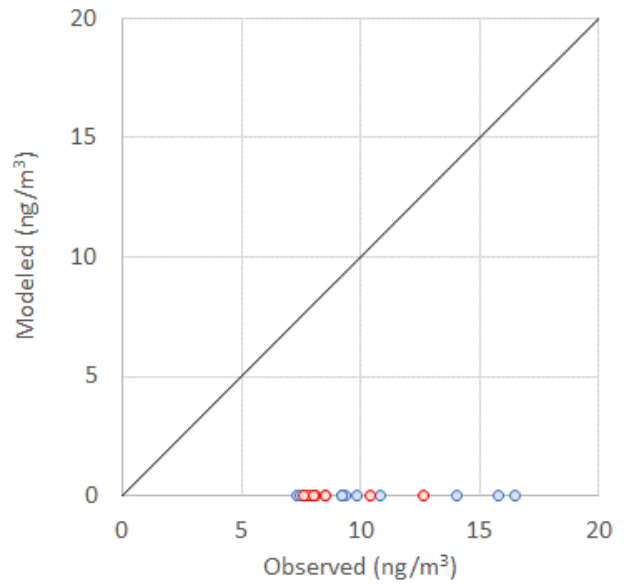


Figure 4.4: 24-hr average concentrations of observed PM_{2.5} EC vs. modeled diesel PM_{2.5} at Oakland West, San Jose-Jackson St., Vallejo and Livermore. Winter, spring, summer, and fall are defined as January-February-December, March-April-May, June-July-August, and September-October-November, respectively.

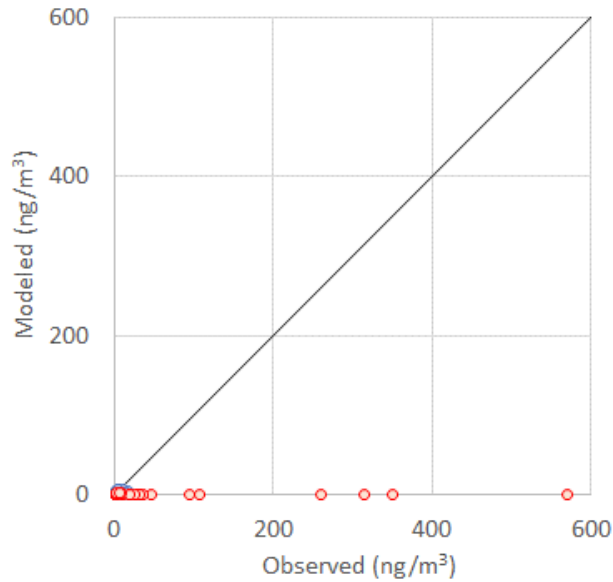
(a) Nickel



(b) Cadmium



(c) Lead



(d) Particulate bound mercury

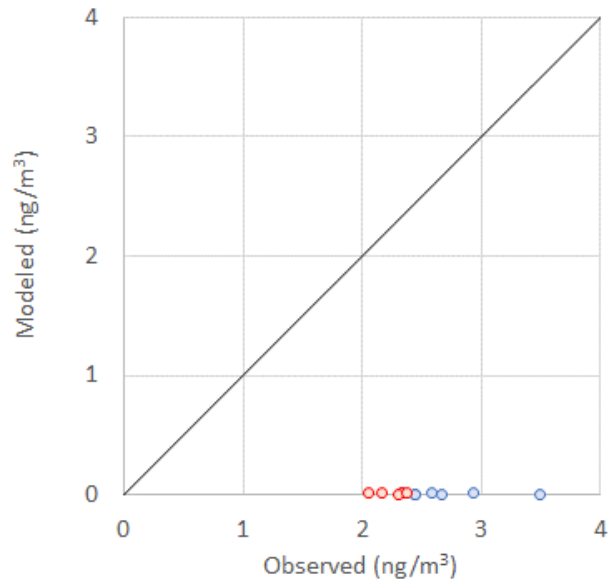


Figure 4.5: Observed vs. modeled 24-hr average concentrations of PM_{2.5} nickel, cadmium, lead and mercury at Oakland West, Vallejo, Livermore, and San Jose-Jackson St. (values at the Oakland West site are shown in red).

5. Risk Evaluation

As described in Section 1.1, cancer risk estimates for the modeled air toxics were calculated using inhalation unit risk factors. Cancer risk associated with modeled air toxics was calculated by multiplying annual average concentrations of each air toxic compound with its respective unit risk factor (Table 1.1) and then the resulting values were summed. The results were expressed as the number of expected excess cancer incidences per million people and are shown in Figure 5.1.

The highest number of estimated excess cancer incidences are modeled to occur east of Half Moon Bay (around 3,200 per million) which coincides with the location having the highest concentration of hexavalent chromium.³ Other than that, the spatial distribution of cancer risk in the Bay Area is similar to that of diesel PM concentrations (Figure 3.10), with the next highest cancer risks occurring at the San Francisco International Airport (about 2,600 per million). The number of estimated excess cancer incidences ranges from 1,000 to 2,000 per million at San Jose International Airport as well as in the area surrounding San Francisco International Airport. The excess cancer incidence estimates along the I-880 corridor connecting Oakland and San Jose, and along the US-101 corridor between San Jose and Palo Alto range from 500 to 1,000 per million.

³ The largest source of hexavalent chromium emissions in the emissions inventory is mineral processes, an area source that is spatially distributed based on the location of sand and gravel facilities.

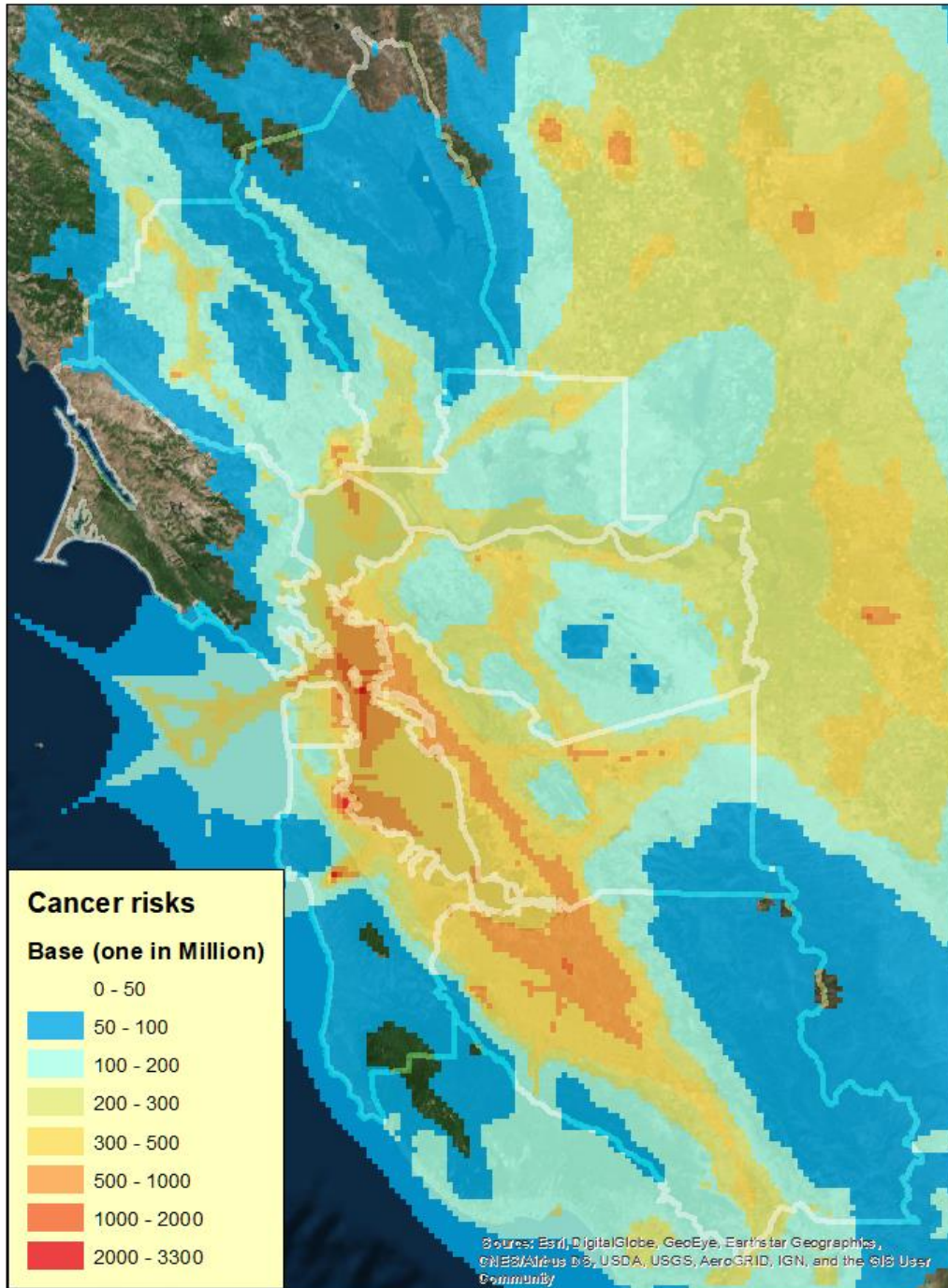


Figure 5.1: Expected excess cancer incidences per million.

6. Summary and Discussion

A total of 11 air toxics were simulated for 2016 over the entire Bay Area using the US EPA's CMAQ model at 1-km grid. Toxic included diesel particulate matter (DPM), 5 toxic gases (acetaldehyde, acrolein, benzene, 1,3-butadiene, and formaldehyde), and 5 trace metals (cadmium, chromium VI, lead, mercury, and nickel). Excess cancer risks were estimated for individual air toxics species as well as for all species combined. Previous analyses have indicated that DPM and the 5 toxic gases cumulatively account for more than 90% of toxic air contaminant emissions in the Bay Area (Tanrikulu et al., 2011).

Toxics measurement stations are sparsely distributed in the Bay Area, and samples are collected on a schedule of either 1 in 6 days or 1 in 12 days. A significant number of toxics measurements are below the instrument minimum detection limit, which makes it difficult to develop a conceptual model of air toxics formation and transport in the Bay Area. Nevertheless, comparisons between simulated and the available observed concentrations show reasonable agreement.

The District simulated DPM and the same five toxics gases for 2005 (Tanrikulu et al., 2009) and with projected emissions for 2015 (Tanrikulu et al., 2011) and estimated associated excess cancer risk. Both simulations were performed with the Comprehensive Air Quality Model with Extensions (CAMx). Because of limited computational resources, the prior simulations were conducted for only 2 weeks in January and 2 weeks in August.

Findings of this recent simulation were compared against the previous simulations and the recent simulations are determined to be improved estimates. Comparison between the new and old simulations, however, was not discussed in this report because the old simulations did not cover the entire year and their emission estimates relied on an older version of air toxics speciation.

Future related work includes updates to the spatial distribution of emissions data and to estimates of residential woodburning emissions. Recent PM modeling (Tanrikulu et al., 2019) showed that woodburning emissions may be significantly underestimated in the North Bay. As a result, concentrations of EC, formaldehyde and acetaldehyde, as well as associated cancer risk, may be underestimated.⁴

⁴ Note that the CMAQ modeling does not account for emissions from wildfires, which also have health impacts. However, the episodic and variable nature of these emissions present challenges for evaluating long-term exposures.

7. References

AMAP/UNEP, 2013. Technical Background Report for the Global Mercury Assessment 2013. Arctic Monitoring and Assessment Programme, Oslo, Norway/UNEP Chemicals Branch, Geneva, Switzerland.

BAAQMD, 2017. Final 2017 Clean Air Plan: Spare the Air, Cool the Climate. Bay Area Air Quality Management District, San Francisco, CA (April).

Emery, C., E. Tai, and G. Yarwood, 2001. Enhanced Meteorological Modeling and Performance Evaluation for Two Texas Ozone Episodes. Report to the Texas Natural Resources Conservation Commission, prepared by ENVIRON International Corp, Novato, CA.

<http://www.tceq.state.tx.us/assets/public/implementation/air/am/contracts/reports/mm/EnhancedMetModelingAndPerformanceEvaluation.pdf>.

Hutzell, W.T., Luecken, D.J., Appel, K.W., and Carter, W.P.L., 2012. Interpreting predictions from the SAPRC07 mechanism based on regional and continental simulations. *Atmos. Environ.*, 46, 417-429, doi:10.1016/j.atmosenv.2011.09.030.

Knoderer, C., Nguyen, D., Alrick, D., Hoag, K., 2017. 2016 Air Monitoring Network Plan. Meteorology, Measurement and Rules Division, Bay Area Air Quality Management District. http://www.baaqmd.gov/~media/files/technical-services/2016_network_plan-pdf.pdf

Tanrikulu, S., Martien, P., Tran, C., 2009. Toxics modeling to support the community air risk evaluation (CARE) program. Bay Area Air Quality Management District (June).

Tanrikulu, S., Martien, P., Tran, C., 2011. 2015 toxics modeling to support the community air risk evaluation (CARE) program. Bay Area Air Quality Management District (January).

Tanrikulu, S., Reid, S., Koo, B., Jia, Y., Cordova, J., Matsuoka, J., Fang, Y., 2019. Fine particulate matter data analysis and regional modeling in the San Francisco Bay Area to support AB617. Bay Area Air Quality Management District (January).

Zemba, S., Damiano, L., Little, H., Doris, J., Estabrooks, M., 2019. Formaldehyde: a leading air toxic. *EM Magazine*, January.

Appendix A – Toxics Emissions Inventory

This appendix provides additional information on the emissions inventory used for the 2016 air toxics modeling, including summary tables and emissions density plots (note that tables and plots for DPM are provided in the main body of the report).

A1. Gaseous Species

Five gaseous air toxics were modeled explicitly in CMAQ: acetaldehyde, acrolein, benzene, 1,3-butadiene, and formaldehyde. Tables A1 through A5 show emissions of these species by geographic area and source sector. Figures A1 through A5 show the spatial distribution of these species across the 1-km modeling domain.

Table A1: Summary of 2016 acetaldehyde emissions (tons/day) by geographic area and source sector.

Geographic Area	Area	Nonroad	Onroad	Point	Total
Alameda	0.04	0.08	0.30	0.03	0.45
Contra Costa	0.03	0.04	0.14	0.02	0.23
Marin	0.01	0.02	0.03	0.00	0.06
Napa	0.00	0.01	0.03	0.00	0.05
San Francisco	0.02	0.09	0.07	0.00	0.18
San Mateo	0.02	0.19	0.07	0.02	0.29
Santa Clara	0.04	0.06	0.23	0.02	0.35
Solano	0.01	0.04	0.06	0.01	0.11
Sonoma	0.01	0.03	0.08	0.00	0.12
<i>BAAQMD Subtotal</i>	<i>0.18</i>	<i>0.55</i>	<i>1.01</i>	<i>0.09</i>	<i>1.84</i>
Non-BAAQMD Counties	0.13	0.16	0.69	0.45	1.44
Domain Total	0.31	0.72	1.71	0.54	3.28

Table A2: Summary of 2016 acrolein emissions (tons/day) by geographic area and source sector.

Geographic Area	Area	Nonroad	Onroad	Point	Total
Alameda	0.03	0.02	0.03	0.05	0.13
Contra Costa	0.02	0.00	0.01	0.01	0.05
Marin	0.00	0.00	0.00	0.00	0.01
Napa	0.00	0.00	0.00	0.00	0.01
San Francisco	0.01	0.00	0.01	0.00	0.02
San Mateo	0.01	0.08	0.01	0.01	0.11
Santa Clara	0.02	0.02	0.02	0.01	0.06
Solano	0.01	0.02	0.00	0.01	0.03
Sonoma	0.01	0.00	0.01	0.00	0.02
<i>BAAQMD Subtotal</i>	<i>0.11</i>	<i>0.14</i>	<i>0.09</i>	<i>0.09</i>	<i>0.43</i>
Non-BAAQMD Counties	0.04	0.02	0.06	0.11	0.23
Domain Total	0.15	0.16	0.15	0.20	0.66

Table A3: Summary of 2016 benzene emissions (tons/day) by geographic area and source sector.

Geographic Area	Area	Nonroad	Onroad	Point	Total
Alameda	0.19	0.10	0.39	0.20	0.89
Contra Costa	0.20	0.08	0.25	0.49	1.01
Marin	0.03	0.04	0.08	0.03	0.18
Napa	0.03	0.02	0.04	0.01	0.10
San Francisco	0.06	0.05	0.09	0.02	0.22
San Mateo	0.09	0.11	0.15	0.09	0.43
Santa Clara	0.21	0.11	0.40	0.26	0.98
Solano	0.05	0.03	0.08	0.07	0.23
Sonoma	0.05	0.03	0.11	0.01	0.21
<i>BAAQMD Subtotal</i>	<i>0.90</i>	<i>0.57</i>	<i>1.60</i>	<i>1.19</i>	<i>4.25</i>
Non-BAAQMD Counties	0.96	0.30	0.90	5.57	7.73
Domain Total	1.86	0.87	2.50	6.76	11.99

Table A4: Summary of 2016 1,3-butadiene emissions (tons/day) by geographic area and source sector.

Geographic Area	Area	Nonroad	Onroad	Point	Total
Alameda	0.07	0.10	0.04	0.05	0.25
Contra Costa	0.02	0.08	0.02	0.02	0.14
Marin	0.00	0.04	0.01	0.00	0.05
Napa	0.00	0.03	0.00	0.01	0.04
San Francisco	0.01	0.05	0.01	0.00	0.07
San Mateo	0.01	0.10	0.01	0.02	0.14
Santa Clara	0.14	0.10	0.04	0.03	0.30
Solano	0.01	0.03	0.01	0.01	0.05
Sonoma	0.01	0.03	0.01	0.02	0.07
<i>BAAQMD Subtotal</i>	<i>0.28</i>	<i>0.56</i>	<i>0.14</i>	<i>0.15</i>	<i>1.13</i>
Non-BAAQMD Counties	0.08	0.20	0.08	0.20	0.56
Domain Total	0.36	0.76	0.22	0.35	1.69

Table A5: Summary of 2016 formaldehyde emissions (tons/day) by geographic area and source sector.

Geographic Area	Area	Nonroad	Onroad	Point	Total
Alameda	0.09	0.24	0.22	0.68	1.23
Contra Costa	0.19	0.12	0.11	1.79	2.21
Marin	0.02	0.05	0.03	0.06	0.16
Napa	0.01	0.04	0.02	0.07	0.14
San Francisco	0.05	0.25	0.05	0.20	0.54
San Mateo	0.06	0.60	0.06	0.18	0.88
Santa Clara	0.10	0.19	0.18	1.02	1.49
Solano	0.07	0.12	0.04	0.10	0.33
Sonoma	0.03	0.08	0.06	0.32	0.48
<i>BAAQMD Subtotal</i>	<i>0.60</i>	<i>1.68</i>	<i>0.76</i>	<i>4.42</i>	<i>7.47</i>
Non-BAAQMD Counties	0.43	0.61	0.49	1.56	3.09
Domain Total	1.04	2.29	1.25	5.97	10.55

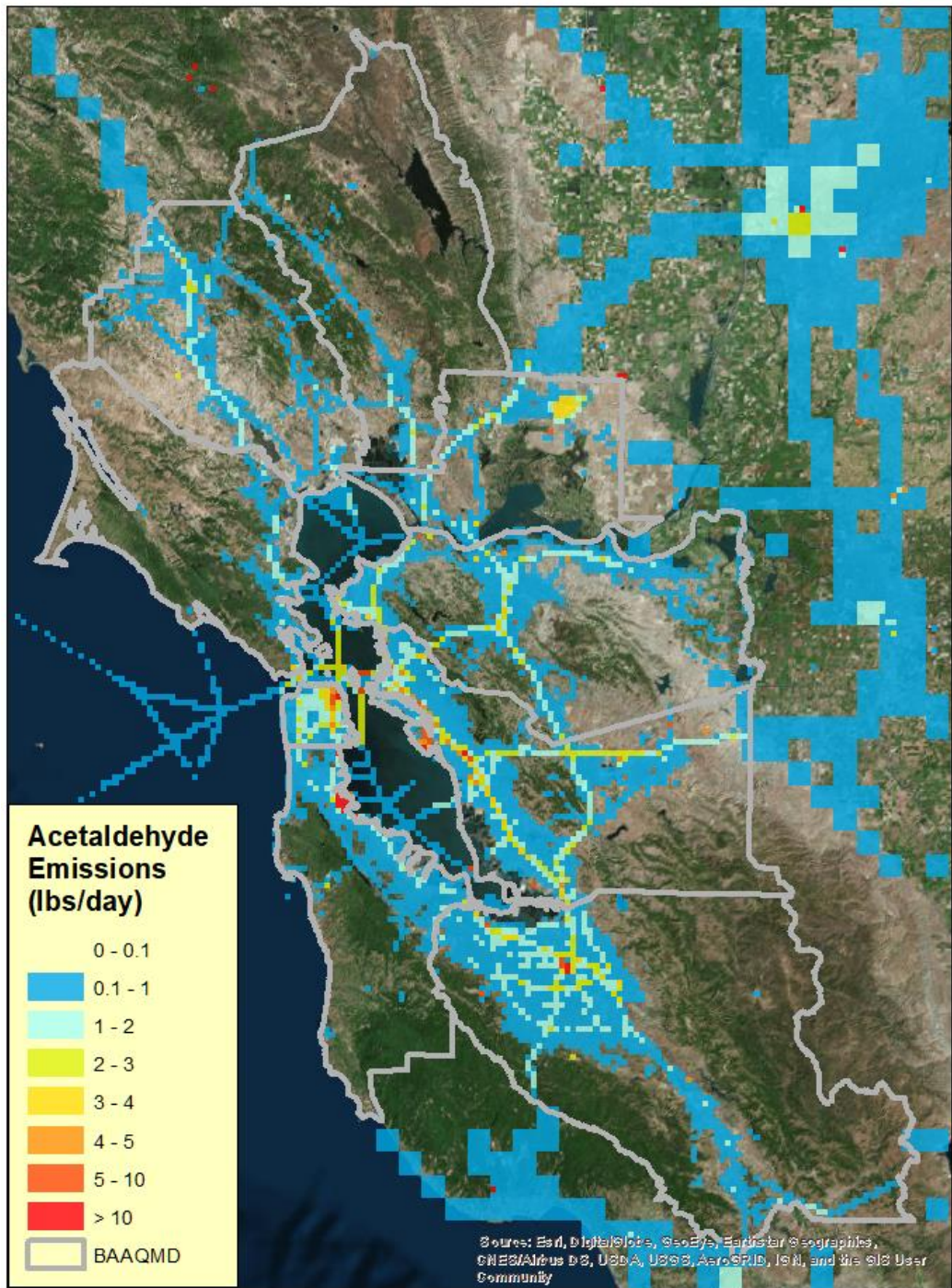


Figure A1: Spatial distribution of 2016 annual average acetaldehyde emissions for the 1-km modeling domain.

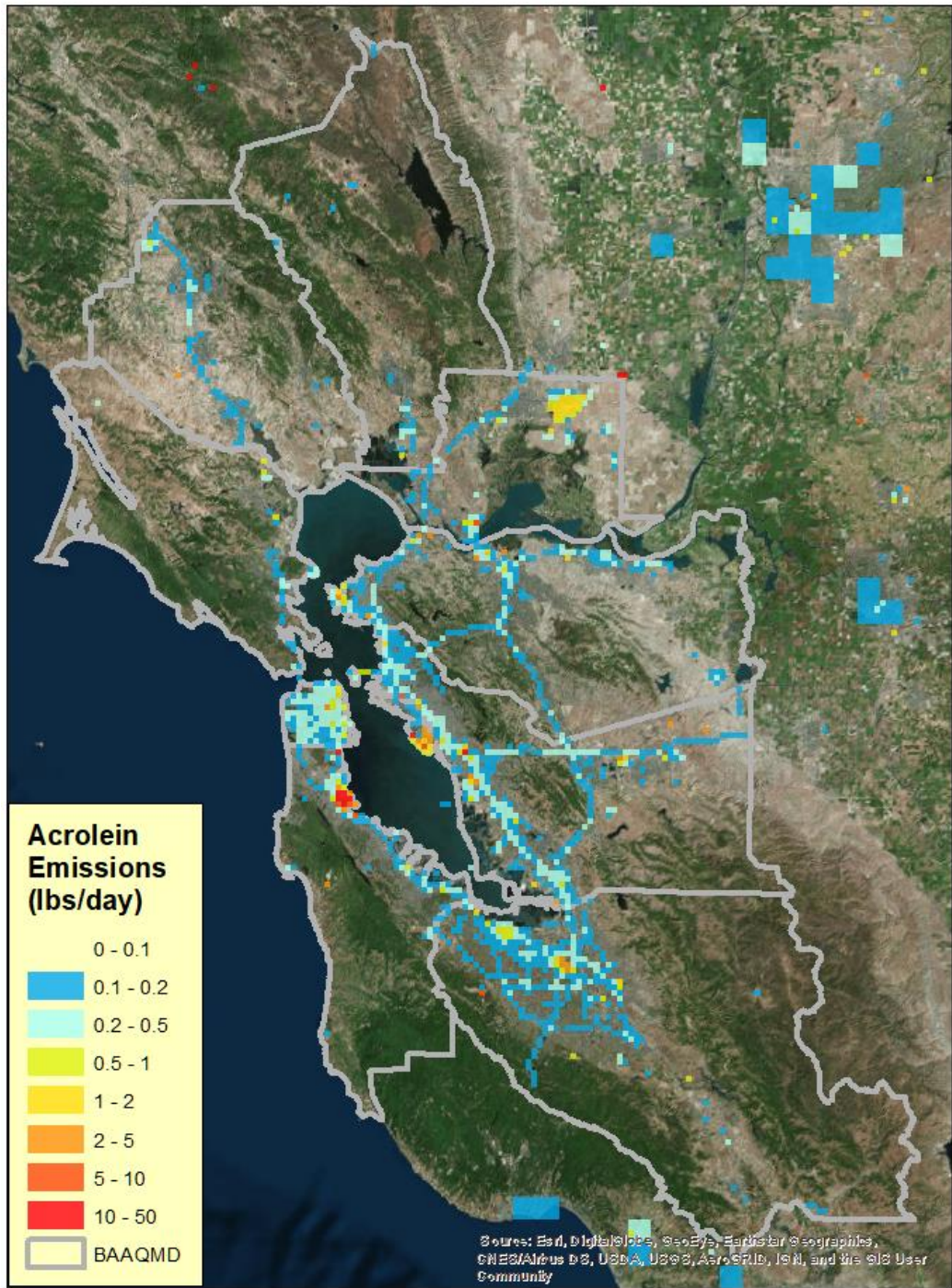


Figure A2: Spatial distribution of 2016 annual average acrolein emissions for the 1-km modeling domain.

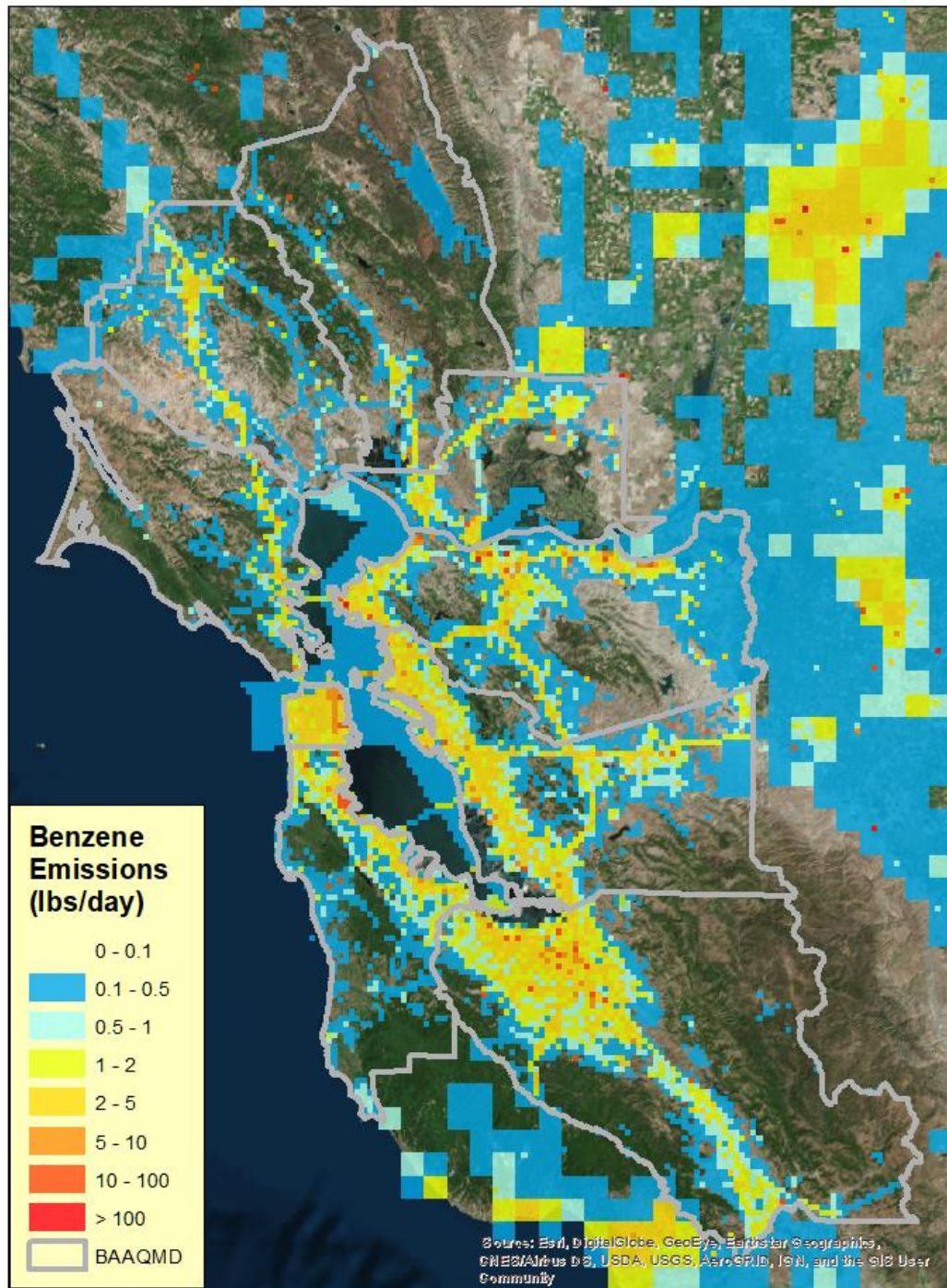


Figure A3: Spatial distribution of 2016 annual average benzene emissions for the 1-km modeling domain.

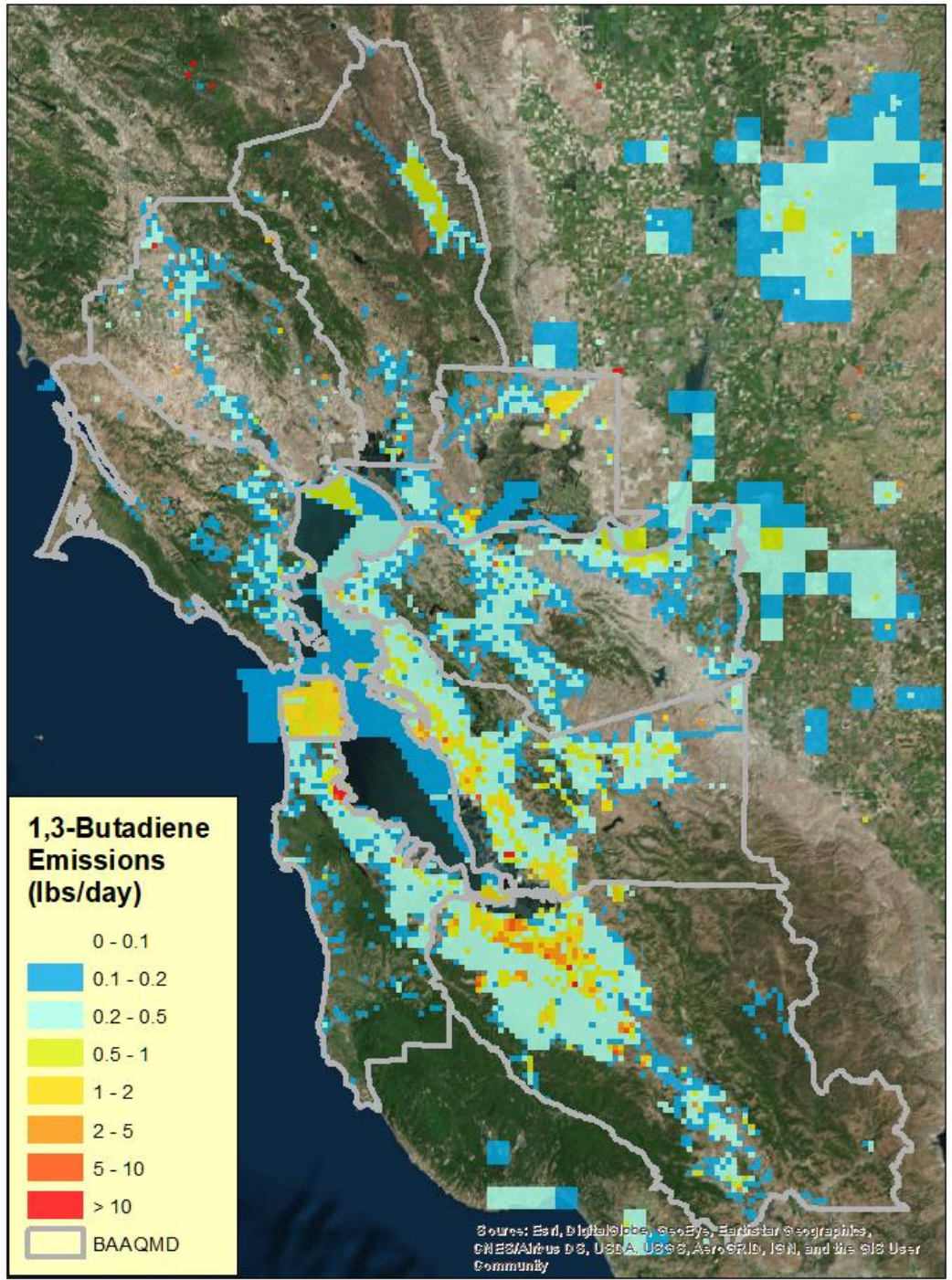


Figure A4: Spatial distribution of 2016 annual average 1,3-butadiene emissions for the 1-km modeling domain.

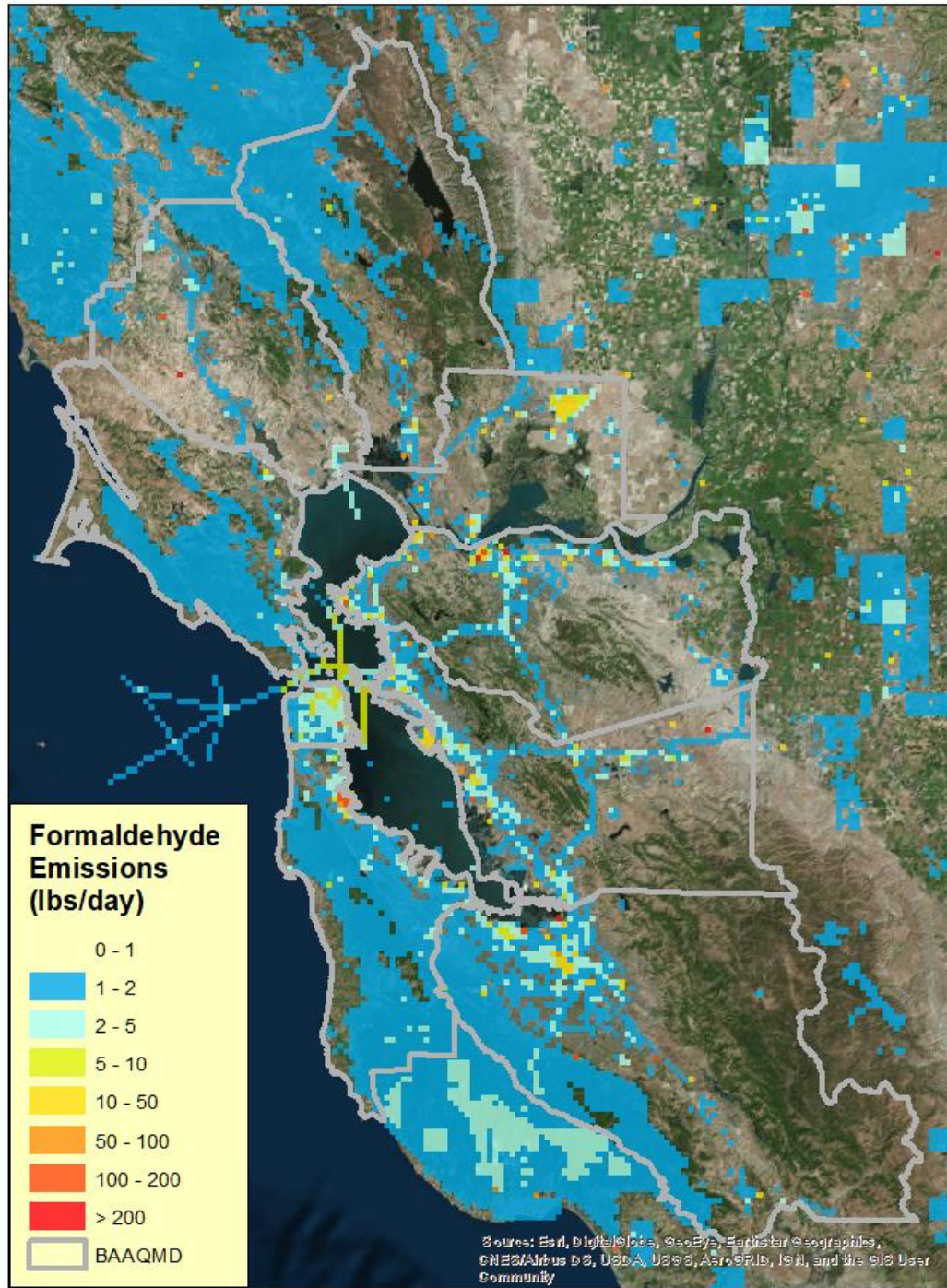


Figure A5: Spatial distribution of 2016 annual average formaldehyde emissions for the 1-km modeling domain.

A2. Trace Metals

Five trace metals were modeled explicitly in CMAQ: cadmium, chromium VI, lead, mercury, and nickel. Tables A6 through A10 show emissions of these species by geographic area and source

sector. Figures A6 through A10 show the spatial distribution of these species across the 1-km modeling domain.

Table A6: Summary of 2016 cadmium emissions (lbs/day) by geographic area and source sector.

Geographic Area	Area	Nonroad	Onroad	Point	Total
Alameda	0.03	0.00	0.00	0.00	0.04
Contra Costa	0.03	0.00	0.00	0.01	0.05
Marin	0.01	0.00	0.00	0.00	0.01
Napa	0.01	0.00	0.00	0.00	0.01
San Francisco	0.02	0.02	0.00	0.00	0.04
San Mateo	0.02	0.00	0.00	0.00	0.02
Santa Clara	0.09	0.00	0.00	0.00	0.09
Solano	0.01	0.00	0.00	0.00	0.02
Sonoma	0.02	0.00	0.00	0.00	0.02
<i>BAAQMD Subtotal</i>	<i>0.24</i>	<i>0.04</i>	<i>0.00</i>	<i>0.02</i>	<i>0.29</i>
Non-BAAQMD Counties	0.13	0.01	0.00	0.16	0.31
Domain Total	0.36	0.05	0.00	0.19	0.60

Table A7: Summary of 2016 chromium VI emissions (lbs/day) by geographic area and source sector.

Geographic Area	Area	Nonroad	Onroad	Point	Total
Alameda	0.05	0.00	0.01	0.00	0.07
Contra Costa	0.01	0.00	0.01	0.12	0.14
Marin	0.01	0.00	0.00	0.00	0.01
Napa	0.00	0.00	0.00	0.00	0.00
San Francisco	0.01	0.01	0.00	0.00	0.02
San Mateo	0.64	0.00	0.01	0.00	0.65
Santa Clara	0.35	0.00	0.01	0.01	0.37
Solano	0.00	0.00	0.00	0.02	0.03
Sonoma	0.15	0.00	0.00	0.00	0.15
<i>BAAQMD Subtotal</i>	<i>1.22</i>	<i>0.02</i>	<i>0.05</i>	<i>0.15</i>	<i>1.44</i>
Non-BAAQMD Counties	1.30	0.01	0.03	0.14	1.48
Domain Total	2.52	0.03	0.08	0.29	2.92

Table A8: Summary of 2016 lead emissions (lbs/day) by geographic area and source sector.

Geographic Area	Area	Nonroad	Onroad	Point	Total
Alameda	0.39	0.00	0.00	5.93	6.33
Contra Costa	1.30	0.01	0.00	3.12	4.43
Marin	0.08	0.00	0.00	1.72	1.81
Napa	0.07	0.00	0.00	0.79	0.86
San Francisco	0.25	0.01	0.00	0.00	0.26
San Mateo	0.39	0.00	0.00	3.02	3.40
Santa Clara	0.71	0.00	0.00	6.11	6.82
Solano	0.17	0.00	0.00	2.20	2.38
Sonoma	0.17	0.00	0.00	1.84	2.01

<i>BAAQMD Subtotal</i>	3.53	0.02	0.00	24.73	28.29
Non-BAAQMD Counties	1.70	0.03	0.00	13.59	15.32
Domain Total	5.22	0.05	0.00	38.32	43.60

Table A9: Summary of 2016 mercury emissions (lbs/day) by geographic area and source sector.

Geographic Area	Area	Nonroad	Onroad	Point	Total
Alameda	0.16	0.01	0.01	0.00	0.19
Contra Costa	0.08	0.01	0.00	0.15	0.24
Marin	0.02	0.00	0.00	0.00	0.02
Napa	0.01	0.00	0.00	0.00	0.02
San Francisco	0.06	0.01	0.00	0.00	0.07
San Mateo	0.06	0.00	0.00	0.00	0.06
Santa Clara	0.14	0.01	0.01	0.41	0.57
Solano	0.02	0.00	0.00	0.01	0.04
Sonoma	0.03	0.00	0.00	0.00	0.03
<i>BAAQMD Subtotal</i>	<i>0.58</i>	<i>0.05</i>	<i>0.04</i>	<i>0.57</i>	<i>1.25</i>
Non-BAAQMD Counties	0.18	0.04	0.02	0.07	0.31
Domain Total	0.76	0.09	0.06	0.65	1.56

Table A10: Summary of 2016 nickel emissions (lbs/day) by geographic area and source sector.

Geographic Area	Area	Nonroad	Onroad	Point	Total
Alameda	1.79	1.41	2.51	0.05	5.76
Contra Costa	0.85	1.55	1.38	1.75	5.54
Marin	0.07	1.74	0.41	0.00	2.22
Napa	0.03	0.81	0.20	0.00	1.03
San Francisco	0.17	1.37	0.59	0.01	2.15
San Mateo	0.16	1.03	1.00	0.02	2.21
Santa Clara	1.45	1.16	2.45	0.10	5.16
Solano	0.07	0.73	0.47	1.12	2.39
Sonoma	0.28	0.67	0.45	0.00	1.41
<i>BAAQMD Subtotal</i>	<i>4.87</i>	<i>10.46</i>	<i>9.47</i>	<i>3.06</i>	<i>27.86</i>
Non-BAAQMD Counties	5.17	3.82	4.82	3.89	17.71
Domain Total	10.04	14.29	14.29	6.95	45.57

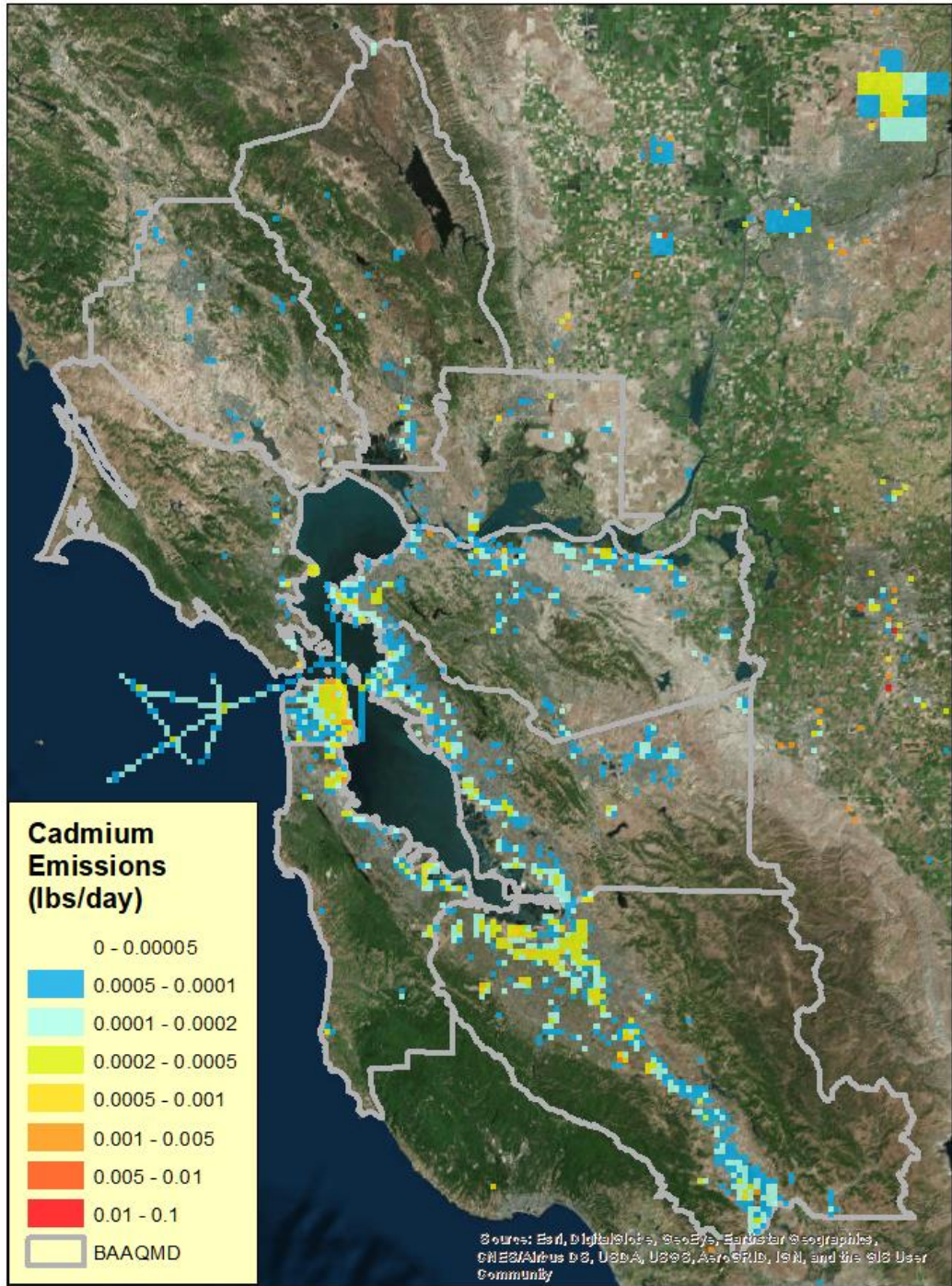


Figure A6: Spatial distribution of 2016 annual average cadmium emissions for the 1-km modeling domain.

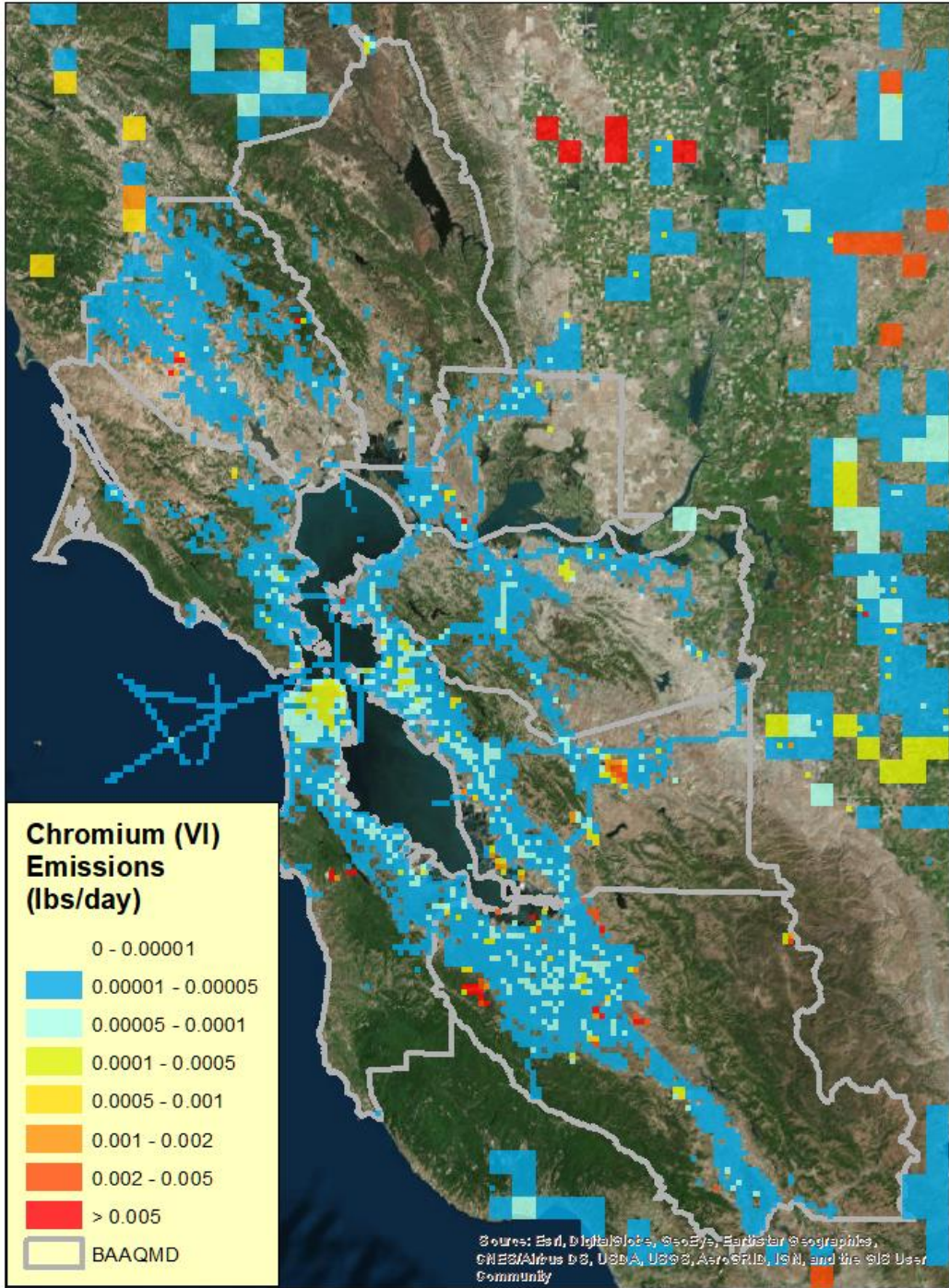


Figure A7: Spatial distribution of 2016 annual average chromium VI emissions for the 1-km modeling domain.

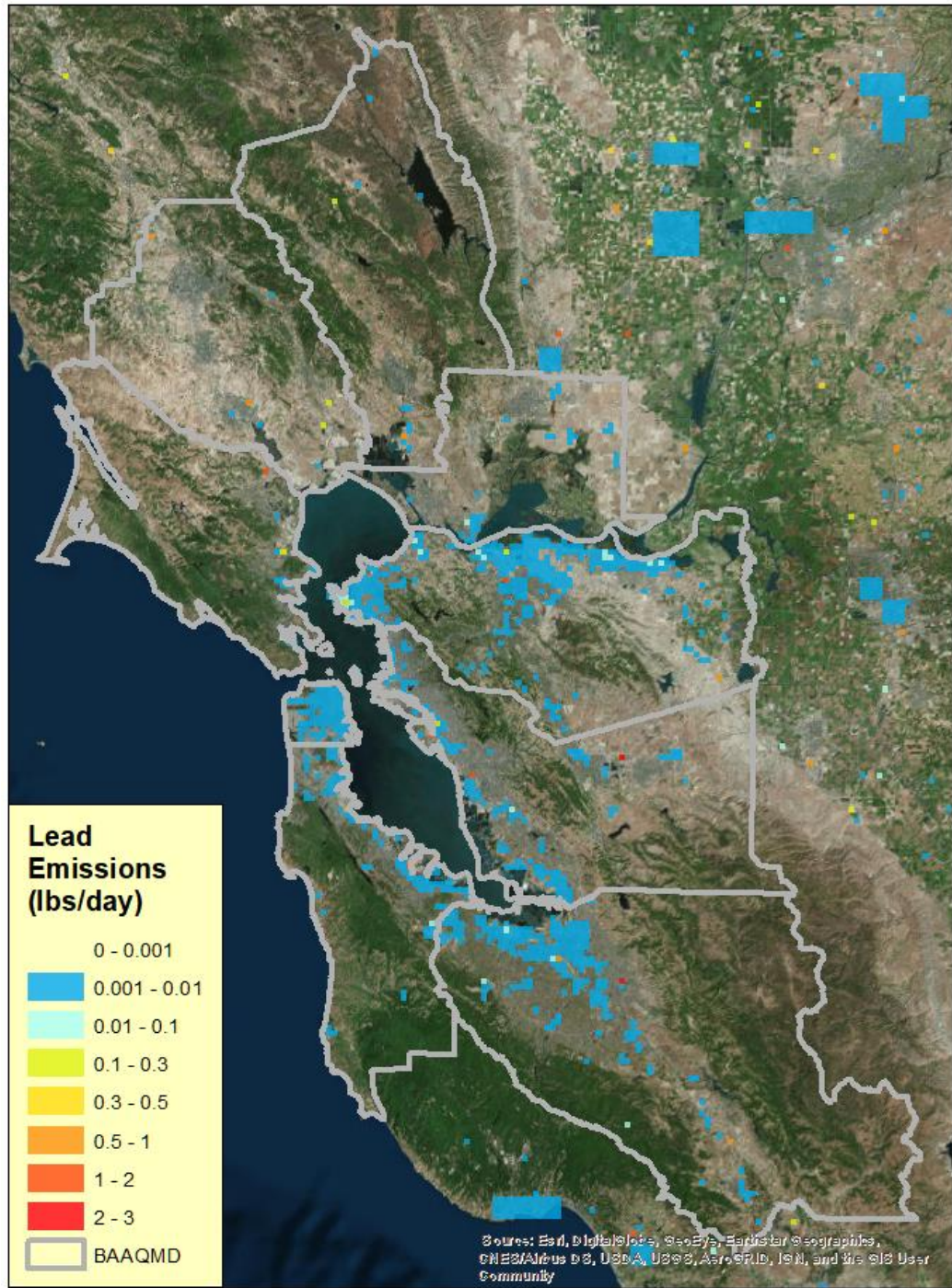


Figure A8: Spatial distribution of 2016 annual average lead emissions for the 1-km modeling domain.

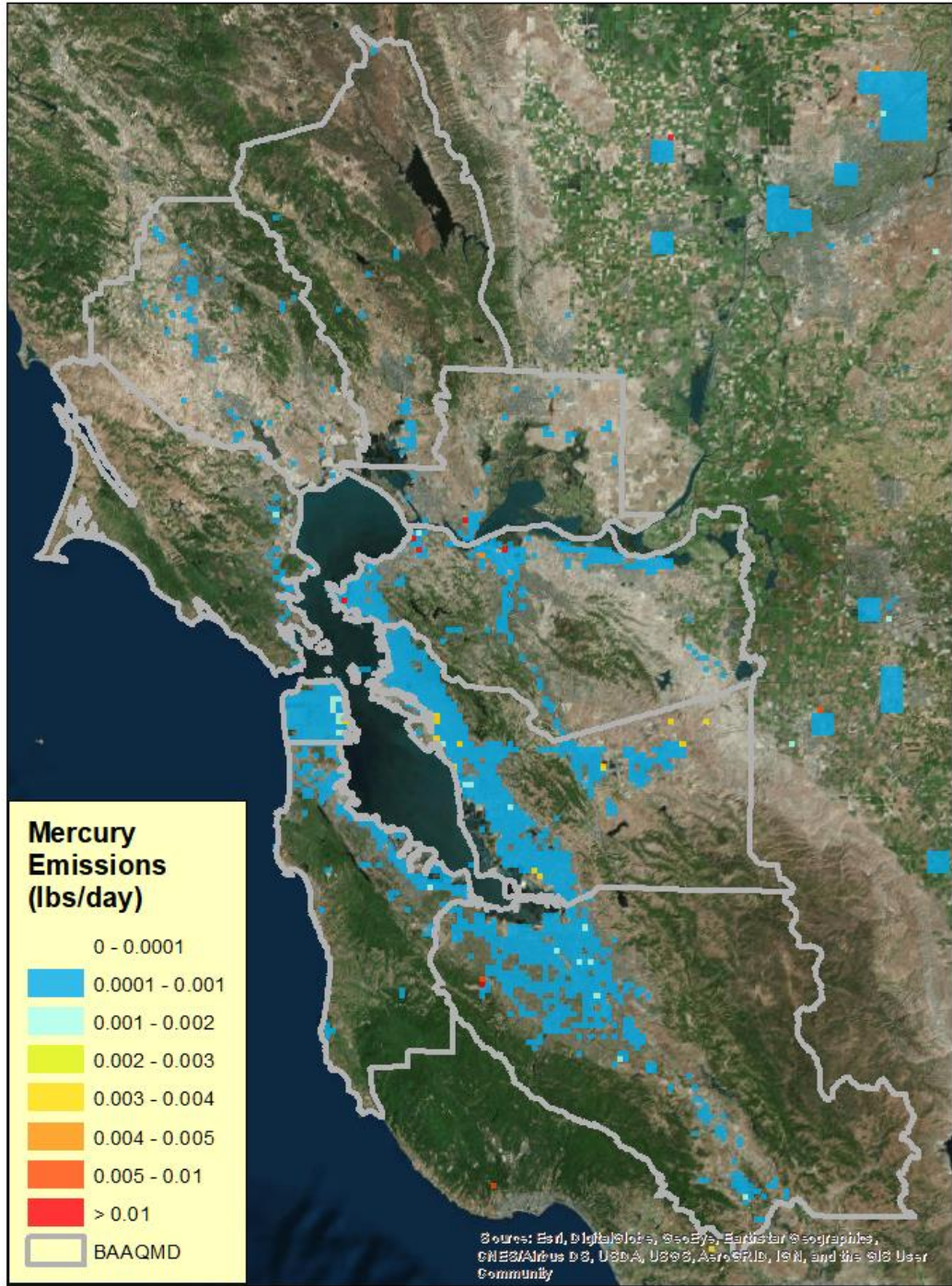


Figure A9: Spatial distribution of 2016 annual average mercury emissions for the 1-km modeling domain.

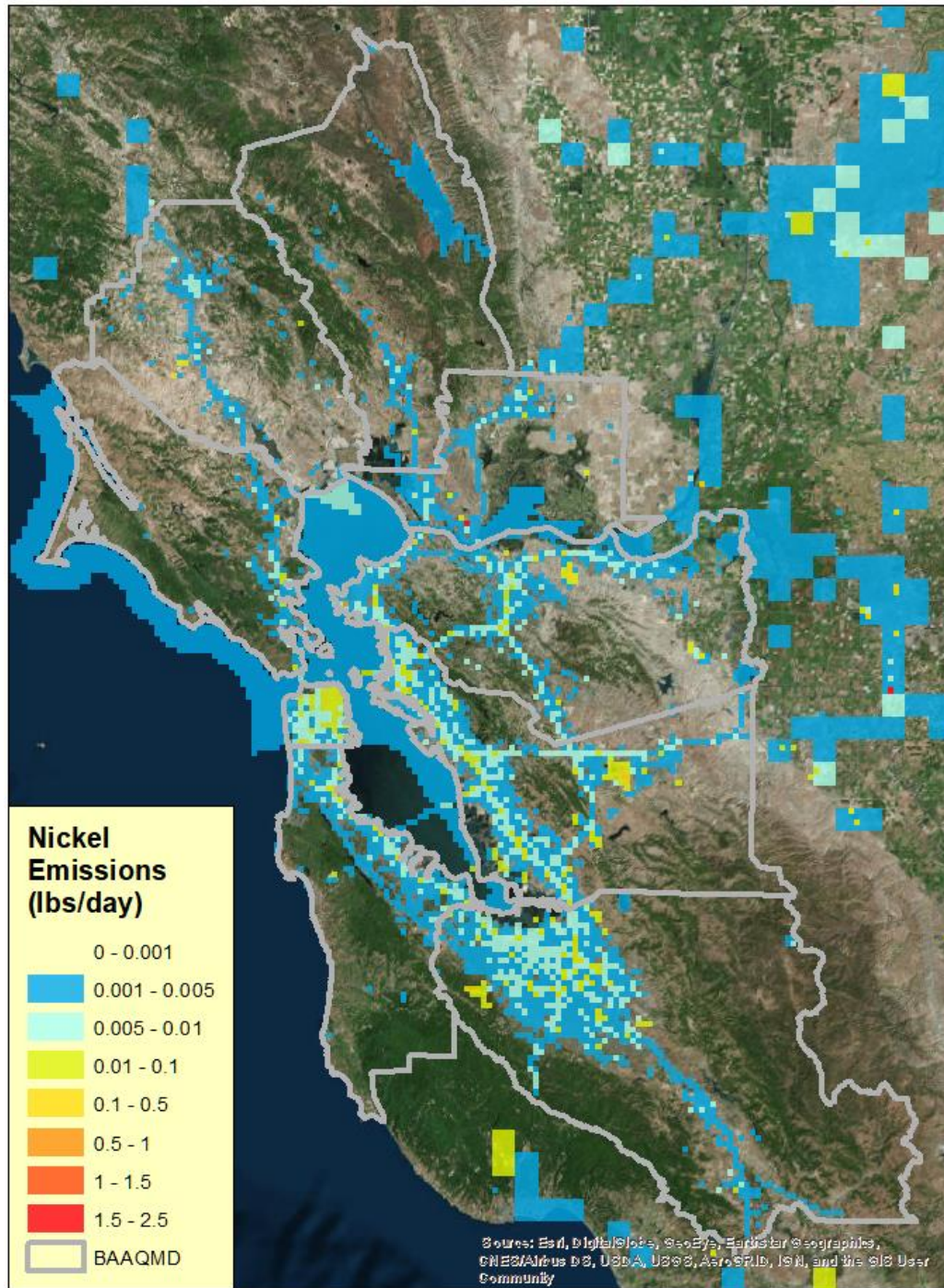


Figure A10: Spatial distribution of 2016 annual average nickel emissions for the 1-km modeling domain.

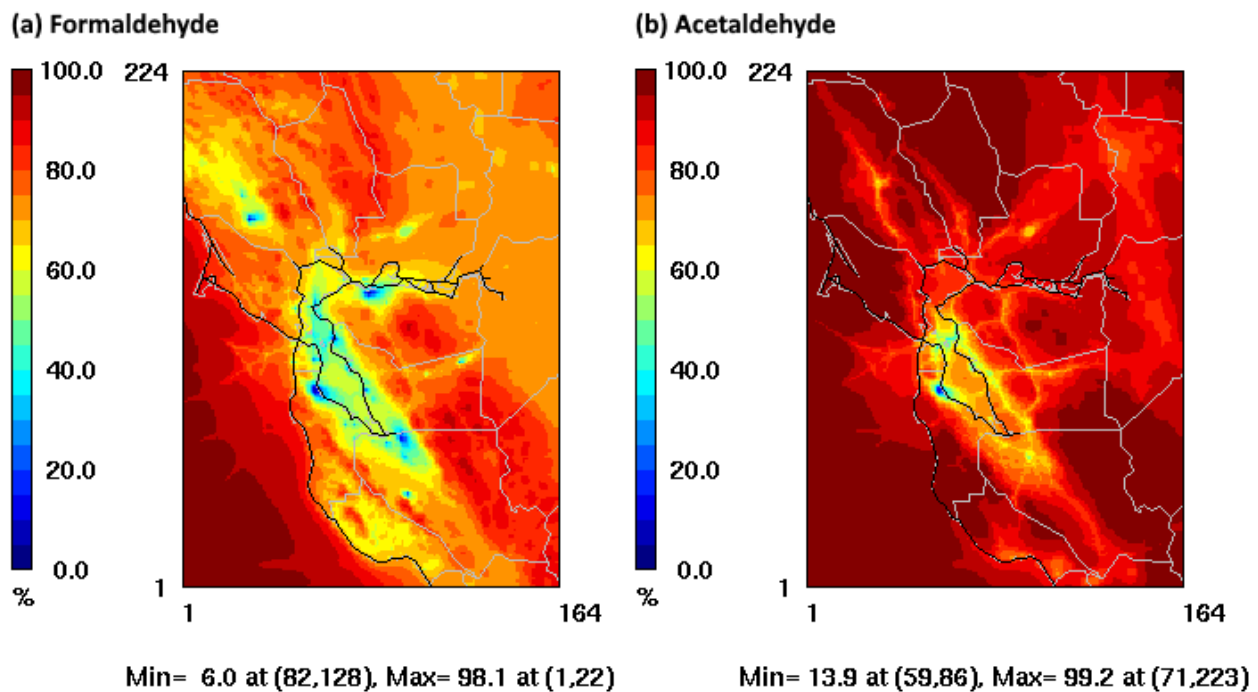
Appendix B: Simulated Primary vs Secondary Air Toxics

Some air toxic compounds have both primary components (i.e., direct emissions) and secondary components (i.e., production in the atmosphere via chemical reactions of other hydrocarbons). For example, formaldehyde and acetaldehyde are primarily formed from atmospheric oxidation of other biogenic (e.g., isoprene emitted from plants) and anthropogenic (e.g., ethene and propene from petrochemical facilities) VOCs. Acrolein is one of the major products of the photochemical oxidation of 1,3-butadiene.

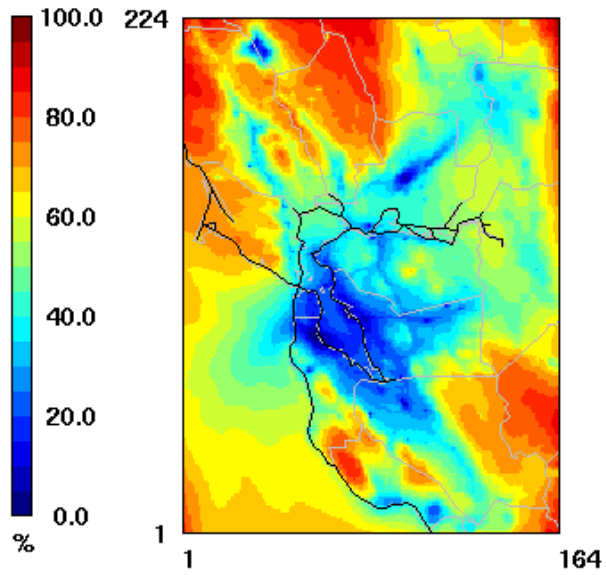
To assess the relative importance of the primary and secondary contributions, CMAQ's SAPRC07TC chemistry mechanism explicitly tracks primary emissions of formaldehyde, acetaldehyde and acrolein, as well as their photochemical production.

Figure B1 shows fractions of secondary contributions to annual average formaldehyde, acetaldehyde and acrolein concentrations in the 1-km modeling domain. Secondary production is the predominant source of formaldehyde and acetaldehyde in most areas of the modeling domain except in the immediate vicinity of emissions sources. Contributions of primary acrolein are generally higher than those of primary formaldehyde and acetaldehyde.

Figure B2 displays relative contributions of primary and secondary formaldehyde, acetaldehyde and acrolein over the West Oakland receptor domain. The primary contributions are relatively higher in this area, which indicates substantial local source influences.



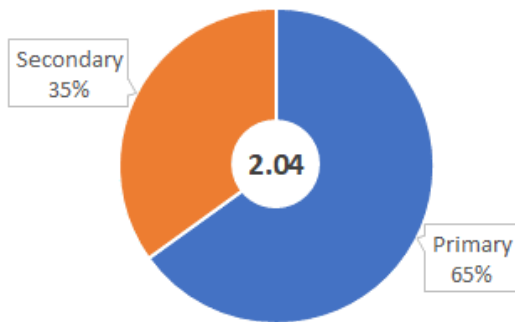
(c) Acrolein



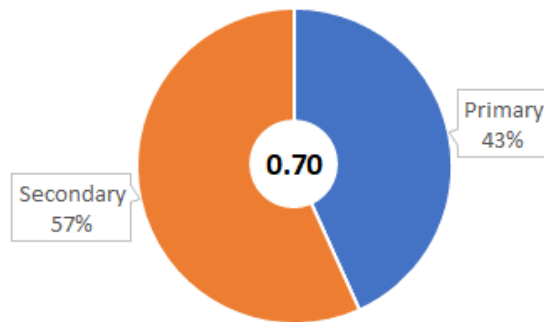
Min= 1.2 at (59,86), Max= 93.0 at (164,224)

Figure B1: Percent contributions of secondary production to annual average formaldehyde, acetaldehyde and acrolein concentrations in the 1-km modeling domain.

(a) Formaldehyde



(b) Acetaldehyde



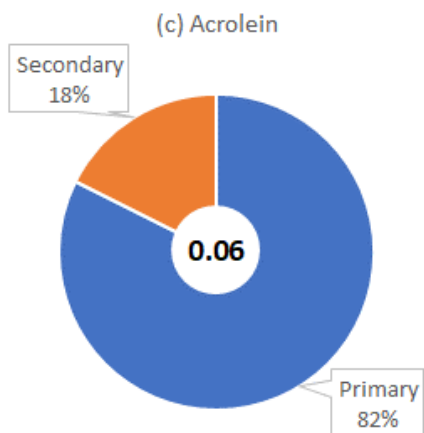


Figure B2: Percent contributions of secondary production to annual average formaldehyde, acetaldehyde and acrolein concentrations over the West Oakland Receptor domain. The numbers in the center represent total (primary plus secondary) concentrations.

Appendix C: Simulated Trace Metals

Figures C1 through C5 show the annual average concentrations of hexavalent chromium, cadmium, lead, nickel, and mercury, respectively. Mercury concentrations are shown as sum of all three forms of atmospheric mercury (gaseous elemental mercury, gaseous oxidized mercury, and particulate bound mercury). Note that the trace metal concentrations in these figures are given in nanograms per cubic meter (ng/m^3) to better represent their typical atmospheric concentration ranges.

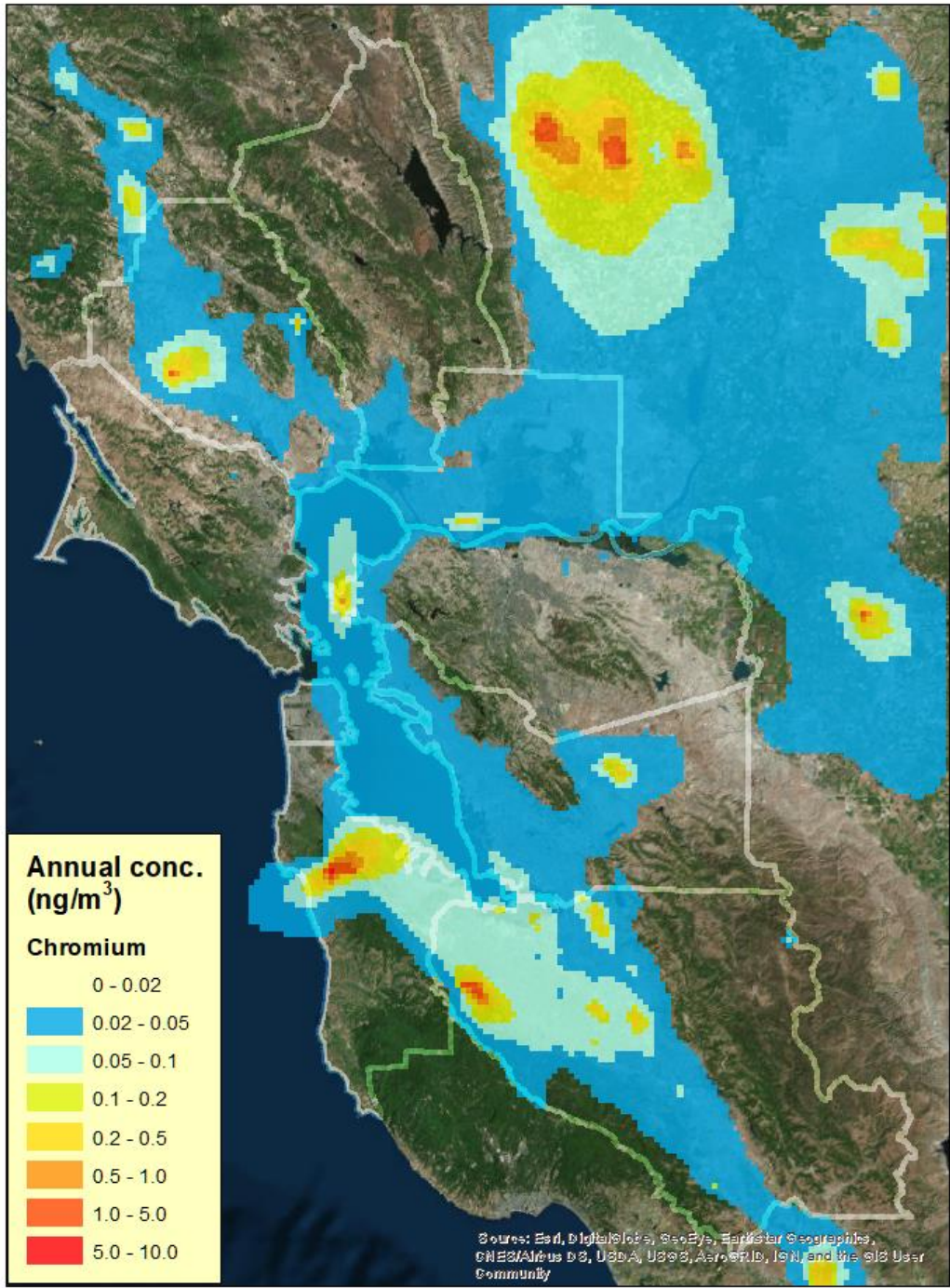
The highest annual average concentration of hexavalent chromium is simulated to occur east of Half Moon Bay ($8.3 \text{ ng}/\text{m}^3$). Concentrations above $1 \text{ ng}/\text{m}^3$ are seen northwest of Petaluma and west of Cupertino. Each of these areas are associated with mineral processing activities in the NATA area source inventory. Outside of the Bay Area, the Stockton and Sacramento areas also show above $1 \text{ ng}/\text{m}^3$ concentrations.

The simulated annual average cadmium concentration peaks at Lathrop ($0.9 \text{ ng}/\text{m}^3$). Simulated concentrations are below $0.05 \text{ ng}/\text{m}^3$ in the Bay Area except for Islais Creek Channel ($0.06 \text{ ng}/\text{m}^3$).

Simulated hot spots for lead are located at local airports such as Reid-Hillview Airport ($39.0 \text{ ng}/\text{m}^3$), Palo Alto Airport ($37.0 \text{ ng}/\text{m}^3$), Livermore Municipal Airport ($33.9 \text{ ng}/\text{m}^3$), Watsonville Municipal Airport ($28.2 \text{ ng}/\text{m}^3$), San Carlos Airport ($25.2 \text{ ng}/\text{m}^3$), Hayward Executive Airport ($23.6 \text{ ng}/\text{m}^3$), Nut Tree Airport ($23.1 \text{ ng}/\text{m}^3$) and Buchanan Field Airport ($22.9 \text{ ng}/\text{m}^3$). Lead concentrations quickly diminish as distance from the source increases.

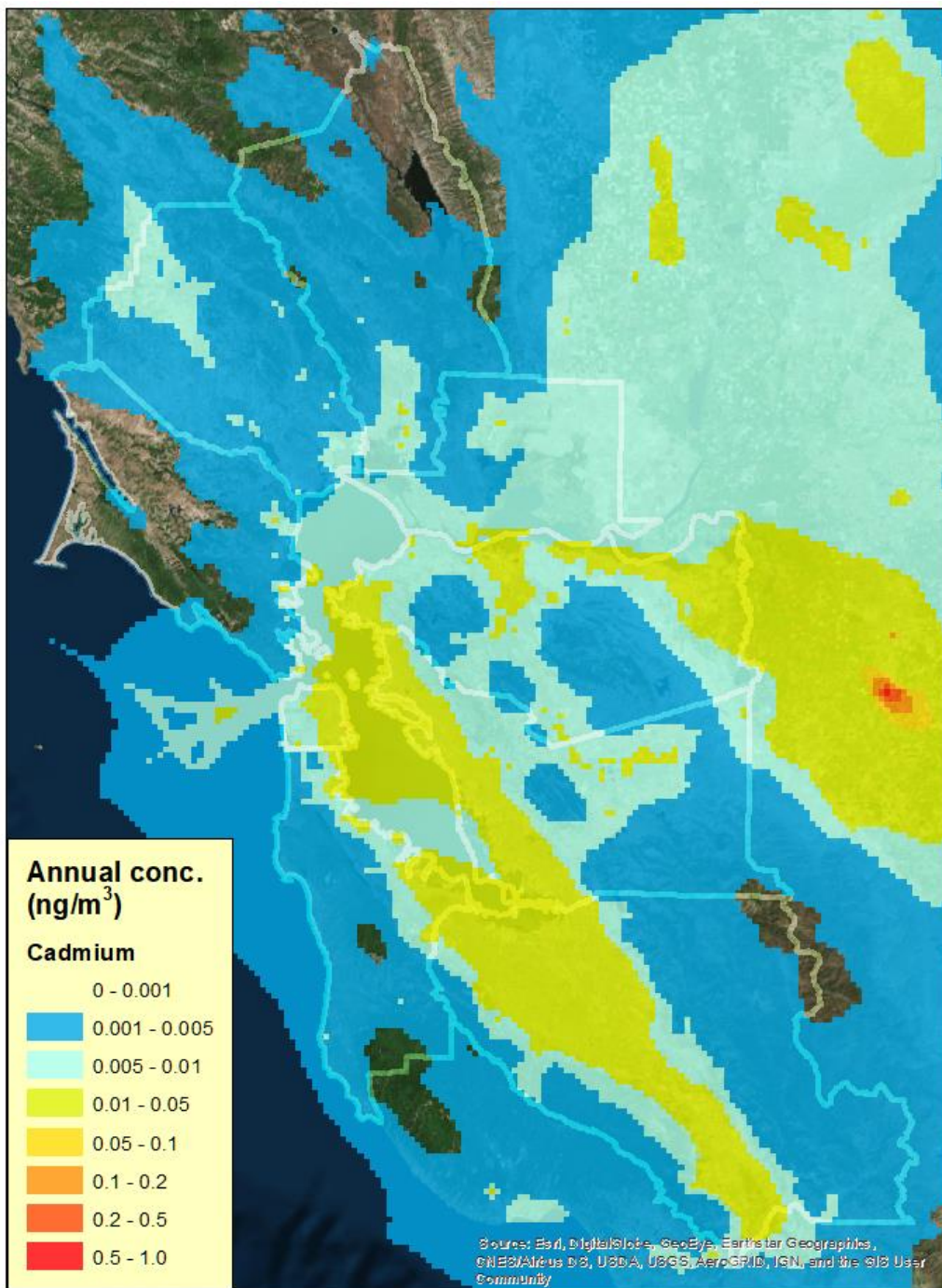
The simulated annual average nickel concentration is highest at Lathrop ($31.5 \text{ ng}/\text{m}^3$). The second highest is at Benicia near the Valero Refinery ($17.9 \text{ ng}/\text{m}^3$). Other hot spots in the Bay Area are Livermore ($7.8 \text{ ng}/\text{m}^3$), Richmond ($6.1 \text{ ng}/\text{m}^3$) and west of Cupertino ($5.4 \text{ ng}/\text{m}^3$).

The highest annual average mercury concentration of $1.8 \text{ ng}/\text{m}^3$ is simulated to occur just west of Cupertino, with the surrounding areas showing above $0.5 \text{ ng}/\text{m}^3$. Simulated concentrations are below $0.5 \text{ ng}/\text{m}^3$ for all other areas except for Rodeo which shows $0.6 \text{ ng}/\text{m}^3$.



Maximum: 8.3

Figure C1: Simulated annual average hexavalent chromium concentrations for 2016.



Maximum: 0.9

Figure C2: Simulated annual average cadmium concentrations for 2016.

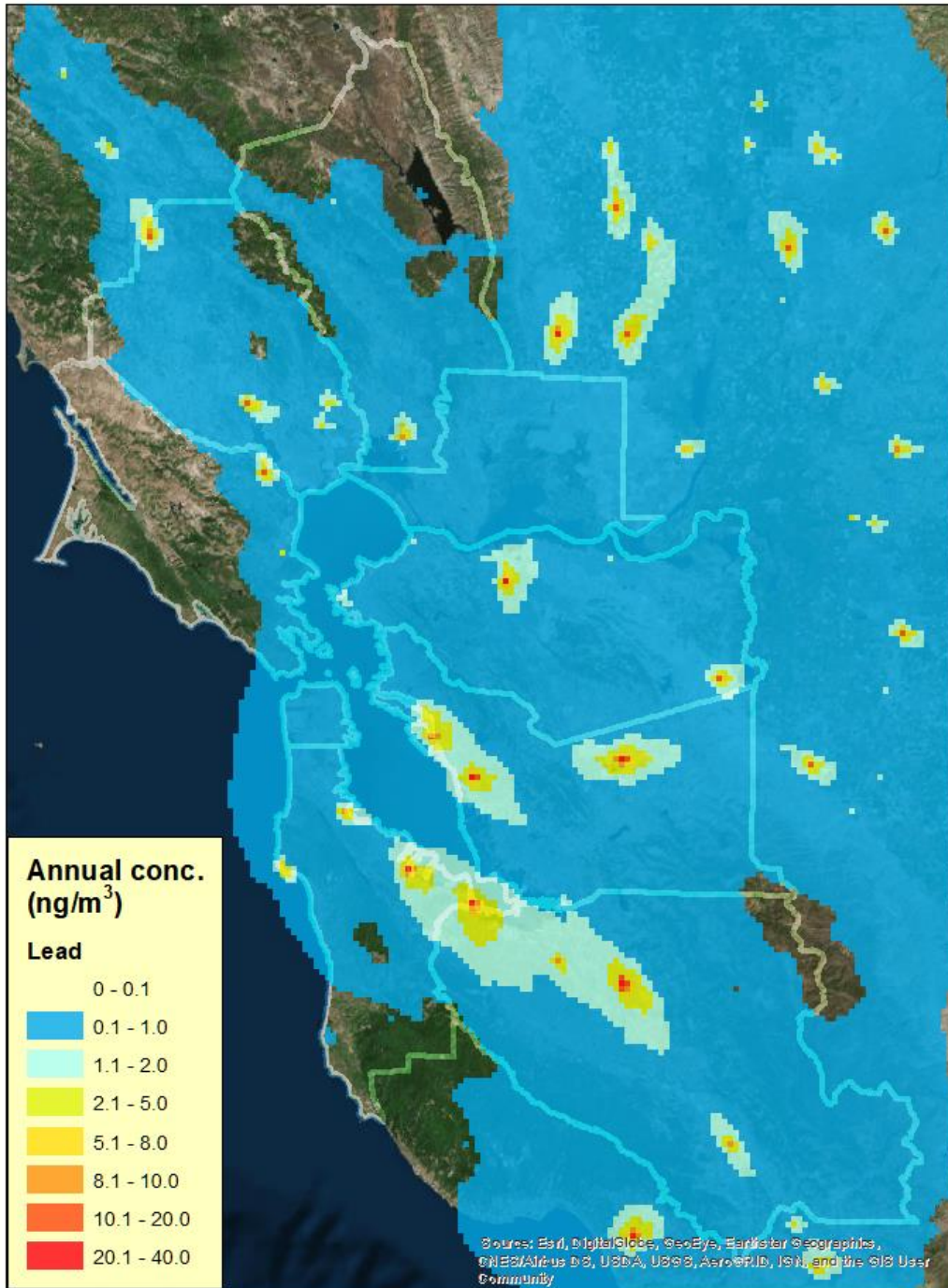
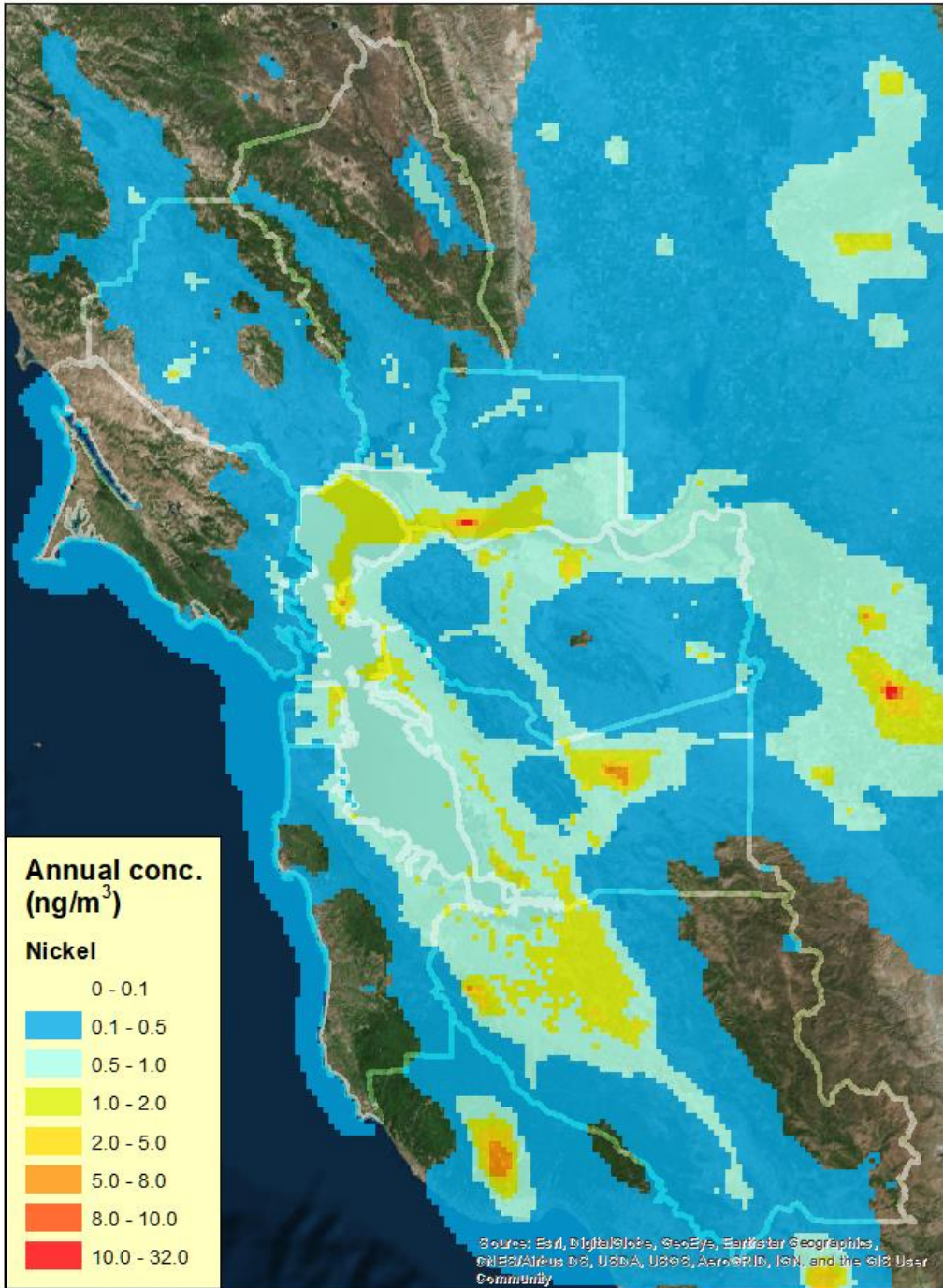
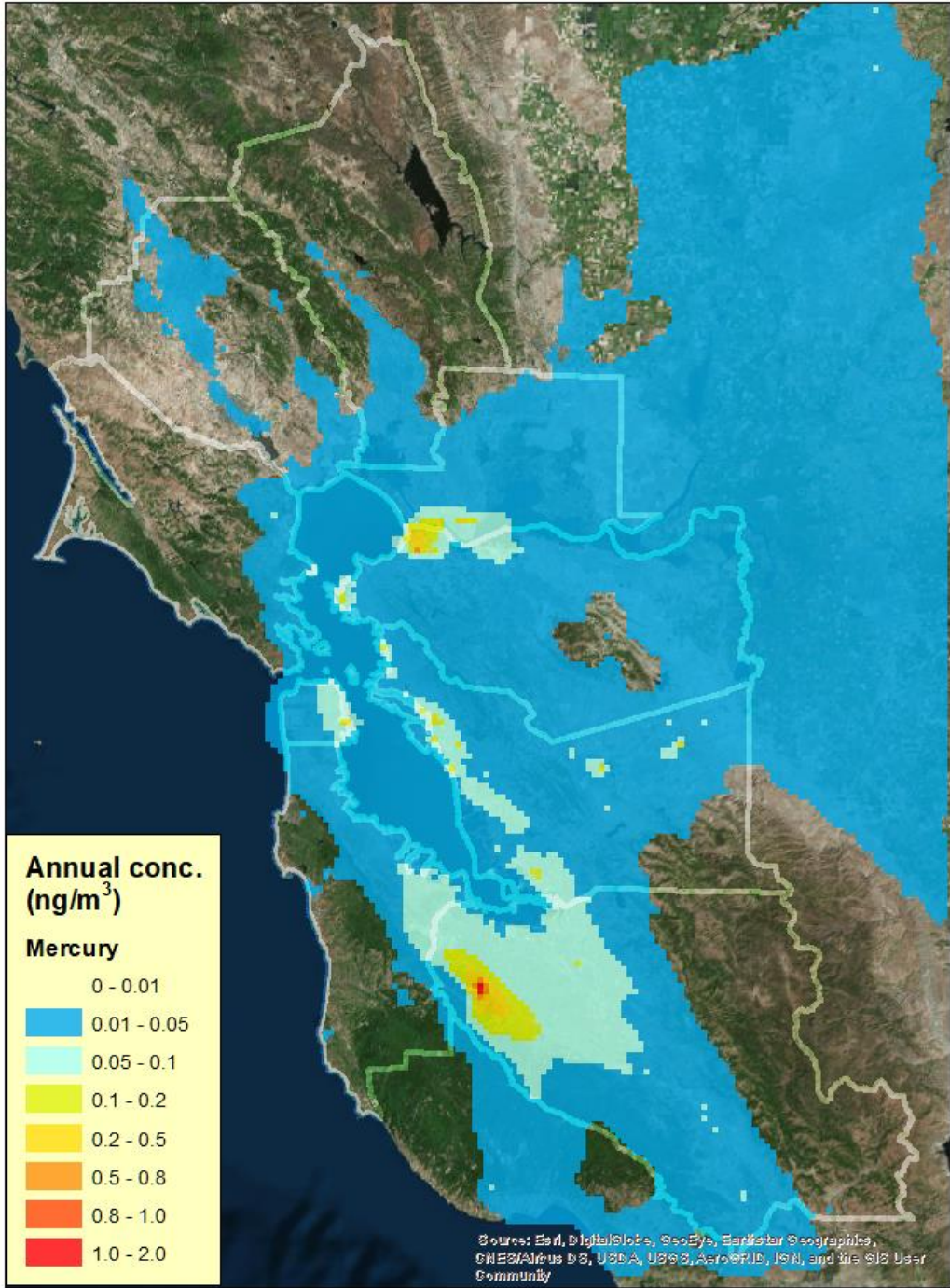


Figure C3: Simulated annual average lead concentrations for 2016.



Maximum: 31.5

Figure C4: Simulated annual average nickel concentrations for 2016.



Maximum: 1.8

Figure C5: Simulated annual average mercury concentrations for 2016.

Appendix D: Excess Cancer Risk in West Oakland

As mentioned in Section 3, in addition to the base case, a “control case” simulation was conducted with all anthropogenic emissions from the West Oakland source domain removed, which provides regional background contributions to air toxics in the West Oakland. The differences between the base and control cases represent contributions from the local anthropogenic sources in West Oakland.

Figures D1 through D4 present the base case annual average concentrations of the air toxics and show significant mass concentrations in the West Oakland receptor domain (formaldehyde, acetaldehyde, benzene, and diesel PM). Annual average formaldehyde concentrations range from 1.3 to 5.1 $\mu\text{g}/\text{m}^3$. The northwestern section of the West Oakland community (the community border is indicated by the red line in the figure) shows the highest concentration.

The highest annual average acetaldehyde concentration (0.83 $\mu\text{g}/\text{m}^3$) within the West Oakland receptor domain is located outside of the West Oakland community, at a grid cell in the northwestern corner of the receptor domain. The concentration gradient of acetaldehyde is not as dramatic as that of formaldehyde. The highest acetaldehyde concentration in the West Oakland community is 0.75 $\mu\text{g}/\text{m}^3$.

The annual average benzene concentration is highest (0.68 $\mu\text{g}/\text{m}^3$) at the northeastern corner of the West Oakland receptor domain. Within the West Oakland community border, the concentration ranges from 0.4 to 0.6 $\mu\text{g}/\text{m}^3$ except for the small area in the northeastern corner of the community.

The annual average diesel PM concentrations peak at the northwestern corner of the receptor domain (1.3 $\mu\text{g}/\text{m}^3$), suggesting significant contributions from diesel traffic over the Bay Bridge. Within the West Oakland community, the concentration remains below 0.9 $\mu\text{g}/\text{m}^3$.

Figure D5 shows relative fractions of individual air toxics mass concentrations averaged over the 5x4 grid cells within the West Oakland receptor domain. Formaldehyde accounts for almost half of the total air toxic concentration. The next highest is diesel PM, which makes up 19% of the total mass concentration, followed by acetaldehyde (17%) and benzene (13%). The combined toxic metals contribute less than 0.1%.

Figure D6 shows expected excess cancer incidences per million people for the base case, which was calculated as described in Section 4, combining impacts from all the air toxics. The spatial pattern of the cancer risk is similar to that of diesel PM concentrations, with the highest number of excess cancer incidences (1069 per million) occurring at the northwestern corner of the receptor domain, and the lowest (496 per million) occurring at the grid cell that partially overlaps the southwestern tip of the West Oakland community. This is expected, as more than 80% of the combined cancer risk is attributed to diesel PM (see Figure D7). Although formaldehyde is the largest contributor in terms of mass concentration in the area, excess cancer risk is dominated by diesel PM due to its high risk factor.

Figure D8 shows the same plot as Figure D6, but for the control case. The spatial gradient of the excess cancer risk somewhat decreased compared to Figure D6, but the northwestern corner grid cell still shows the highest value, indicating the importance of non-local contributions from the Bay Bridge.

Figure D9 shows the differences in the excess cancer risk between the base and control cases. The Chinatown area (the southeastern corner of the West Oakland receptor domain) would benefit the most (485 cancer incidences per million avoided) from eliminating all anthropogenic emissions in the West Oakland source domain. Similarly, significant benefit is expected at the northwestern corner of the receptor domain, although the population in this grid cell is very small. Within the West Oakland community, the cancer incidences avoided range from 174 to 365 per million.

Figure D10 is the same as Figure D9 except the relative contributions of local vs. background toxics to excess cancer risks is shown on a percentage basis. Local sources account for about 50% of cancer risk in the China Town area, and about 40% in the West Oakland community. The lowest local source contribution to cancer risk is about 27% and is located at a cell in the southwestern corner of the domain.

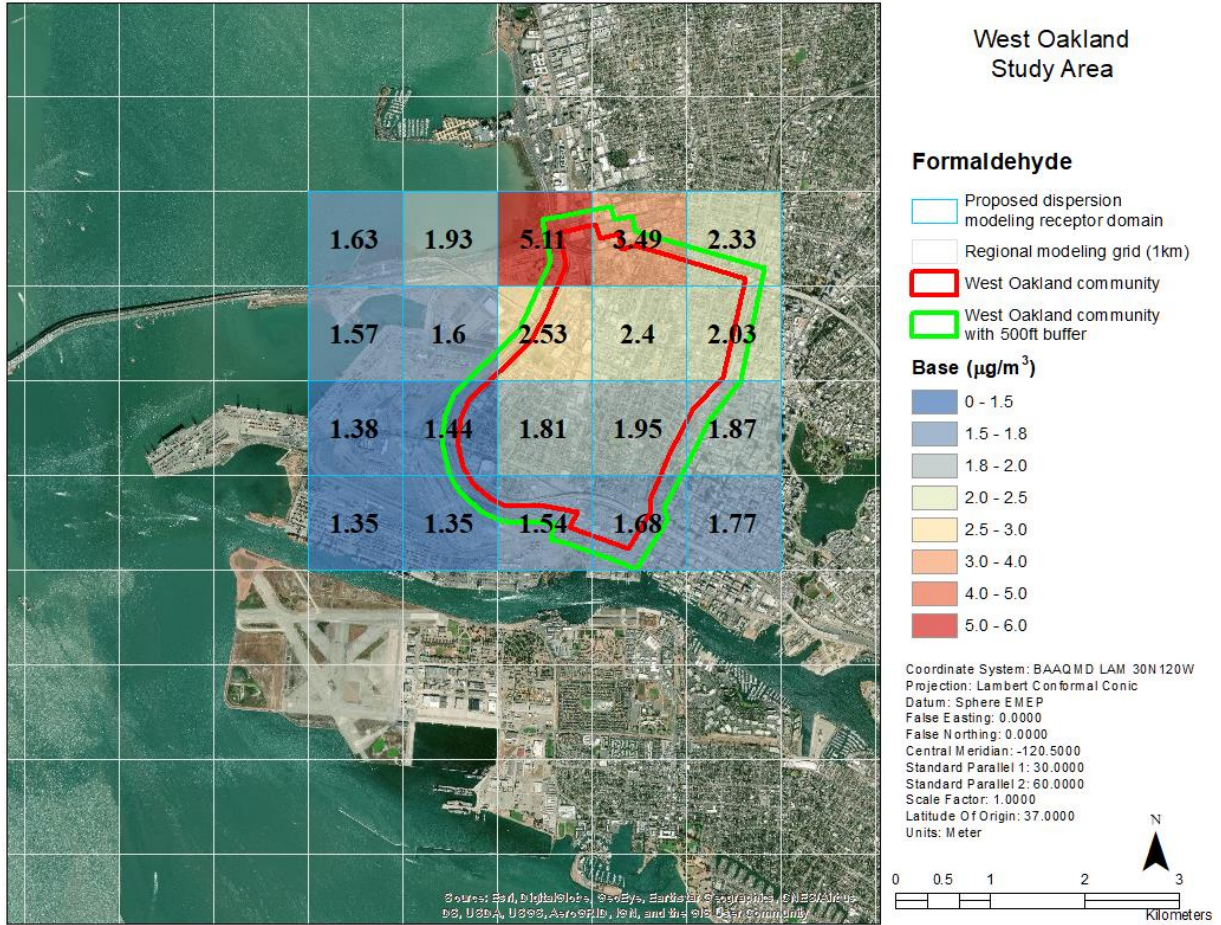


Figure D1: Annual average concentrations of formaldehyde in the West Oakland receptor domain for the base case.

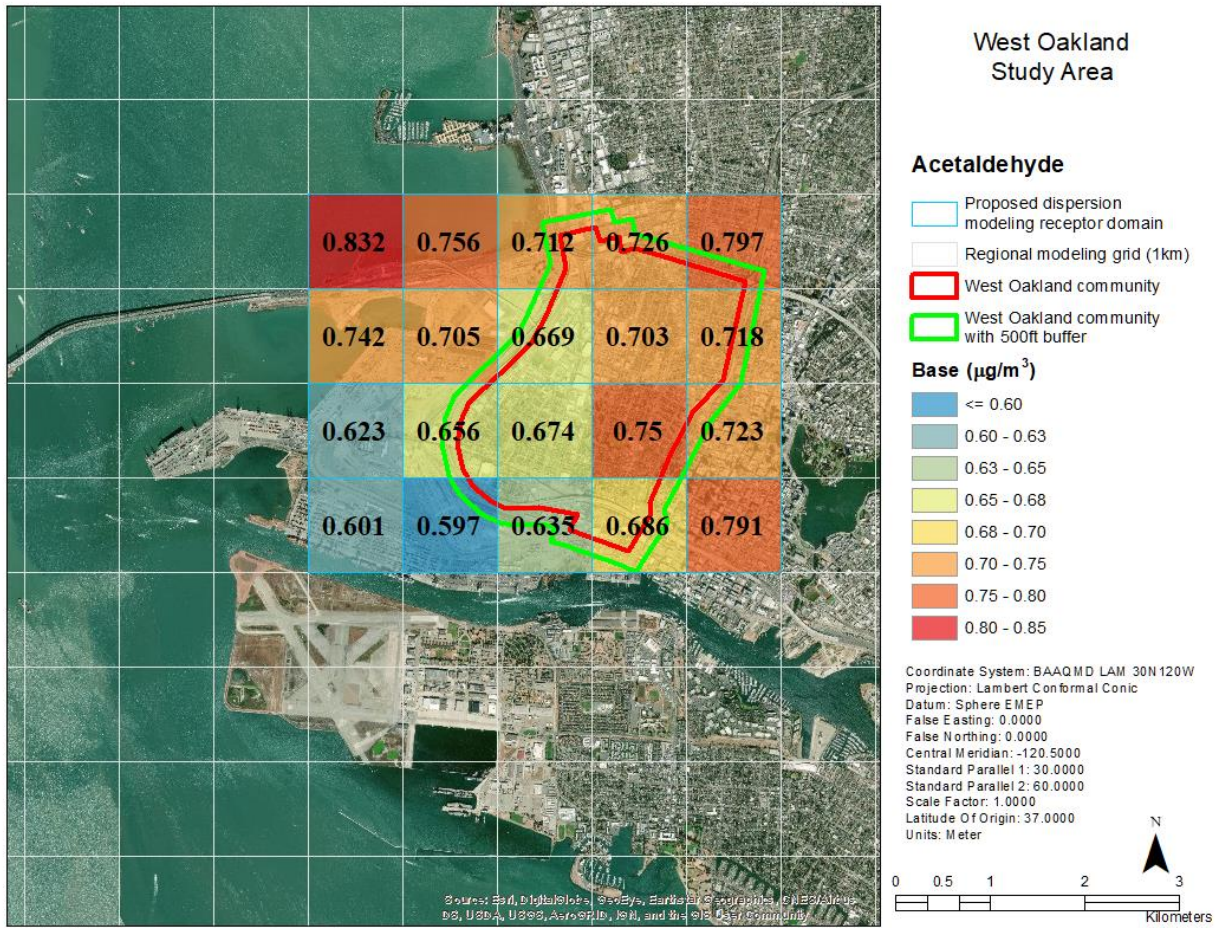


Figure D2: Annual average concentrations of acetaldehyde in the West Oakland receptor domain for the base case.

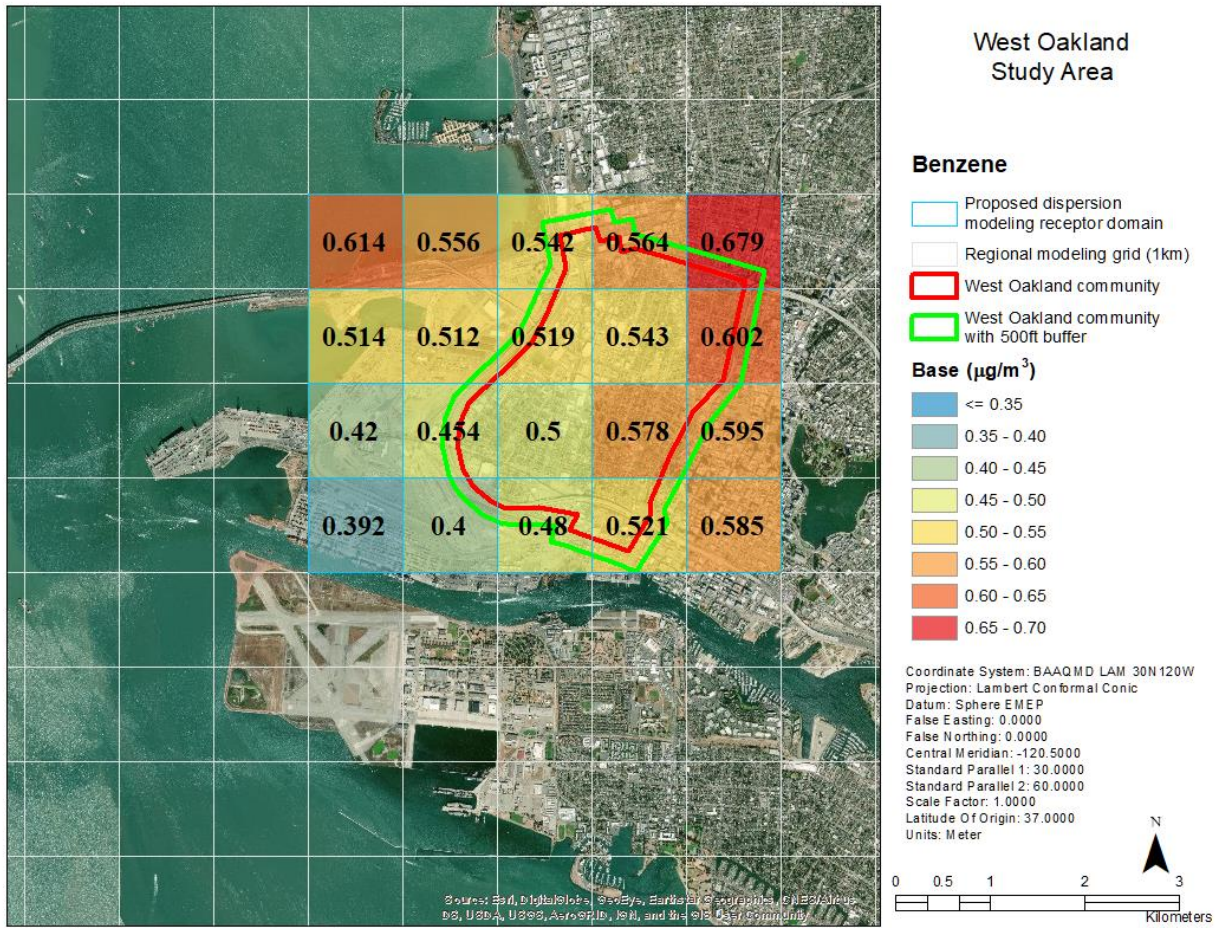


Figure D3: Annual average concentrations of benzene in the West Oakland receptor domain for the base case.

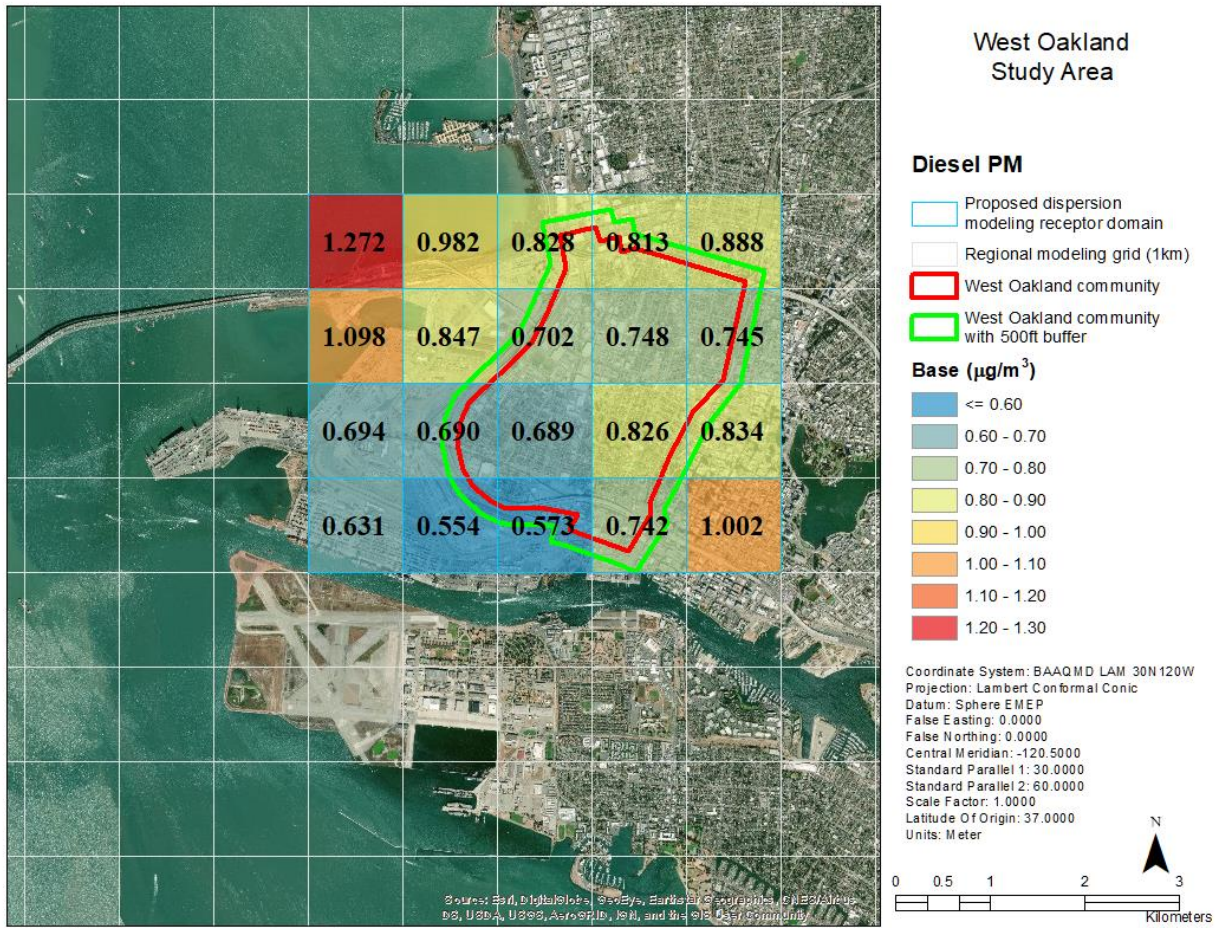


Figure D4: Annual average concentrations of diesel PM in the West Oakland receptor domain for the base case.

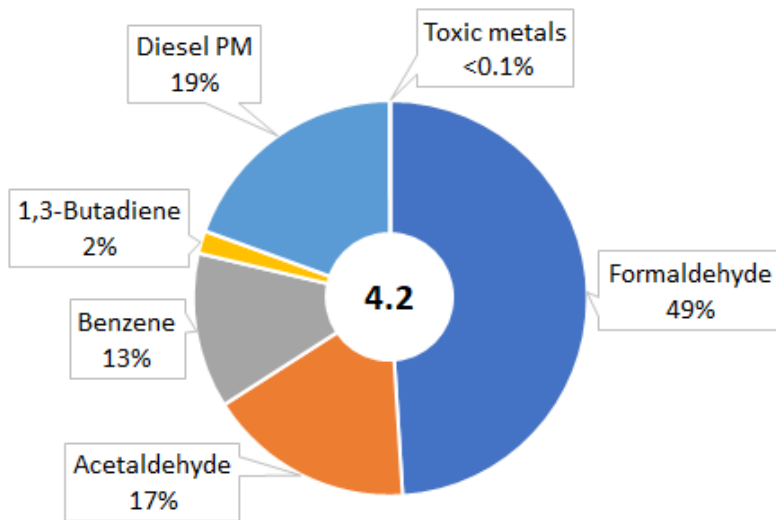


Figure D5: Relative contributions of individual air toxics to total air toxics mass concentration in West Oakland. The number in the center represents the combined annual average concentration ($\mu\text{g}/\text{m}^3$) of all air toxics modeled, averaged over the 5x4 grid cells within the West Oakland receptor domain.

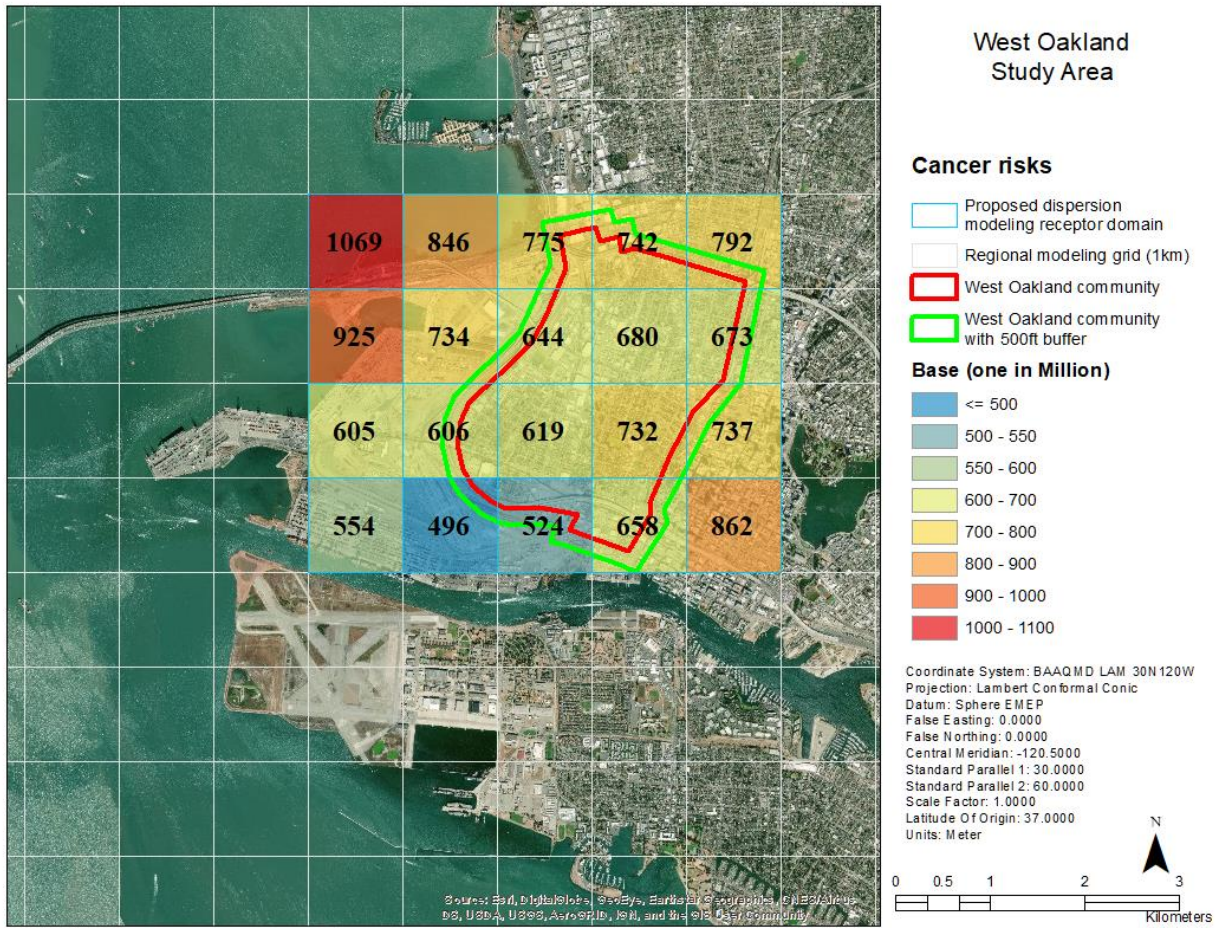


Figure D6: Expected excess cancer incidences per million in the West Oakland receptor domain (base case).

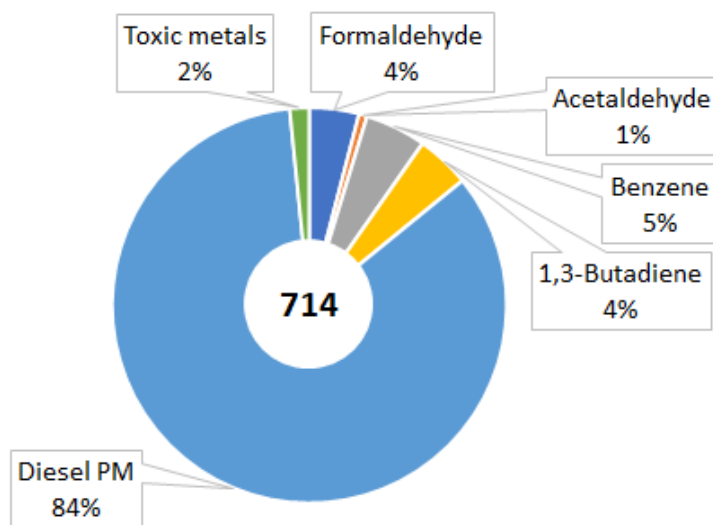


Figure D7: Relative contributions of individual air toxics to total excess cancer risk in West Oakland. The number in the center represents the combined excess cancer incidences (per million people) due to all air toxics modeled, averaged over the 5x4 grid cells within the West Oakland receptor domain.

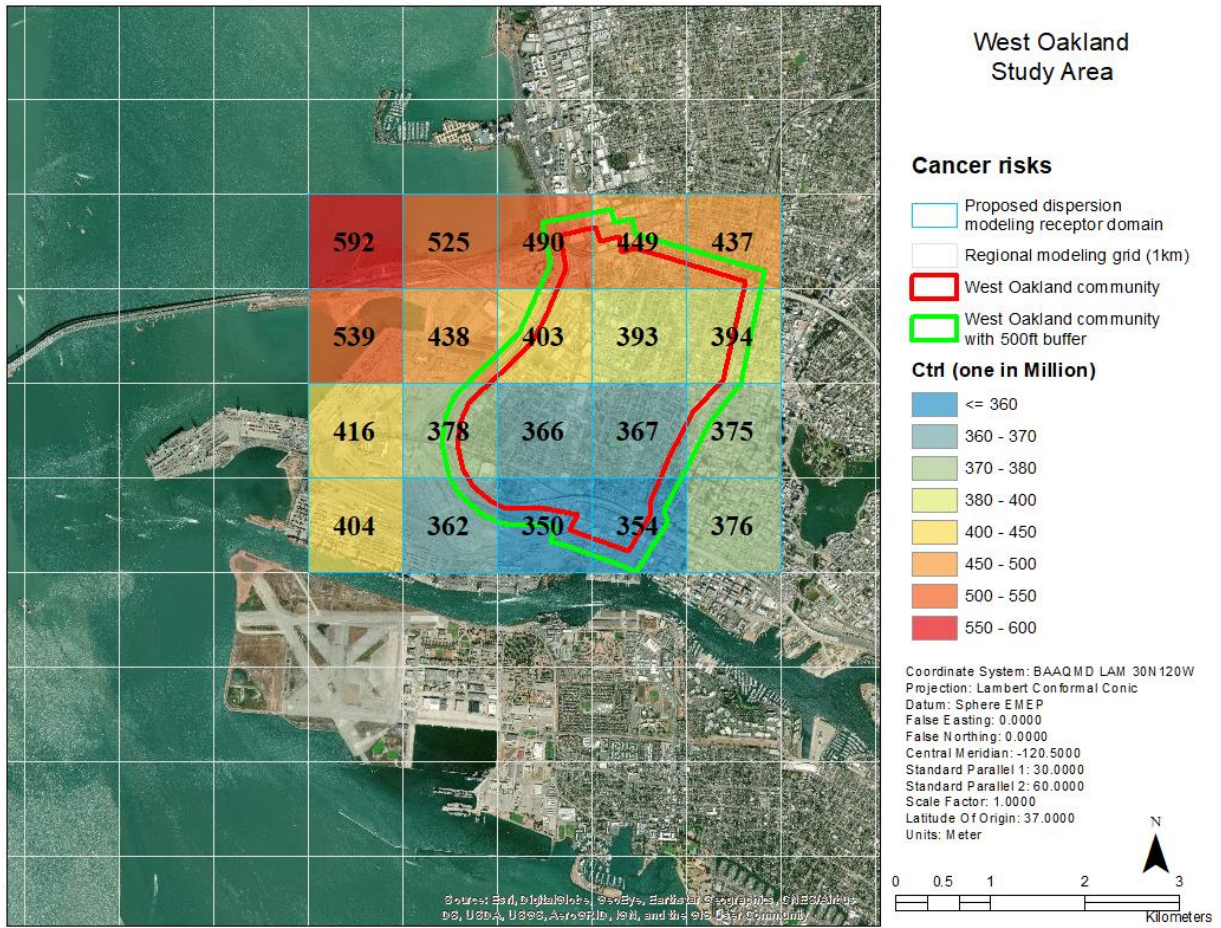


Figure D8: Expected excess cancer incidences per million in the West Oakland receptor domain (control case).

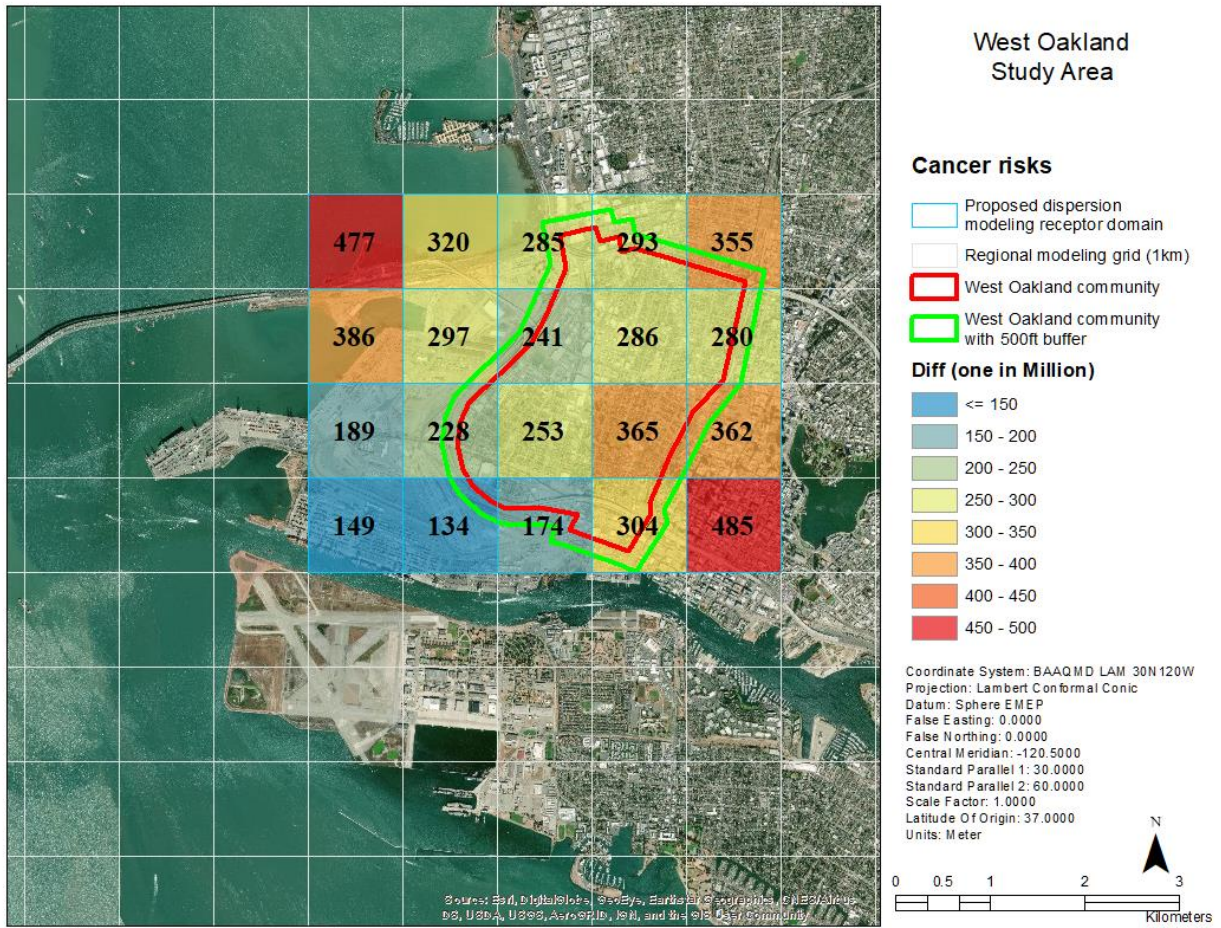


Figure D9: Differences in expected excess cancer incidences per million in the West Oakland receptor domain between the base and control cases.

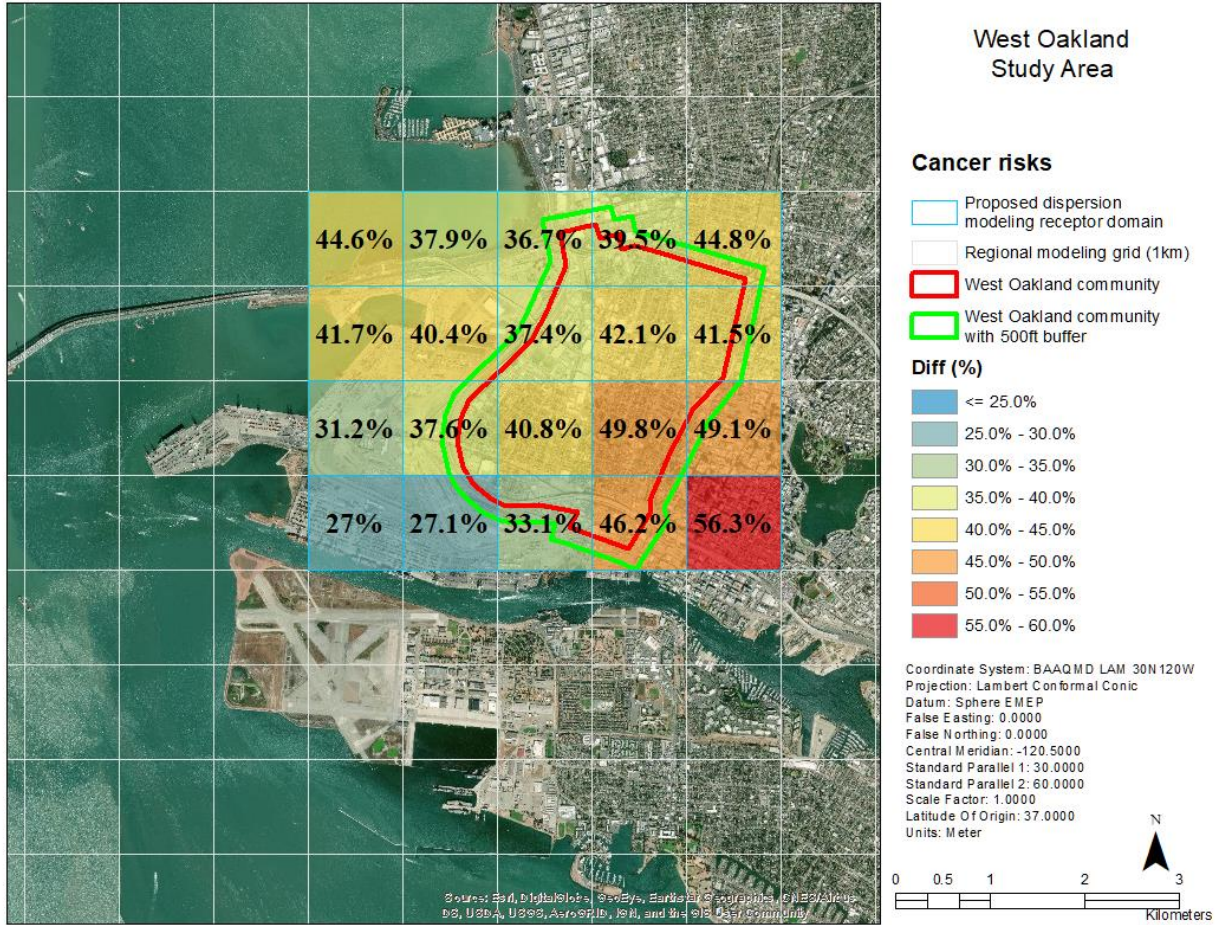
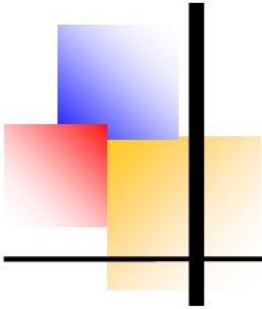


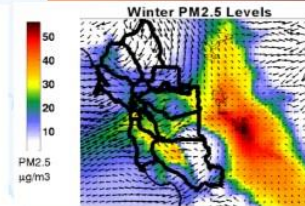
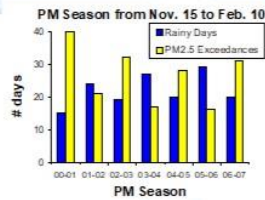
Figure D10: Percentage contribution of cancer risks due to the local anthropogenic emissions within West Oakland.



Fine Particulate Matter Data Analysis and Regional Modeling In the San Francisco Bay Area to Support AB617

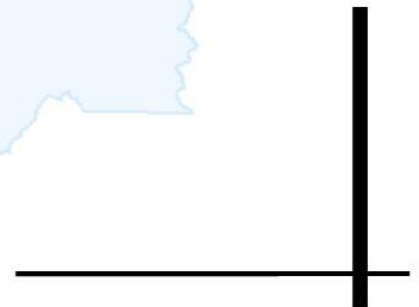
Draft Report—Version 1

January, 2019



Prepared by the Air Quality Modeling and Analysis Section:

Saffet Tanrikulu, Manager
Stephen Reid, Senior Atmospheric Modeler
Bonyoung Koo, Senior Atmospheric Modeler
Yiqin Jia, Atmospheric Modeler
James Cordova, Air Quality Meteorologist
Jeff Matsuoka, Research Analyst
Yuanyuan Fang, Statistician



Disclaimer

This draft report presents results from analyses of ambient measurement data and air quality modeling performed by the District. The models were tested and evaluated for many cases in the Bay Area, and their performance has been iteratively improved. In addition, ambient and emissions data used in the analyses were carefully evaluated. The simulations in this report utilize the best-performing configurations of the models. However, the results presented should be viewed as interim because further refinements may still be made to emissions estimates, meteorological fields, and other modeling-related data. The District plans to improve upon these interim results and minimize uncertainties via its on-going modeling and analysis efforts. As significant improvements are made, this draft report may be updated.

Executive Summary

E1. Background

The adoption of Assembly Bill 617 (AB617) established collaborative programs to reduce community exposure to air pollutants in neighborhoods most impacted by air pollution. Air District staff have been working closely with the California Air Resources Board (ARB), other local air districts, community groups, community members, environmental organizations, regulated industries, and other key stakeholders to reduce harmful air pollutants in Bay Area communities.

The purpose of this data analysis and regional modeling effort is to support the District's AB617 activities by assessing pollutant formation, quantifying the relative contribution of emission sources to ambient pollution levels, and assessing population exposures and the benefits of emission controls in impacted communities around the Bay Area. Our initial assessments focus on fine particulate matter (PM_{2.5}) concentrations in West Oakland, and follow-up analyses will include air toxics evaluations in West Oakland and expansion of our technical assessments to other communities.

For the PM_{2.5} analyses, we evaluated ambient meteorological and air quality data, and applied the U.S. EPA's Community Multi-Scale Air Quality (CMAQ) model to simulate pollutant concentrations at a 1-km horizontal resolution over the entire Bay Area for 2016. Then we repeated the simulation with West Oakland's anthropogenic emissions removed from the modeling inventory, leaving all other model input parameters unchanged. We calculated annual average PM_{2.5} concentrations using the output of each simulation. The first simulation provided the annual average PM_{2.5} concentrations for 2016 over the entire Bay Area, which will be used for PM_{2.5} exposure analyses and health impacts assessments. The second simulation provided an estimate of background PM_{2.5} levels in West Oakland (i.e., the PM_{2.5} concentrations that would exist in the absence of local West Oakland sources). Background PM_{2.5} concentrations will then be combined with local-scale modeling of West Oakland sources using the AERMOD dispersion model to provide a complete picture of PM_{2.5} levels in the community and the relative contribution of different emission sources to those levels.

E2. Major Findings

E2.1 Regional PM_{2.5} Concentrations

The CMAQ model generally captured the observed PM_{2.5} pattern within the 1-km domain (Figure E1). High concentrations in both simulations and observations are evident in the northern San Joaquin Valley, along the I-580 and I-880 corridors from Richmond to the Oakland Airport, along the I-101 corridor near Redwood City, and in the San Jose metropolitan area. In the Sacramento area, the model shows overestimation biases and PM_{2.5} concentrations do not compare as well to observations as in the Bay Area. For Sacramento and other counties outside

the Bay Area, we relied on the ARB's emission inventories, and further evaluation of these data may be warranted. The model also shows high concentrations along the I-880 corridor from Oakland Airport to San Jose and along the Delta from Antioch to Brentwood, although observations are unavailable in these areas.

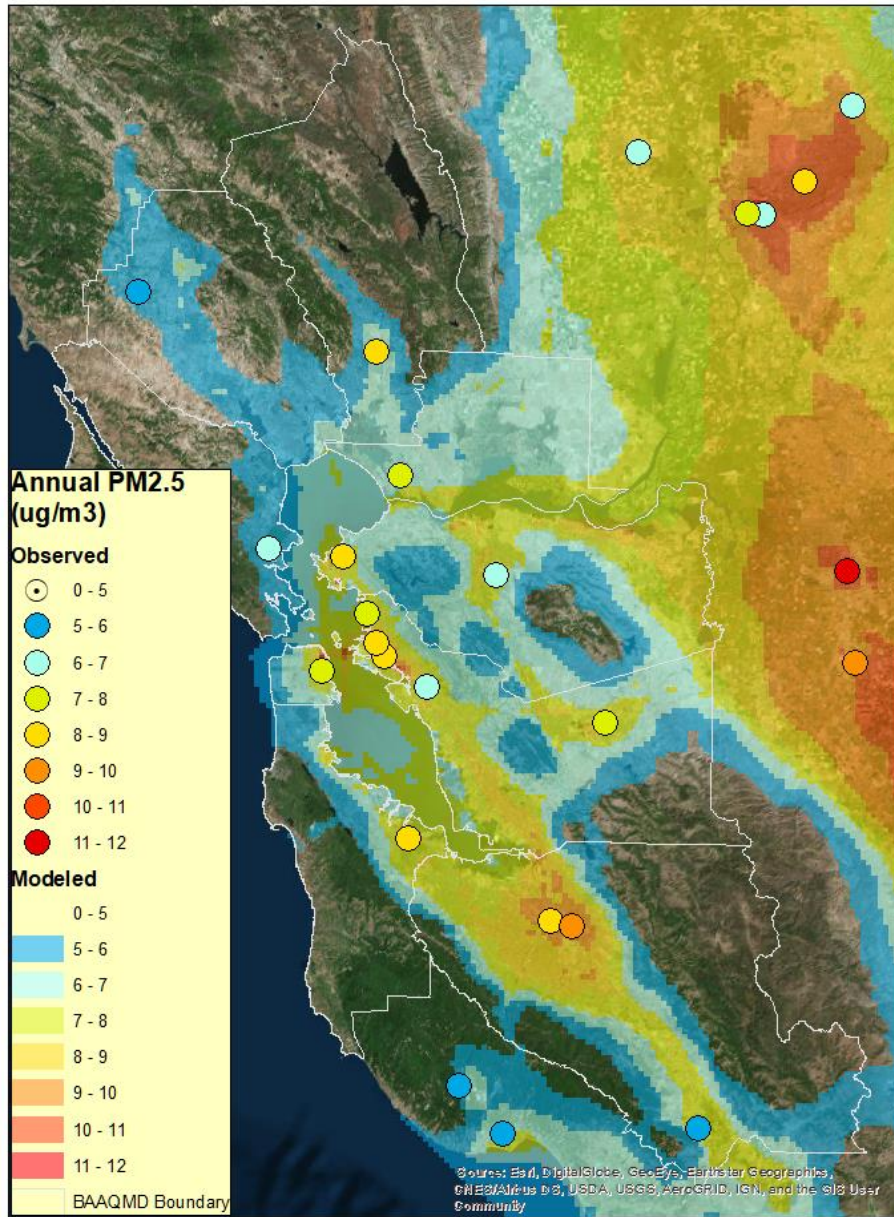


Figure E1: Spatial distribution of simulated and observed annual average PM_{2.5} concentrations within the 1-km modeling domain.

Site by site comparisons between the simulations and observations (Figure E2) show that at most Bay Area sites (including the West Oakland Air Monitoring Station), the simulated annual average PM_{2.5} concentrations are within $\pm 1.0 \mu\text{g}/\text{m}^3$ of observations. At a few sites (Concord,

Oakland and Gilroy), the annual average PM_{2.5} concentrations were overestimated, and at one site (Napa), the annual average PM_{2.5} concentration was underestimated by as much as 2.1 µg/m³. Causes of these over and underestimations are under investigation.

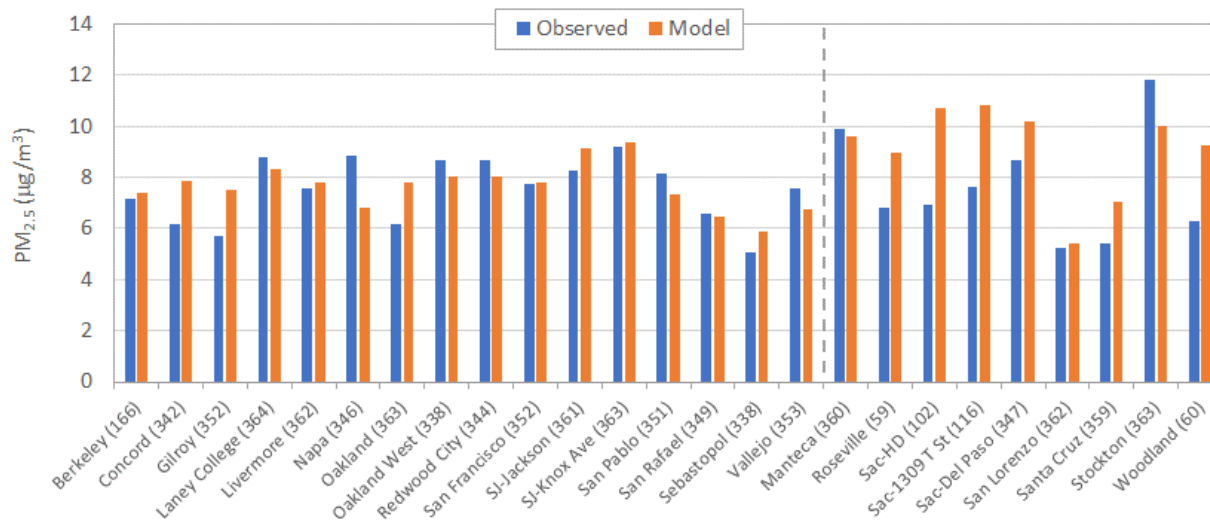


Figure E2: Annual mean observed vs. modeled PM_{2.5} concentrations at monitoring sites within the 1-km modeling domain. The number of valid observations is shown in parentheses for each site.

E2.2 Estimating Background PM_{2.5} in West Oakland

Figure E3 shows the annual average PM_{2.5} concentrations for the base case within the West Oakland local-scale modeling domain that will be used for AERMOD. The highest and lowest annual average PM_{2.5} concentrations are 9.3 µg/m³ and 7.1 µg/m³, respectively. A concentration gradient is evident within the domain. Cells with relatively higher concentrations extend along the eastern boundary and northwestern corner of the domain. A concentration gradient is also evident in the West Oakland community, an area within the red border in the figure. The eastern half of the community has slightly higher concentrations than the western half.

The spatial distribution of the annual average PM_{2.5} concentrations is similar to the spatial distribution of West Oakland’s emissions (Figure E4). The Chinatown area in the southeastern corner of the West Oakland local-scale domain has the highest emissions and concentrations. The cell along the southern boundary with the area’s lowest concentration (7.1 µg/m³) also has the lowest emissions (1.4 lbs/day).

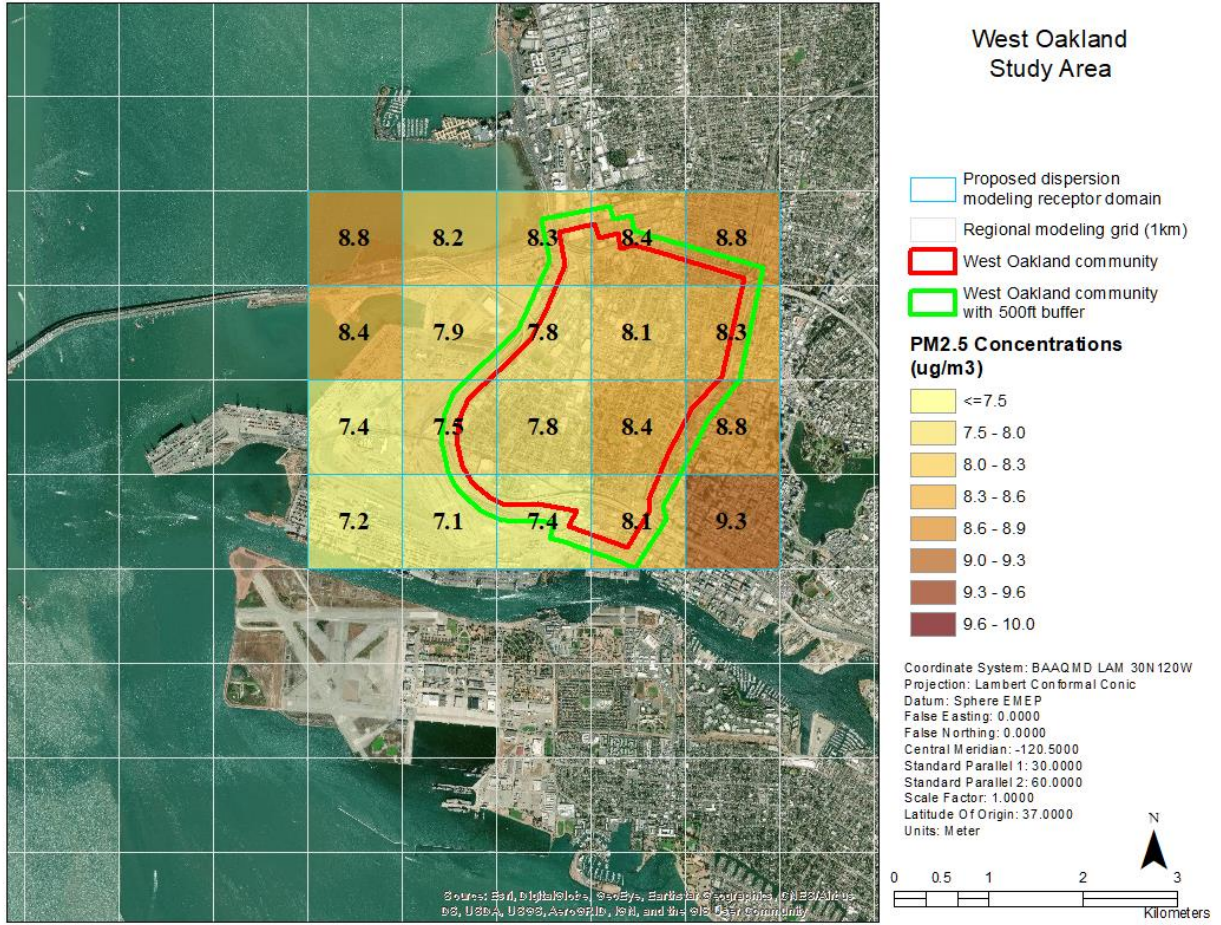


Figure E3: Spatial distribution of the simulated annual average PM_{2.5} concentrations in the West Oakland modeling domain.

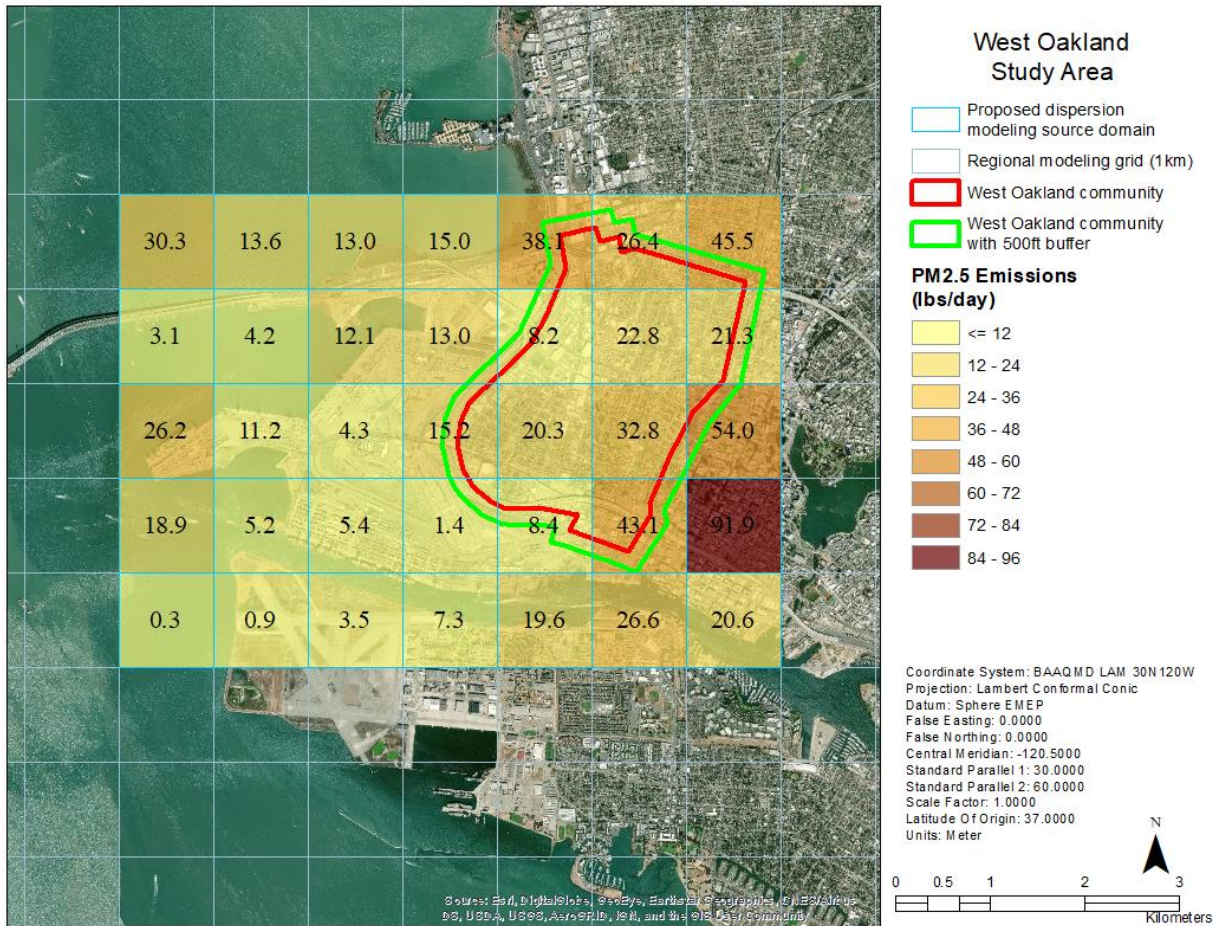


Figure E4: Spatial distribution of annual average PM_{2.5} emissions in West Oakland.

Figure E5 shows the annual average PM_{2.5} concentrations for the control case, i.e., a simulation without West Oakland’s anthropogenic emissions. Compared to Figure E3, the spatial gradient in the annual average concentrations decreased significantly in the absence of West Oakland emissions across the local-scale domain. The location of the maximum annual average PM_{2.5} concentrations has shifted from Chinatown to near the Bay Bridge, suggesting the influence of transport from the northwest corner of the domain.

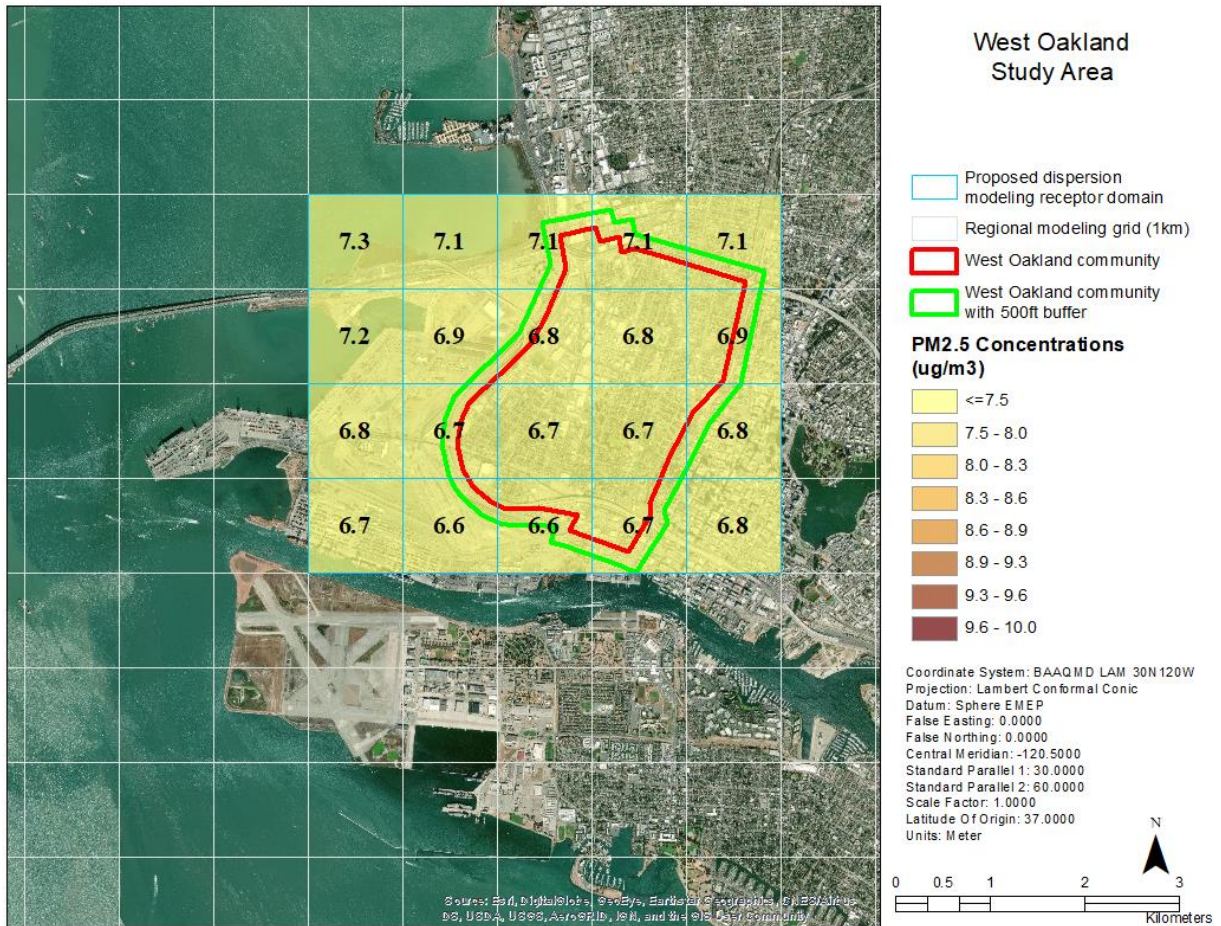


Figure E5: Spatial distribution of the simulated PM_{2.5} concentrations without West Oakland’s anthropogenic emissions.

Figure E6 shows the difference between the base and control cases. Based on the figure, the Chinatown area would benefit the most (2.5 µg/m³) from zeroing out all anthropogenic emissions in the West Oakland local-scale domain. The West Oakland community (within the red border) would benefit by PM_{2.5} reductions ranging from 0.8 µg/m³ to 1.7 µg/m³. The southwest corner of the modeling domain would be the least benefitted area, with a reduction of about 0.5 µg/m³.

Note that these PM_{2.5} concentrations and reductions represent the average value across a 1x1 km grid cell. Higher concentrations and reductions are possible at the sub-grid cell level, and these finer-scale gradients will be investigated with the local-scale AERMOD modeling.

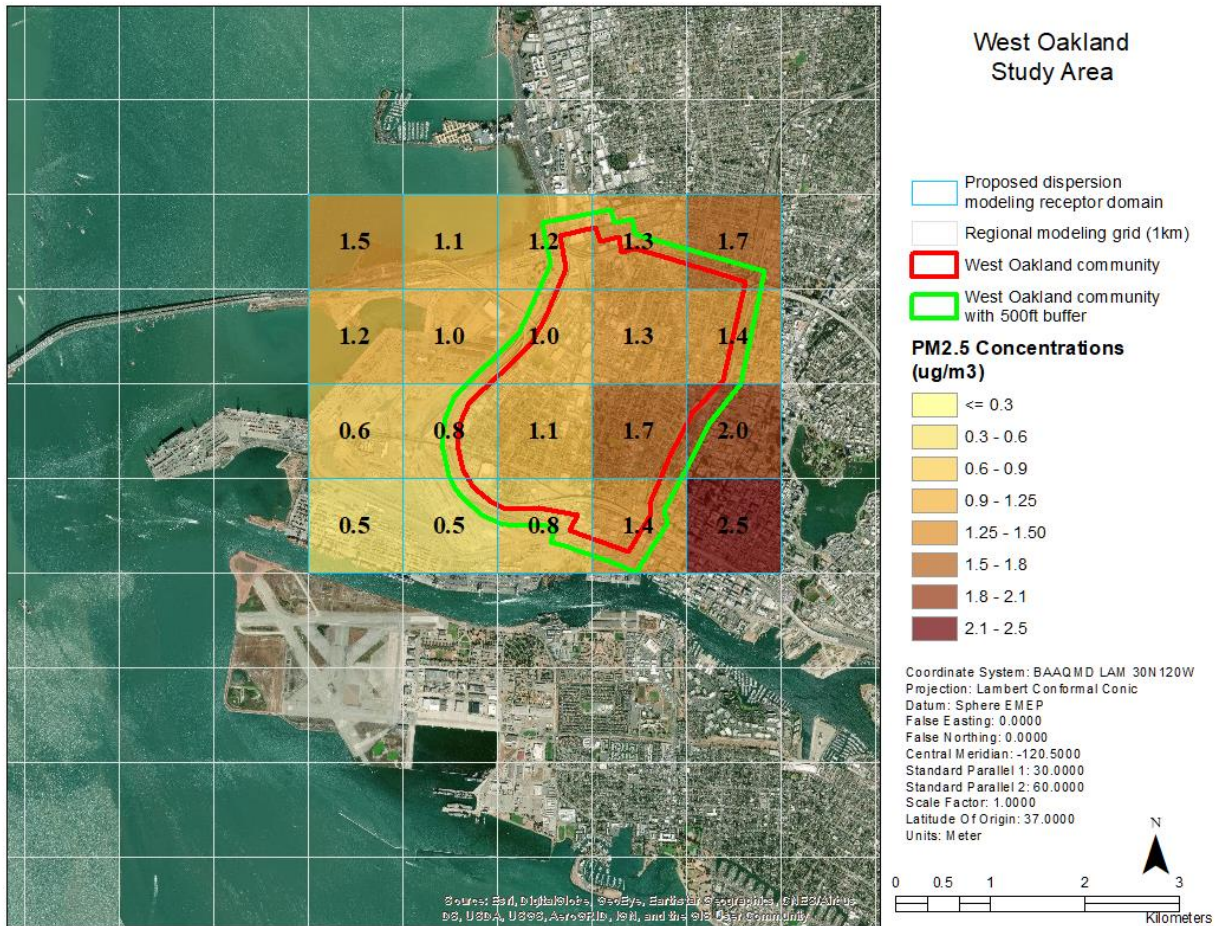


Figure E6: Difference between the simulated annual average base and control case PM_{2.5} concentrations.

E3. Discussion

West Oakland is a unique area in terms of its geographic location, emissions, meteorology and air quality. In the West Oakland local-scale domain, annual average PM_{2.5} emissions are 0.35 tons per day (tpd), about 1% of the Bay Area total. Onroad and nonroad mobile sources account for 66% of total PM_{2.5} emissions. Area sources account for 24% of total PM_{2.5} emissions, a significantly smaller percentage compared to the Bay Area total PM_{2.5} emissions (Figure E7).

West Oakland is also impacted by pollutant transport from outside sources for all seasons. During spring, summer and fall, prevailing winds from the west, northwest and, to a lesser degree, from the southwest transport pollutants from downtown San Francisco, the San Francisco Peninsula, and shipping emissions from the Pacific Ocean and the Bay. During winter, occasional easterly airflow transports polluted air from the Central Valley through the Delta. West Oakland is also open for sea salt intrusion, which mostly occurs during spring, and the

transport of wildfire emissions from the Sierras, other northern California locations and state of Oregon during the wildfire season. Transport to West Oakland from southern California, neighboring counties and intercontinental transport are also possible.¹

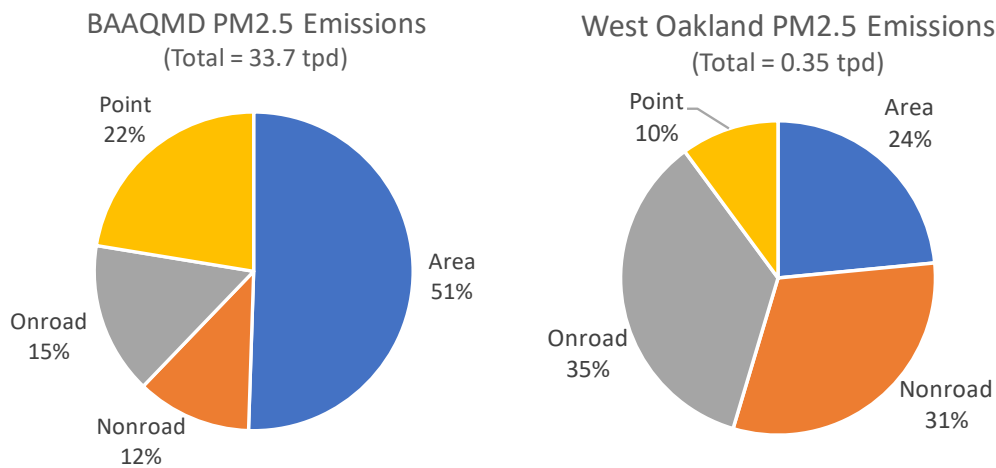


Figure E7: PM_{2.5} emissions by source sector for the District (left) and West Oakland (right).

February, September and December usually exhibit the highest PM_{2.5} concentrations in West Oakland (Figure E8). PM is elevated in February because of the contribution of wood burning emissions, secondary PM formation and near stagnant atmospheric conditions. Elevated PM in September is mainly influenced by wildfire emissions. In December, PM levels are significantly influenced by wood burning and cooking, which generally increases during the holidays, and relatively calm and foggy atmospheric conditions.

The remaining months exhibit PM levels around 8 µg/m³, except July, August and October. The strong afternoon seabreeze in July and August lowers concentrations through atmospheric mixing, while October is a month with relatively low wind speeds and highly variable wind directions. The usual transport from nearby sources are not dominant during this month.

The CMAQ model is generally able to replicate the month-to-month variation in observed PM_{2.5} concentrations in West Oakland (Figure E8). The model slightly overestimates PM during winter months and underestimates PM during summer months, a pattern that is typical of the CMAQ modeling system. The somewhat significant underestimation in September is likely due to lack of wildfire emissions in the CMAQ simulations.

¹ Note that this analysis did not seek to quantify the impact of various sources of transported pollution on West Oakland. Rather, to be consistent with AB617 goals, the focus was on the impact of local emissions.

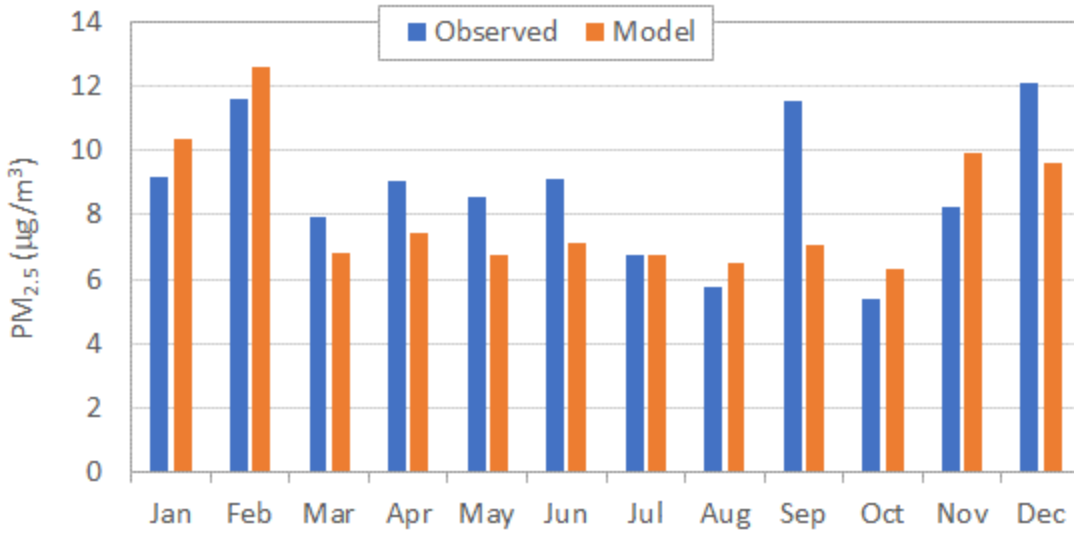


Figure E8: Monthly average simulated and observed PM_{2.5} concentrations in West Oakland.

Fine Particulate Matter Data Analysis and Regional Modeling in the San Francisco Bay Area to Support AB617

1. Introduction

The adoption of Assembly Bill 617 (AB617) established collaborative programs to reduce community exposure to air pollutants in neighborhoods most impacted by air pollution. Air District staff have been working closely with the California Air Resources Board (ARB), other local air districts, community groups, community members, environmental organizations, regulated industries, and other key stakeholders to reduce harmful air pollutants in Bay Area communities.

The purpose of this data analysis and regional modeling effort is to support the District's AB617 activities by assessing pollutant formation, quantifying the relative contribution of emission sources to ambient pollution levels, and assessing population exposures and the benefits of emission controls in impacted communities around the Bay Area. Our initial assessments focus on fine particulate matter (PM_{2.5}) concentrations in West Oakland, and follow-up analyses will include air toxics evaluations in West Oakland and expansion of our technical assessments to other communities.

For the PM_{2.5} analyses, we evaluated ambient meteorological and air quality data, and applied the U.S. EPA's Community Multi-Scale Air Quality (CMAQ) model to simulate pollutant concentrations at a 1-km horizontal resolution over the entire Bay Area for 2016 (Figure 1.1). Then we repeated the simulation with West Oakland's anthropogenic emissions removed from the modeling inventory, leaving all other model input parameters unchanged. We calculated annual average PM_{2.5} concentrations using the output of each simulation. The first simulation provided the annual average PM_{2.5} concentrations for 2016 over the entire Bay Area, which will be used for PM_{2.5} exposure analyses and health impacts assessments. The second simulation provided an estimate of background PM_{2.5} levels in West Oakland (i.e., the PM_{2.5} concentrations that would exist in the absence of local West Oakland sources).

Background PM_{2.5} concentrations will be combined with local-scale modeling of West Oakland sources using the AERMOD dispersion model to provide a complete picture of PM_{2.5} levels in the community and the relative contribution of different emission sources to those levels. Figure 1.2 shows the AERMOD modeling domain for West Oakland. The area outlined in blue represents the "source domain," and all significant emissions sources in that area will be modeled in the AERMOD simulations. The red hatched area represents the "receptor domain," or the area for which pollutant concentrations will be calculated by AERMOD.

The application of the CMAQ model involves the preparation of meteorological and emissions inputs, model runs, analysis of simulated pollutant concentrations, and the evaluation of model performance via comparison between simulated and observed pollutant concentrations. A

simulation year of 2016 was selected because (1) this is a recent year that is likely to be representative of current conditions in West Oakland and other communities; and (2) special measurement studies that took place in 2016 provide additional ambient data to support evaluations of model performance.

District staff have been applying and evaluating the CMAQ model in the Bay Area over the last several years, along with the Weather Research and Forecasting (WRF) model, which provides meteorological inputs for CMAQ. Findings from previous modeling work are documented in a District report on PM_{2.5} data analysis and modeling (Tanrikulu et al., 2009) and in the District’s 2017 Clean Air Plan (BAAQMD, 2017). Both the CMAQ and WRF models were tested and evaluated for many cases in the Bay Area and their performance has been iteratively improved. The 2016 simulations used the best-performing configuration of the model. The 2016 emissions inputs have been updated to reflect ARB’s most recent estimates and have been evaluated to the extent possible.

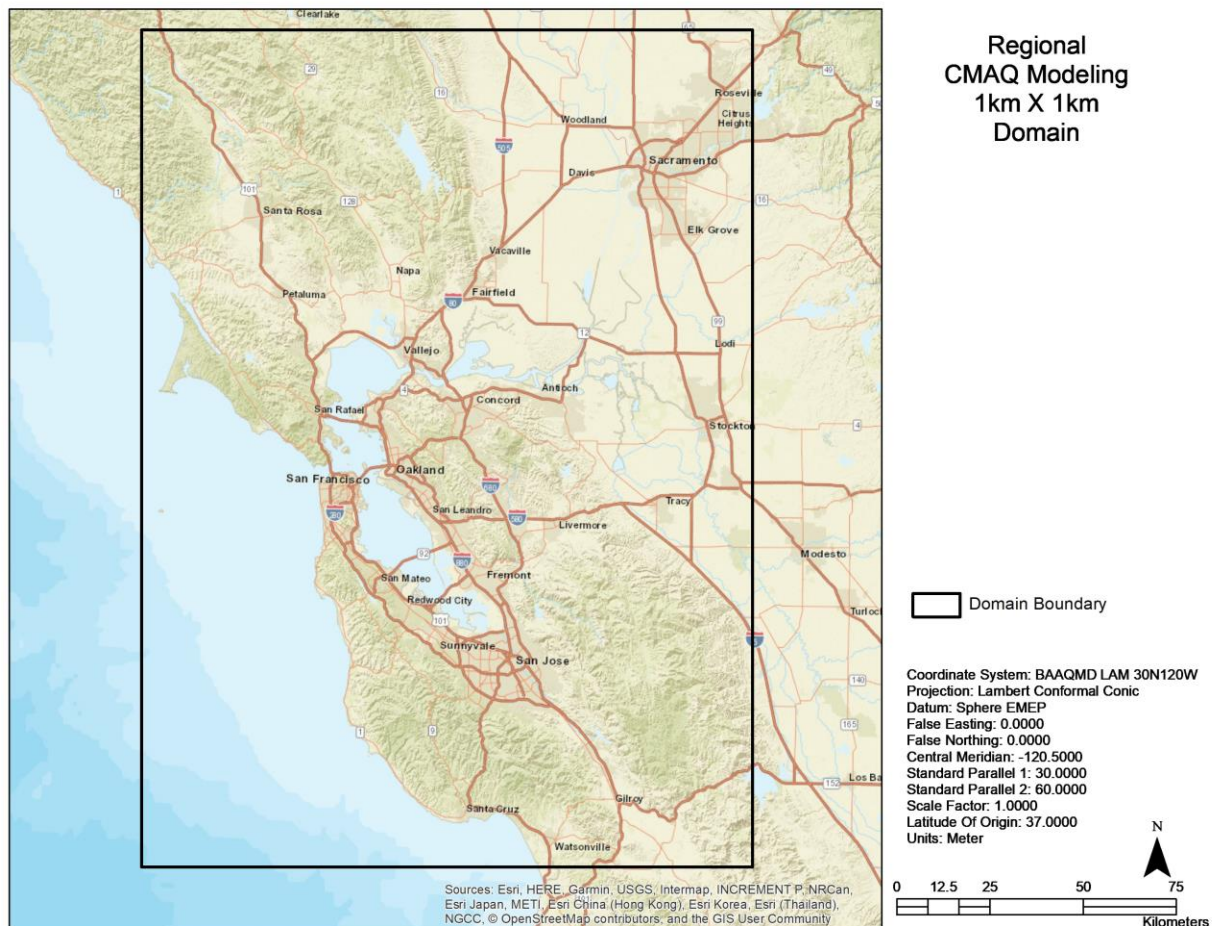


Figure 1.1: The regional 1-km modeling domain used for CMAQ simulations.

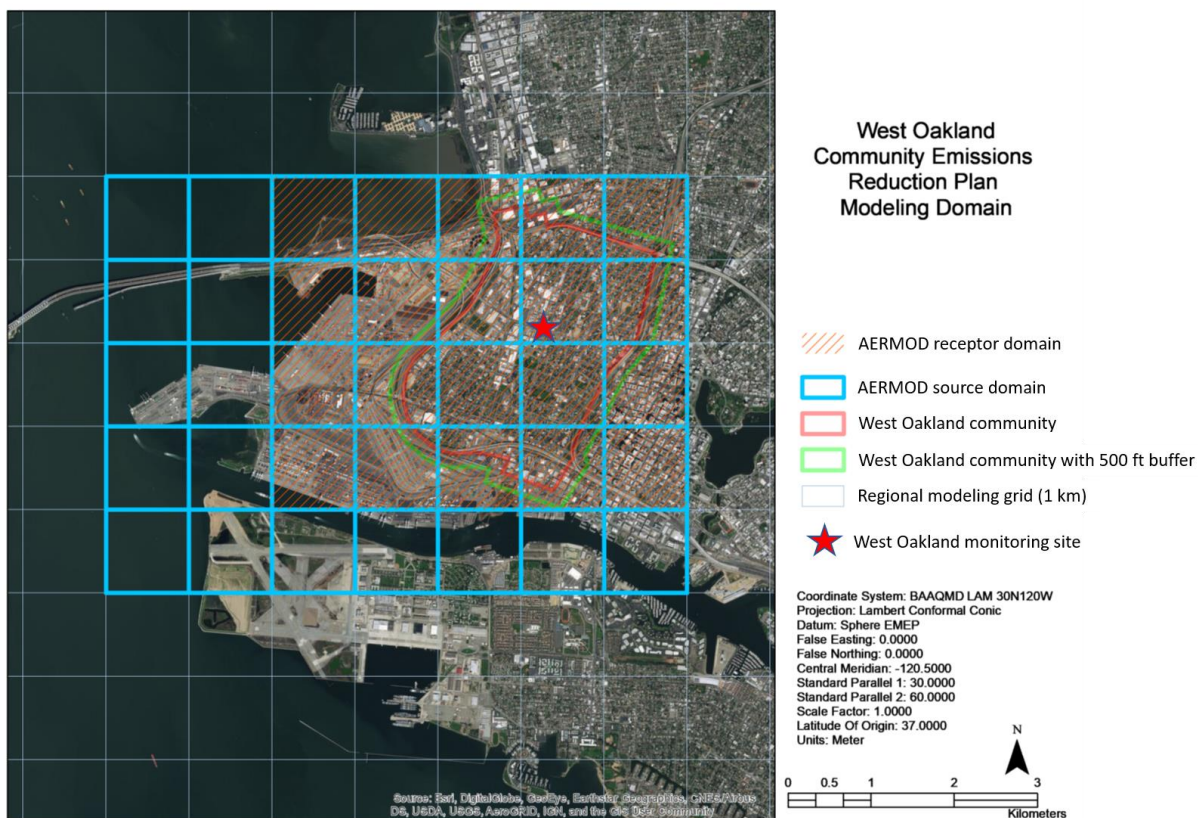


Figure 1.2: The West Oakland AERMOD modeling domain. The area outlined in blue represents the AERMOD source domain, and the red hatched area represents the AERMOD receptor domain.

1.1 PM_{2.5} and Its Health Impacts

PM_{2.5} is a complex mixture of suspended particles and liquid droplets in the atmosphere that have an aerodynamic diameter of 2.5 microns (μm) or less. An individual particle typically begins as a core or nucleus of carbonaceous material, often containing trace metals. These *primary* (directly emitted) particles usually originate from the incomplete combustion of fossil fuels or biomass. Layers of organic and inorganic compounds then deposit onto a particle, causing it to grow in size. These layers are largely comprised of *secondary* material that is not emitted directly. Secondary PM instead forms from chemical reactions of precursor gases released from combustion, agricultural activities, household activities, industrial sources, vegetation, and other sources. As a particle grows larger, gravity eventually causes it to be deposited onto a surface. Naturally emitted dust particles generally have diameters too large to be classified as PM_{2.5}.

Major human health outcomes resulting from PM_{2.5} exposure include: aggravation of asthma, bronchitis, and other respiratory problems, leading to increased hospital admissions; cardiovascular symptoms, including chronic hardening of arteries and acute triggering of heart

attacks; and decreased life expectancy, potentially on the order of years. Smaller particles have increasingly more severe impacts on human health as compared to larger particles. This occurs in part because smaller particles can penetrate more deeply into the human body. For the Bay Area, public health impacts from PM_{2.5} may well exceed the combined impacts of all other currently regulated air pollutants.

District staff have previously evaluated the health and monetary impacts of PM_{2.5} concentrations in the Bay Area for 2010. Findings of this evaluation are documented in a report by Tanrikulu, et al. (2011).

1.2 Formation of PM_{2.5} in the Bay Area

In the Bay Area, PM_{2.5} concentrations can build up during winter months (December, January and February) under stable atmospheric conditions that trap pollutants near the ground. Winters with frequent stagnant periods tend to have a higher number of days with elevated PM_{2.5} than winters with more periods of windy and stormy conditions. Consecutive stagnant, clear winter days are typically required for PM_{2.5} episodes to develop. PM_{2.5} episodes are regional in nature and impact most Bay Area locations.

The Chemical Mass Balance (CMB) model was previously applied for PM_{2.5} source apportionment using specialized measurements mostly obtained during the years 1999-2014. CMB is a statistical receptor model that uses speciated PM_{2.5} measurements to estimate the contribution of individual source categories to observed PM_{2.5} levels. CMB analyses for the Bay Area showed that primary combustion sources (both fossil fuels and biomass) were the largest PM_{2.5} contributors in all seasons. The biomass combustion contribution to peak PM_{2.5} levels was about 2-4 times higher during winter than for other seasons. Secondary PM_{2.5} levels were mostly elevated during the winter months, with ammonium nitrate being the key component of wintertime secondary PM_{2.5}. This semi-volatile PM_{2.5} component is stable in its solid form during the cooler winter months. Secondary ammonium sulfate PM_{2.5} levels were generally low (< 1-2 µg/m³) but non-negligible. Sea salt, geological dust, and tire and brake wear contributed minimally to PM_{2.5} concentrations (Tanrikulu et al., 2009).

Meteorological cluster analysis, a data mining technique, was implemented to determine how weather patterns impact PM_{2.5} levels. Clustering was applied to measurements from every winter day across more than 10 years. This method provided a robust representation of how prevailing weather conditions affected the development of PM_{2.5} episodes. Such episodes generally developed under: stable atmospheric conditions inhibiting vertical dispersion; clear and sunny skies favoring enhanced secondary PM_{2.5} formation; and pronounced overnight drainage (downslope) flows off the Central Valley rims, causing low-level air in the Central Valley to empty through the Delta and into the Bay Area along its eastern boundary. Atmospheric transitions of aloft weather systems profoundly influenced the surface winds that determine PM_{2.5} levels. Surface conditions stagnated whenever an upper-level high pressure

system moved over Central California. Persisting high pressure conditions allowed PM_{2.5} buildup, and Bay Area 24-hour elevated PM_{2.5} generally occurred after 2-4 days.

A refined cluster analysis further characterized the upwind Central Valley conditions during Bay Area episodes. Two distinct inter-regional air flow patterns were associated with different types of Bay Area episodes. Most elevated PM days were associated with winds from the Sacramento Valley to the northeast entering the Bay Area through the Delta. Peak PM_{2.5} levels typically occurred along the Delta and at San Jose for this type of episode. A minority of elevated PM days were associated with winds from the San Joaquin Valley from the southeast entering the Bay Area through the Delta. Peak PM_{2.5} levels typically occurred along the Delta and in the East Bay (at Livermore, Concord, Vallejo or San Rafael, and to a lesser degree at Oakland and San Francisco) for this type of episode. The remaining relatively moderate episodes could not be associated with any distinct inter-regional transport pattern linking the Bay Area and surrounding air basins.

2. Observations and Data Analysis

2.1 Ambient Measurements

Both meteorological and air quality data have been continuously collected in the Bay Area and surrounding regions for many years. In 2016, there were twenty-six PM monitoring stations within the 1-km modeling domain - sixteen in the Bay Area and ten outside the region. Table 2.1 lists PM monitoring stations used in this study with their annual and quarterly average PM_{2.5} values. Figure 2.1 shows the spatial distribution of monitored annual average PM_{2.5} concentrations for 2016. A complete list of monitoring stations, types of measurements, and the purpose of their use in this study is provided in Appendix A. The air quality monitoring network plan published by BAAQMD (Knoderer et al., 2017) provides additional details on the District's monitoring network.

All ambient data used in this study were subjected to quality assurance checks and validated prior to being used. These data were used for the development of a conceptual model of PM formation in the region, establishment of relationships among emissions, meteorology and air quality, evaluation of models, and four-dimensional data assimilation (FDDA), in which meteorological observations are used by the meteorological model to “nudge” simulations toward observations.

Hourly average data are used for most analyses and model evaluation, but monthly, quarterly or annual averages are presented here for brevity.

2.2 Data Analysis

In 2016, the annual average PM_{2.5} concentrations (Table 2.1) at two Bay Area air monitoring stations (Sebastopol and Gilroy) were between 5 µg/m³ and 6 µg/m³. These two sites captured the lowest PM_{2.5} levels in the Bay Area. At three other air monitoring stations (Concord, Oakland and San Rafael), PM_{2.5} concentrations were between 6 µg/m³ and 7 µg/m³, and at four other stations (Berkeley Aquatic Park, Livermore, San Francisco and Vallejo), they were between 7 µg/m³ and 8 µg/m³. At the remaining seven stations (Napa, San Pablo, Laney College, Oakland West, Redwood City, San Jose - Jackson and San Jose - Knox Avenue), PM_{2.5} levels were above 8 µg/m³. San Jose - Knox Avenue had the highest Bay Area annual average PM_{2.5} concentration (9.2 µg/m³).

Outside of Napa, the stations with annual average PM_{2.5} concentrations above 8 µg/m³ extend from the north Bay to the south Bay. Previous analyses showed that PM_{2.5} levels at these locations were influenced by local sources and the transport of pollutants from the Central Valley. Elevated concentrations at Napa are mostly due to local residential wood burning and the transport of PM from both residential wood burning and wildfire emissions.

While PM_{2.5} levels at several Bay Area stations, such as Laney College, West Oakland and Livermore, showed little change from one quarter to another, another set of stations (including Napa, Vallejo and San Francisco) had significant differences between quarters (Table 2.1). These stations are impacted by transport and seasonal changes in meteorology and/or emissions, such as wood burning.

Table 2.1: PM stations in the 1-km modeling domain with their annual and quarterly average PM_{2.5} values.

Station Name	PM _{2.5} Averages (µg/m ³) for 2016				
	ANNUAL	QTR_01	QTR_02	QTR_03	QTR_04
Stations in the Bay Area					
Berkeley Aquatic Park	7.2	-- ^a	-- ^a	7.7	6.6
Concord	6.2	6.0	4.3	4.6	9.4
Gilroy	5.7	5.9	6.1	6.8	4.1
Laney College	8.8	8.9	9.4	8.7	8.1
Livermore	7.6	7.4	7.2	8.4	7.3
Napa	8.9	6.5	7.2	10.4	11.1
Oakland	6.2	5.2	5.9	6.4	7.2
Oakland West	8.7	9.6	8.9	7.6	8.6
Redwood City	8.7	6.8	10.3	10.6	6.7
San Francisco	7.8	8.5	8.1	5.9	8.4
San Jose - Jackson	8.3	8.0	8.0	8.8	8.4
San Jose - Knox Avenue	9.2	9.0	8.6	9.9	9.2
San Pablo	8.1	7.6	8.9	7.8	8.2
San Rafael	6.6	7.0	6.1	5.9	7.1
Sebastopol	5.1	4.9	4.6	4.0	6.5
Vallejo	7.6	8.4	5.6	6.0	10.2
Stations outside the Bay Area					
Manteca	9.9	10.8	7.5	8.8	12.3
San Lorenzo Valley Middle School	5.3	5.4	5.2	4.7	5.8
Roseville - N Sunrise Ave	6.8	6.7	5.7	6.7	8.3
Sacramento Health Department - Stockton Blvd.	6.9	7.8	5.7	6.6	8.3
Sacramento - 1309 T Street	7.6	7.2	5.6	7.1	10.9
Sacramento - Bercut Drive	-- ^a	-- ^a	-- ^a	-- ^a	14.6
Sacramento - Del Paso Manor	8.7	8.6	6.1	7.2	13.2
Santa Cruz	5.4	5.8	5.9	5.3	4.5
Stockton - Hazelton	11.8	13.9	8.2	10.0	15.2
Woodland - Gibson Road	6.3	5.2	5.4	8.1	6.9

^aData missing or invalidated.

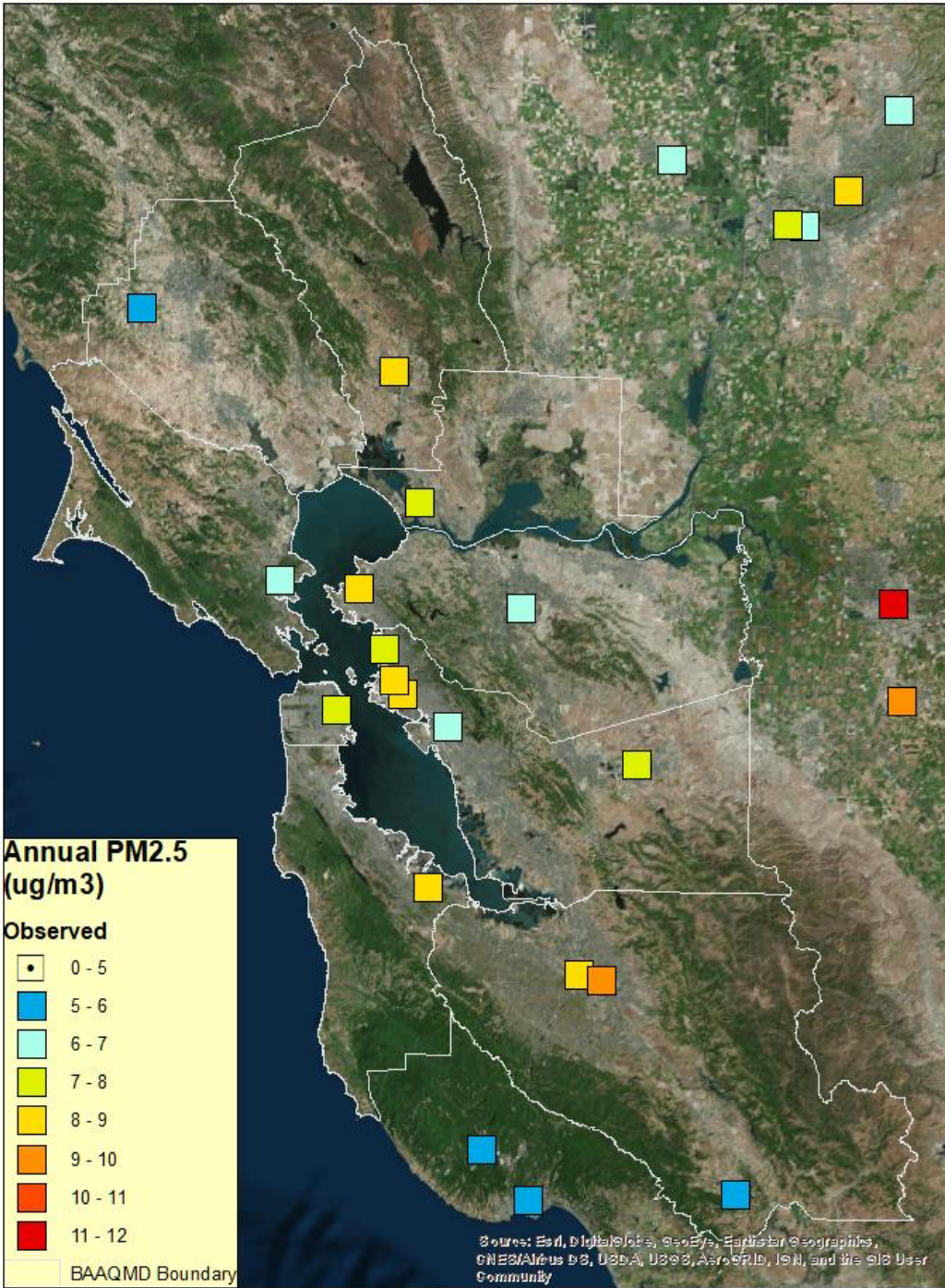


Figure 2.1: Spatial distribution of observed annual average PM_{2.5} concentrations for 2016 within the 1-km modeling domain.

3. Modeling

3.1 Emissions Inventory Preparation

The 2016 modeling emissions inventory includes estimates for area sources,² point sources, onroad mobile sources, nonroad mobile sources, and biogenic sources. The inventory was assembled from a variety of data sources, including the District's in-house emissions estimates, emissions data from ARB, and outputs from ARB's EMFAC2017 model (see Table 3.1). ARB emissions data were used for all anthropogenic sources in non-BAAQMD counties with the exception of onroad mobile sources. County- and facility-level ARB emissions data for the entire state of California were downloaded from ARB's FTP site in June 2018. These data were in SMOKE-ready format and were consistent with the current version of ARB's online repository of emissions inventory data that was developed to support the preparation of ozone State Implementation Plans (SIPs) for non-attainment areas in California. At the time of this work, the latest version of ARB's SIP inventory was version 1.05, which was prepared for a base year of 2012 and projected to various future years, including 2016.³

For area sources, ARB's county-level emissions estimates for residential wood combustion in BAAQMD counties were adjusted to account for the impact of the District's winter Spare the Air program, which prohibits wood burning when air quality is forecast to be unhealthy. This adjustment was based on survey-based wood combustion emissions estimates developed by District staff, comparisons with wood combustion emissions estimates for other air districts, and discussions with ARB staff. Additional details in residential wood combustion emissions are provided in Appendix B.

For onroad mobile sources, ARB's EMFAC2017 model was run for the entire state of California for each month in 2016 to produce county-level, month-specific emissions estimates. EMFAC2017 reports emissions by vehicle type and emission mode (e.g., idling, running exhaust, brake wear, tire wear). EMFAC2017 outputs were converted to SMOKE-ready format using a Perl script developed by BAAQMD staff.

For point sources, ARB emissions estimates for BAAQMD counties were replaced by detailed, in-house data prepared in California Emission Inventory Development and Reporting System (CEIDARS) format. These point source emissions data were representative of calendar year 2012 and were projected to 2016 using industry-specific growth factors from ARB's California Emissions Projection Analysis Model (CEPAM). The CEIDARS data were converted to SMOKE-ready format using a Perl script developed by BAAQMD staff.

Biogenic emissions estimates were prepared using EPA's Biogenic Emission Inventory System (BEIS), version 3.61, which estimates emissions from vegetation and soil using land use data;

² Area sources are stationary sources such as dry cleaners that are too small or numerous to treat as individual point sources.

³ See <http://www.arb.ca.gov/app/emsinv/2016ozsip/2016ozsip/>.

vegetation-specific emission rates for isoprene and other species; and gridded, hourly meteorological data from the WRF model.

3.1.1 SMOKE Processing

Emissions inventory data assembled from the sources described above were processed through version 4.5 of the SMOKE emissions processor to develop CMAQ-ready emissions inputs for each day of 2016. SMOKE uses the processing steps described below to convert “raw” emissions inputs to the spatial, temporal, and chemical resolution required by CMAQ or an equivalent air quality model.

Table 3.1: Summary of data sources used to develop the 2016 modeling inventories.

Region	Source Sector	Data Source
BAAQMD Counties ^a	Area	ARB county-level emissions estimates, with adjustments made to residential wood combustion emissions
	Nonroad	ARB county-level emissions estimates
	Onroad	County-level, month-specific EMFAC2017 outputs
	Point	In-house CEIDARS data
	Biogenic	Hourly outputs from EPA’s BEISv3.61 model
Non-BAAQMD Counties	Area	ARB county-level emissions estimates
	Nonroad	ARB county-level emissions estimates
	Onroad	County-level, month-specific EMFAC2017 outputs
	Point	ARB facility-level emissions estimates
	Biogenic	Hourly outputs from EPA’s BEISv3.61 model

^aAlameda, Contra Costa, Marin, Napa, San Francisco, San Mateo, and Santa Clara counties, plus the southern portion of Sonoma County and the western portion of Solano County.

Spatial allocation

SMOKE assigns county- or facility-level emissions to individual grid cells in the modeling domain. For point sources, emissions are assigned to grid cells based on the location coordinates (i.e., latitude and longitude) of emission release points. For county-level area, nonroad, or onroad emissions estimates, SMOKE allocates emissions to grid cells using spatial allocation factors developed from “surrogate” geospatial data sets such as land use or socioeconomic data. Geospatial data sets used to develop the surrogates used in SMOKE include land use data from the Association of Bay Area Governments (ABAG) (Reid, 2008). For counties in the District’s jurisdiction, gridded surrogate data were available at 1-km grid resolution. However, for counties outside the District, only 4-km surrogate data were available, so these data were parsed to create a set of pseudo 1-km surrogates.

Temporal allocation

SMOKE assigns annualized or average day emissions to the specific dates and hours being modeled using temporal profiles that reflect source-specific activity patterns by month, day of week, and hour of day. Temporal profiles from ARB’s CEIDARS database were used in SMOKE to

temporally allocate area, point, and nonroad mobile source emissions. For onroad mobile sources, temporal profiles that ARB developed from its California Air Resources Board Vehicle Activity Database (CalVAD) were used.⁴

Chemical speciation

SMOKE disaggregates total organic gas (TOG) and PM_{2.5} emissions into a series of model species that CMAQ uses to represent atmospheric chemistry. For the 2016 CMAQ modeling, speciation profiles developed for the SAPRC07 chemical mechanism were applied to TOG emissions from all sources, and profiles developed for the AERO6 aerosol module were applied to PM_{2.5} emissions from all sources.

The SMOKE system includes an implementation of EPA's Biogenic Emission Inventory System (BEIS), version 3.61, which estimates biogenic emissions using land use data; vegetation specific emission rates for isoprene and other species; and gridded, hourly meteorological data from the WRF model. BEISv3.61 was run within SMOKE to prepare 2016 biogenic emissions estimates for the 1-km modeling domain.

Once SMOKE runs were completed, a number of quality assurance checks were performed on the resulting emissions data. First, plots of gridded emissions were generated to examine the spatial distribution of emissions. Similarly, diurnal plots were generated to examine hourly variations in emissions by source sector and to ensure that the patterns make sense. In addition, SMOKE's SMKREPORT utility was used to generate tabular summaries of emissions by pollutant, county, grid cell, hour, and source category. This information was used in a variety of ways, including:

- Comparing emissions before and after key processing steps to ensure that any changes in the mass of emissions make sense. For example, for counties that only partially lie within the modeling domain, total emissions should decrease after the gridding step.
- Sorting emissions by source category code (SCC) or facility ID to identify key contributors to total emissions for each pollutant and to identify potential outliers.
- Summarizing emissions by pollutant and county to ensure that geographic distributions make sense (e.g., SO₂ emissions are highest in Contra Costa County where refineries are concentrated).
- Extracting emissions for grid cells in the West Oakland AERMOD modeling domain to identify key sources and compare emissions by source sector with the District as a whole.

These checks identified several issues, including PM_{2.5} hotspots at two landfills in eastern Alameda County. Our modelers worked with staff from the District's Emissions & Community Exposure Assessment section to correct the emissions from these and other point sources.

⁴ The CalVAD database fuses available data sources such as Caltrans Weigh-in-Motion (WIM) data and Highway Performance Monitoring System (HPMS) data to produce a best estimate of vehicle activity by class.

3.1.2 Emissions Summaries

This subsection provides emissions density plots and summary tables for PM_{2.5}, and similar information for additional pollutants can be found in Appendix B. Figure 3.1 shows annual average PM_{2.5} emissions for the 1-km modeling domain. Table 3.2 summarizes the annual average PM_{2.5} emissions by county and source sector, as reported by the SMOKE emissions model. Within the District's jurisdiction, annual average PM_{2.5} emissions total 33.7 tons per day (tpd). The area source sector accounts for about half of this total (17 tpd), and individual source categories that are key contributors to total PM_{2.5} emissions include residential wood combustion, fugitive dust from roadways and construction sites, and commercial cooking.

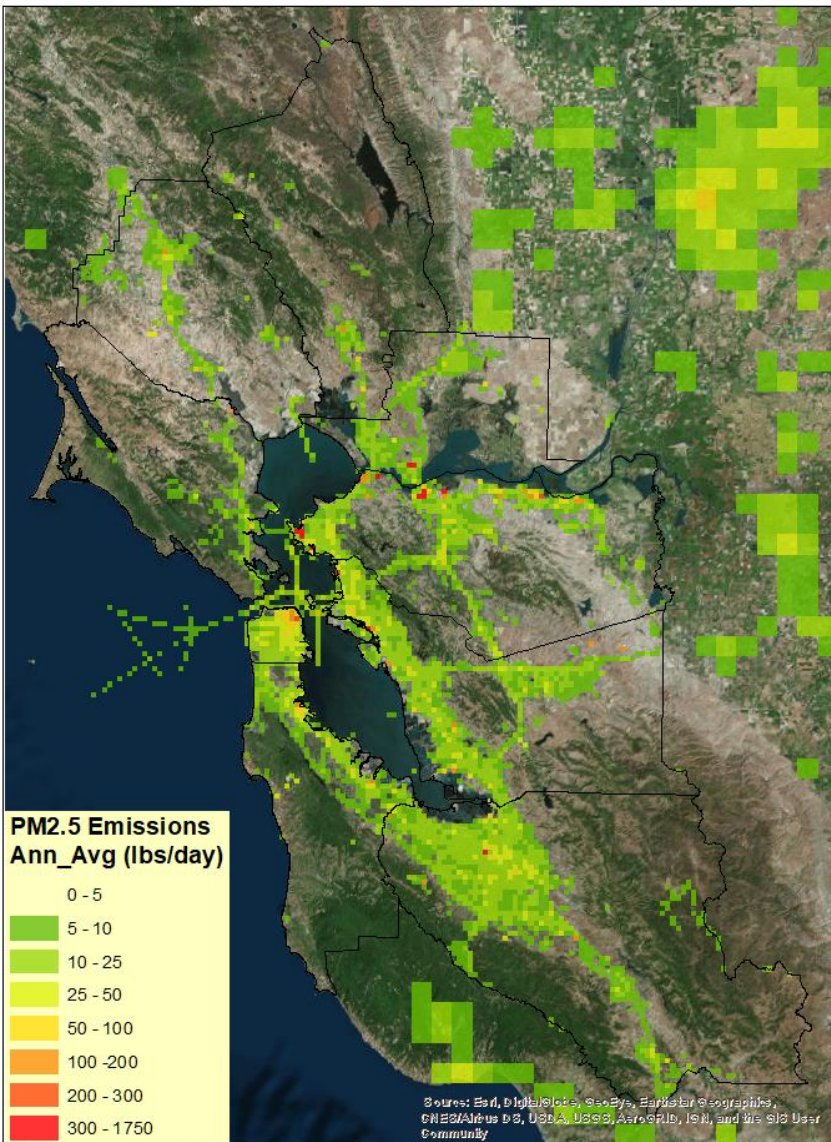


Figure 3.1: Spatial distribution of annual average PM_{2.5} emissions for the 1-km modeling domain.

Table 3.2: Summary of 2016 PM_{2.5} anthropogenic emissions (tpd) by geographic area and source sector.

Geographic Area	Area	Nonroad	Onroad	Point	Total
Alameda	3.0	0.5	1.4	1.3	6.2
Contra Costa	3.1	0.5	0.8	4.2	8.7
Marin	0.8	0.2	0.2	0.1	1.3
Napa	0.8	0.2	0.1	0.1	1.2
San Francisco	1.2	1.0	0.3	0.1	2.7
San Mateo	1.4	0.5	0.5	0.4	2.7
Santa Clara	3.9	0.6	1.3	0.7	6.5
Solano ^a	1.3	0.1	0.3	0.5	2.1
Sonoma ^a	1.4	0.3	0.3	0.2	2.2
<i>BAAQMD Subtotal</i>	<i>17.0</i>	<i>3.9</i>	<i>5.2</i>	<i>7.5</i>	<i>33.7</i>
Non-BAAQMD Counties	23.7	2.2	2.9	2.4	31.2
Domain Total	40.7	6.1	8.0	9.9	64.9

^aEmissions totals for Solano and Sonoma counties only include the portion of those counties in BAAQMD's jurisdiction.

For the West Oakland AERMOD modeling domain, annual average PM_{2.5} emissions total 0.35 tpd, or about 1% of the BAAQMD total. Figure 3.2 shows that the distribution of emissions by source sector in West Oakland differs from the District as a whole. In West Oakland, onroad and nonroad mobile sources account for 66% of total PM_{2.5} emissions, while the same sources only account for 27% of total PM_{2.5} emissions districtwide. Figure 3.3 shows the spatial distribution of PM_{2.5} emissions across the 1-km grid cells that coincide with the local-scale AERMOD modeling domain.

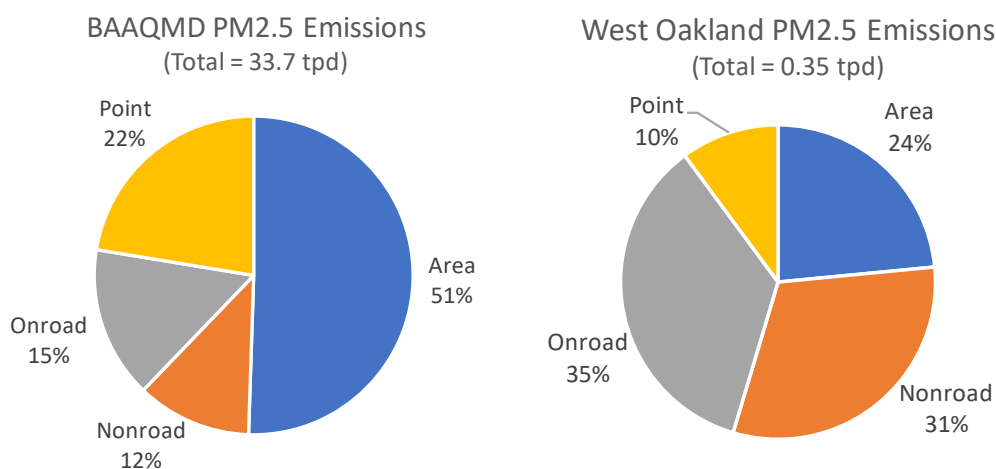


Figure 3.2: PM_{2.5} emissions by source sector for the District (left) and West Oakland (right).

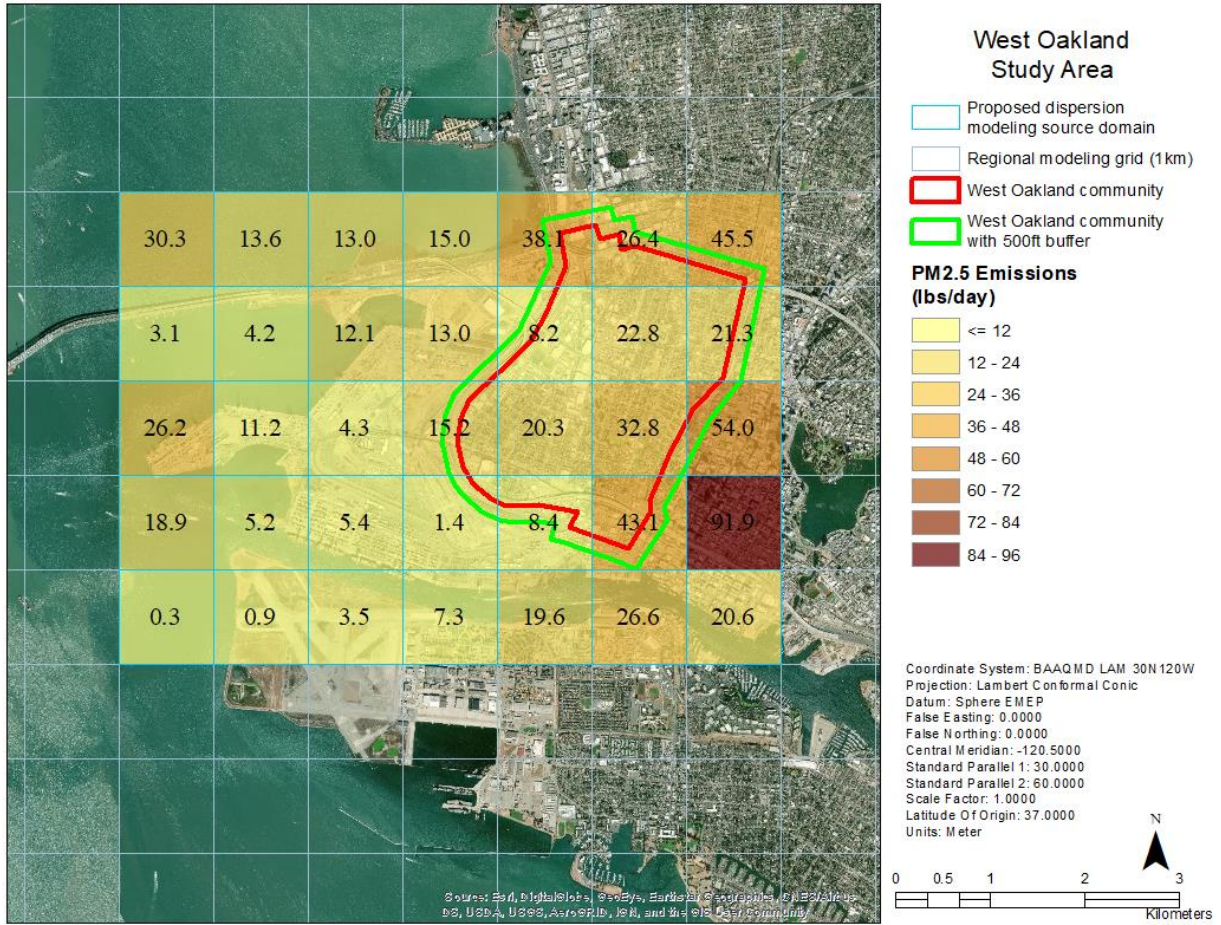


Figure 3.3: Spatial distribution of annual average PM_{2.5} emissions in West Oakland.

3.2 Meteorological Modeling

The Weather Research and Forecasting (WRF) Model version 3.8 was used to prepare meteorological inputs to CMAQ. Four nested modeling domains were used (Figure 3.4). The outer domain covered the entire western United States at 36-km horizontal grid resolution to capture synoptic (large-scale) flow features and the impact of these features on local meteorology. The second domain covered California and portions of Nevada at 12-km horizontal resolution to capture mesoscale (sub-regional) flow features and their impacts on local meteorology. The third domain covered Central California at 4-km resolution to capture localized air flow features. The 4-km domain included the Bay Area, San Joaquin Valley, and Sacramento Valley, as well as portions of the Pacific Ocean and the Sierra Nevada mountains. The fourth domain covered the Bay Area and surrounding regions at 1-km resolution. All four domains employed 50 vertical layers with thickness increasing with height from the surface to the top of the modeling domain (about 18 km).

Meteorological variables are estimated at the layer midpoints in WRF. The thickness of the lowest layer nearest the surface was about 25 m. Thus, meteorological variables near the surface were estimated for a height of about 12.5 m above ground level. The model configuration was tested using available physics options, including: (1) planetary boundary layer processes and time-based evolution of mixing heights; (2) choice of input database for WRF; (3) four-dimensional data assimilation (FDDA) strategy; (4) horizontal and vertical diffusion; (5) advection scheme; and (6) initial and boundary conditions. The final choice of options was the one proved to best characterize meteorology in the domain.

WRF was applied for 2016 to estimate parameters required by the air quality model, including hourly wind speed and direction, temperature, humidity, cloud cover, rain and solar radiation levels. Observations are assimilated into the model during the simulations to minimize the difference between simulations and real-world measurements. Two types of nudging methods were employed (analysis and observation). The NCEP North America Mesoscale (NAM) 12-km analyzed meteorological fields were used for analysis nudging as well as for initializing the model. The NCEP ADP Global Surface and Upper Air Observational Weather Data were used for observational nudging. A list of these stations for the 1-km domain is given in Appendix A.

The analysis nudging was applied to the 36-km and 12-km domains. Frequency of surface analysis nudging was every three hours, while the frequency of 3D analysis nudging was every six hours. The 3D analysis nudging of winds was performed over all model layers, but the 3D analysis nudging of temperature and humidity was limited to layers above the planetary boundary layer. The observation nudging of wind was applied to all four domains every three hours.

The WRF model was rigorously evaluated for accuracy. Observations used to evaluate WRF were taken from the EPA's Air Quality System, the BAAQMD meteorological network, and the National Climate Data Center. A list of these stations for the 1-km domain is given in Appendix A. Hourly and daily time series plots of observed and simulated wind, temperature

and humidity were generated at each observation station and compared to each other hour by hour and day by day. Simulated hourly areal plots of wind, temperature, humidity, planetary boundary layer height, pressure and other fields were generated and quantitatively compared against observations where observations were available.

WPS Domain Configuration

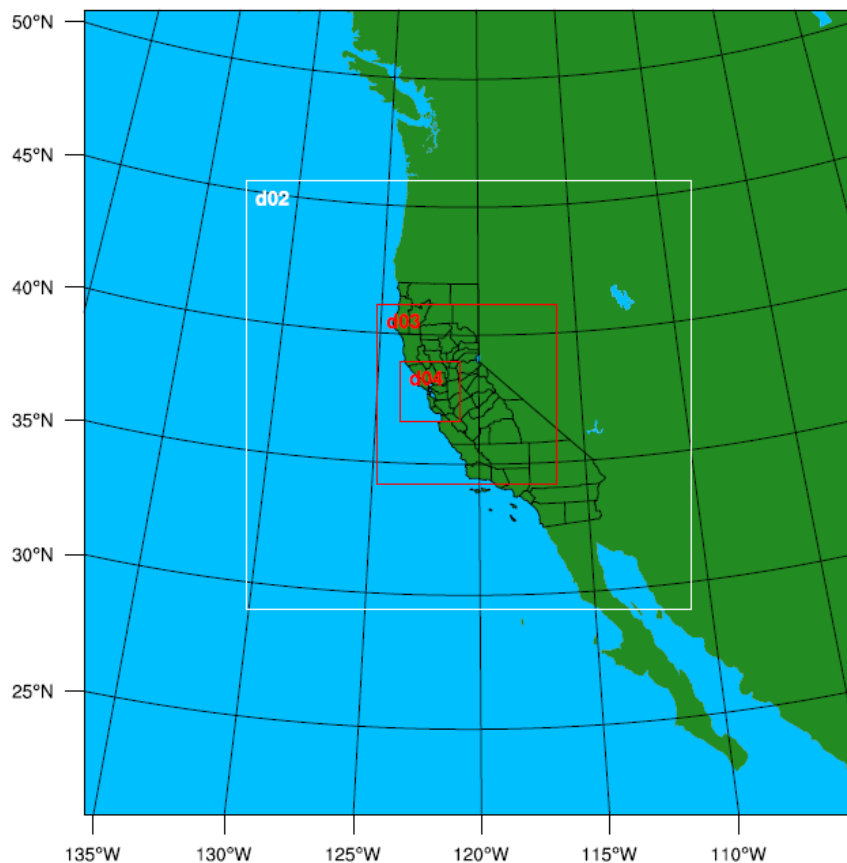


Figure 3.4: Nested WRF modeling domains.

These plots were also qualitatively evaluated for known meteorological features of the modeling domain, especially at 4-km and 1-km resolutions. These features include slope flows, channeled flows, sea breeze and low-level jet. The vertical profile of observed and simulated meteorological fields was compared at several upper air meteorological stations, including Oakland, Medford, Reno and Las Vegas, and at a temporary station established at Bodega Bay. RAMBOLL's METSTAT program (Emery et al., 2001) was used to statistically evaluate the performance of WRF. The statistical metrics used in this evaluation are defined in Appendix C.

The WRF model performed reasonably well in every evaluation category. The estimated bias, gross error, root mean square error (RMSE), and index of agreement (IOA) are within established criteria for acceptable model performance for every day of 2016. In other words,

performance obtained from the Bay Area applications of WRF is similar or slightly better than performance obtained from applications elsewhere, available from literature.

Performance statistics were generated for all days of 2016. Samples from ten winter (December 1-10) and ten summer (July 1-10) days are shown in Table 3.3, while Table 3.4 shows maximum and minimum skill scores of WRF for all of 2016.

Simulated and observed wind speed, wind direction, temperature and humidity, for both hourly and annual time periods, were compared at each station. Time series comparisons for West Oakland, Vallejo and San Jose are shown in Appendix C. These three stations were selected because West Oakland is the area of interest for this study. Vallejo is strategically located in the Delta to capture air flow between the Bay Area and the Central Valley. San Jose is an important sub-region of the Bay Area representing outflows. Good model performance at Vallejo and San Jose is critical to simulate representative meteorological features in West Oakland.

The WRF model was also compared against upper air measurements at Oakland, a site operated by the National Weather Service with twice daily upper air measurements and at Bodega Bay, a temporary site established by the California Baseline Ozone Transport Study with daily ozonesonde and meteorological measurements. Simulated winds, temperatures and humidity matched these upper air measurements very well. Details can be found in Appendix C.

Table 3.3: Sample (December 1-10 and July 1-10) statistical scores of WRF.

Parameter	Metric	Units	12/01	12/02	12/03	12/04	12/05	12/06	12/07	12/08	12/09	12/10
Wind Speed	Bias	(m/s)	-0.21	-0.43	-0.21	-0.68	-0.35	-0.38	-0.67	-0.32	-0.35	-0.77
Wind Speed	Gross Error	(m/s)	1.28	1.61	1.05	1.08	0.91	1.13	1.16	1.49	0.93	1.33
Wind Speed	RMSE	(m/s)	1.68	2.07	1.4	1.5	1.22	1.49	1.48	1.88	1.19	1.7
Wind Speed	IOA	-- ^a	0.78	0.75	0.64	0.67	0.66	0.73	0.71	0.7	0.66	0.79
Wind Direction	Bias	(deg)	2.21	-1.32	-6.78	3.74	4.73	13.09	3.22	5.08	-6.37	6.45
Wind Direction	Gross Error	(deg)	32.17	24.42	57.64	45.58	42.43	43.08	32.72	50.97	38.39	22.33
Temperature	Bias	(K)	1.26	1.25	2.6	0.85	0.35	1.76	2.08	0.75	-0.31	-0.68
Temperature	Gross Error	(K)	32.17	1.72	2.66	1.47	1.18	1.85	2.26	1.64	1.43	0.92
Temperature	RMSE	(K)	2.09	2.25	3.2	1.87	1.53	2.41	2.71	2.09	1.82	1.15
Temperature	IOA	-- ^a	0.93	0.91	0.87	0.94	0.94	0.88	0.82	0.89	0.88	0.87
Parameter	Metric	Units	7/01	7/02	7/03	7/04	7/05	7/06	7/07	7/08	7/09	7/10
Wind Speed	Bias	(m/s)	-0.96	-1.12	-0.96	-1.15	-1.04	-0.95	-1.08	-0.91	-1.27	-0.91
Wind Speed	Gross Error	(m/s)	1.35	1.48	1.37	1.53	1.44	1.43	1.51	1.41	1.7	1.44
Wind Speed	RMSE	(m/s)	1.81	1.91	1.77	2.02	1.99	1.86	2.01	1.8	2.26	1.88
Wind Speed	IOA	-- ^a	0.71	0.76	0.75	0.71	0.71	0.75	0.71	0.7	0.71	0.74

Wind Dir	Bias	(deg)	-0.16	0.36	-3.34	-1.97	-3.95	-1.52	0.97	3.73	3.51	4.82
Wind Dir	Gross Error	(deg)	28.1	27.05	24.63	27.85	24.76	23.07	20.44	21.91	21.83	28.44
Temperature	Bias	(K)	1.3	1.47	0.24	0.39	1.2	1.09	0.87	0.34	0.06	0.59
Temperature	Gross Error	(K)	1.89	1.9	1.21	1.14	1.58	1.36	1.12	1.14	0.87	1.17
Temperature	RMSE	(K)	2.43	2.34	1.56	1.48	1.99	1.69	1.39	1.43	1.09	1.54
Temperature	IOA	-- ^a	0.97	0.96	0.98	0.98	0.96	0.97	0.98	0.98	0.99	0.98

^aThe Index of Agreement (IOA) is a dimensionless quantity.

Table 3.4: Maximum and minimum statistical scores of WRF for 2016.

Parameter	Metric	Units	Max	Min
Wind Speed	Bias	(m/s)	1.02	-0.99
Wind Speed	Gross Error	(m/s)	2.03	0.57
Wind Speed	RMSE	(m/s)	2.5	0.76
Wind Speed	IOA	--	0.92	0.4
Wind Direction	Bias	(deg)	14.84	-12.56
Wind Direction	Gross Error	(deg)	81.37	13.5
Temperature	Bias	(K)	2.99	-1.62
Temperature	Gross Error	(K)	3.24	0.72
Temperature	RMSE	(K)	5.22	0.9
Temperature	IOA	--	0.98	0.47

3.3 Air Quality Modeling

Air quality modeling was conducted using the U.S. EPA’s Community Multiscale Air Quality (CMAQ) modeling system version 5.2. Two nested domains were used. The outer domain coincides with the third domain of the meteorological model and covers the Bay Area, San Joaquin Valley, and Sacramento Valley, as well as portions of the Pacific Ocean and the Sierra Nevada mountains at 4-km horizontal resolution. The inner domain covers the Bay Area and surrounding regions at 1-km horizontal resolution.

Both CMAQ modeling domains had 28 vertical layers. Below 1,500 m, the CMAQ layers match the WRF layers, while some upper-level meteorological model layers above 1,500 m were collapsed while preparing meteorological inputs for CMAQ to reduce computational time. This is a common practice in air quality modeling, as pollutant levels in layers aloft are relatively low and do not significantly impact concentrations at the surface. The thickness of CMAQ model layers was also increasing with height from the surface to the top of the modeling domain (about 18 km). The thickness of the first layer of CMAQ was kept the same as in WRF (about

25 m), meaning that pollutant concentrations are estimated at around 12.5 m above the surface (the midpoint of the first layer).

The outer domain provides initial conditions and hourly boundary conditions to the 1-km domain. As a result, the inner domain accounts for the contribution of emissions sources outside of the Bay Area to Bay Area PM levels. The outer domain was initialized and its boundary conditions were updated every six hours using outputs from a global air quality model (MOZART), available from the National Center for Atmospheric Research (NCAR).

CMAQ simulates both primary and secondary PM_{2.5}, with secondary PM_{2.5} formation being dependent upon photochemistry. The chemical mechanism used in this simulation was the Statewide Air Pollution Research Center version 2007 (SAPRC-07) mechanism. Secondary PM formulation was simulated using the Models-3 AE6 aerosol module.

Each month was simulated separately to distribute simulations over 12 computer nodes for computational efficiency. Each monthly simulation includes the last three days of the previous month as a spin-up period except for January, which includes the last five days of December 2015. Model outputs from the spin-up periods were not used in analyses.

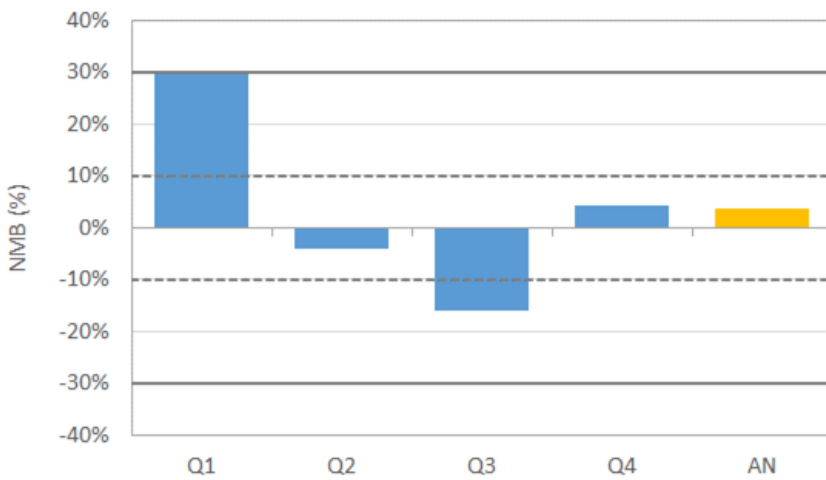
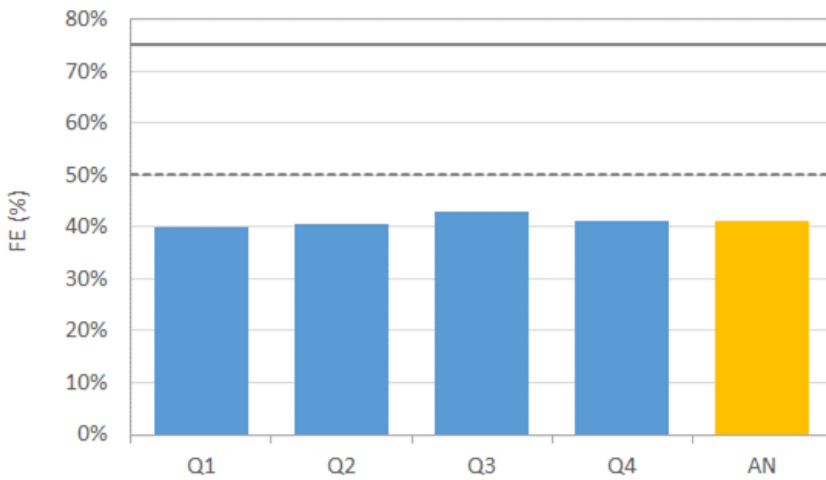
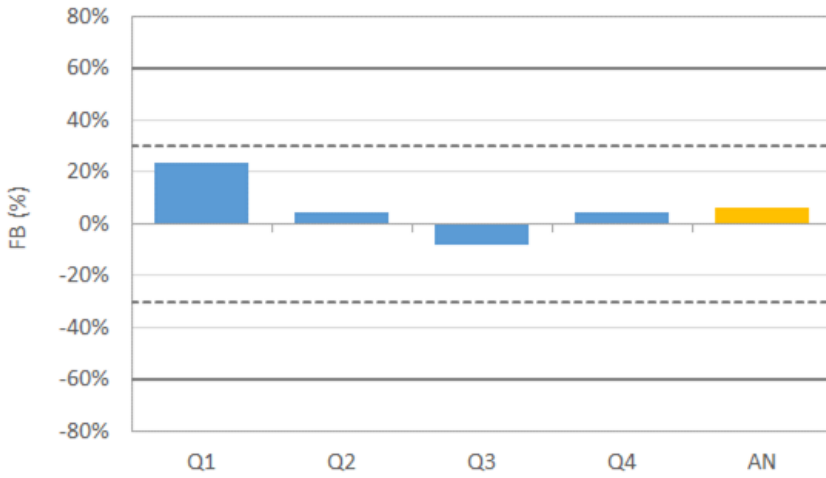
3.3.1 CMAQ Evaluation

The CMAQ model was rigorously evaluated for accuracy. Observations used to evaluate CMAQ were taken from the District's Data Management System and the EPA's Air Quality System. Hourly and daily time series plots of observed and simulated PM_{2.5} concentrations were generated at each observation station and compared to each other hour by hour and day by day. This evaluation also provided an opportunity to identify gaps in measurements and outliers. Hourly, daily, monthly, quarterly and annual average spatial plots of PM and precursor concentrations were generated for observed and simulated values, and simulated values were quantitatively compared against observations where observations were available.

These plots were also qualitatively evaluated for known air quality features that may be impacted by meteorology, emissions, chemistry and other environmental parameters. Examples include local and regional transport of pollutants, proximity of polluted areas to emission sources such as freeways, and the behavior of atmospheric chemistry.

Various statistical metrics were used to evaluate the performance of CMAQ. Standard statistical measures used for CMAQ evaluation are described in EPA's latest modeling guidance (EPA, 2018) and in Appendix D. These metrics were applied for daily average simulated PM_{2.5} concentrations over quarterly and annual periods. The CMAQ model performed reasonably well, meeting the performance goals proposed by Boylan and Russell (2006) and criteria by Emery et al. (2017), two well-known references for PM model evaluation. Figure 3.5 shows fractional bias, fractional error, normalized mean bias and normalized mean error for quarterly

and annual periods. The performance goals (dashed lines) and criteria (solid lines) are also shown in the figure as references.



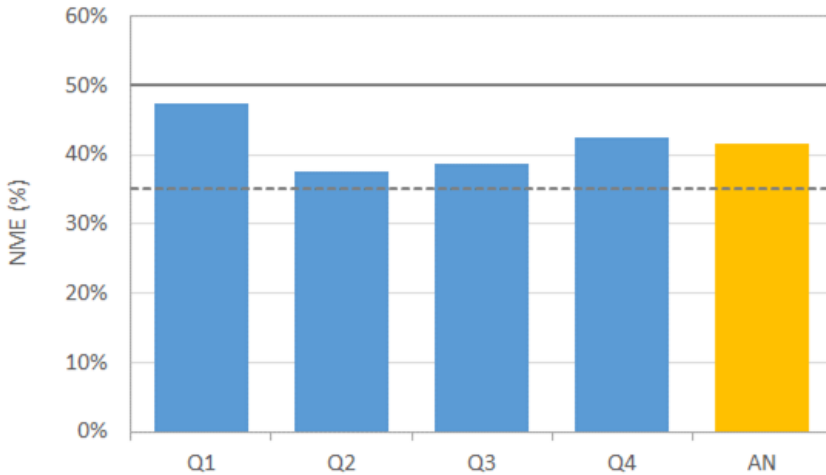


Figure 3.5: Quarterly and annual performance statistics for simulated PM_{2.5} over the 26 air monitoring sites within the 1-km modeling domain with performance goals (dashed lines) and criteria (solid lines) proposed by Boylan and Russell (2006) and Emery et al. (2017). FB stands for fractional bias, FE fractional error, NMB normalized mean bias and NME normalized mean error.

Additional comparisons between simulated and observed PM_{2.5} are discussed in Section 4 (Results) and in Appendix D. These comparisons largely focus on three selected Bay Area sites (West Oakland, Vallejo and San Jose) that are particularly relevant to West Oakland study.

4. Results

Comparison between the annual average simulated and observed PM_{2.5} concentrations (Figure 4.1) shows that the CMAQ model generally captured the observed PM_{2.5} pattern within the 1-km domain. High concentrations in both simulations and observations are evident in the northern San Joaquin Valley, along the I-580 and I-880 corridors from Richmond to the Oakland Airport, along the I-101 corridor near Redwood City, and in the San Jose metropolitan area. In the Sacramento area, the model shows overestimation biases and PM_{2.5} concentrations do not compare as well to observations as in the Bay Area. For Sacramento and other counties outside the Bay Area, we relied on the ARB's emission inventories, and further evaluation of these data may be warranted. The model also shows high concentrations along the I-880 corridor from Oakland Airport to San Jose and along the Delta from Antioch to Brentwood, although observations are unavailable in these areas.

Site by site comparisons between the model predictions and observations (Figure 4.2) show that at most Bay Area sites, the simulated annual average PM_{2.5} concentrations are within ± 1.0 $\mu\text{g}/\text{m}^3$ of observations. At a few sites (Concord, Oakland and Gilroy), the annual average PM_{2.5} concentrations were overestimated, and at one site (Napa), the annual average PM_{2.5} concentration was underestimated by as much as 2.1 $\mu\text{g}/\text{m}^3$.

Further analyses of model output showed that at sites with overestimated PM_{2.5}, both primary and secondary PM_{2.5} concentrations appear to be overestimated. This suggests that there may be multiple causes of overestimation. Primary PM_{2.5} concentrations can be overestimated due to overestimation of emissions, transport, and stability of the atmosphere. Secondary PM_{2.5} can be overestimated due to overestimation of precursor emissions, chemical conversion of the precursors to PM, transport of secondary PM_{2.5} or its precursors, and stability of the atmosphere.

Underestimation of PM_{2.5} at Napa is likely due to an underestimation of wood burning emissions or the transport of wildfire emissions to the North Bay. Wildfire emissions are not included in the modeling emissions inventory.

Figure 4.3 shows time-series plots of observed and simulated daily PM_{2.5} concentrations at three key Bay Area sites relevant to the West Oakland study: West Oakland, Vallejo and San Jose. It is evident from this figure that PM_{2.5} is generally overestimated during winter months and underestimated during summer months. However, on a monthly average basis, the CMAQ model is generally able to replicate the month-to-month variation in observed PM_{2.5} concentrations in West Oakland (Figure 4.4). The somewhat significant underestimation in September is likely due to lack of wildfire emissions in the CMAQ simulations.

During winter months, especially in February, the atmosphere is relatively sunny, calm and cool in the Bay Area, ideal conditions for the formation of secondary PM and for allowing

ammonium nitrate to remain in particle form. All of these suspected causes of overestimation are under further investigation and evaluation.

Wintertime overestimation and summertime underestimation of $PM_{2.5}$ by the WRF-CMAQ couple have also been reported elsewhere, and developers of the modeling system are aware of this problem (Appel et al., 2017; Simon et al., 2012). Efforts are underway by the model developers and District staff to minimize errors and to improve model performance for both winter and summer.

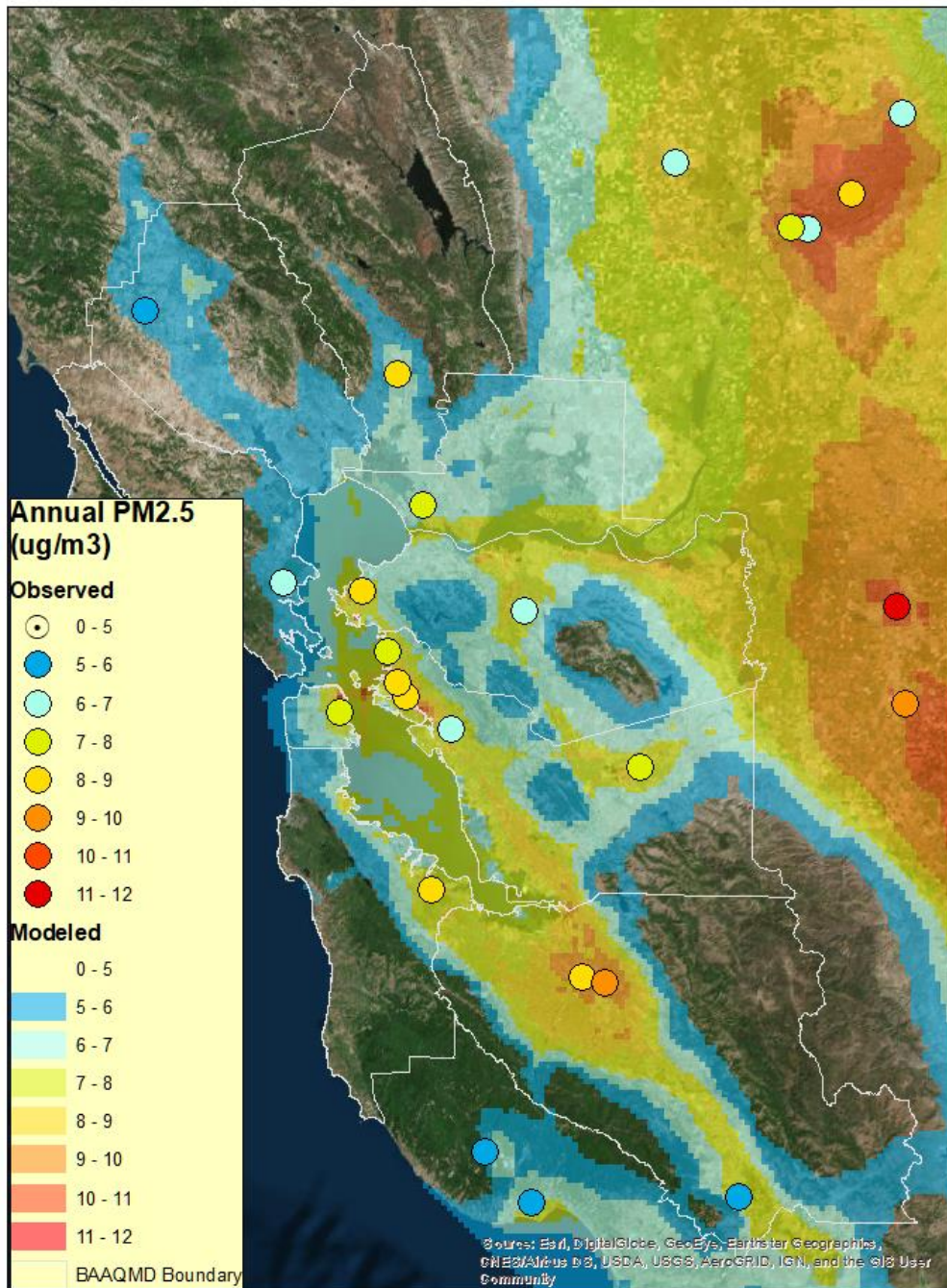


Figure 4.1: Spatial distribution of simulated and observed annual average PM_{2.5} concentrations within the 1-km modeling domain.

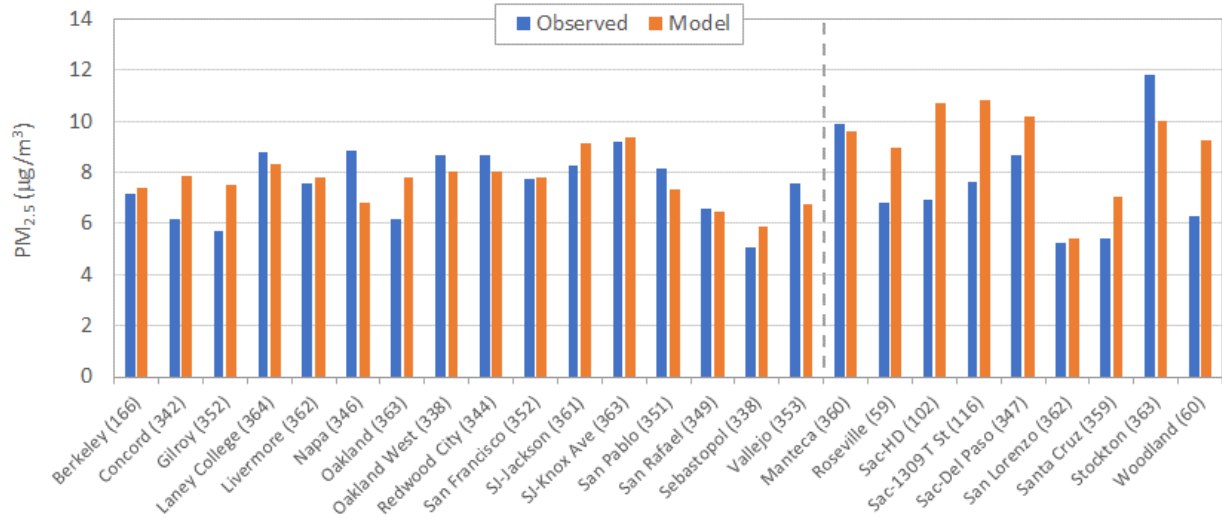
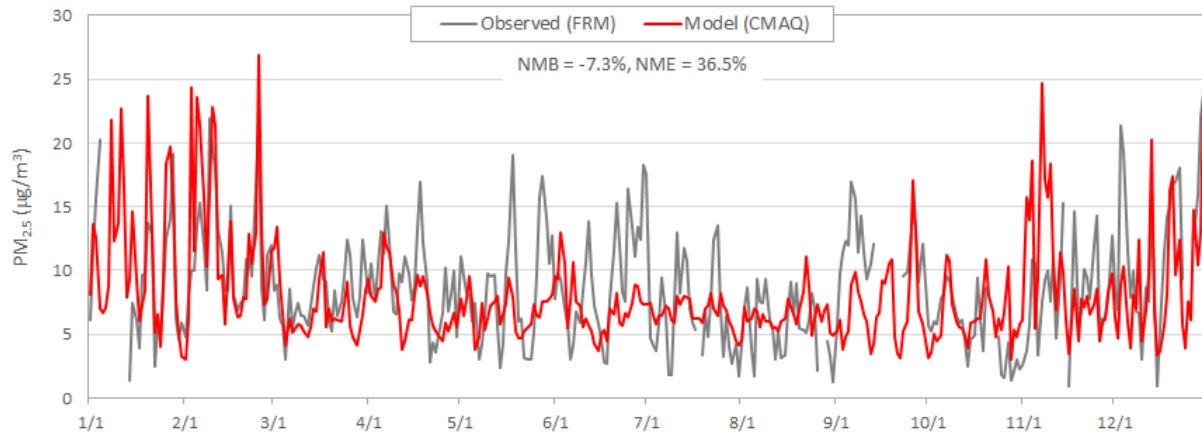
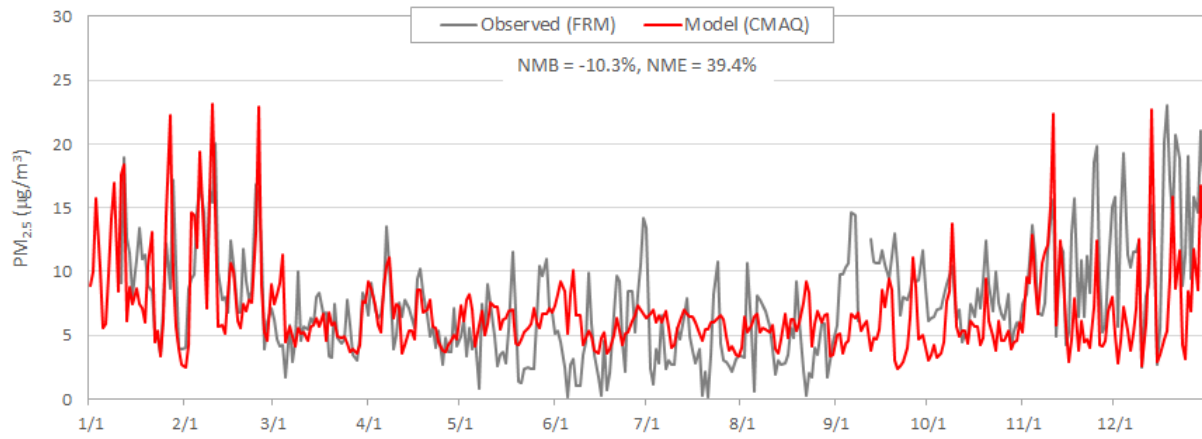


Figure 4.2: Annual mean observed vs. modeled PM_{2.5} concentrations at monitoring sites within the 1-km modeling domain. The annual means are calculated over the days with valid observations. The number of valid observations is shown in parentheses for each site. The Berkeley site is missing observations for January through June. Two Sacramento sites (Health Department - Stockton Blvd. and 1309 T Street) have observations every 3rd day. The Roseville and Woodland sites have observations every 6th day. The Sacramento - Bercut Drive site has data only for December, so its annual mean is not shown.

(a) Oakland West



(b) Vallejo



(c) San Jose – Knox Avenue

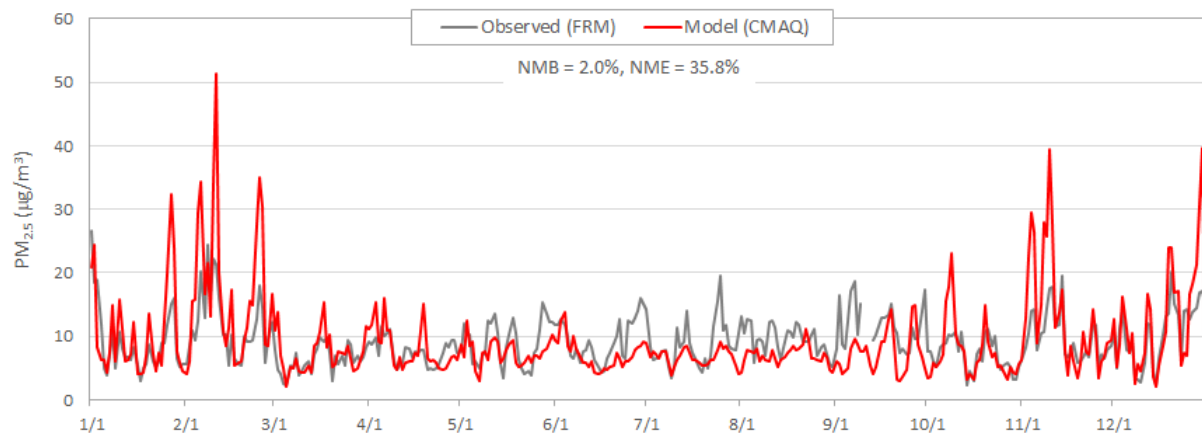


Figure 4.3: Time-series plots of observed vs. modeled daily PM_{2.5} concentrations at (a) Oakland West, (b) Vallejo, and (c) San Jose monitoring sites.

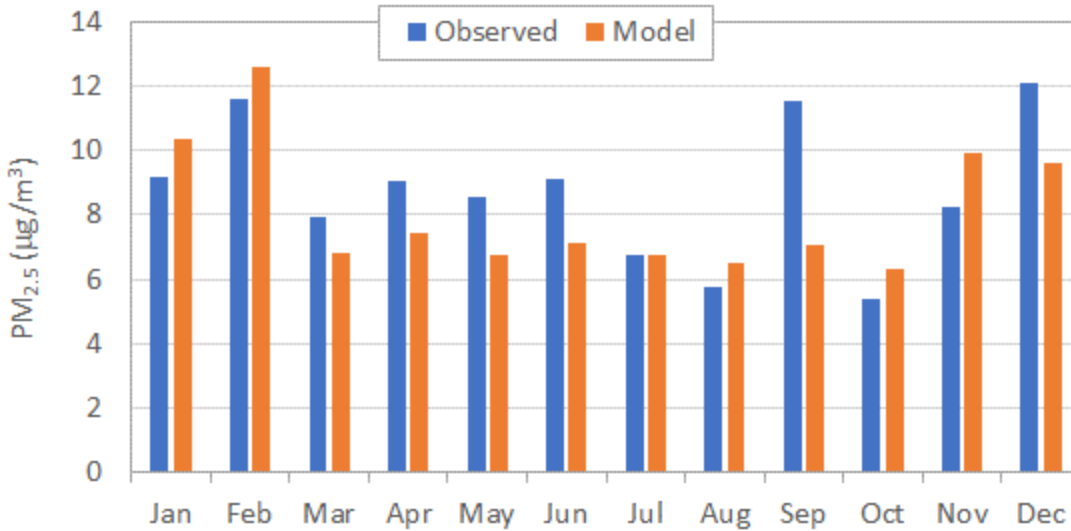


Figure 4.4: Monthly average simulated and observed PM_{2.5} concentrations in West Oakland.

4.1 Estimating Background PM_{2.5} in West Oakland

As mentioned in Section 1, we have simulated pollutant concentrations at a 1-km horizontal resolution over the entire Bay Area for 2016 (base case). Then we repeated the simulation with all anthropogenic emissions removed from the modeling inventory in the West Oakland source domain (control case), leaving all other model input parameters unchanged.

Figure 4.5 shows the annual average PM_{2.5} concentrations for the base case within the West Oakland receptor domain. The highest and lowest annual average PM_{2.5} concentrations are 9.3 µg/m³ and 7.1 µg/m³, respectively. A concentration gradient is evident within the domain. Cells with relatively higher concentrations extend along the eastern boundary and northwestern corner of the domain. A concentration gradient is also evident in the West Oakland community, an area within the red border in the figure. The eastern half of the community has slightly higher concentrations than the western half.

The spatial distribution of the annual average PM_{2.5} concentrations is similar to the spatial distribution of West Oakland’s emissions (Figure 3.3). The Chinatown area in the southeastern corner of the West Oakland domain has the highest emissions and concentrations. The cell along the southern boundary with the area’s lowest concentration (7.1 µg/m³) also has the lowest emissions (1.4 lbs/day).

Figure 4.6 shows the annual average PM_{2.5} concentrations for the control case, i.e., a simulation without West Oakland’s anthropogenic emissions. Compared to Figure 4.5, the spatial gradient in the annual average concentrations decreased significantly in the absence of West Oakland emissions across the receptor domain. The location of the maximum annual average PM_{2.5} concentrations has shifted from Chinatown to near the Bay Bridge, suggesting the influence of transport from the northwest corner of the domain.

Figure 4.7 shows the difference between the base and control cases. Based on the figure, the Chinatown area would benefit the most ($2.5 \mu\text{g}/\text{m}^3$) from zeroing out all anthropogenic emissions in the West Oakland source domain. The West Oakland community (within the red border) would benefit by $\text{PM}_{2.5}$ reductions ranging from $0.8 \mu\text{g}/\text{m}^3$ to $1.7 \mu\text{g}/\text{m}^3$. The southwest corner of the receptor domain would be the least benefitted area, with a reduction of about $0.5 \mu\text{g}/\text{m}^3$.

Note that these $\text{PM}_{2.5}$ concentrations and reductions represent the average value across a 1×1 km grid cell. Higher concentrations and reductions are possible at the sub-grid cell level, and these finer-scale gradients will be investigated with local-scale AERMOD modeling.

Bias in the simulated annual average $\text{PM}_{2.5}$ concentrations for both base and control cases are expected to be similar. Since reductions are estimated from the difference between the two simulations, the impact of model bias on estimated reductions is expected to be insignificant.

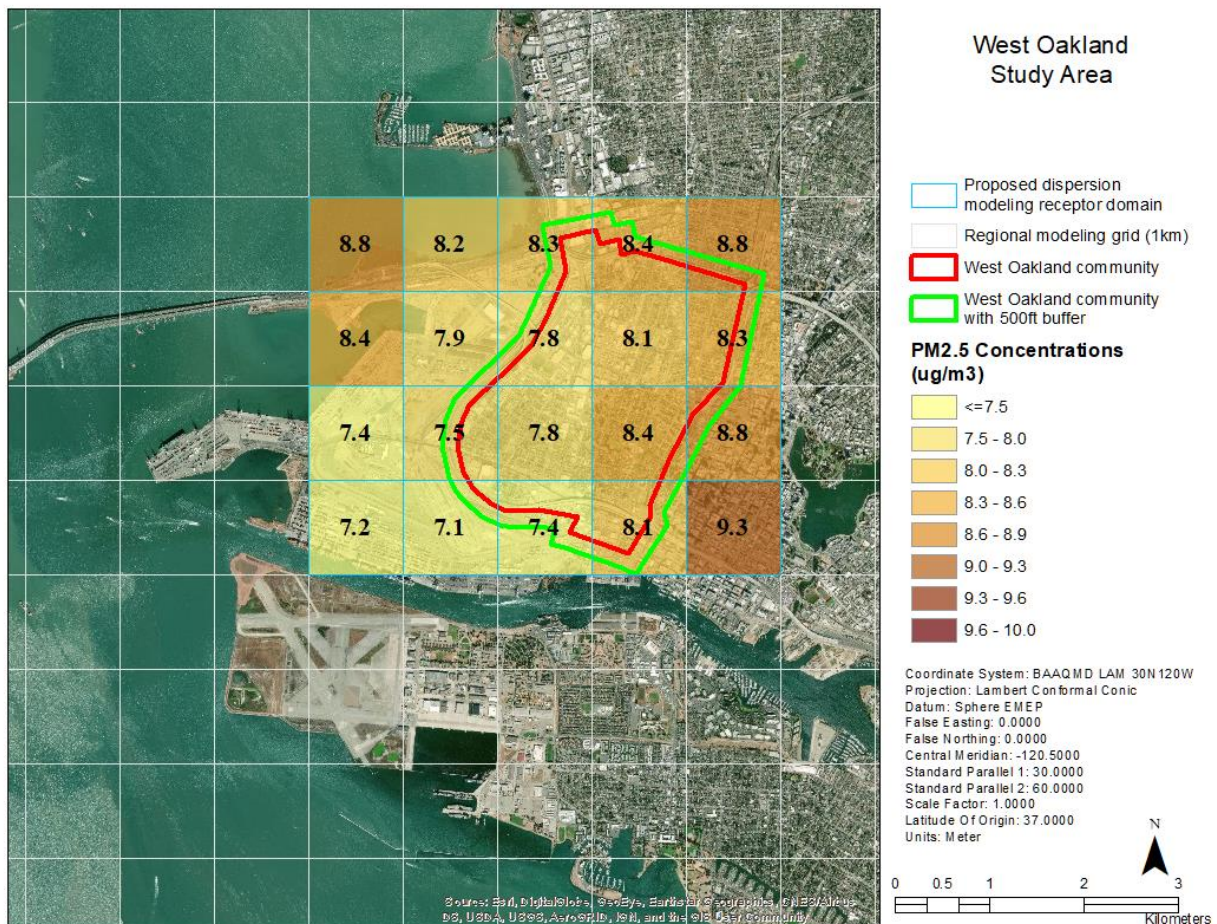


Figure 4.5: Spatial distribution of the simulated annual average $\text{PM}_{2.5}$ concentrations in the West Oakland receptor domain (base case).

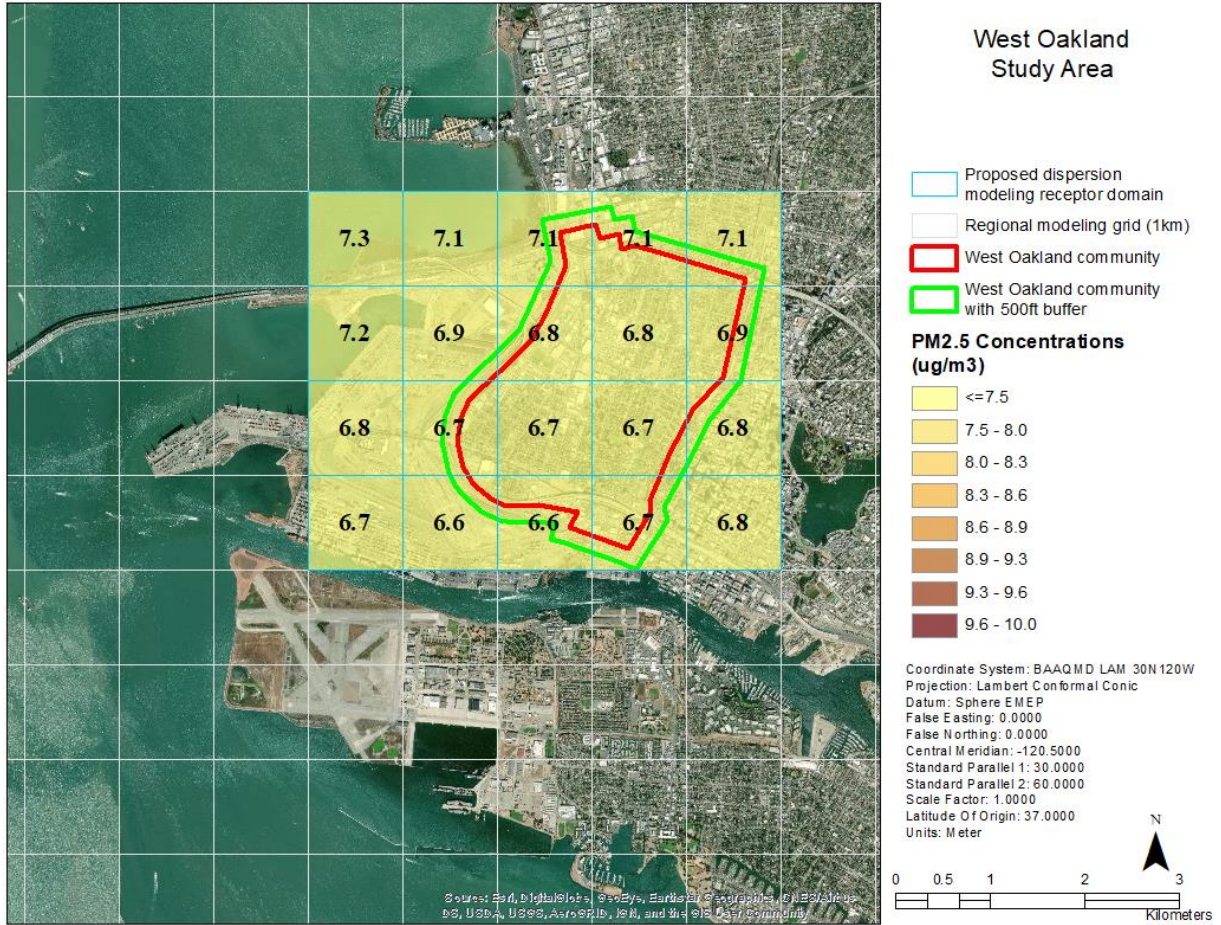


Figure 4.6: Spatial distribution of the simulated PM_{2.5} concentrations without West Oakland’s anthropogenic emissions (control case).

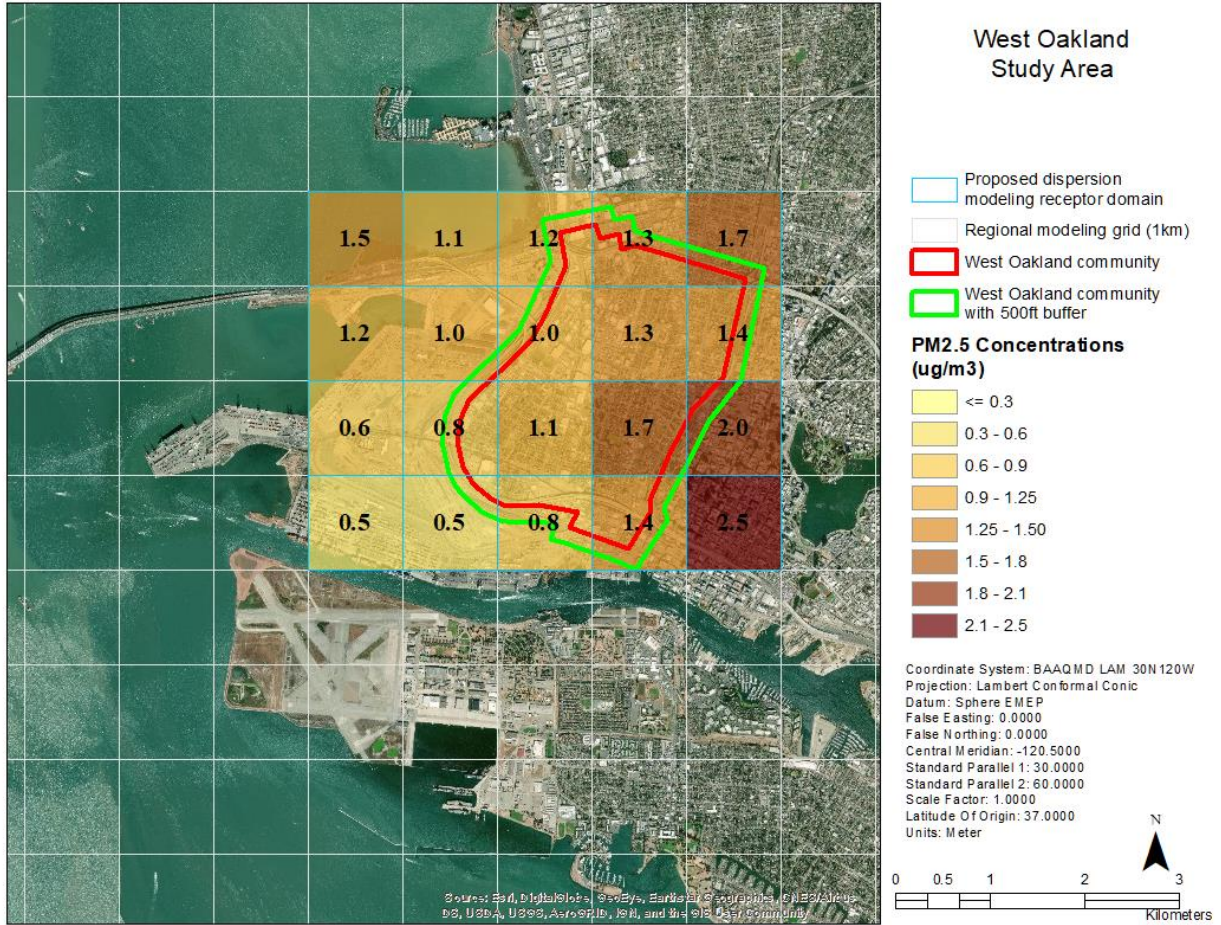


Figure 4.7: Difference between the simulated annual average base and control case PM_{2.5} concentrations.

Appendix A – Observational Data

A1. Description of Observations

Table A1 lists all aerometric stations within the 1-km modeling domain from which data were used in this study. It also shows data sources, data types, and purpose of the data. Under the monitoring location column, the first two subsections list PM_{2.5} stations within and outside of the Bay Area. The subsequent subsections list meteorological measurement stations within and outside of the Bay Area, followed by a list of upper air measurement stations. Meteorological measurement stations within the Bay Area are further separated based on whether or not they are operated by the District. Some stations measure both PM_{2.5} and meteorology. These stations are listed under both the PM_{2.5} and meteorology measurement sections and identified through checkmarks under columns titled “PM” and “Met.”

Hourly PM_{2.5} and meteorological data were obtained from the District’s Data Management System (DMS) in October 2018, and hourly PM_{2.5} and meteorological data were obtained from the U.S. EPA’s Air Quality System (AQS) at around the same time. Hourly meteorological data were also obtained from the NCAR/UCAR ADP data archive and twice daily upper air data were obtained from NOAA’s National Climatic Data Center.

The ADP and National Climatic Data Center data were used for the four-dimensional data assimilation (FDDA) in the WRF model. FDDA is a method to nudge the WRF model results towards observations. The WRF model includes a post-processing utility computer program that prepares the ADP and NCDC data for FDDA. The utility program also quality assures and quality checks both the ADP and National Climatic Data Center data. Meteorological data from the other sources listed in Table A1 were not used in FDDA because they do not include pressure, which is required for the nudging process. All the observed meteorological data listed in the column titled “Met” were used for WRF model validation using a software tool called METSTAT. The METSTAT program has a module for applying consistency checks to the data being used.

PM_{2.5} data obtained from DMS and AQS were compared against each other and no differences were found. PM_{2.5} data were used for both data analysis and CMAQ model validation. For consistency in data format, only data downloaded from AQS were used for data analysis and model validation.

As explained in the main text of this document, time series and spatial plots of simulated and observed hourly PM_{2.5} concentrations were generated and compared against each other. This process allowed identification of gaps and outliers in the PM_{2.5} data. Statistical formulas were developed in an Excel spreadsheet to evaluate the observations, such as assessing gaps in measurements, calculating daily, monthly, seasonal and annual averages, and assessing high and low values. Statistical formulas were also developed to assess bias, normalized bias and root mean square error in simulations by comparing simulated values to observations.

Table A1: Description of observations used in this study.

Monitoring Location	Source	PM	Met (ws, wd, t, rh)*	FDDA	Model Validation	
					WRF	CMAQ
<i>San Francisco Bay Area PM Stations</i>						
Berkeley Aquatic Park	DMS	x				x
Concord	DMS	x	x			x
Gilroy	DMS	x				x
Laney College	DMS	x				x
Livermore	DMS	x	x			x
Napa	DMS	x	x			x
Oakland	DMS	x				x
Oakland West	DMS	x				x
Redwood City	DMS	x				x
San Francisco	DMS	x				x
San Jose - Jackson	DMS	x				x
San Jose - Knox Avenue	DMS	x				x
San Pablo	DMS	x				x
San Rafael	DMS	x				x
Sebastopol	DMS	x				x
Vallejo	DMS	x	x			x
<i>PM Stations Outside the San Francisco Bay Area</i>						
Manteca	AQS	x				x
Roseville - N Sunrise Ave	AQS	x	x			x
Sacramento Health Department - Stockton Blvd.	AQS	x				x
Sacramento - 1309 T Street	AQS	x	x			x
Sacramento - Bercut Drive	AQS	x				x
Sacramento - Del Paso Manor	AQS	x	x			x
San Lorenzo Valley Middle School	AQS	x				x
Santa Cruz	AQS	x				x
Stockton - Hazelton	AQS	x	x			x
Woodland - Gibson Road	AQS	x				x
<i>BAAQMD Met Stations</i>						
Bethel Island	DMS		x		x	
Chabot	DMS		x		x	
Concord	DMS	x	x		x	
Fairfield	DMS		x		x	
Ft. Funston	DMS		x		x	
Livermore	DMS	x	x		x	
Napa	DMS	x	x		x	
Oakland STP	DMS		x		x	
Patterson Pass	DMS		x		x	
Pleasanton	DMS		x		x	
Pt. San Pablo	DMS		x		x	

Monitoring Location	Source	PM	Met (ws, wd, t, rh)*	FDDA	Model Validation	
					WRF	CMAQ
Rio Vista	DMS		x		x	
San Carlos	DMS		x		x	
San Martin	DMS		x		x	
San Ramon	DMS		x		x	
Sonoma Baylands	DMS		x		x	
Vallejo	DMS	x	x		x	
Valley Ford	DMS		x		x	
<i>Non-BAAQMD Met Stations in the Bay Area</i>						
Berkeley Lab	DMS		x		x	
Concord KCCR	ADP		x	x	x	
Hayward KHWD	ADP		x	x	x	
Livermore KLVK	ADP		x	x	x	
Moffett NASA/Mountain View KNUQ	ADP		x	x	x	
Napa KAPC	ADP		x	x	x	
Novato KDVO	ADP		x	x	x	
Oakland KOAK	ADP		x	x	x	
Palo Alto KPAO	ADP		x	x	x	
Petaluma KO69	ADP		x	x	x	
San Carlos KSQL	ADP		x	x	x	
San Francisco KSFO	ADP		x	x	x	
San Francisco STP	DMS		x		x	
San Jose KSJC	ADP		x	x	x	
San Jose/Reid KRHV	ADP		x	x	x	
San Martin KE16	ADP		x	x	x	
Santa Rosa KSTS	ADP		x	x	x	
Travis AFB KSUU	ADP		x	x	x	
<i>Met Stations Outside the Bay Area</i>						
Davis - UCD Campus	AQS		x		x	
Davis KEDU	ADP		x	x	x	
Elk Grove - Bruceville Road	AQS		x		x	
Half Moon Bay KHAF	ADP		x	x	x	
Hollister KCVH	ADP		x	x	x	
Lincoln KLHM	ADP		x	x	x	
Mather Field KMHR	ADP		x	x	x	
McClellan AFB KMCC	ADP		x	x	x	
Modesto KMOD	ADP		x	x	x	
Roseville - N Sunrise Ave	AQS	x	x		x	
Sacramento - 1309 T Street	AQS	x	x		x	
Sacramento - Del Paso Manor	AQS	x	x		x	
Sacramento KSAC	ADP		x	x	x	
Salinas KSNS	ADP		x	x	x	
Sanford MUNI KSMF	ADP		x	x	x	

Monitoring Location	Source	PM	Met (ws, wd, t, rh)*	FDDA	Model Validation	
					WRF	CMAQ
Stockton KSCK	ADP		x	x	x	
Stockton - Hazelton	AQS	x	x		x	
Tracy - Airport	AQS		x		x	
Vacaville KVCB	ADP		x	x	x	
Watsonville KWVI	ADP		x	x	x	
<i>Upper Air Stations</i>						
Oakland Sounding	NCDC		x	x	x	

*ws=wind speed; wd=wind direction; t=temperature; rh=relative humidity.

A2. Spatial Distribution of Observation Stations

Figure A1 shows spatial distribution of meteorological observation stations in the 1-km modeling domain. They are grouped based on whether they are operated by BAAQMD or other agencies (non-BAAQMD) and whether they are inside or outside of the District boundaries. BAAQMD sites collocated with PM_{2.5} measurements are also marked.

The spatial distribution of PM_{2.5} monitoring stations in the 1-km modeling domain is shown in Figure A2. These stations are grouped based on whether they are inside or outside of the District boundaries. All stations within the District are operated by the District.

Note that both the meteorological and air quality models have nested domains. Meteorological and air quality measurements outside of the 1-km domain were obtained from various databases and used for FDDA and model evaluation along with data for the 1-km domain. These data are stored on modeling computers and are available on request.

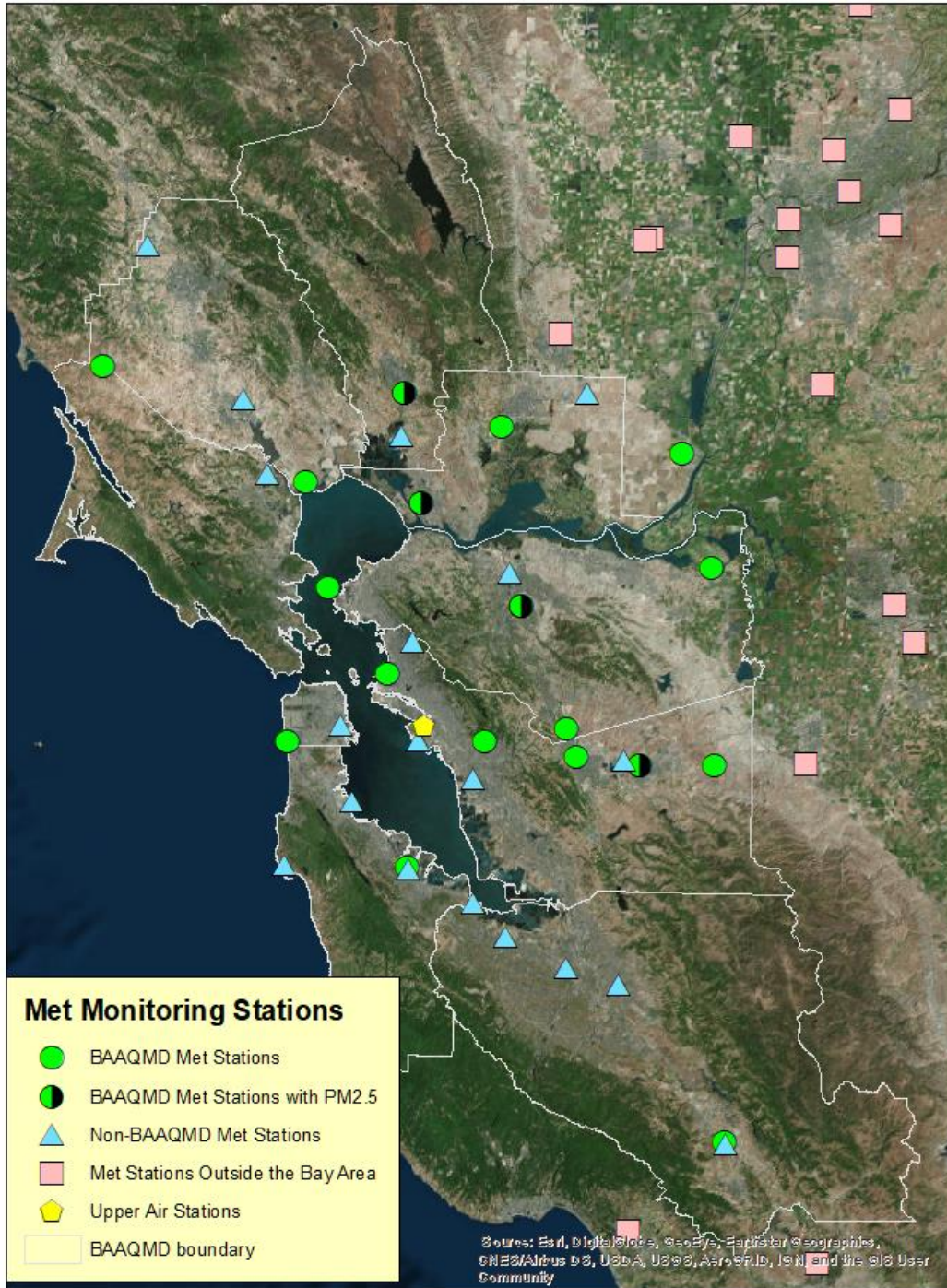


Figure A1: Spatial distribution of meteorological monitoring sites in the 1-km modeling domain.

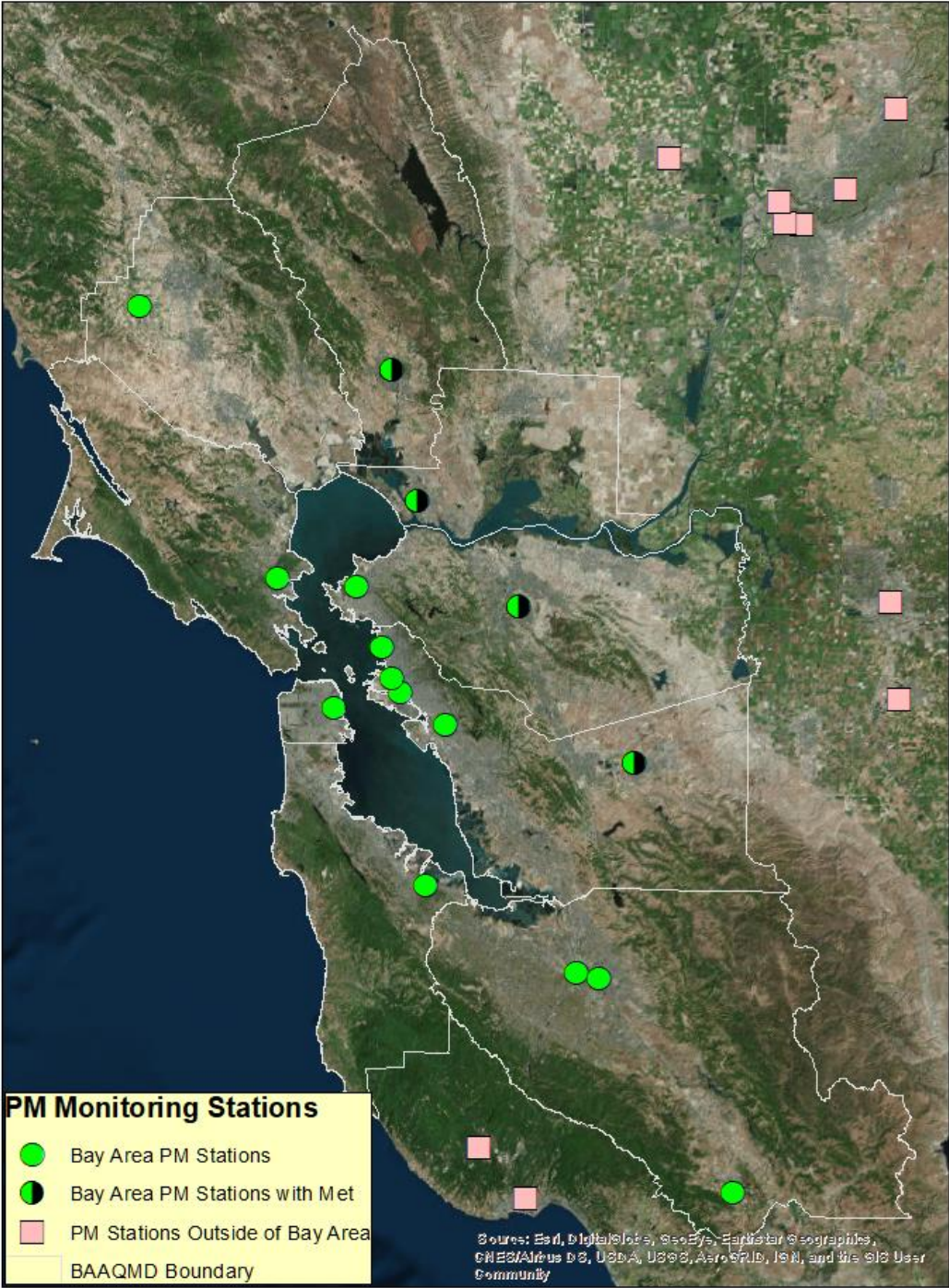


Figure A2: Spatial distribution of PM_{2.5} monitoring stations in the 1-km modeling domain.

Appendix B – Emissions Inventory

This appendix provides additional details on the development of emissions estimates for residential wood combustion, an important PM_{2.5} source during winter pollution episodes. This appendix also contains additional summary tables and emissions density plots that characterize the emissions inventory used for the 2016 CMAQ modeling.

B1. Residential Wood Combustion

ARB emissions estimates for residential wood combustion are based on county-level populations of fireplaces and woodstoves, wood consumption rates by device type, and emission factors that represent the quantity of emissions per ton of fuel burned. Where possible, ARB estimates device populations and wood consumption rates using local survey data, such as data collected as part of the District's Spare the Air Tonight Study (BAAQMD, 2007). ARB residential wood combustion emissions estimates for the District were compared to internal estimates derived from survey data, as well as estimates from neighboring air districts.

Figure B1 shows annual average PM_{2.5} emissions from residential wood combustion for the two BAAQMD inventories, as well as inventories for the Sacramento Metropolitan Air Quality Management District (SMAQMD) and the San Joaquin Valley Unified Air Pollution Control District (SJVUAPCD). The internal BAAQMD inventory is somewhat higher than the ARB inventory for BAAQMD, and both BAAQMD inventories are significantly higher than emissions estimates for SMAQMD and SJVUAPCD. After additional investigations and discussions with ARB, it was determined that:

- ARB's PM_{2.5} emissions estimates for winter compared well with the District's internal estimates; however, the District's estimates for summer (which were extrapolated from winter survey results based on temperature data) are significantly higher than ARB's estimates. These summer estimates do not appear to be realistic and result in the higher annual average PM_{2.5} emissions in the District's internal inventory.
- Higher residential wood combustion emissions estimates for BAAQMD relative to SMAQMD and SJVUAPCD likely result from a failure to account for the impact of the District's Spare the Air Program.

Based on these findings, it was decided that ARB's residential wood combustion estimates for the District would be reduced by 50% as an initial estimate of the impact of the District's Spare the Air program. Figure B2 shows the final monthly average PM_{2.5} emissions from residential wood combustion that were included in the CMAQ modeling inventories. Monthly average emissions range from 0.20 tpd in August to 8.39 tpd in January, with an annual average of 3.93 tpd.

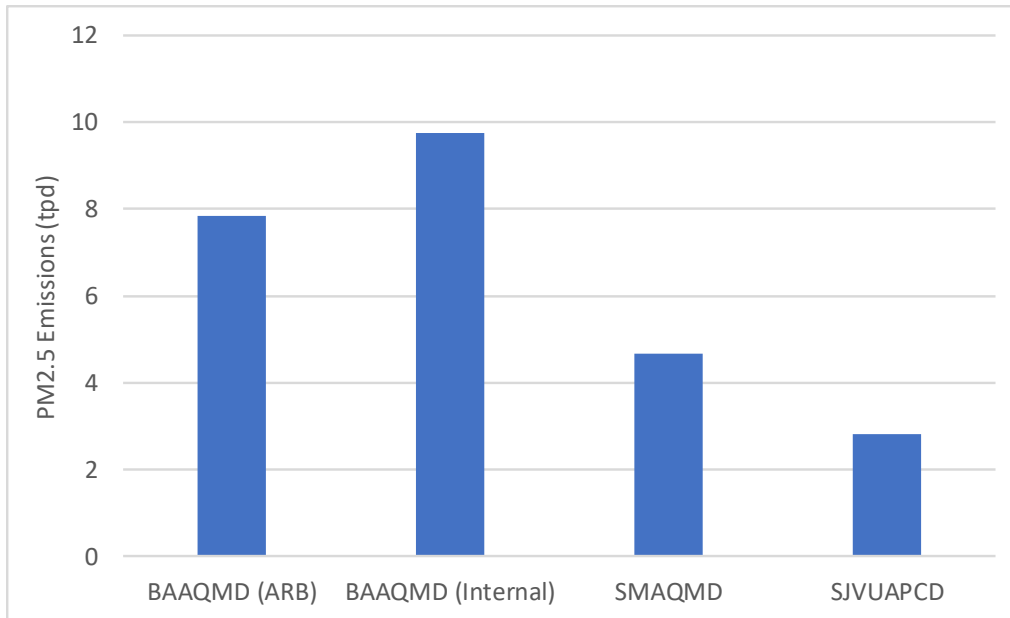


Figure B1: Comparison of 2016 annual average PM_{2.5} emissions inventories for residential wood combustion.

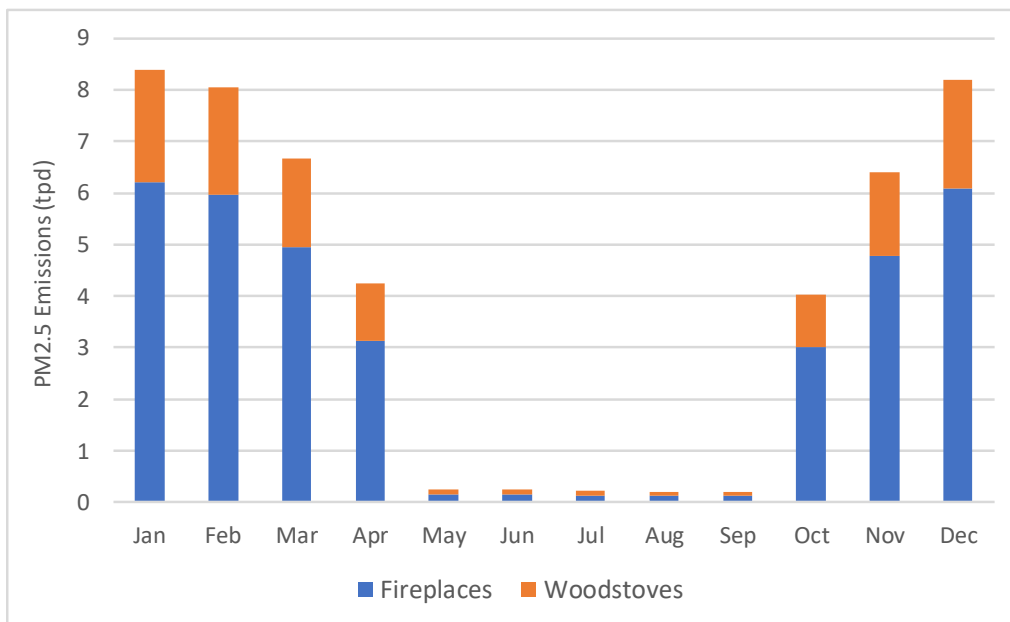


Figure B2: 2016 monthly average PM_{2.5} emissions for BAAQMD from residential wood combustion.

B2. Emissions Inventory Summaries

This section provides additional summary information on the emissions inventory used for the 2016 CMAQ modeling. Tables B1 through B4 show emissions of PM_{2.5} precursors (TOG, NO_x, SO₂, and NH₃) by geographic area and source sector. Key sources of TOG emissions include landfills, natural gas transmission losses, petroleum refining, and solvent usage. Key sources of NO_x emissions include onroad and nonroad mobile sources, especially diesel-powered vehicles.

Key sources of SO₂ emissions include petroleum refining and ocean-going vessels. Key sources of NH₃ emissions include farming operations such as livestock waste and fertilizer application.

Table B1: Summary of 2016 TOG emissions (tons/day) by geographic area and source sector.

Geographic Area	Area	Nonroad	Onroad	Point	Total
Alameda	42.6	8.0	12.4	64.1	127.1
Contra Costa	51.0	6.3	7.7	43.9	109.0
Marin	16.2	2.9	2.5	15.2	36.8
Napa	6.8	1.9	1.4	3.6	13.6
San Francisco	18.1	6.2	2.9	3.0	30.2
San Mateo	18.9	7.1	4.4	25.1	55.5
Santa Clara	57.6	8.1	12.2	50.8	128.7
Solano	14.3	2.1	2.6	8.7	27.7
Sonoma	25.4	3.0	3.5	9.1	41.1
<i>BAAQMD Subtotal</i>	<i>251.0</i>	<i>45.6</i>	<i>49.6</i>	<i>223.4</i>	<i>569.6</i>
Non-BAAQMD Counties	502.5	22.7	29.0	80.9	635.1
Domain Total	753.5	68.3	78.6	304.3	1,204.7

Table B2: Summary of 2016 NO_x emissions (tons/day) by geographic area and source sector.

Geographic Area	Area	Nonroad	Onroad	Point	Total
Alameda	3.4	12.0	27.2	3.2	45.8
Contra Costa	4.3	11.8	13.8	15.5	45.4
Marin	0.9	3.8	3.6	0.3	8.5
Napa	0.3	2.2	3.0	0.2	5.7
San Francisco	2.1	34.4	4.5	1.4	42.4
San Mateo	2.1	18.9	6.7	0.7	28.5
Santa Clara	4.2	10.0	22.2	8.5	45.0
Solano	1.0	3.9	5.4	3.8	14.1
Sonoma	0.9	7.9	6.7	0.4	15.9
<i>BAAQMD Subtotal</i>	<i>19.3</i>	<i>104.8</i>	<i>93.0</i>	<i>34.0</i>	<i>251.2</i>
Non-BAAQMD Counties	19.0	37.3	60.5	4.2	121.1
Domain Total	38.4	142.1	153.5	38.3	372.3

Table B3: Summary of 2016 SO₂ emissions (tons/day) by geographic area and source sector.

Geographic Area	Area	Nonroad	Onroad	Point	Total
Alameda	0.1	0.4	0.2	1.4	2.0
Contra Costa	0.1	0.9	0.1	16.6	17.7
Marin	0.0	0.0	0.0	0.1	0.2
Napa	0.0	0.0	0.0	0.0	0.0
San Francisco	0.1	0.4	0.0	0.1	0.6
San Mateo	0.1	0.9	0.1	0.1	1.1
Santa Clara	0.1	0.1	0.2	2.9	3.3
Solano	0.0	0.2	0.0	0.4	0.6

Sonoma	0.0	0.1	0.0	0.0	0.2
<i>BAAQMD Subtotal</i>	<i>0.5</i>	<i>3.1</i>	<i>0.7</i>	<i>21.6</i>	<i>25.9</i>
Non-BAAQMD Counties	1.6	0.3	0.4	1.9	4.2
Domain Total	2.1	3.4	1.1	23.4	30.1

Table B4: Summary of 2016 NH₃ emissions (tons/day) by geographic area and source sector.

Geographic Area	Area	Nonroad	Onroad	Point	Total
Alameda	3.0	0.0	1.5	0.4	4.9
Contra Costa	3.1	0.0	0.9	2.1	6.1
Marin	2.5	0.0	0.3	0.3	3.0
Napa	0.5	0.0	0.2	0.1	0.8
San Francisco	1.4	0.0	0.3	0.0	1.7
San Mateo	1.3	0.0	0.5	0.2	2.1
Santa Clara	3.6	0.0	1.6	1.5	6.7
Solano	1.9	0.0	0.3	0.1	2.3
Sonoma	3.3	0.0	0.4	0.3	4.0
<i>BAAQMD Subtotal</i>	<i>20.7</i>	<i>0.1</i>	<i>6.0</i>	<i>5.0</i>	<i>31.7</i>
Non-BAAQMD Counties	46.9	0.0	3.3	7.0	57.3
Domain Total	67.6	0.1	9.3	12.0	89.0

B3. Emissions Density Plots

This section provides emissions density plots that show the spatial distribution of key PM_{2.5} precursors (an emissions density plot for primary PM_{2.5} is provided in the main body of this report in Figure 3.1). The emissions density plot for NO_x (Figure B3) shows elevated emissions along major freeways and shipping lanes and in urban cores. Note that high emissions along shipping lanes in San Pablo Bay to the south of Marin County may be overestimated due to the spatial surrogate used for commercial marine vessel emissions, which does not include offshore shipping lanes for Sonoma County.

The emissions density plot for SO₂ (Figure B4) shows the presence of point sources in the 1-km domain that emit this pollutant, as well as emissions from commercial marine vessels along shipping lanes. The emissions density plot for NH₃ (Figure B5) shows elevated emissions in San Joaquin County in the eastern part of the modeling domain, an area with significant agricultural activity.

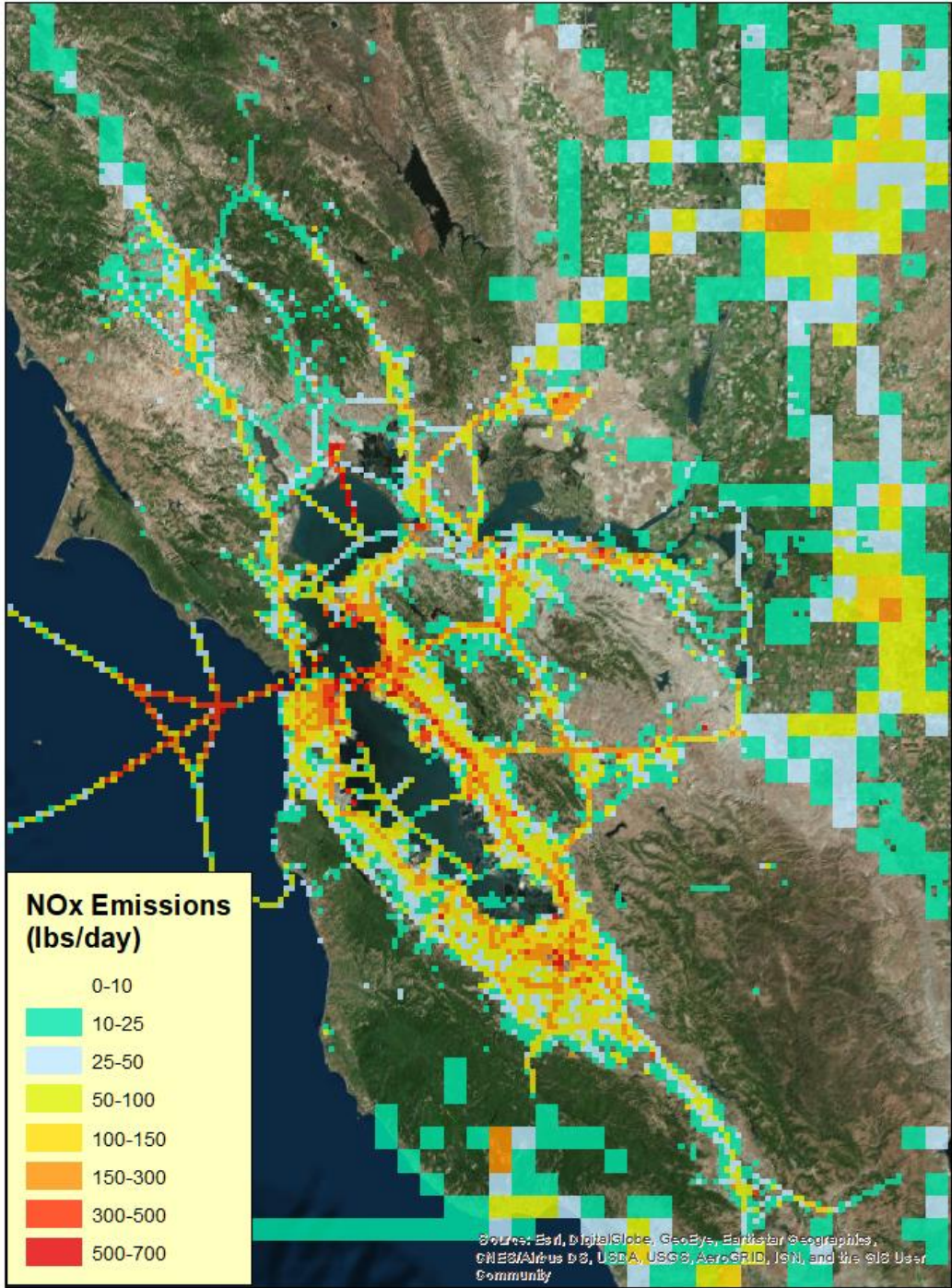


Figure B3: Spatial distribution of annual average NO_x emissions for the 1-km modeling domain.

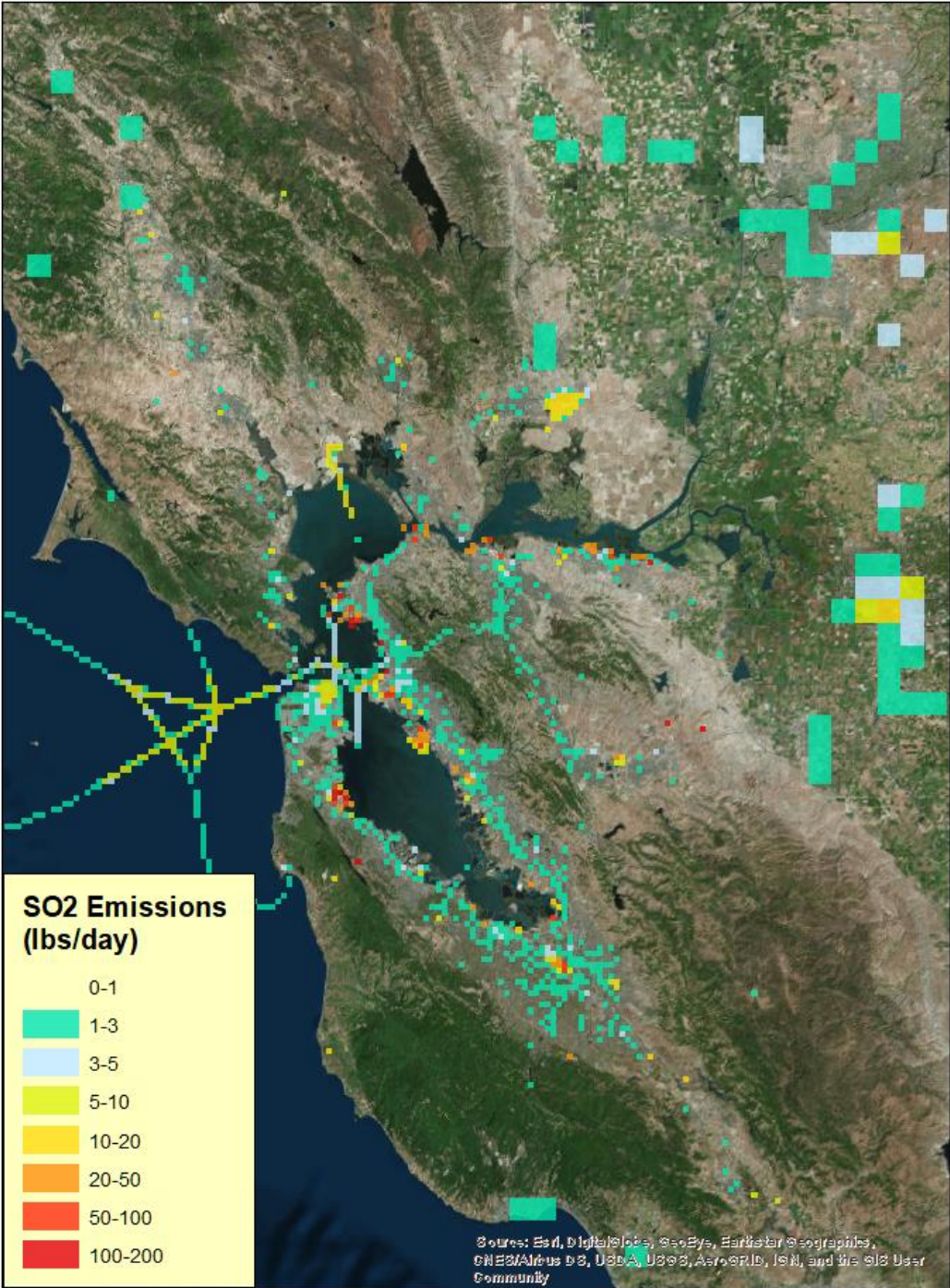


Figure B4: Spatial distribution of annual average SO₂ emissions for the 1-km modeling domain.

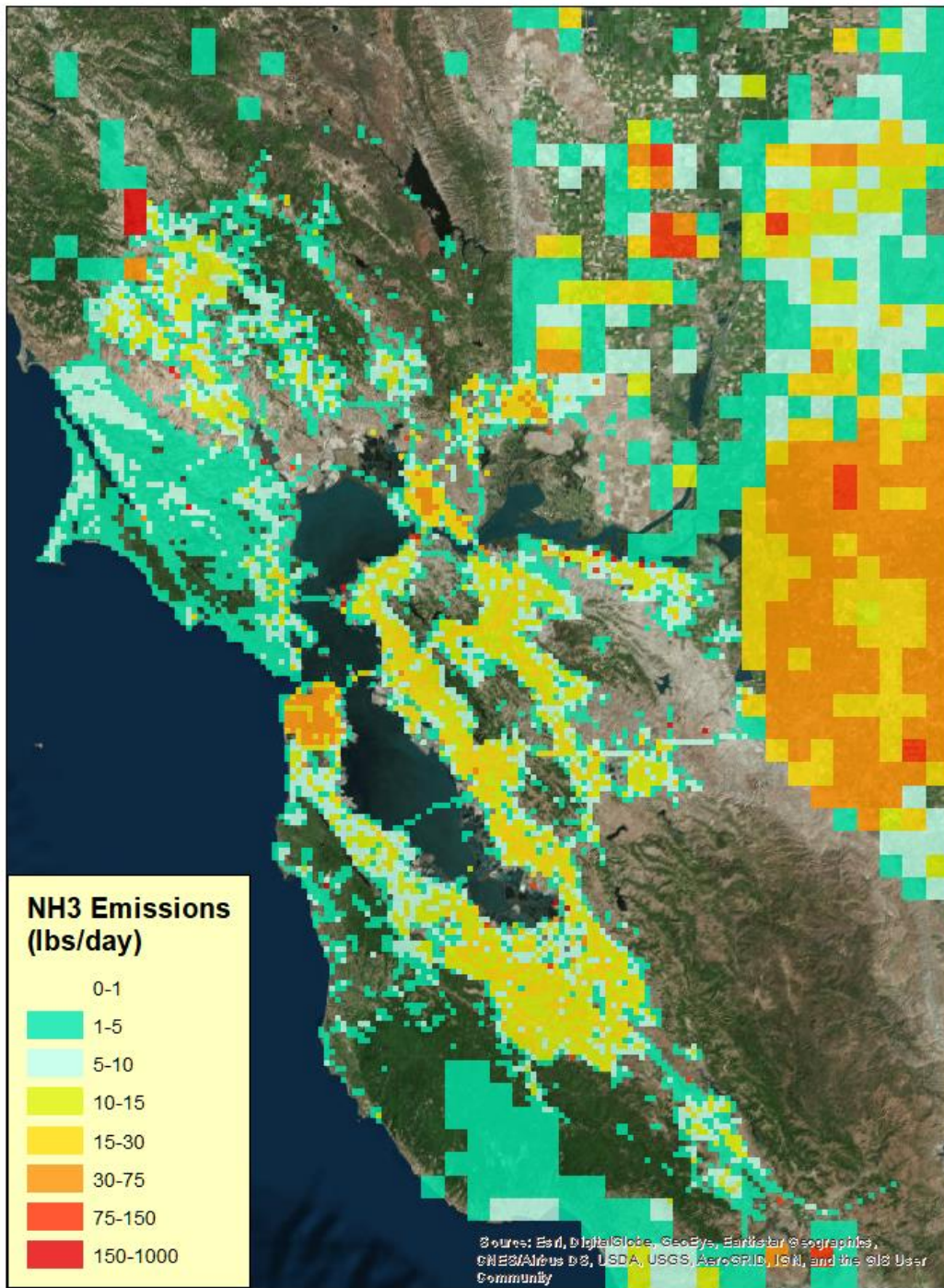


Figure B5: Spatial distribution of annual average NH₃ emissions for the 1-km modeling domain.

APPENDIX C – Meteorological Model Evaluation

C1. Statistical Evaluation

The ENVIRON METSTAT program (Emery et al., 2001) was used to compare the WRF-generated meteorological fields against hourly surface observations archived at NCAR. METSTAT is a statistical analysis software package that calculates and graphically presents statistics such as mean observation, mean simulation, bias error, gross error, and index of agreement.

Hourly time series of observed and simulated surface-layer wind and temperature are presented to evaluate the model performance. Statistics are defined as follows:

Mean observation (M_o): calculated from all sites with valid data within a given analysis region and for a given time period (hourly or daily):

$$M_o = \frac{1}{IJ} \sum_{j=1}^J \sum_{i=1}^I O_j^i$$

where O_j^i is the individual observed quantity at site i and time j , and the summations are over all sites (I) and time periods (J).

Mean prediction (M_p): calculated from simulation results that are interpolated to each observation used to calculate the mean observation (hourly or daily):

$$M_p = \frac{1}{IJ} \sum_{j=1}^J \sum_{i=1}^I P_j^i$$

where P_j^i is the individual simulated quantity at site i and time j . Note that mean observed and simulated winds are vector-averaged (for east-west component u and north-south component v), from which the mean wind speed and mean resultant direction are derived.

Bias error (B): calculated as the mean difference in prediction-observation pairings with valid data within a given analysis region and for a given time period (hourly or daily):

$$B = \frac{1}{IJ} \sum_{j=1}^J \sum_{i=1}^I (P_j^i - O_j^i)$$

Gross Error (E): calculated as the mean *absolute* difference in prediction-observation pairings with valid data within a given analysis region and for a given time period (hourly or daily):

$$E = \frac{1}{IJ} \sum_{j=1}^J \sum_{i=1}^I |P_j^i - O_j^i|$$

Note that the bias and gross error for winds are calculated from the predicted-observed residuals in speed and direction (not from vector components u and v). The direction error for a given prediction-observation pairing is limited to range from 0 to $\pm 180^\circ$.

Root Mean Square Error (RMSE): calculated as the square root of the mean squared difference in prediction-observation pairings with valid data within a given analysis region and for a given time period (hourly or daily):

$$RMSE = \left[\frac{1}{IJ} \sum_{j=1}^J \sum_{i=1}^I (P_j^i - O_j^i)^2 \right]^{1/2}$$

The RMSE, as with the gross error, is a good overall measure of model performance.

Index of Agreement (IOA): calculated following the approach of Willmont (1981). This metric condenses all the differences between model estimates and observations within a given analysis region and for a given time period (hourly and daily) into one statistical quantity. It is the ratio of the total RMSE to the sum of two differences – between each prediction and the observed mean, and each observation and the observed mean:

$$IOA = 1 - \left[\frac{IJ \cdot RMSE^2}{\sum_{j=1}^J \sum_{i=1}^I |P_j^i - M_o| + |O_j^i - M_o|} \right]$$

Viewed from another perspective, the index of agreement is a measure of the match between the departure of each prediction from the observed mean and the departure of each observation from the observed mean. Thus, the correspondence between predicted and observed values across the domain at a given time may be quantified in a single metric and displayed as a time series. The index of agreement has a theoretical range of 0 to 1, the latter score suggesting perfect agreement.

C2. Time Series Comparisons

To further evaluate model performance and to understand the meteorology at specific regions of concern, the simulated results were compared to wind and temperature measurements from monitoring sites in West Oakland, San Jose and Vallejo. Figures C2 through C9 show time series comparing daily average WRF-simulated surface wind speed and temperature to observations at Oakland, San Jose and Vallejo for each quarter of 2016.

The WRF-simulated wind and temperature matched the observed trends very well for the whole year of 2016. There were no significant differences between the predicted and the observed values. The best performance was observed at Vallejo site, especially for wind speed performance. Underestimations of wind speed were noticeable at Oakland and San Jose

throughout 2016. Investigations into this wind speed performance problem are on-going.

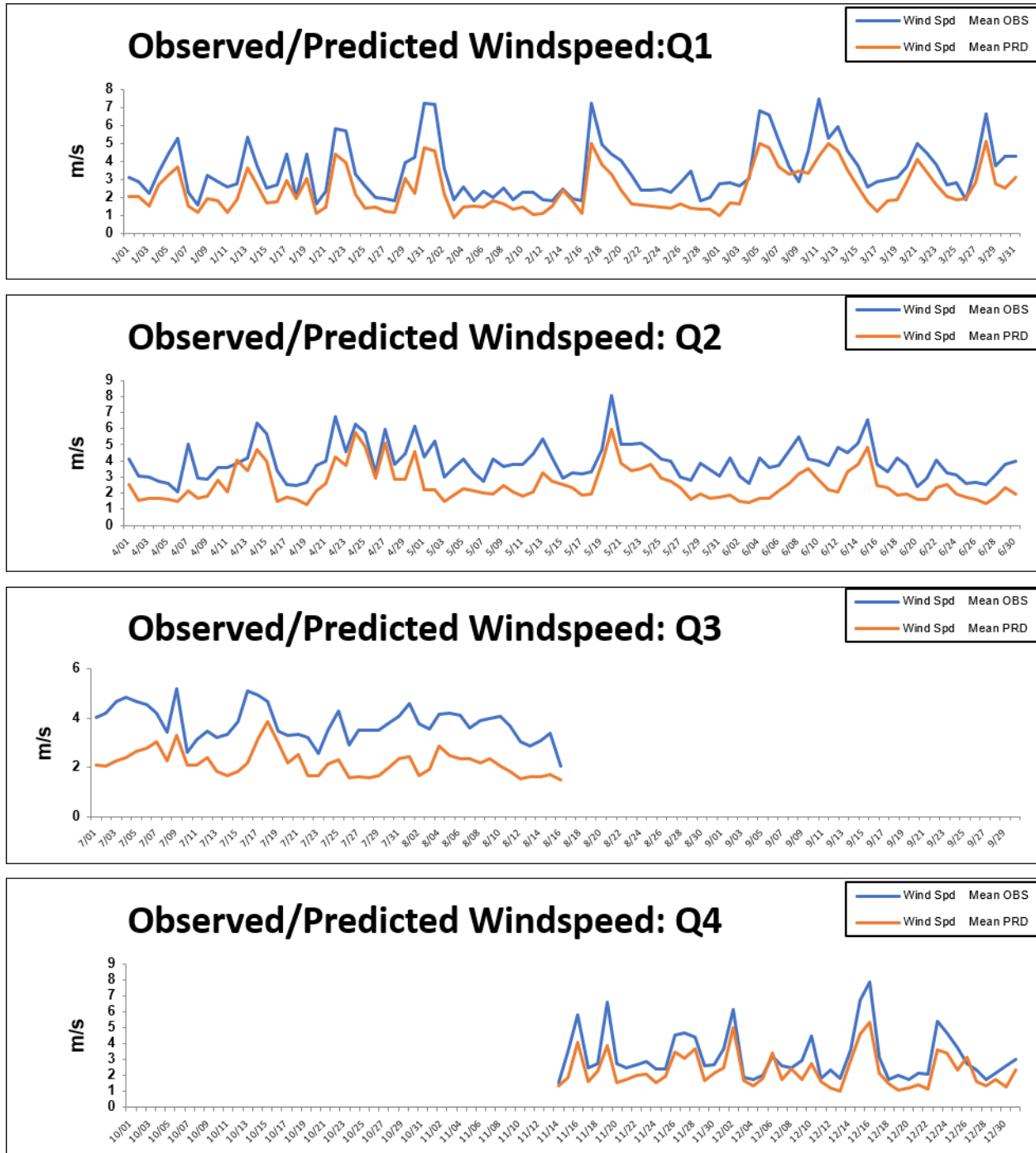


Figure C1: Daily time series of observed and simulated wind speed at West Oakland for 2016 are displayed quarterly. Observation data from mid-August through mid-November were not available. “Mean OBS” is for all observations averaged over the 1-km domain. “Mean PRD” is for all prediction fields at the observation sites averaged over the 1-km domain.

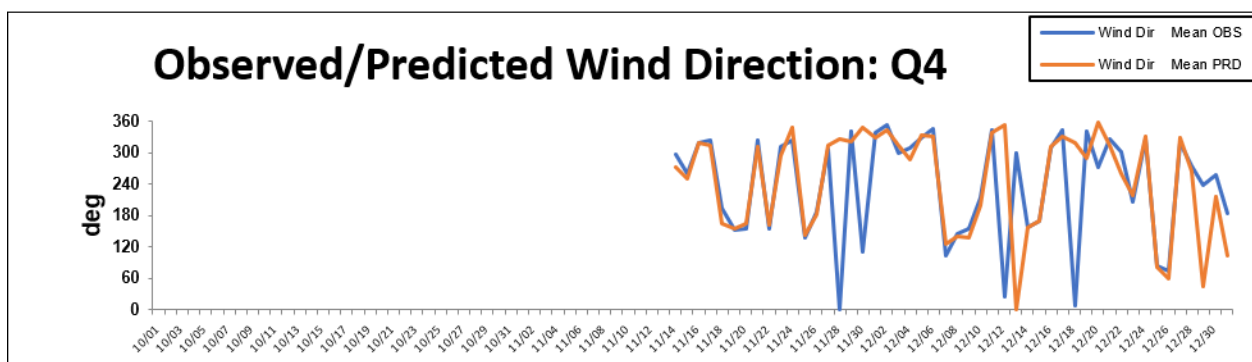
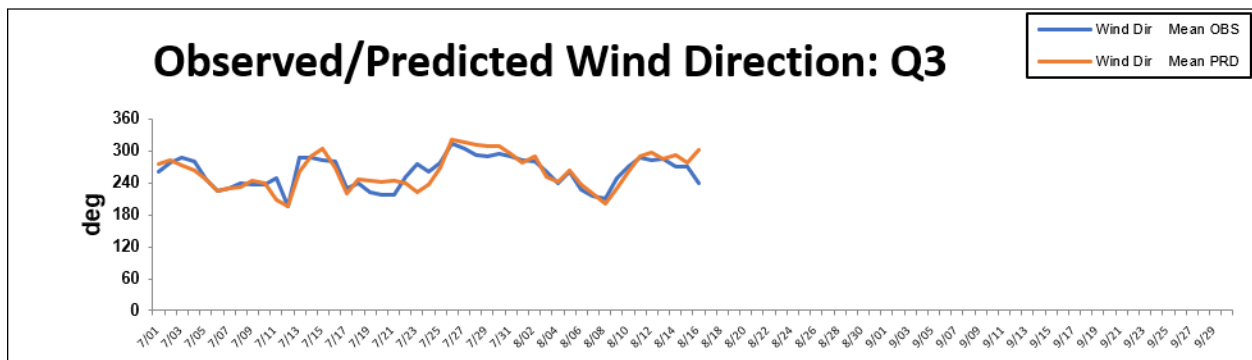
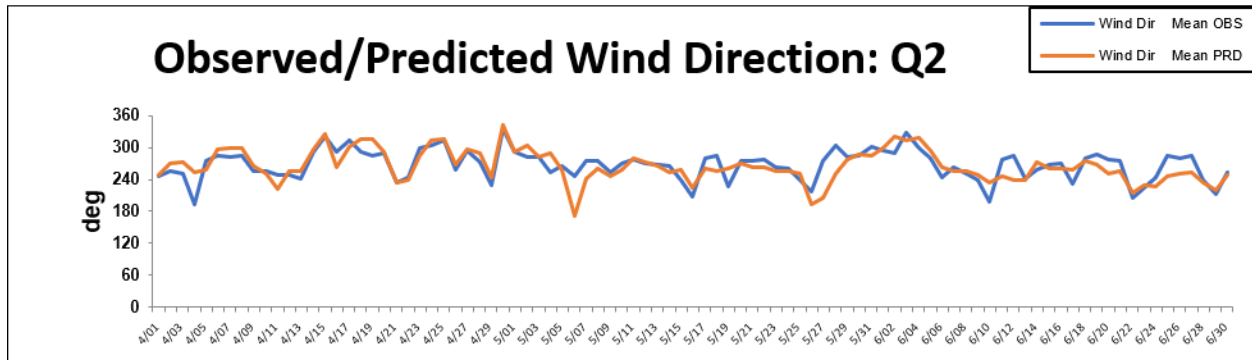
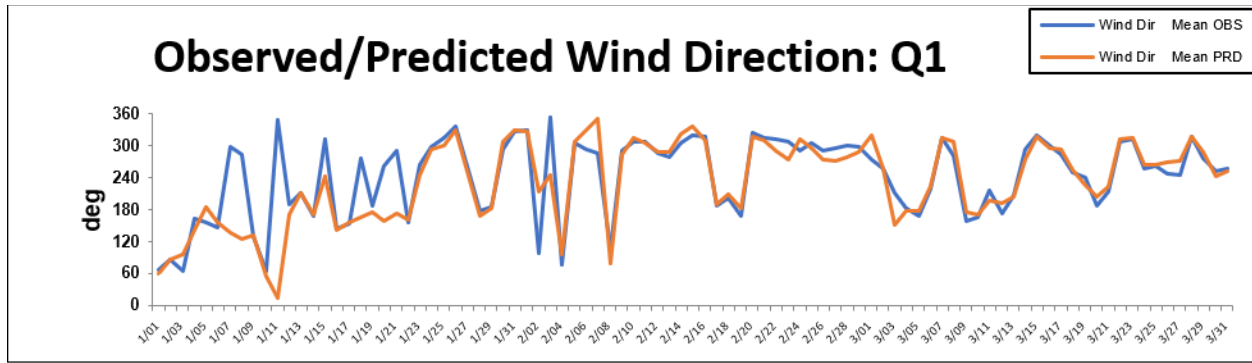


Figure C2: Daily time series of observed and simulated wind direction at West Oakland for 2016.

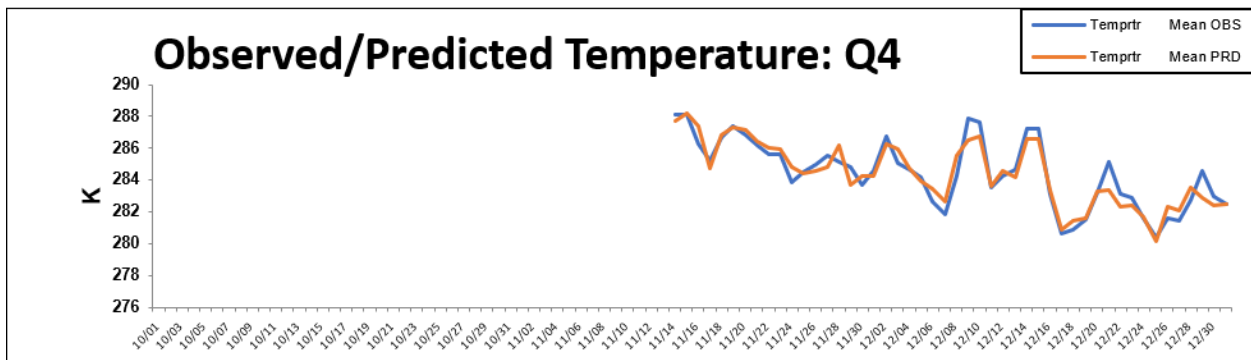
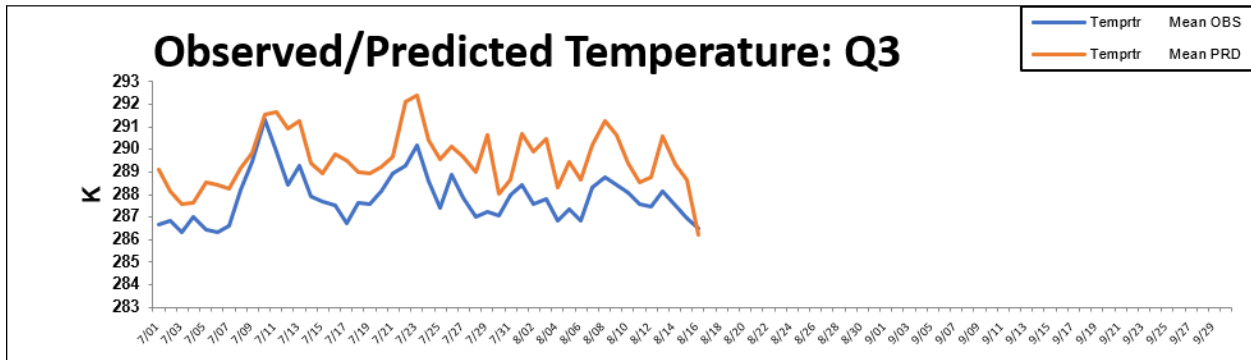
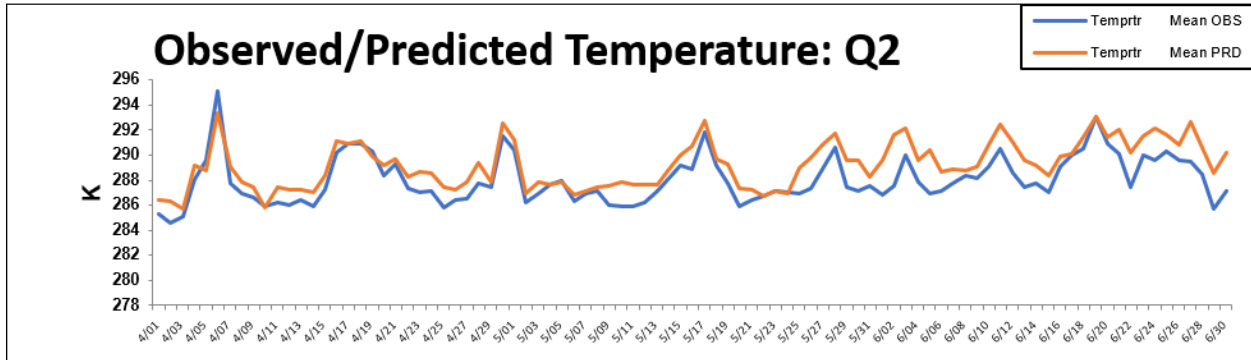
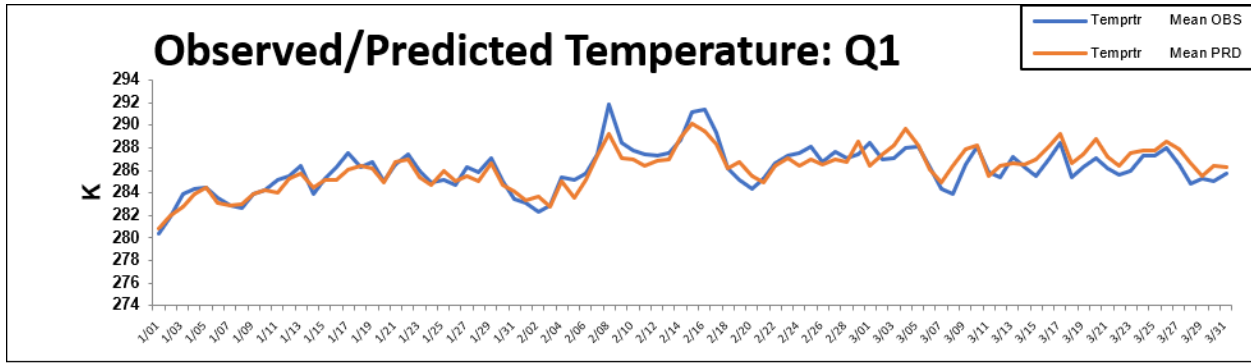


Figure C3: Daily time series of observed and simulated temperatures at West Oakland for 2016.

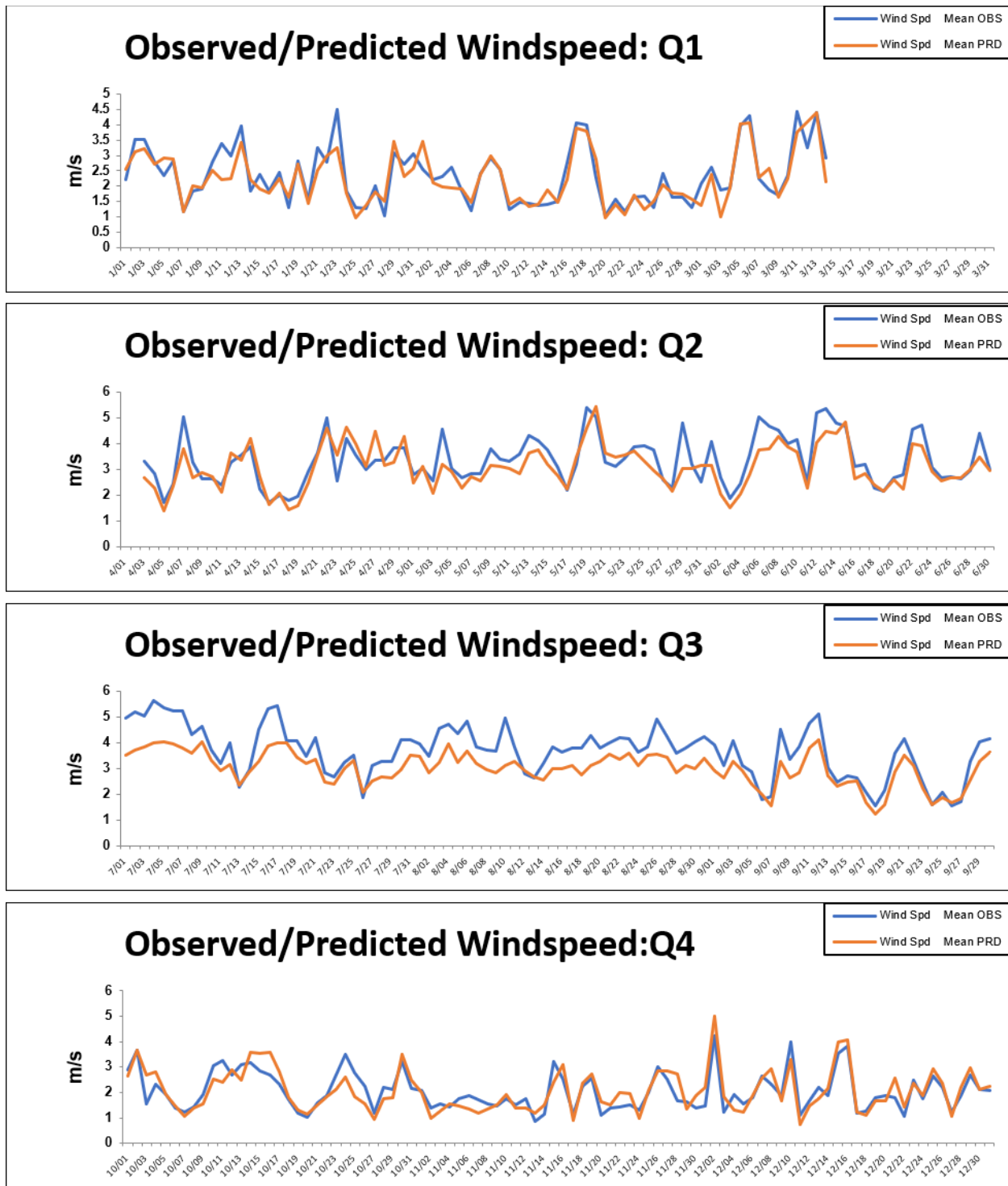


Figure C4: Daily time series of observed and simulated wind speed at Vallejo for 2016.

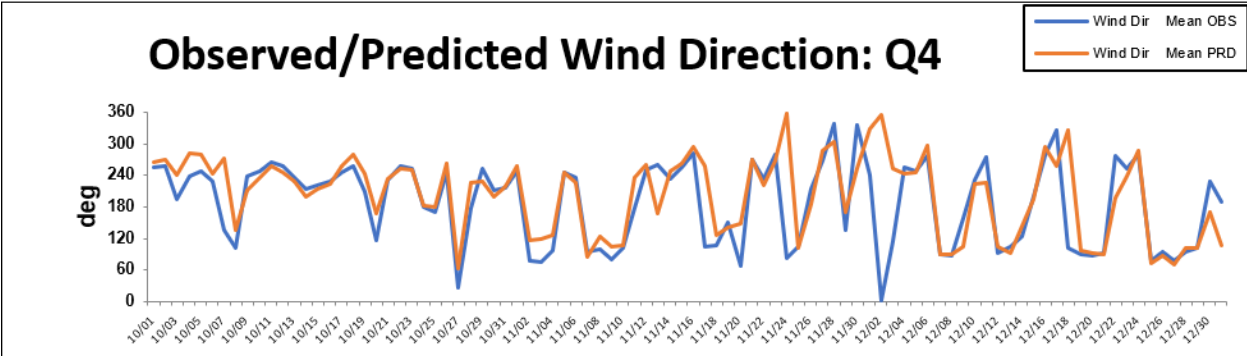
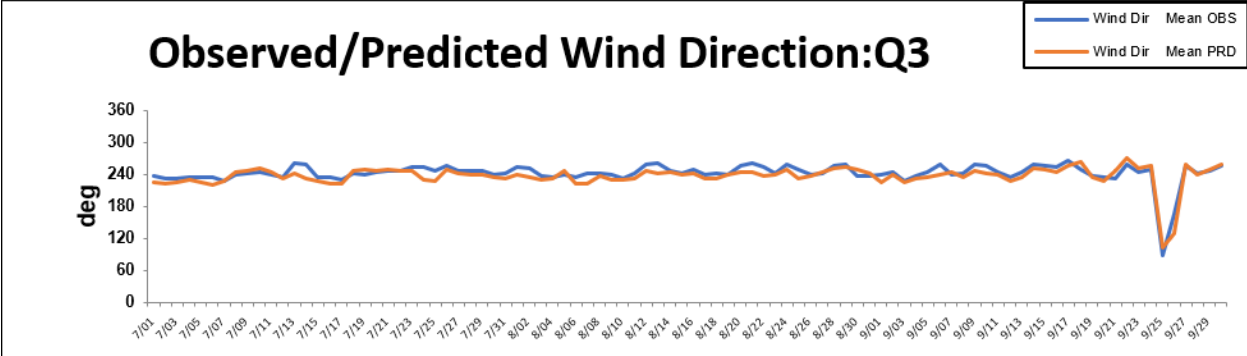
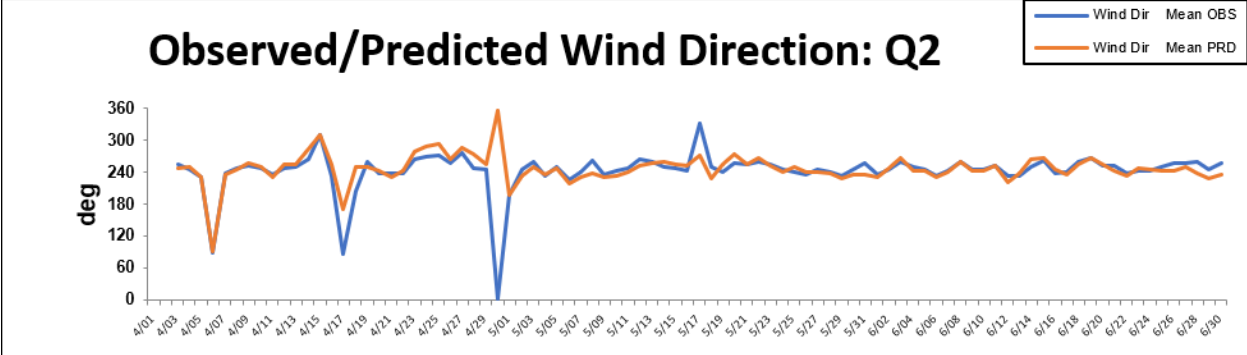
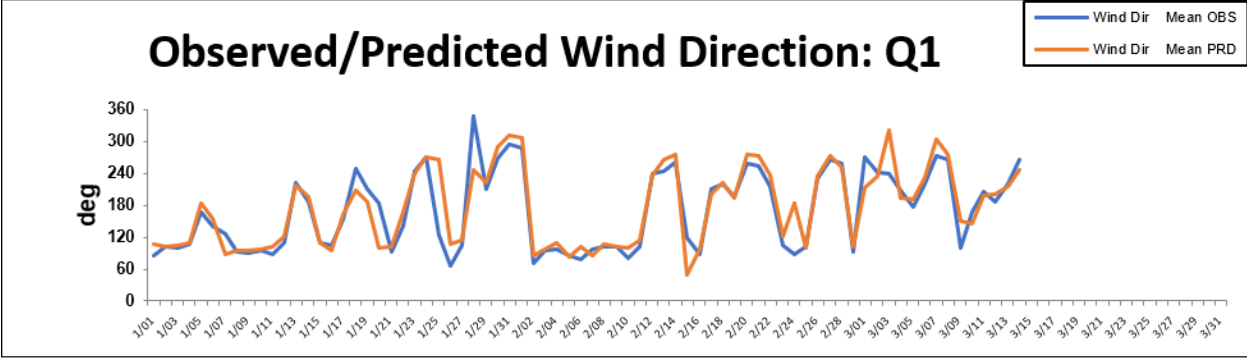


Figure C5: Daily time series of observed and simulated wind direction at Vallejo for 2016.

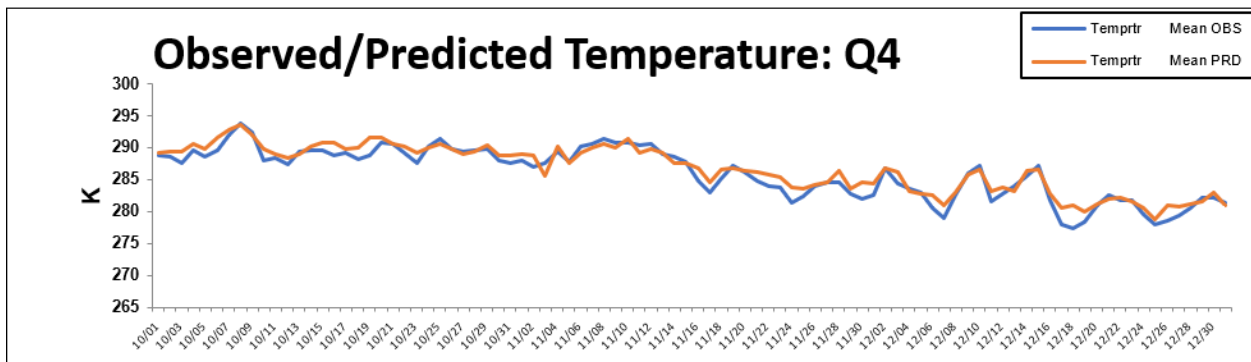
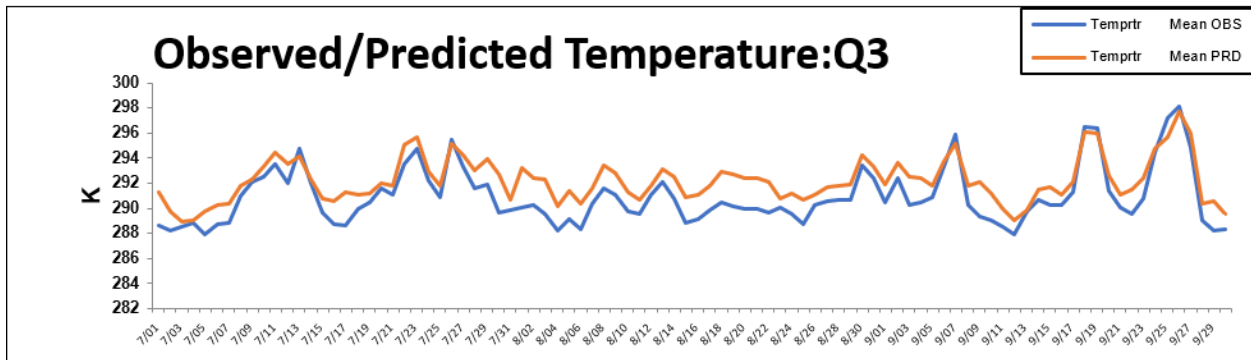
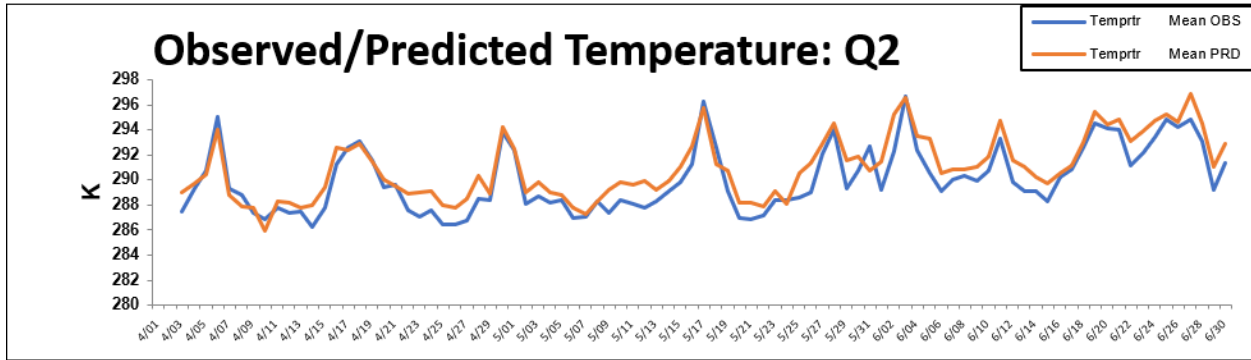
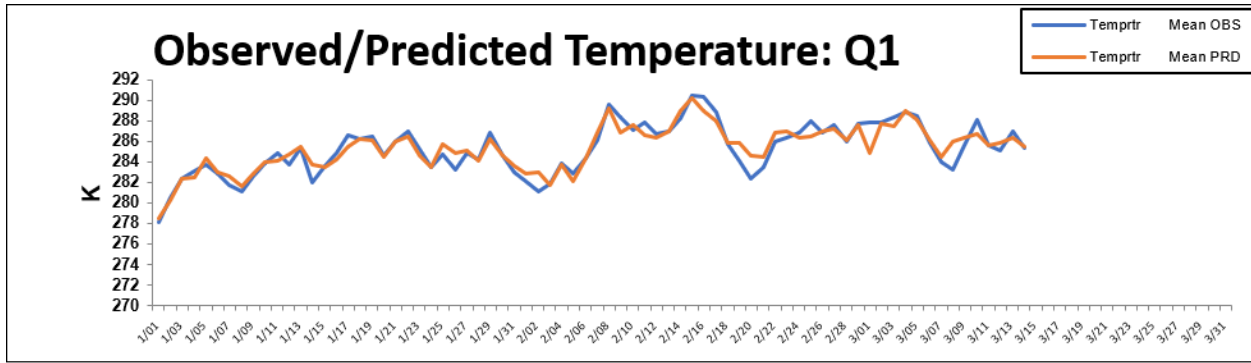


Figure C6: Daily time series of observed and simulated temperatures at Vallejo for 2016.

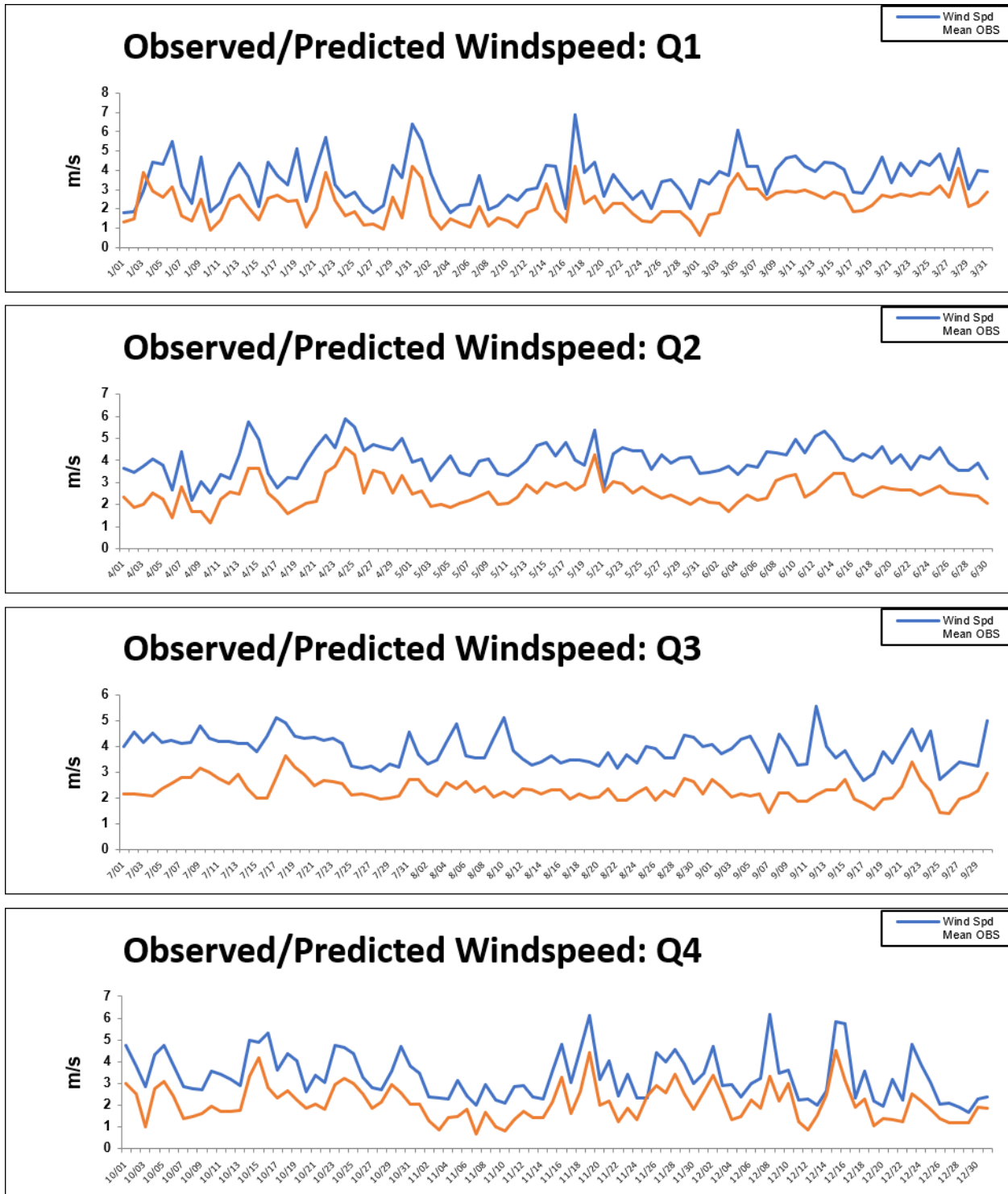


Figure C7: Daily time series of observed and simulated wind speed at San Jose for 2016.

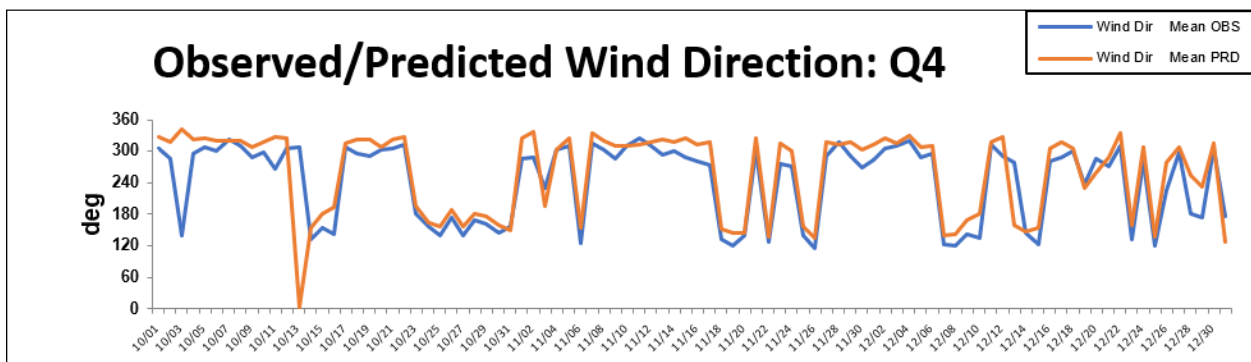
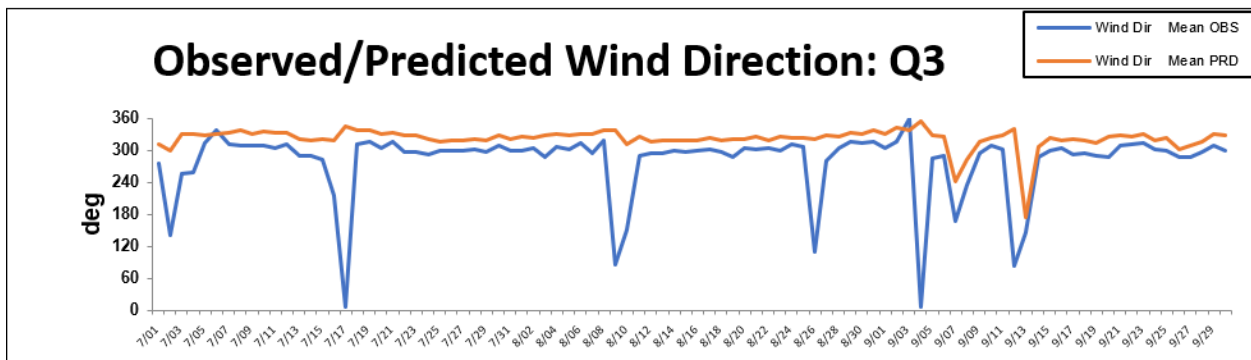
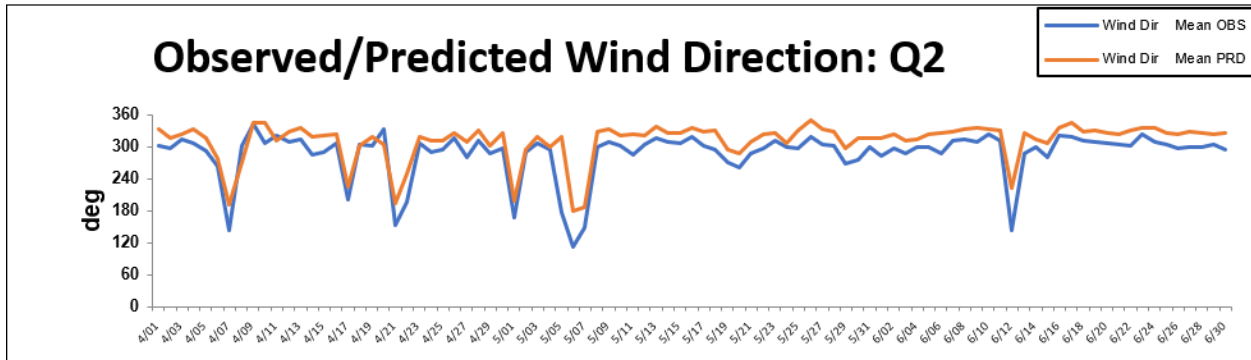
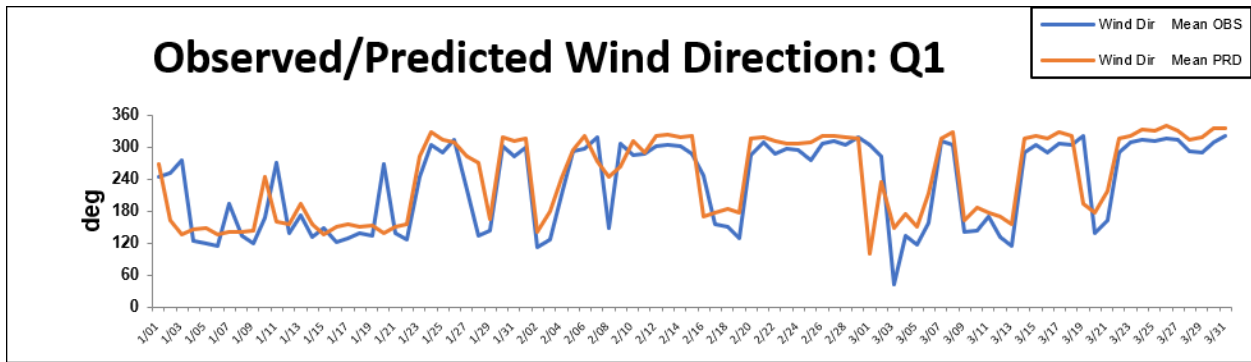


Figure C8: Daily time series of observed and simulated wind direction at San Jose for 2016.

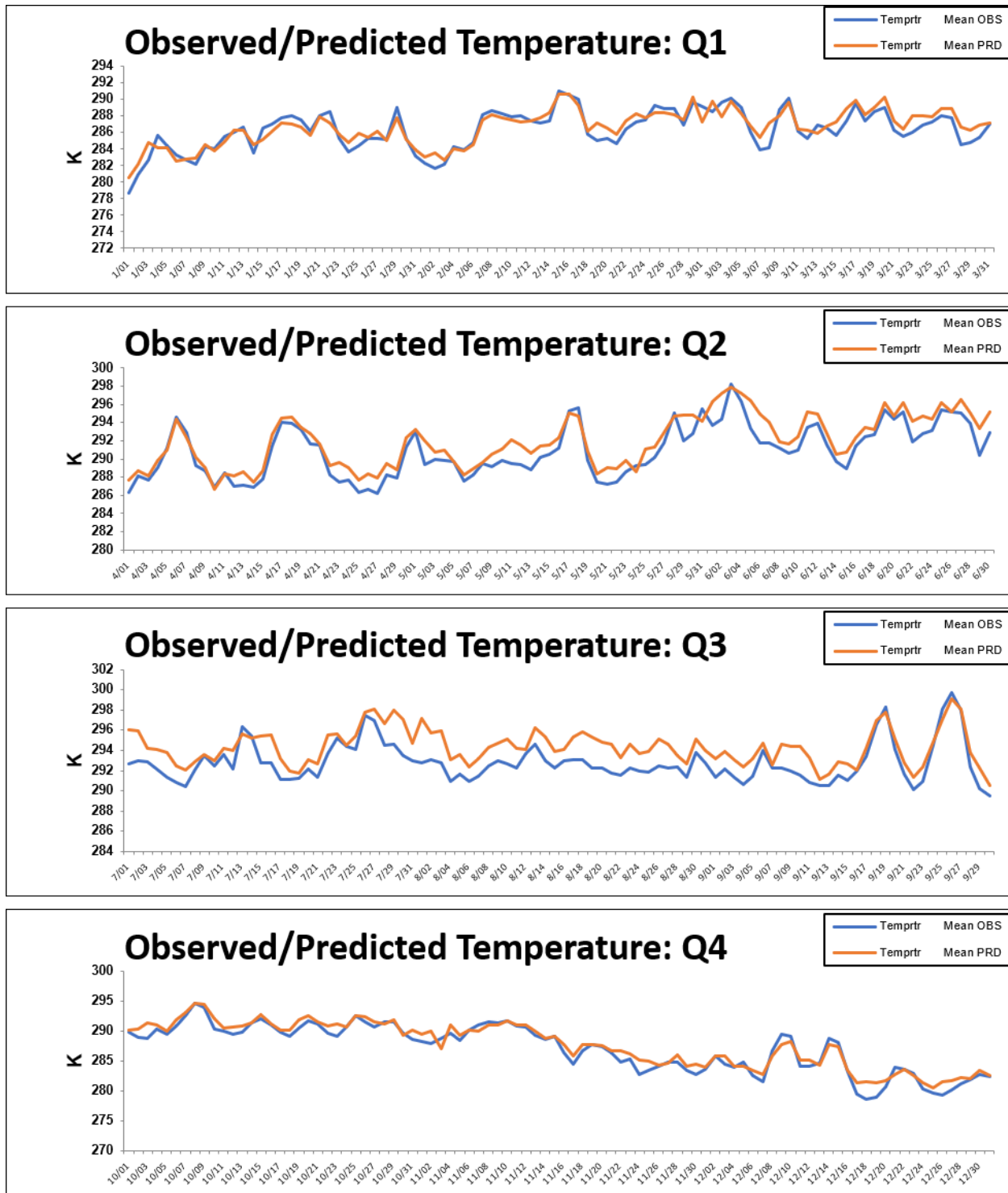


Figure C9: Daily time series of observed and simulated temperatures at San Jose for 2016.

C3. Evaluating WRF Against Upper Air Measurements

There were two upper air stations within the 1-km WRF modeling domain that were operating in 2016. One of them was in Oakland, where the National Weather Service made twice daily measurements at 00 GMT and 12 GMT (4:00 pm and 4:00 am PST, respectively) throughout the year. The other station was at Bodega Bay, where midday measurements were made from May through August, 2016. This was a temporary station established in support of the California Baseline Ozone Transport Study.

Outputs from the 1-km WRF model were compared against measurements at both stations. Day by day, simulations matched observations exceptionally well. Figures C10 and C11 show simulated and observed upper air meteorological data from one winter day (January 10, 2016 at 12 GMT) and from one summer day (June 4, 2016 at 12 GMT) at Oakland. Simulated temperature and dew point (dashed lines) follow observations (solid lines) very well.

Figure C12 shows observed and simulated temperatures at 1:00 pm at Bodega Bay. The simulated temperature matches observations very well.

These are randomly selected plots for the purpose of displaying observed vs. simulated meteorological parameters. They do not necessarily show the best or worst match between the simulation and observations.

Station = 72493 Lat = 37.7 Lon = -122.2 Date = 2016-01-10_12

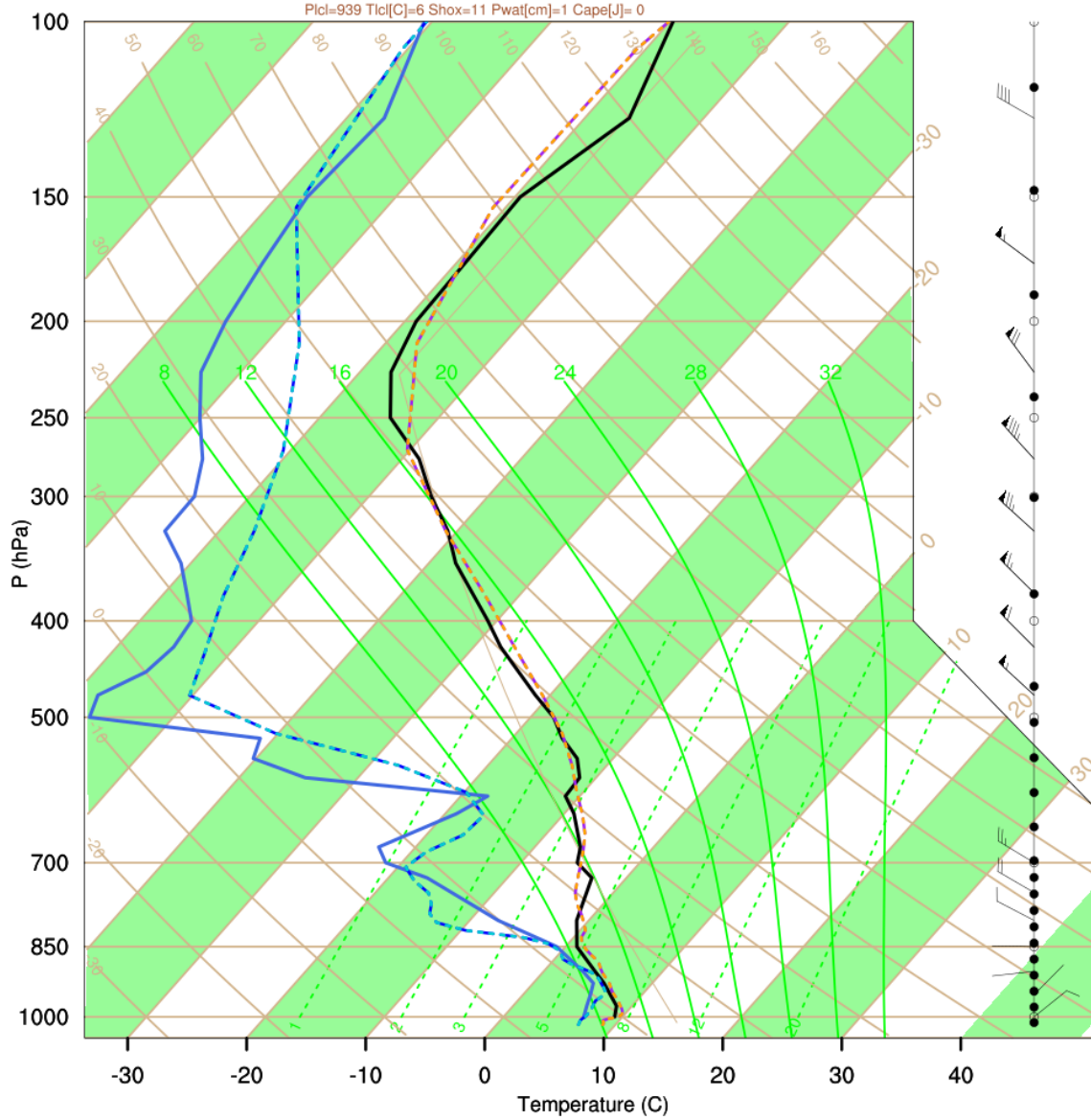


Figure C10: A skew-T plot showing simulated (dashed lines) and observed (solid lines) temperatures (orange and black) and humidity (blue) at Oakland on January 10, 2016 at 12 GMT. Observed wind barbs at pressure levels are shown on the right y-axis.

Station = 72493 Lat = 37.7 Lon = -122.2 Date = 2016-06-04_12

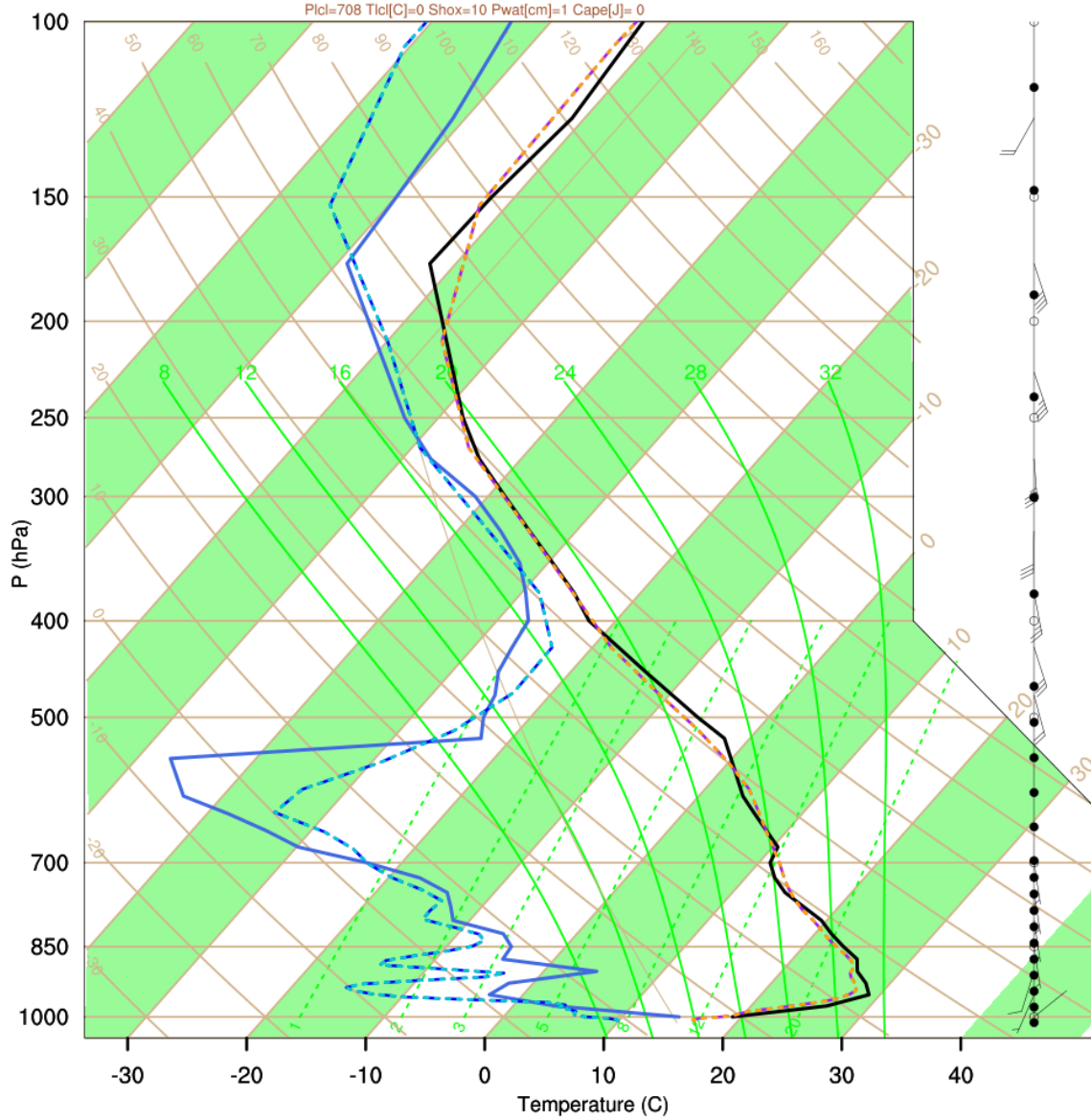


Figure C11: A skew-T plot showing simulated (dashed lines) and observed (solid lines) temperatures (orange and black) and humidity (blue) at Oakland on June 4, 2016 at 12 GMT. Observed wind barbs at pressure levels are shown on the right y-axis.

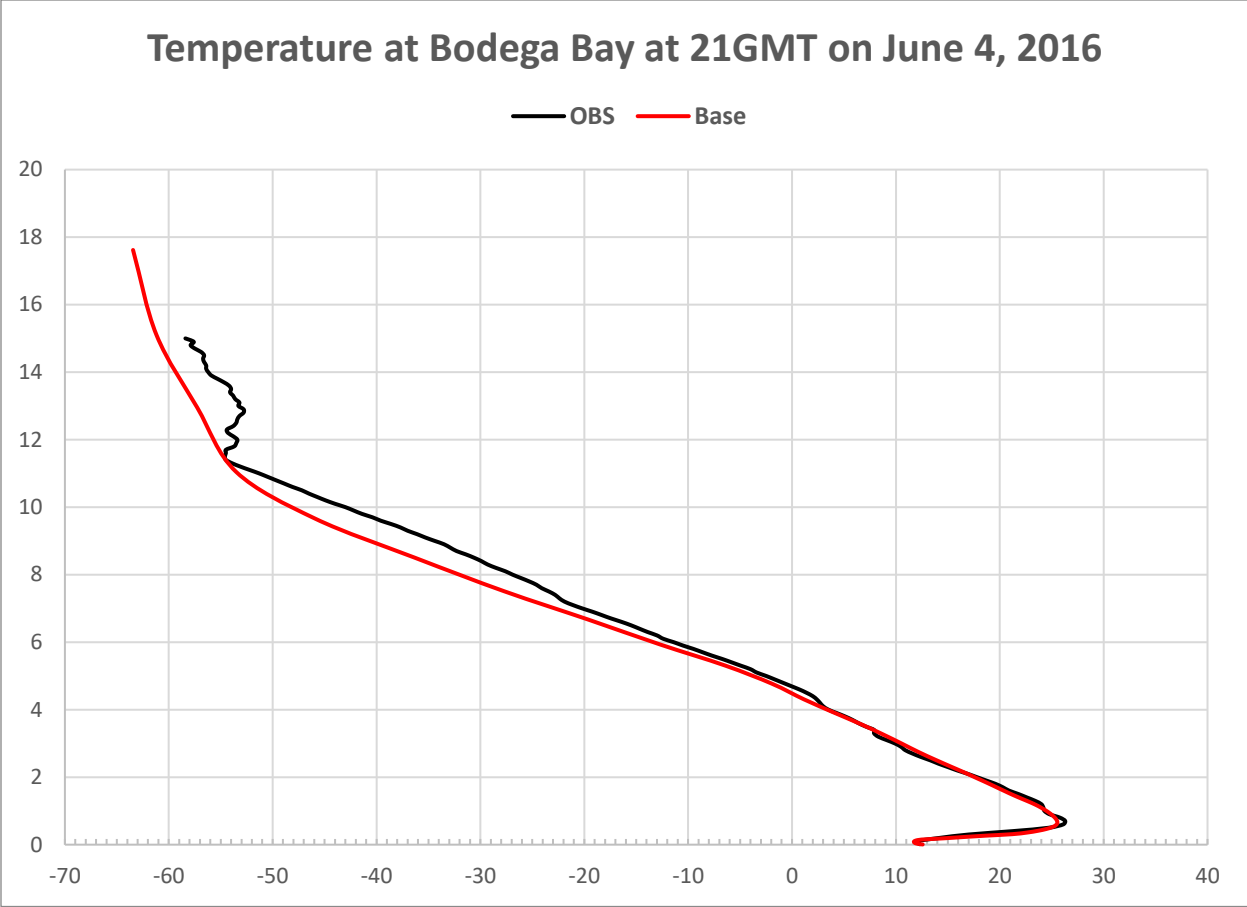


Figure C12: A plot showing simulated (red) and observed (black) temperatures at Bodega Bay at 1:00 pm PST.

Appendix D – Evaluation of the CMAQ Model

D1. Statistical Metrics

Table D1 shows statistical metrics used for CMAQ evaluation. Statistical metrics were calculated from paired daily observed and simulated PM_{2.5} concentrations over quarterly and annual periods. Q1, Q2, Q3 and Q4 represent the 1st, 2nd, 3rd and 4th quarters, respectively. They are defined as January-March, April-June, July-September and October-December.

Table D1. Quarterly and annual statistical model performance metrics.

Metric	Definition ¹	Q1	Q2	Q3	Q4	Annual
Mean bias (MB, µg/m ³)	$\frac{1}{N} \sum (P_i - O_i)$	2.3	-0.3	-1.2	0.4	0.3
Mean error (ME, µg/m ³)	$\frac{1}{N} \sum P_i - O_i $	3.6	2.7	2.9	3.6	3.2
Root mean square error (RMSE, µg/m ³)	$\sqrt{\frac{1}{N} \sum (P_i - O_i)^2}$	5.5	3.4	3.7	5.3	4.6
Fractional bias (FB, %)	$100 \times \frac{2}{N} \sum \frac{P_i - O_i}{P_i + O_i}$	23%	5%	-8%	4%	6%
Fractional error (FE, %)	$100 \times \frac{2}{N} \sum \frac{ P_i - O_i }{P_i + O_i}$	40%	40%	43%	41%	41%
Normalized mean bias (NMB, %)	$100 \times \frac{\sum (P_i - O_i)}{\sum O_i}$	30%	-4%	-16%	4%	4%
Normalized mean error (NME, %)	$100 \times \frac{\sum P_i - O_i }{\sum O_i}$	47%	38%	39%	42%	42%
Correlation coefficient (r)	$\frac{\sum [(P_i - \bar{P})(O_i - \bar{O})]}{\sqrt{\sum (P_i - \bar{P})^2 \sum (O_i - \bar{O})^2}}$	0.69	0.35	0.32	0.61	0.56

¹ The summations are taken over all pairs of predictions (P_i) and valid observations (O_i) by site and day, and N is the total number of data pairs. Overbars represent means over the N data.

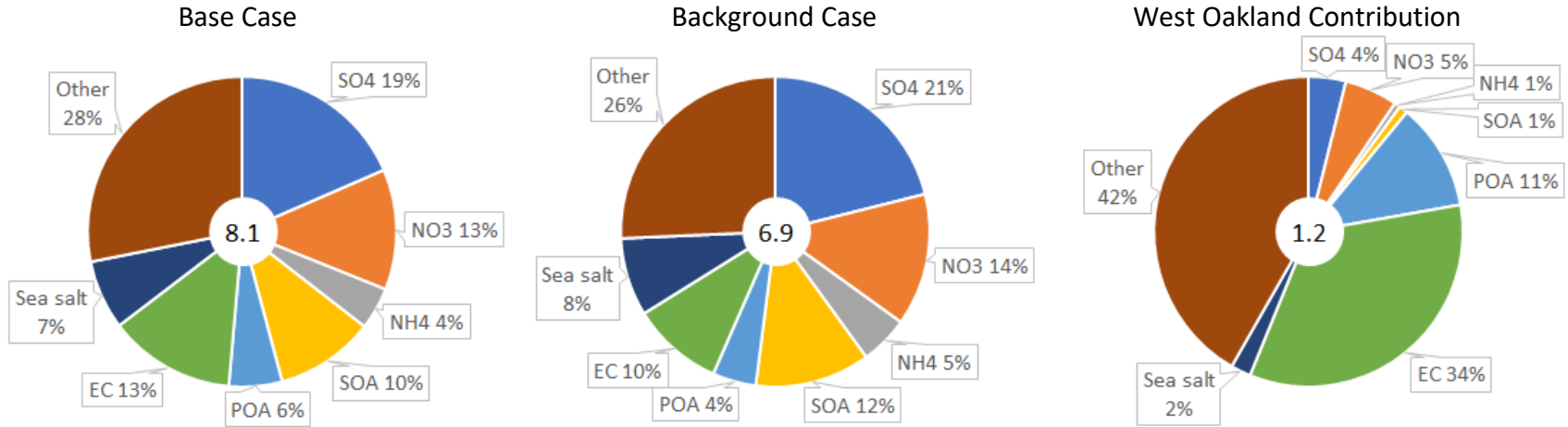
The annual mean bias in simulated PM_{2.5} concentrations is 0.3 µg/m³. On a quarter by quarter basis, the mean bias ranges from -0.3 to 2.3 µg/m³. Among the quarters, Q1 has the highest bias. As explained in the main text, the model is significantly overestimating PM_{2.5} during winter months, especially in February. Possible reasons for the overestimation are under investigation.

Overall, the model shows acceptable PM_{2.5} performance, meeting the goals by Boylan and Russell (2006) and criteria by Emery et al. (2017) for the whole year as well as all 4 quarters.

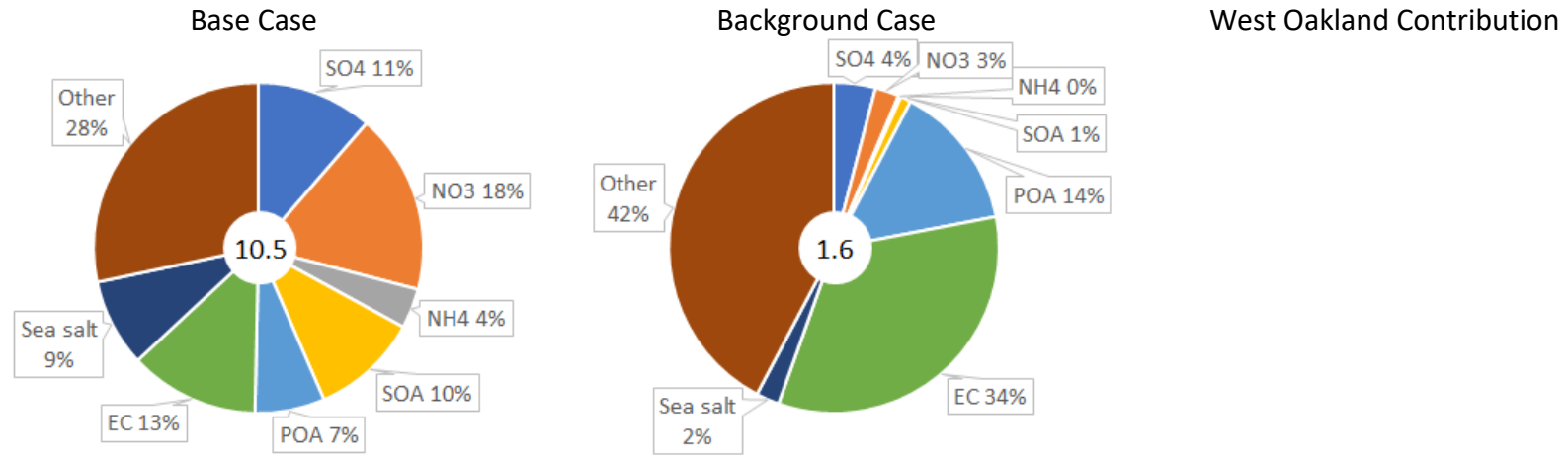
D2. West Oakland PM_{2.5} Composition

Figure D1 shows annual and quarterly average PM_{2.5} compositions over the West Oakland receptor domain for the base and control (i.e., a simulation without West Oakland's anthropogenic emissions) cases as well as the West Oakland contributions (i.e., the difference between the base and control cases). The "Other PM_{2.5}" fractions (primary PM_{2.5} mass other than carbonaceous material and sea salt; mostly fugitive dust in this region) are generally the largest component except for the 3rd quarter, where sulfate is the dominant PM_{2.5} component. Secondary PM_{2.5} fractions (ammonium sulfate, ammonium nitrate, and secondary organic aerosol) account for approximately half of total PM_{2.5} mass (ranging from 41% to 63%). The base and control cases exhibit similar PM_{2.5} compositions, indicating that the regional background influence is dominating. The West Oakland contributions are heavily weighted by primary fractions (84% to 93%) from the local sources.

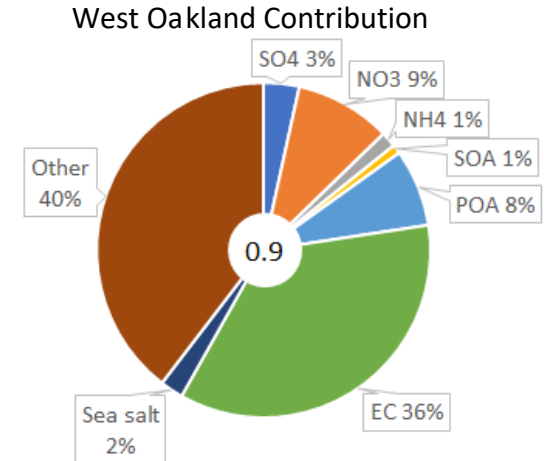
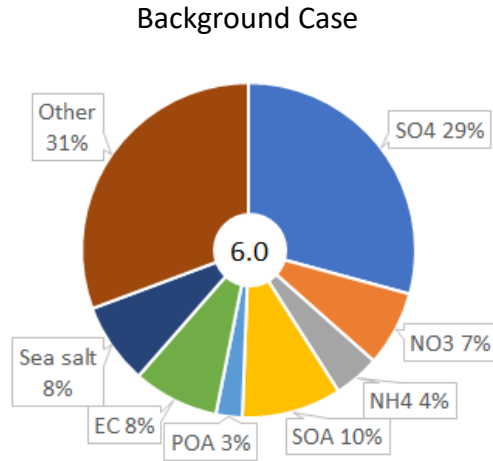
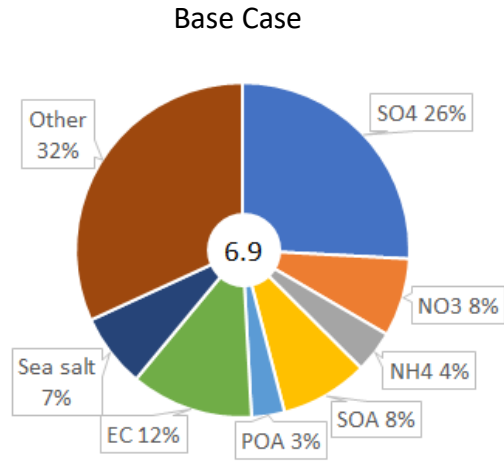
(a) Annual Average PM_{2.5} Composition (West Oakland Receptor Region)



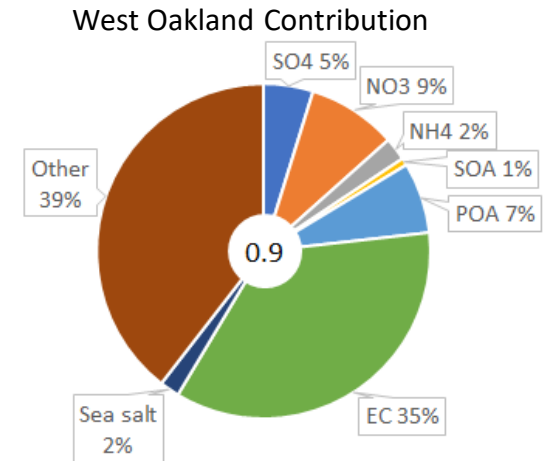
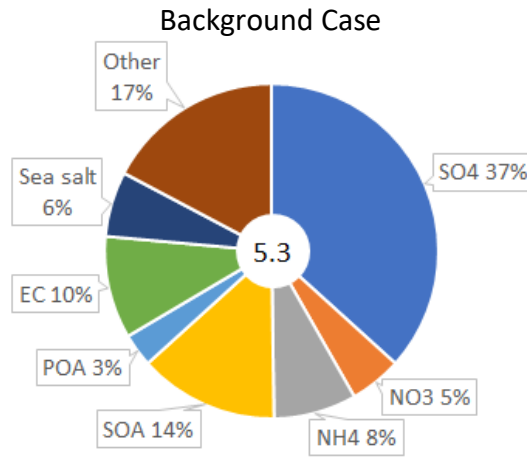
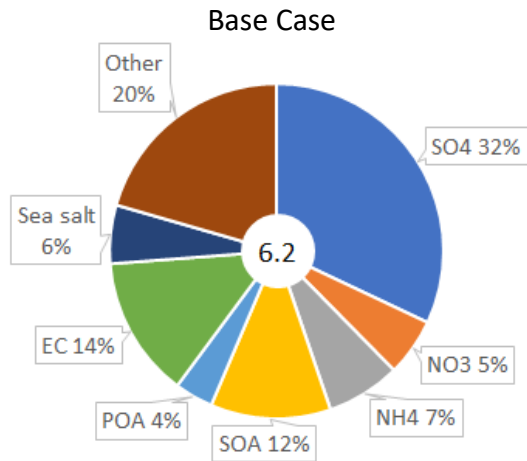
(b) Quarter 1 Average PM_{2.5} Composition (West Oakland Receptor Region)



(c) Quarter 2 Average PM_{2.5} Composition (West Oakland Receptor Region)



(d) Quarter 3 Average PM_{2.5} Composition (West Oakland Receptor Region)



(e) Quarter 4 Average PM_{2.5} Composition (West Oakland Receptor Region)

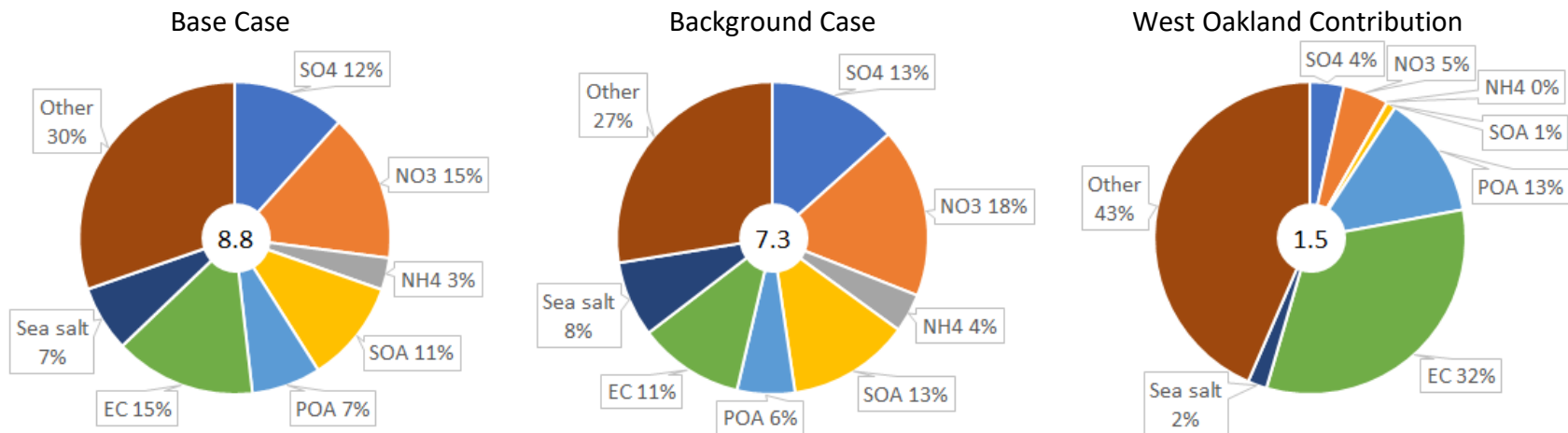


Figure D1: Annual and quarterly average PM_{2.5} compositions over the West Oakland Receptor Region for the base and control cases and their differences (i.e., contributions from the West Oakland anthropogenic emissions). Numbers in the center are total PM_{2.5} concentrations in μg/m³.

References

Appel, W., Napelenok, S., Foley, K., Pye, H., Hogrefe, C., Luecken, D., Bash, J., Roselle, S., Pleim, J., Foroutan, H., Hutzell, B., Pouliot, G., Sarwar, G., Fahey, K., Gantt, B., Gilliam, R.C., Heath, N., Kang, D., Mathur, R., Schwede, D., Spero, T., Wong, D., and Young, J., 2017. Description and evaluation of the Community Multiscale Air Quality (CMAQ) modeling system version 5.1. Geoscientific Model Development. Copernicus Publications, Katlenburg-Lindau, Germany, 10:1703-1732.

BAAQMD, 2007. Spare the air tonight study, 2007-2008 winter wood smoke season. Bay Area Air Quality Management District, San Francisco, CA (March).

BAAQMD, 2017. Spare the air, cool the climate. Bay Area Air Quality Management District, San Francisco, CA (April).

Boylan, J.W. and Russell, A.G., 2006. PM and light extinction model performance metrics, goals, and criteria for three-dimensional air quality models. *Atmos. Environ.*, 40, 4946-4959, doi:10.1016/j.atmosenv.2005.09.087.

Emery, C., Tai, E., and Yarwood, G., 2001. Enhanced meteorological modeling and performance evaluation for two Texas ozone episodes. Prepared for the Texas Natural Resource Conservation Commission by ENVIRON International Corp., Novato, CA (August).

Emery, C., Liu, Z., Russell, A.G., Odman, M.T., Yarwood, G. and Kumar, N., 2017. Recommendations on statistics and benchmarks to assess photochemical model performance. *J. Air & Waste Manage. Assoc.*, 67:5, 582-598, doi:10.1080/10962247.2016.1265027.

EPA, 2018. Modeling guidance for demonstrating air quality goals for ozone, PM_{2.5}, and regional haze. U.S. Environmental Protection Agency, Research Triangle Park, NC (EPA-454/R-18-009).

Knoderer, C., Nguyen, D., Alrick, D., and Hoag, K., 2017. 2016 air monitoring network plan. Bay Area Air Quality Management District, San Francisco, CA (July).

Reid, S.B., 2008. Documentation of the preparation of year-2005 emission inventories of toxic air contaminants for the San Francisco Bay Area. Technical memorandum prepared for the Bay Area Air Quality Management District by Sonoma Technology, Inc., Petaluma, CA (January).

Simon, H., Baker, K., and Phillips, S., 2012. Compilation and interpretation of photochemical model performance statistics published between 2006 and 2012. *Atmos. Environ.*, 61, 124-139, doi:10.1016/j.atmosenv.2012.07.012.

Tanrikulu, S., Soong, S., Tran, C., and Beaver, S., 2009. Fine particulate matter data analysis and modeling in the Bay Area. Bay Area Air Quality Management District, San Francisco, CA (October).

Tanrikulu, S., Tran, C., and Beaver, S., 2011. Health impact analysis of fine particulate matter in the San Francisco Bay Area. Bay Area Air Quality Management District (September).